

Insertion Reactions and QSSR Modeling of Donor/Donor Rhodium Carbenes for the Synthesis of
Indanes, Indolines, and Benzodihydrofurans

By

LUCAS WILLIAM SOUZA
DISSERTATION

Submitted in partial satisfaction of the requirements for the degree of

DOCTOR OF PHILOSOPHY

in

Chemistry

in the

OFFICE OF GRADUATE STUDIES

of the

UNIVERSITY OF CALIFORNIA

DAVIS

Approved:

Jared T. Shaw, Chair

Dean J. Tantillo

David E. Olson

Committee in Charge

2022

To Lynn Kipp, Stephen Kipp, and Bill Souza: This was for you.

Acknowledgements

I would like to acknowledge my graduate student mentor Dr. Richard Squitieri for believing in me. And my mentor Dr. Jared Shaw and fellow graduate students Dr. Leslie Nickerson, Dr. Stephen Laws, and Dr. Lucas Moore for their help in becoming the chemist I am today. My family, including my brother Sean Kipp who has been there for me when no one else was. Lastly, I would like to thank Dr. Anna Lo. Without you this would not have been possible.

ABSTRACT OF DISSERTATION

The creation of new carbon–carbon bonds with a high degree of stereocontrol is a powerful strategy employed in targeted synthesis of complex organic molecules. Chiral benzene-fused 5-membered rings represent a significant portion of medicinally relevant molecules. This dissertation describes the construction of benzodihydrofurans, indanes and indolines by C–H insertion reactions of donor/donor carbenes. Chapter one discusses the development of a stereochemically predicative model for insertion reactions to form benzodihydrofurans. From this study, a predictive model for diastereoselectivity was established. Chapter two discusses methodology development for insertion reactions to make indolines and indanes. These cores were produced in high yields, with a high degree of stereocontrol and functional group tolerance.

TABLE OF CONTENTS

Chapter 1: QSSR Study of C–H Insertion Reactions for the Formation of Benzodihydrofurans

1. Introduction.....	1
1.1 Cheminformatics: An Emerging Approach in the Field of Asymmetric Catalysis ...	1
1.2 Early QSSR Work Utilizing Local Parameterization	3
1.3 Global Parameterization Methods	4
1.4 Spatial Molding of Approach Ridged Targets (SMART) Descriptors	6
2. Results	9
2.1 Substrate and Catalyst Chemical Space Mapping	9
2.2 Catalyst Chemical Space Mapping	11
2.3 New Catalyst Development	12
2.4 QSSR Modeling	15
3. Conclusion.....	20
4. Experimental	20
5. References	34

Chapter 2: Enantioselective C–H Insertion Reactions of Donor/donor Carbenes for the Formation of Indolines and Indanes

2.1 Introduction.....	65
2.1.1 Metal Carbene Reactivity and History	65
2.1.2 Donor/Donor Metal Carbene Precursors	66
2.1.3 Catalysts Used in Donor/Donor Metal Carbene Precursors	68
2.1.4 Reactions Mechanisms and Scope of Donor/Donor Carbene Insertions	70
2.1.4.1 Mechanisms of Insertion Reactions of Non-C–H Bonds with Donor/Donor Carbenes	70
2.1.4.2 Scope of Insertion Reactions of Non-C–H Bonds with Donor/Donor Carbenes	72
2.1.4.3 C–H Insertion Reactions of Donor/Donor Carbenes	79
2.1.4.4 Diazo-free Insertion Reactions of Donor/Donor Carbenes	82
2.2 Results	89
2.2.1 Indolines	89
2.2.2 Mechanistic Studies	92
2.2.3 Indanes	96
2.2.4 Targeted Synthesis of Patented Indane Drug	97

2.3 Conclusion.....	102
2.4 Experimental Procedures	103
2.5 References	146

Chapter 1. QSSR Study of C–H Insertion Reactions for the Formation of Benzodihydrofurans

1 Introduction

1.1 Cheminformatics: An Emerging Approach in the Field of Asymmetric Catalysis

The relationship between structure and reactivity is a foundational principle of the organic chemist. Since the first alchemists put mortar to pestle, this relationship has been the basis for the prediction and rationalization of chemical transformations. Advances in computational techniques in recent decades have coincided with advances in the field of catalyst development^{1,2}. A complementary approach to this methodology has been the emerging field of cheminformatics. Cheminformatics has long been used in the area of drug development and has recently been extended to the area of asymmetric catalysis in the form of “quantitative structure selectivity relationships” (QSSR).³ A general workflow for this technique is described eloquently by Denmark et al. (Figure 1).⁴

Framework of 3D-QSAR Guided Catalyst Optimization

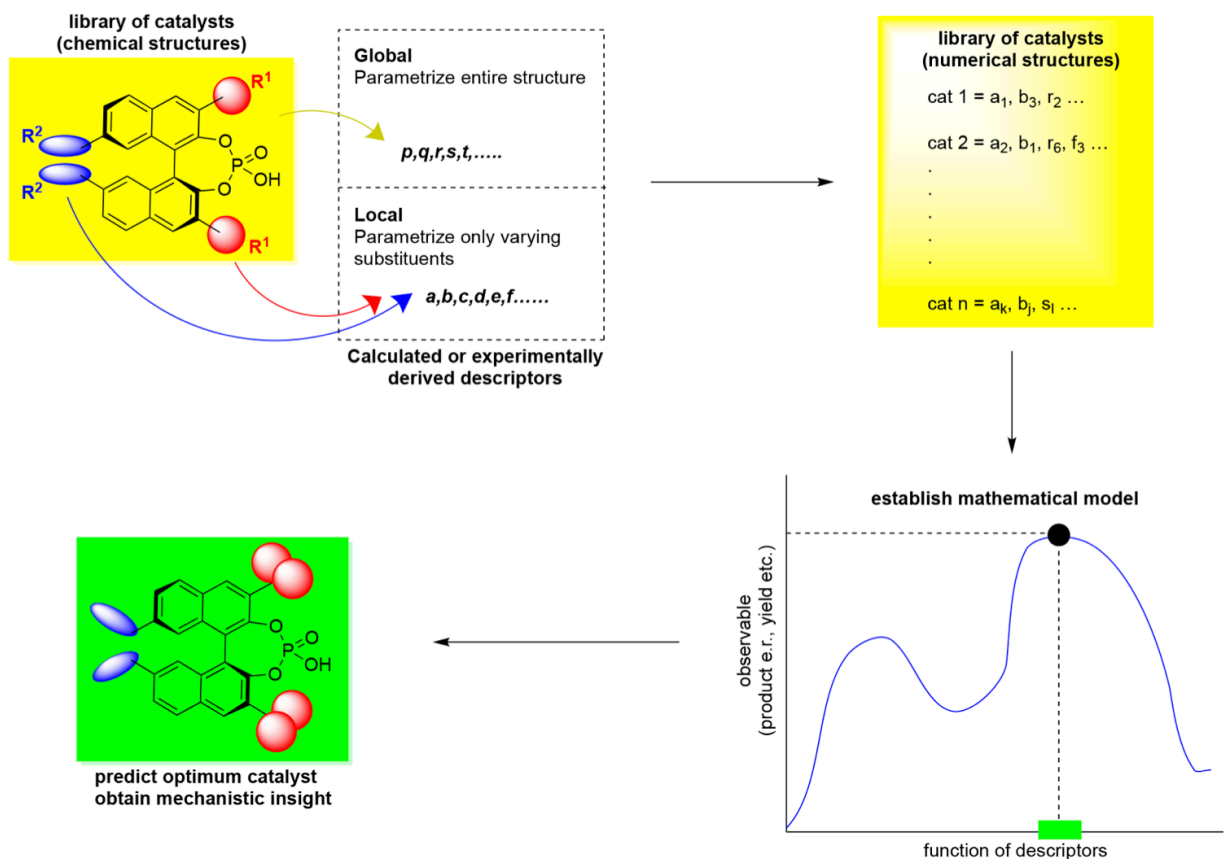


Figure 1. QSSR workflow overview as described by Denmark et. al.

Catalyst design begins with a library of catalysts with diverse structures. Structural components are then parametrized into measurable quantities. This can be done in numerous ways but generally these parametrizations fall into two classes: (1) local parameterizations, i.e. parameterizations of some individual structural components of the catalyst, or (2) global parameterization, wherein the entire shape of the catalyst is parameterized. These catalyst structures can then be simplified into a series of “numerical” catalyst structures by describing the molecule in terms of these numerical descriptors. Following parameterization, mathematical models can be developed that create a relationship between catalyst descriptors and observed activity (QSAR) or

stereoselectivity (QSSR). This model can then be used to predict optimal catalyst structures and improve the reaction performance *without* the use of time intensive DFT calculations. While work done by Tantillo and others has made much progress in our understanding of dirhodium catalysis^{5,6}, this method allows us to examine reactions with complex catalyst architectures that are expensive to model in their entirety by existing DFT methods.

1.2 Early QSSR Work Utilizing Local Parameterization

Linear free energy relationships are a fundamental topic of physical organic chemistry. Conceptually, they represent a relationship between a substituent parameter and reactivity. A classic example of a LFER is a Hammett correlation⁷, wherein the relative acidity of substituted benzoic acid can be correlated to a substituent descriptor to derive a numerical value σ . While relatively unsophisticated by today's standards, this concept represents a key innovation: the effective transformation of a local qualitative structural element (substituent) into a quantitative numerical value (σ). By extension, it is possible to apply this concept to enantioselective catalysis, where specific catalyst or substrate structural features are parametrized and modeled to predict stereochemical outcomes.

Early work in QSSR involved the use of Charton values (ν) as descriptors by Miller and Sigman wherein they construct LEFR's in the enantioselective Nozaki-Hiyama-Kishi (NHK) reaction (Figure 2).⁸ Charton values are derived from the relative influence certain groups have on the rate of hydrolysis of methyl esters. Charton was able to fit these measurements to calculated values derived from the van der Waals radii of the

substituent.⁹ In this study, five catalysts with differing carbamate groups R were evaluated. A linear relationship was established in the reaction of three different substrates when Charton values are plotted against the logarithm of product enantiomeric ratios. While not particularly complex by today's standards, this study represents one of the earliest demonstrations that structural information can be quantified and modeled to generate a predictive model for stereochemical outcome.

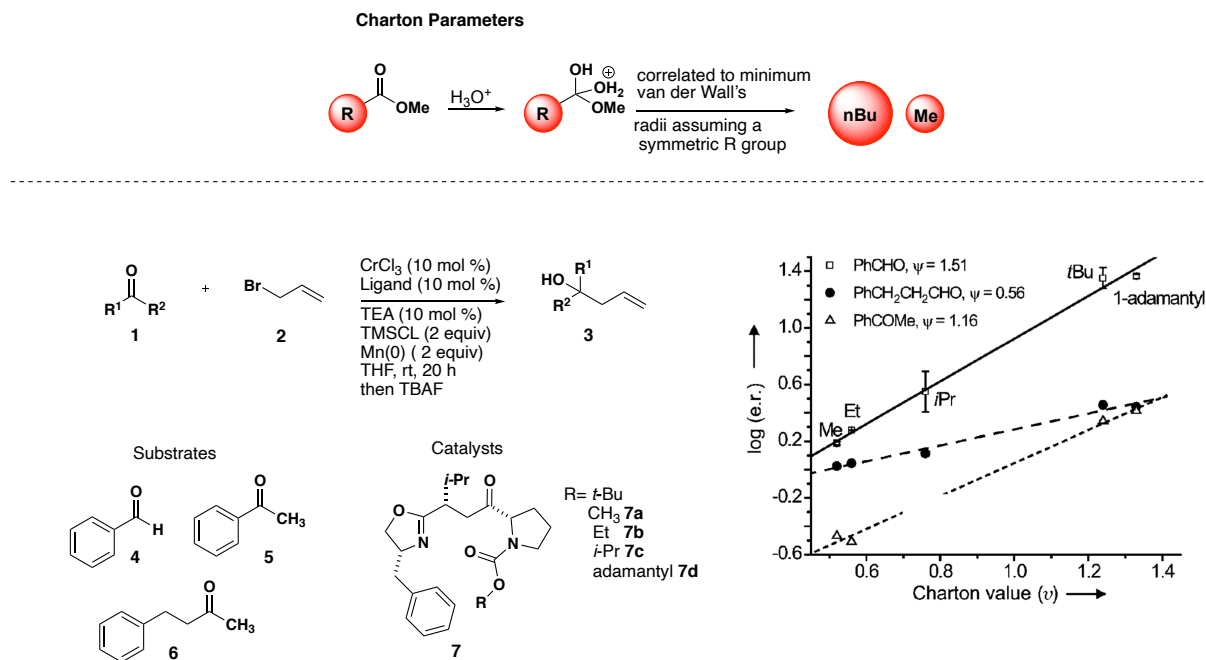


Figure 2. Summary of Charton values and Miller and Sigman's LEFR study of the enantioselective NHK reaction.

1.3 Global Parametrization Methods

While early studies focused on single structural component variation (local parametrization), it soon became apparent that the subtleties of stereinduction are often not captured by variation of a single substituent. Indeed, modern catalysts are understood to interact with substrates in a variety of complex ways and thus require

parameterization methods that elucidate more structural detail . As a result, new global descriptors have been developed that capture catalyst structure in its entirety. Early efforts towards this aim were undertaken by Carbo and coworkers for the copper-catalyzed cyclopropanation of styrene and diazo esters (Figure 3).¹⁰ The authors suggested quadrant diagrams may be used to quantify specific catalyst steric effects in a more wholistic fashion. The steric parameterization of each quadrant is constructed by a twofold approach. First, Charton values of each R group in each quadrant were obtained, then the distance weighted volume of each quadrant was calculated using equation 1.

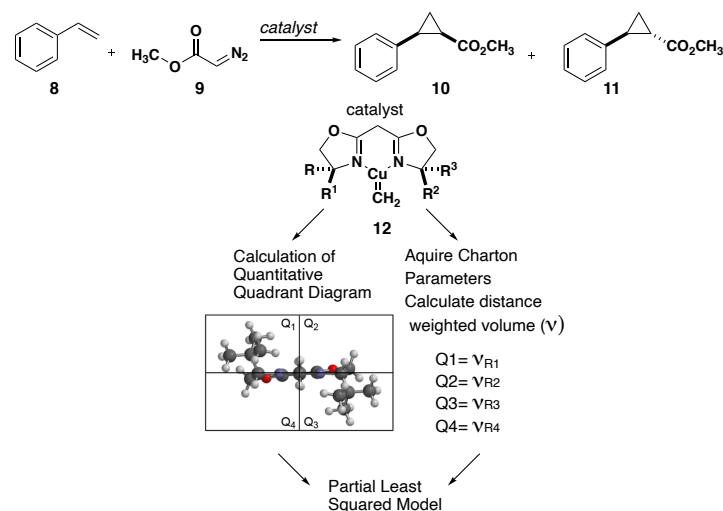


Figure 3. Global parametrization workflow developed by Carbo and coworkers

$$V_{w,k,l} = \sum_{i=1}^n \frac{r_i^k}{d_i^l}$$

Equation 1. Equation for distance weighted volume

In this equation $V_{w,k,l}$ is the distance weighted volume, r is the Van der Waals radius of a given atom and d is the distance between that atom and the central copper atom of catalyst **12**. w , k and l are exponents that can be given by values of 0, 1, 2, or 3. The authors found that distance weighted volume measurements showed only slightly worse correlation to the energy differential between diastereomeric transition states than Charton values. This proof-of-concept study indicates that global parameterization of catalysts is indeed possible and competitive with existing local descriptors. Refinement of this seminal work by others has established a wide range of complex global parameterization methods that have become the standard for modern QSSR studies of complex catalytic systems.⁴

1.4 Spatial Molding Of Approach Ridged Targets (SMART) Descriptors

While much progress has been made over the last few decades in the development of global descriptors to quantify catalyst reactivity, capturing three dimensional structural features of complex catalyst architectures remains a formidable challenge. Specifically, dirhodium paddlewheel complexes present a unique challenge as their reactive site topologies are often difficult to quantify by existing methods.¹¹ Recently, Cammarota et. al. developed new global descriptors, dubbed “SMART”, for dirhodium catalyst parameterization and applied them to study C–H insertion reactions of donor/acceptor carbenes. (Figure 4).¹²

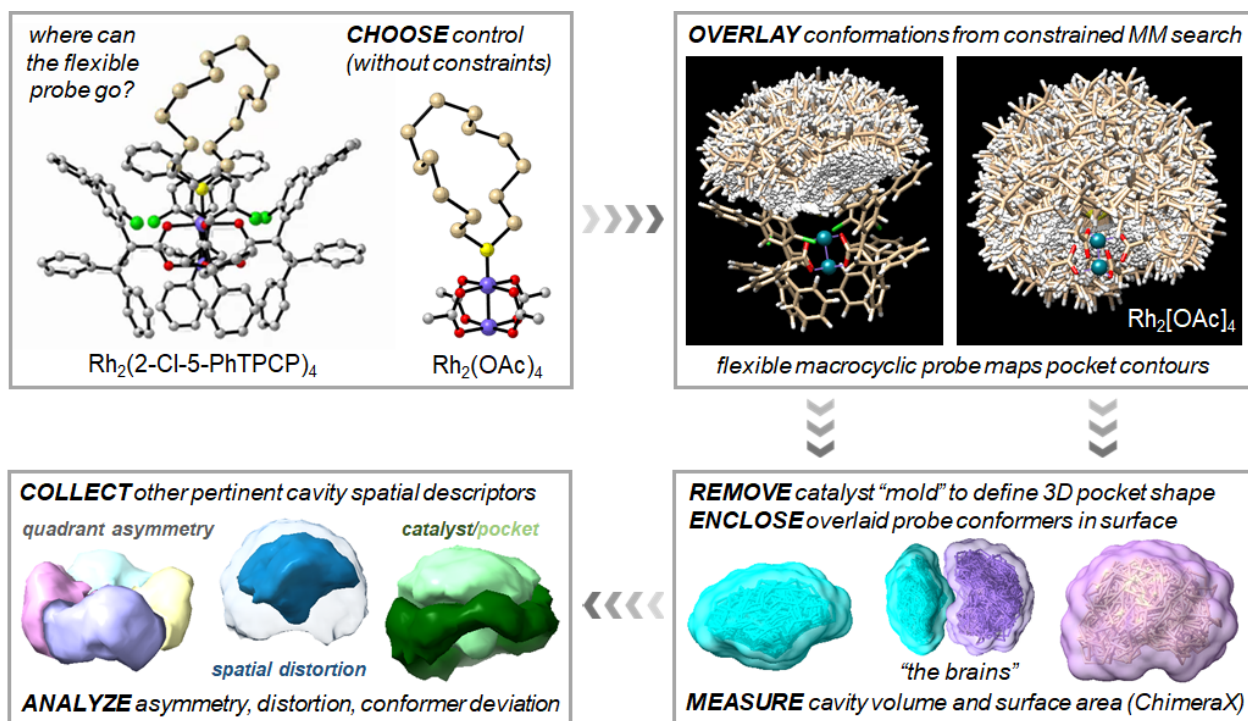


Figure 4: Workflow for SMART descriptor definition.

The SMART approach treats the reactive catalyst conformer as an approachable rigid target into which a macrocyclic probe molecule can be docked. The shape of the catalyst pocket can be directly captured by assessing what space the probe molecule can occupy in a constrained conformational search, where all atoms belonging to the catalyst are frozen. All conformations of the probe can then be overlaid and enclosed in a surface using UCSF ChimeraX 1.11¹³ to generate what is colloquially called a "brain" (or spatial mold). From this point, various novel SMART descriptors can be extracted from the "brains" and used as inputs for catalyst performance via statistical modeling. With this tool in hand, we set out to conduct a QSSR study of donor/donor carbenes with the aim of creating a predictive model for diastereoselectivity and enantioselectivity for C–H insertion reactions of donor/donor carbenes to form benzodihydrofurans. (Figure 5)

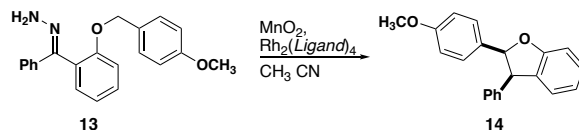


Figure 5: C–H insertion reaction of Donor/Donor carbenes to form benzodihydrofurans

We envisioned a holistic approach to model development. (Figure 6)

We wanted to create a system in which both novel substrates and catalysts could be virtually screened to predict stereochemical outcomes. We also wanted to develop a system to determine which substrate catalyst combination would be best suited for achieve a particular stereochemical outcome.

While each piece of this vision has been achieved by other groups on other systems, few have combined them in a holistic fashion. Furthermore, a tool of this nature would be of

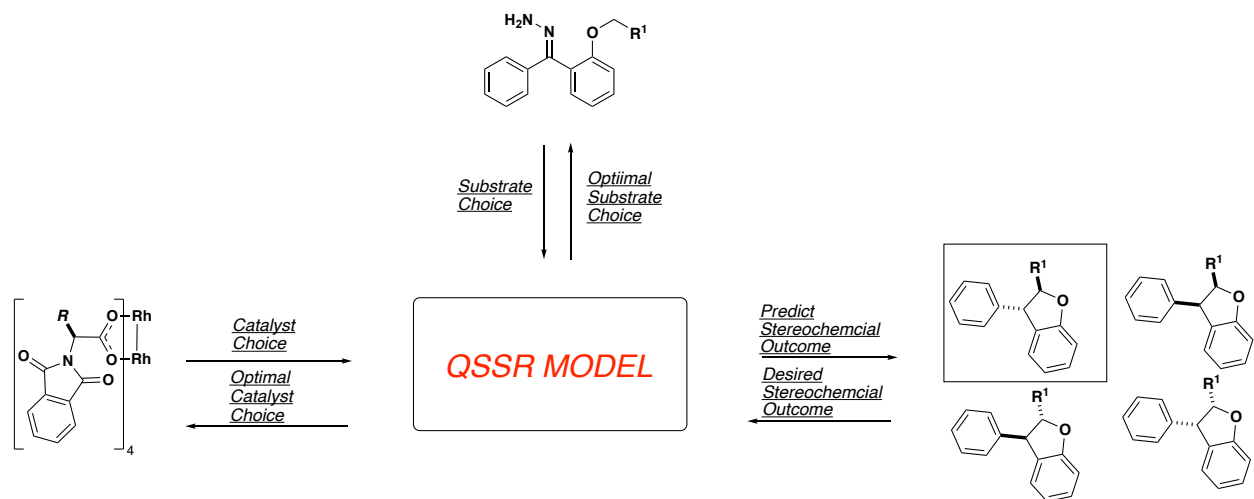


Figure 6. Vision for QSSR model of benzodihydrofuran

great use to the synthetic organic chemist as it could potentially cut down on intensive catalyst screens, substrate scope exploration, and other time intensive aspects of method development.

2 Results

2.1 Substrate and Catalyst Chemical Space Mapping.

Initially, we set out to construct a comprehensive chemical space map of both catalysts and substrates. We hypothesized that the greatest amount of substrate chemical variance could be achieved by modulating the steric bulk and electronics of the functional groups closest to the carbon undergoing C–H insertion. To this end, we recognized that our synthetic route could be leveraged to modulate the structural components closest to the insertion center by careful selection of the alkyl bromide used in the initial alkylation of benzophenone 15. (Figure 7)

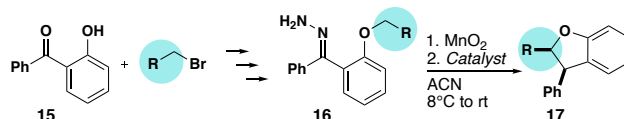


Figure 7: Synthesis of benzodihydrofurans.

We then conducted a principal component analysis (PCA) of 3000 commercially available alkyl bromides utilizing Mordred descriptors implemented through RDKit (Figure 8). This analysis yielded an extremely high number of results, however it quickly became apparent that conducting this study on a large number of substrates would prove too synthetically challenging.

As such, we opted to examine a smaller yet representative area of chemical space to limit the total number of substrates. We found that potential substrates clustered in areas of similar structure and defined five distinct substrate groups alkyl (red), allyl (purple), EW benzyl (blue), ED benzyl (green), and extended benzyl (pink) (Figure 8). Finally, within each group we chose several bromides to maximize substrate diversity.

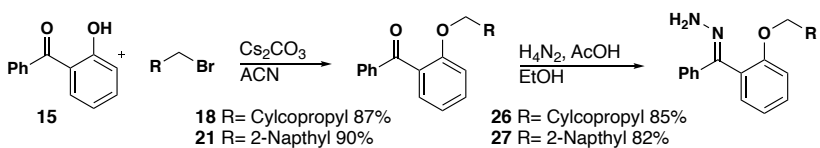
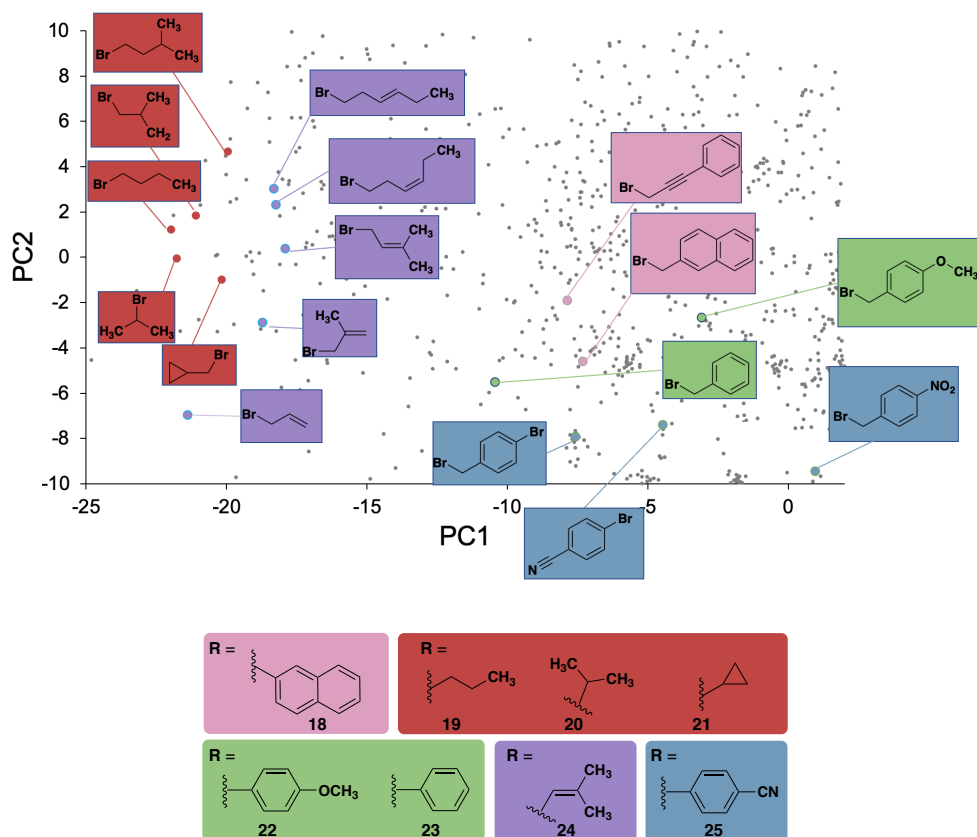


Figure 9: PCA analysis of commercially available alkyl bromides and novel substrate synthesis

PC1 and PC2 represent linear combinations of substrate descriptors with the greatest variance.

2.2 Catalyst Chemical Space mapping

We conducted a similar PCA for the dirhodium catalyst space. 36 catalysts donated to us by Professor Joseph Fox and his group at University of Delaware were analyzed based on 23 descriptors including SMART descriptors developed by Sigman (Figure 9). Similarly to our substrate analysis, catalysts were grouped and compounds from each group were selected as representative of the larger chemical space. This effort afforded 14 catalysts to serve as the basis of our training set (Figure 10). PC1 and PC2 represent linear combinations of the above mentioned descriptors with the greatest variance.

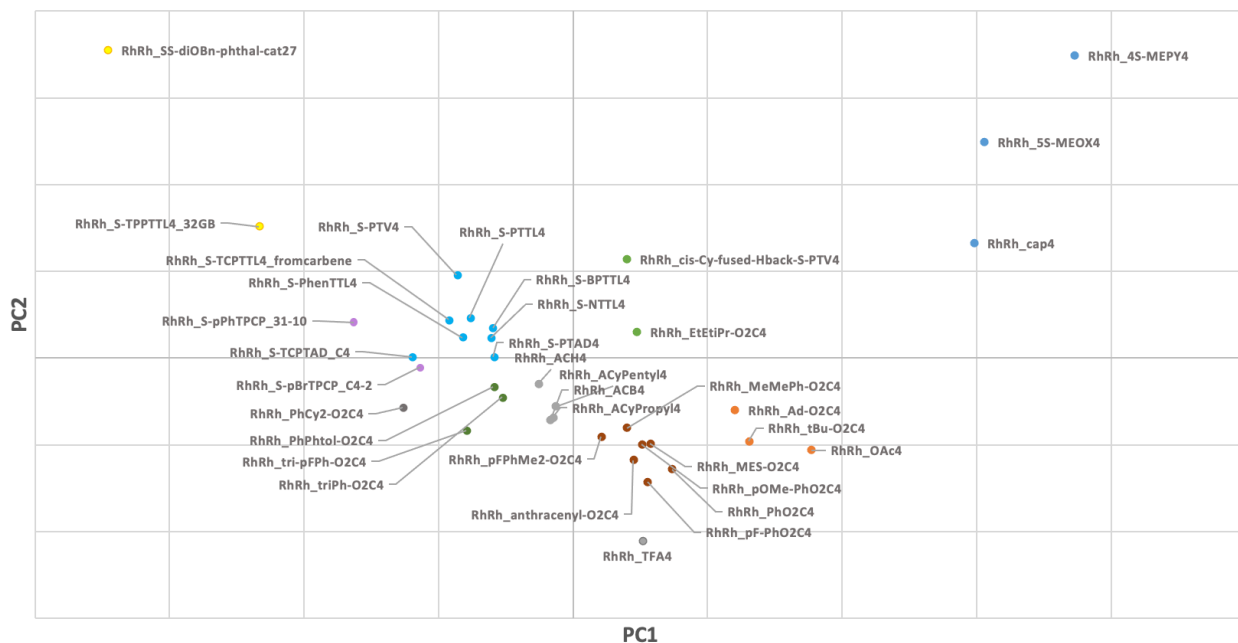


Figure 9. Catalyst space PCA

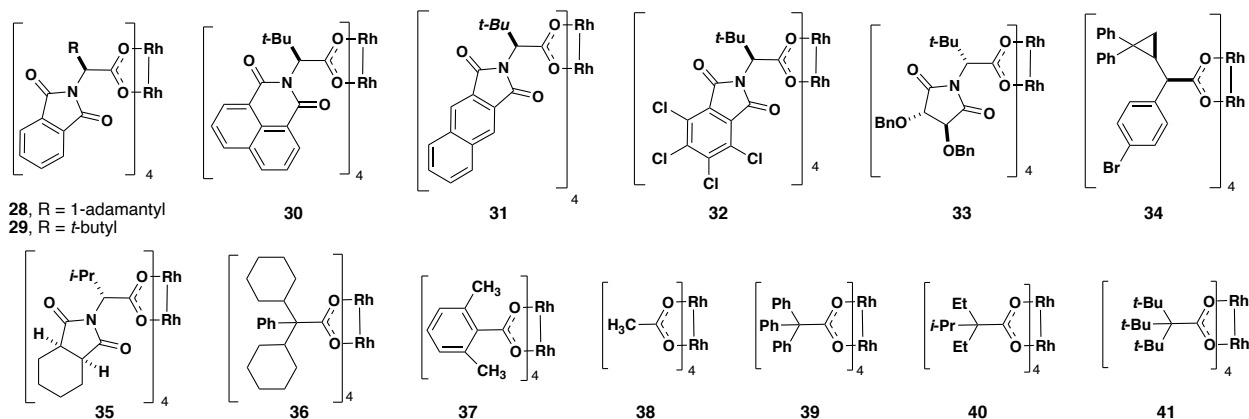


Figure 10. Training set catalysts

2.3 New catalyst Development

In our lab, we have been lucky to find that our best results in both reactivity and stereoselectivity can be achieved by a single catalyst, $\text{Rh}_2(\text{PTAD})_4$. While this has helped us to create efficient methodologies for C–H insertion reactions, we often struggle to get similar levels of reactivity and selectivity out of achiral catalysts. We saw this study as an opportunity to develop achiral catalysts with similar reactivity to $\text{Rh}_2(\text{PTAD})_4$. Our chemical intuition and preliminary modeling data informed our decision to consider some relatively underexplored cycloalkane-phthalamido catalysts resembling $\text{Rh}_2(\text{PTTC})_4$ as possible “PTAD like” (Figure 11).

Catalysts were synthesized by phthalamidation of commercially available amino acids **42** followed by treatment with rhodium acetate in refluxing chlorobenzene. Crystal structures were obtained for all catalysts including the first reported for $\text{Rh}_2(\text{PTTC})_4$ (**49**).

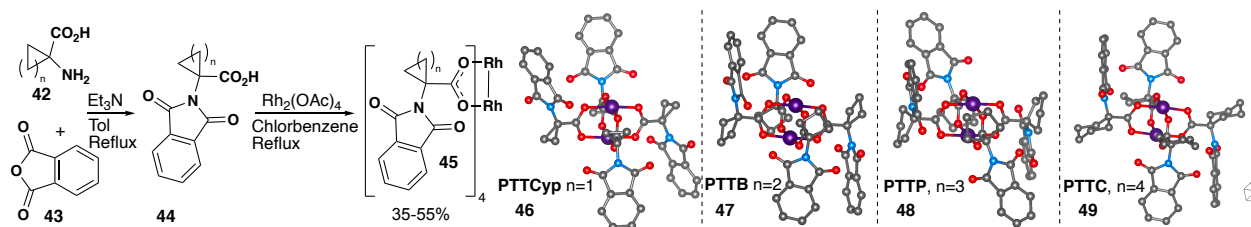


Figure 11. Synthesis of $\text{Rh}_2(\text{PTCC})_4$ related catalysts.

Having had success with the PTCC family of catalysts, We attempted to synthesize a number of other dirhodium catalysts we intuitively predicted would give us high levels of reactivity and selectivity. (Figure 12)

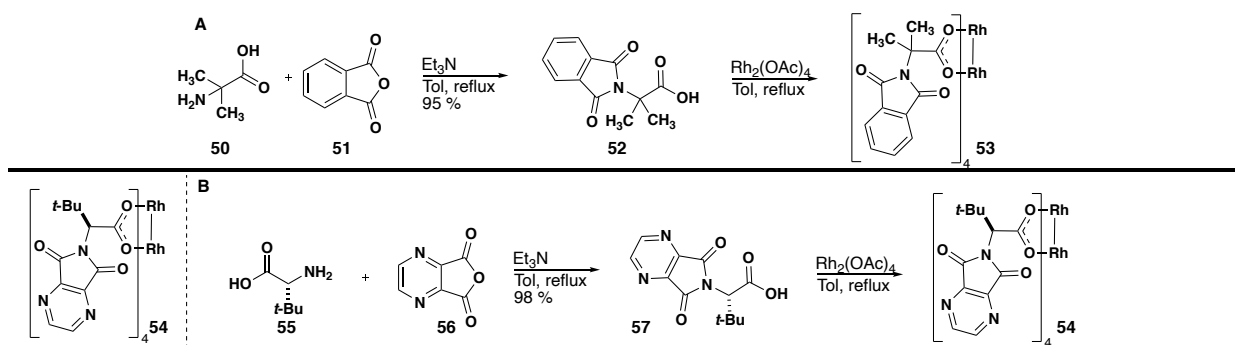


Figure 12. Attempts to synthesize catalysts with electron withdrawing groups.

Firstly, attempts were made to synthesize dimethyl derived catalyst **53**. (Figure 12A) We hoped this would serve as a more freely rotating version of our previously successful cyclopropane catalyst $\text{Rh}_2(\text{PTCC})_4$. While the phthalimidation and ligand exchange worked well, **53** proved insoluble and difficult to work with so it was abandoned.

In general, it is believed that increased electrophilicity of metal carbenes increases their reactivity.¹⁴ Two attempts were made to synthesize more electron withdrawing catalysts **54** (Figure 12b) and **61**. (Table 1) The phthalimidation reaction and ligand

exchange to synthesize **54** worked well. However, the final product again proved highly insoluble in organic solvents and too difficult to work with.

We hypothesized that the addition of fluorine to the catalyst $\text{Rh}_2(\text{PTTL})_4$ (**59**) may sufficiently increase the electronegativity of the resultant metal carbene. To this end, attempts were made to fluorinate malonic ester derivative **59**. (Table 1).

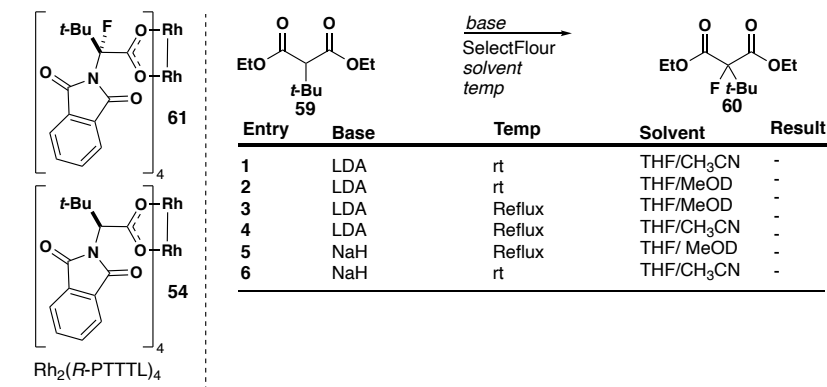


Table 1. Attempts to synthesize fluorine derivative **61**.

Firstly, a literature procedure utilizing LDA at room temperature in a mixture of THF and CH₃CN was performed with no product observed (entry 1). We believed steric issues due to the large *t*-Butyl group might be causing either slow addition to the fluoride source or slow enolization. To test this, the reaction was carried out in deuterated methanol with the hope that the deuterium exchange could give us an idea of the degree to which **59** was enolizing. Unfortunately, no deuterium exchange was observed by ¹HNMR. Similar experiments were performed with NaH and at reflux (entries 2 -6). In all cases no enolization or fluoride addition was observed. As a result of already having several new catalysts that showed higher levels of reactivity this effort was abandoned.

2.4 QSSR Modeling

Having established a list of catalysts and substrates as well as synthesizing novel catalysts, we then set out to collect selectivity data for both enantiomeric and diastereomeric ratios (Table 2 and 3). Reaction conditions were identical for every experiment and chiral HPLC and ¹HNMR were used to gather enantiomeric and diastereomeric ratios respectively. A representative data set is shown in tables 2 and 3.

1. MnO₂
2. 0.1% Catalyst
ACN 8°C to rt

119 Total Reactions

Catalyst	R =	R =	R =	R =	R =
	d.r. (e.r.)	d.r. (e.r.)	d.r. (e.r.)	d.r. (e.r.)	d.r. (e.r.)
31	84:16	84:16	89:11	90:10	90:10
35	68:32	52:48	72:28	86:14	88:12
36	62:38	39:61	68:31	80:20	80:20
30	46:54 (92:8)	50:50 (55:45)	82:18 (100:0)	100:0 (6:94)	100:0 (94:6)
26	85:15 (97:3)	89:11 (97:3)	93:7 (100:0)	97:3 (96:4)	100:0 (99:1)
33	72:28 (63:37)	72:28 (69:31)	85:15 (60:40)	90:10 (47:53)	87:13 (46:54)
29	94:6 (—)	74:26 (72:28)	— (—)	94:6 (84:16)	94:6 (77:23)
28	77:23 (90:10)	— (—)	97:3 (93:7)	— (—)	— (—)

Catalyst	R =	R =	R =
	d.r. (e.r.)	d.r. (e.r.)	d.r. (e.r.)
36	85:15	85:15	85:15
38	84:16	95:5	94:6
39	68:32	88:12	87:13
37	95:5	91:9	97:3
38	100:0 (90:10)	90:10 (93:7)	89:11 (80:20)
26	100:0 (97:3)	100:0 (94:6)	100:0 (94:6)
31	100:0 (94:6)	94:6 (93:7)	96:4 (3:97)
32	92:8 (100:0)	100:0 (100:0)	98:2 (100:0)

cis:trans diastereomeric ratios obtained by integration of crude ¹H NMR
enantiomeric ratios measured by chiral HPLC

Table 2 & 3. Representative examples of training set data.

We also collected additional diastereoselectivity data on our new catalysts in the hopes it could be used as a validation set for our model (Table 4). We were pleased to see that qualitatively these catalysts performed well across our substrate classes which indicated that our preliminary modeling data was predicting effective catalyst architectures.

Entry	Catalyst	d.r.	d.r.	d.r.	d.r.	d.r.	d.r.	d.r.	d.r.
1	49	84:16	93:7	94:6	75:25	67:37	67:37	100:0	89:11
2	48	84:16	92:8	93:7	68:32	58:42	58:42	100:0	87:13
3	47	78:22	93:7	92:8	70:20	71:29	71:29	100:0	89:11
4	46	85:15	94:6	94:6	64:36	60:40	60:40	100:0	84:16

cis:trans diastereomeric ratios obtained by integration of crude ¹H NMR

Table 4. Validation set consisting of novel achiral catalysts.

With this data in hand, we set out to create a model for diastereoselectivity.

To this end, $\Delta\Delta G^\ddagger$ for each reaction combination was calculated and plotted against the experimentally determined $\Delta\Delta G^\ddagger$'s. This was done by utilizing the equation $\Delta\Delta G^\ddagger = -RT\ln(dr)$. Where the dr is defined as the syn : anti ratio of the products and temperature was defined at 293 °K.

Our catalyst conformers were optimized using the B3LYP functional with the GD38BJ empirical dispersion correction, basis set 6-31G** for all non-rhodium atoms and LANL2DZ on the rhodium atoms. Then single points were calculated using the MO6 functional with the GD3 empirical dispersion correction using Basis set def2TZVP on non-rhodium atoms and SSD on rhodium atoms.¹⁵⁻²¹

Substrate and product conformers were optimized at B3LYP/6-31G* level of theory with GD3BJ empirical dispersion correction. Single points were calculated at the M062X/6311G* level with GD3 empirical dispersion correction.²² These experiments were conducted by my collaborators in the laboratory of Mathew Sigman.²³

In order to obtain good statistical correlations, two separate sub-models had to be constructed. (Figure 13).

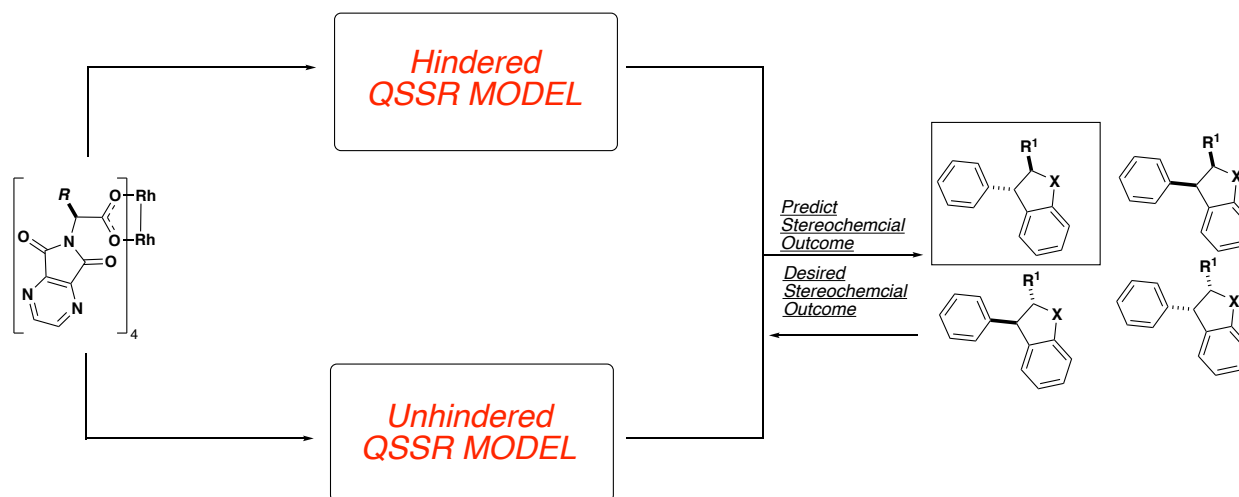


Figure 13. Modified QSSR workflow for Hindered and Unhindered models

In this system, a catalyst considered hindered or unhindered by ligand steric bulk was fed into two different models to predict the stereoselective outcome. We were pleased to find that this strategy proved effective for obtaining a good correlation of both training set and validation set data for hindered catalysts. (Figure 14)


```

Split method: y_equidist
Test ratio: 0.4

Features: x9 + x17 + x45

Parameters:
-1.3405 +
0.3507 * x9 carbene LP*
-0.5128 * x17 sterimol L/B5 WA
0.1865 * x45 prox5_ESA% WA

Training R2 = 0.764
Training Q2 = 0.628
Training MAE = 0.218
Training 4-fold R2 = 0.608 (+/- 0.003)

Test R2 = 0.713
Test MAE = 0.264

```

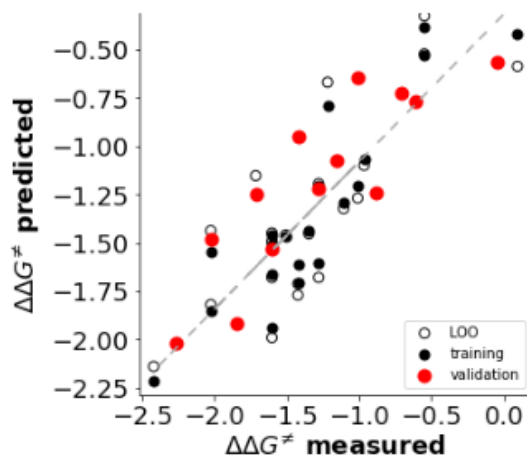


Figure 14. Hindered catalyst model for diastereoselectivity.

An R^2 value of 0.764. was obtained for our test set in the hindered catalyst model. Additionally, our validation set of novel catalyst also correlated well to this model with and R^2 value of 0.713. This indicates that our hindered model is adequate at predicting both effective novel catalyst structures and selectivity outcomes for a given substrate in the training set.

When we tested our hindered model's ability to predict the stereochemical outcome of validation set catalysts and one unmodeled substrate, (Figure 15) we found a weak correlation of $R^2= 0.161$ indicating our model falls short at predicting the stereochemical outcome of novel catalysts with a substrate outside the training set.

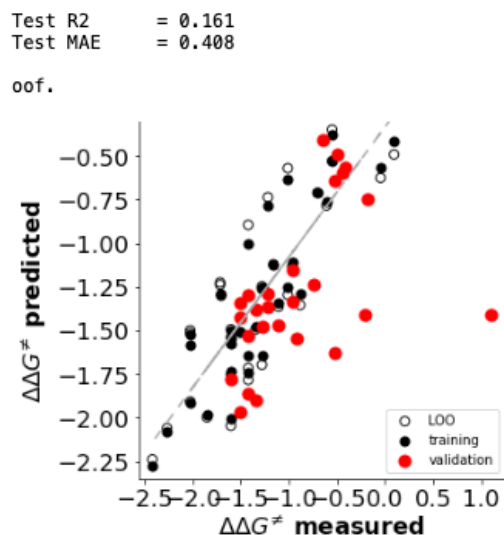


Figure 15. Hindered model with a test set of novel catalysts and one novel substrate.

Our preliminary data for our unhindered model (Figure 16) shows a modest correlation with an R^2 value of 0.5024 for the training set. This data however has yet to be rigorously validated with a validation set.

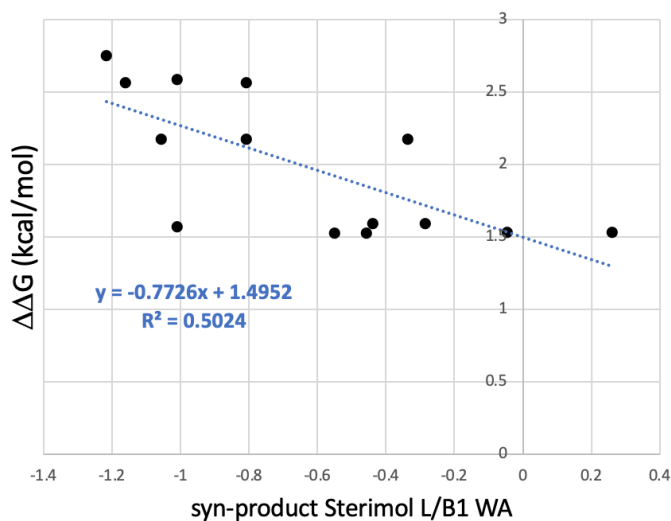


Figure 16. Unhindered catalyst QSSR model

Unfortunately, the enantioselectivity ratios gathered did not produce a modellable training set. We hypothesize that this is due to the relatively low number of data points.

Future work will focus on doing more enantioselective reactions to establish a more robust training set.

3 Conclusion

As our understanding of chemistry deepens, it is becoming increasingly evident that the structural components that govern the outcome of chemical reactions are often increasingly complex and subtle. As catalysts enable more transformations, their structural complexity often increases in equal measure. Herein, I have described in brief how the emerging field of cheminformatics can guide our understanding of asymmetric catalysis. We were able to show that these new methods could be used to create a predictive model for diastereoselectivity of rhodium catalyzed C–H insertion reactions of donor/donor carbenes to form benzodihydrofurans. My hope is this work will inform catalyst design for reactions involving rhodium carbenes and will inspire others to utilize cheminformatics to understand asymmetric reactions involving complex catalyst architectures.

4 Experimental

Instrumentation and General Considerations

Chemicals were purchased and used without further purification. Solvents were dried on a JC Meyer solvent system or purchased anhydrous where required. Reactions requiring anhydrous conditions were performed under argon; glassware was flame dried under vacuum immediately prior to use and allowed to cool under reduced pressure; liquid reagents, solutions or solvents were added via syringe through rubber septa; solid reagents were added under a flow of argon. Reactions were monitored by TLC on

Kieselgel 60 F254 (Merck) plates and detected by examination under UV light (254 nm and 365 nm). Flash column chromatography was performed using silica gel [Merck, 230–400 mesh (40–63 μm)], unless otherwise stated. Microwave reactions were conducted using a Biotage InitiatorTM 2.0, employing 2.45 GHz microwaves. Accurate mass measurements were recorded on positive ESI mode in methanol. Extracts were concentrated *in vacuo* using both a rotary evaporator at a pressure of 15 mmHg (diaphragm pump), and a high vacuum line at a pressure of 0.1 mmHg (oil pump) at room temperature. ¹H and ¹³C spectra were measured in the solvent stated at 400 or 600 MHz and 101 or 151 MHz respectively. ¹H and ¹³C NMR chemical shifts are quoted in parts per million (ppm) and referenced to TMS (TMS: ¹H = 0.0 ppm and ¹³C = 0.0 ppm), coupling constants (*J*) are given in Hertz (Hz). Multiplicities are abbreviated as: br (broad), s (singlet), d (doublet), t (triplet), q (quartet), p (pentet) and m (multiplet) or combinations thereof. Catalysts with known structures were obtained by donation from the laboratory of Professor Joe Fox or were purchased when commercially available.^{24–26}

General Procedure A for alkylation. To a flame dried 50 mL round bottom flask was added 2-hydroxybenzophenone (1.0 equiv.), purged under high vacuum, and backfilled with argon. To the flask was added dry acetonitrile (0.1M), the respective bromide (1.3–1.5 equiv.), and 12-hour oven dried Cs₂CO₃ (3 equiv.). The reaction was stirred at 50 ° C for 12 hours. The reaction mixture was allowed to cool, and solvent was removed by rotatory evaporation. The residue was then resuspended in dichloromethane and washed with deionized water. The organic layer was dried over Na₂SO₄, filtered, and solvent was

removed in vacuo. The resulting crude material was purified by flash column chromatography to yield the desired ketone.

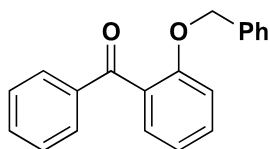
General Procedure B for hydrazone formation. To a solution the respective ketone (1 equiv) in anhydrous EtOH (0.1M) was added AcOH (2 equiv) and anhydrous hydrazine (10 equiv). The reaction mixture was heated in a microwave reactor at 160 °C for 1-3 hours. The reaction was allowed to cool then diluted with Et₂O and washed with water. The organic layer was removed, and the aqueous layer was washed three times with Et₂O. The combined organic layer was washed with water and dried over Na₂SO₄. The crude reaction mixture was purified by flash column chromatography to yield the desired hydrazone

General Procedure C (two-pot insertion). To a flame-dried scintillation vial under argon atmosphere was added the desired hydrazone (1 equiv) followed by anhydrous CH₃CN (0.01 M). To the vial was added MnO₂ (8 equiv). The resulting dark suspension was stirred until full conversion of the starting material was observed by TLC. The reaction mixture was filtered over Celite into a new flame-dried, argon backfilled 20 mL scintillation vial using the same solvent. The magenta solution was cooled to 0 °C and the desired rhodium catalyst was added (0.01 equiv). The reaction mixture was warmed to room temperature and allowed to stir from 10 min to 12 h. The crude reaction mixture was concentrated *in vacuo* and purified by flash column chromatography to yield the desired insertion product. Diastereomeric ratios were determined by crude ¹H NMR in which conversion appeared to be greater than 90%. For known compounds, only

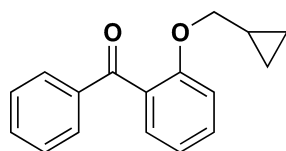
general experimentals and ^1H NMR data were reported. For novel compounds, full characterization and experimental data has been reported including isolated yields. Absolute and relative stereochemistry has been confirmed in previous work from our lab.²⁷⁻²⁹

General Procedure D for Catalyst Synthesis

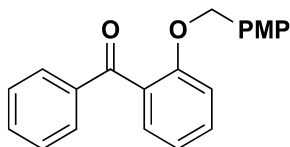
To a flame dried 50 mL round bottom flask was added $\text{Rh}_2(\text{OAc})_4$ (1 equiv) followed by the requisite ligand (4.1 equiv) and chlorobenzene. To the flask was added a 100 mL addition funnel filled with oven dried sodium bicarbonate (30 equiv). A cotton plug was placed in the stopcock in order to prevent solid from falling into the reaction. The stopcock was opened, and the reaction was heated to reflux. A heat gun was used to heat up the glass and the entire reaction vessel was wrapped in aluminum foil. If working correctly, solvent should be refluxing through the arm of the addition funnel and dripping down through the bicarbonate and back into the reaction flask. After 12 hours the reaction mixture was cooled and diluted in Ethyl Acetate (100 mL). The organic layer was washed with sat. NaHCO_3 3x25 mL and 3x with water. The aqueous layer was back extracted with 3x 25 mL of EtOAc. The organic layer was combined, dried over anhydrous Na_2SO_4 , filtered, and solvent was removed by rotary evaporation to yield the crude product.



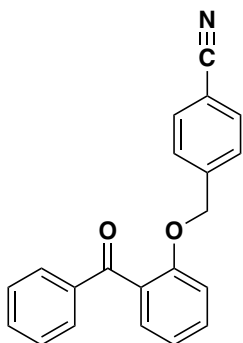
(2-(benzyloxy)phenyl)(phenyl)methanone (23) was synthesized according to general procedure A using 2- hydroxybenzophenone (500 mg, 2.5 mmol), (bromomethyl)benzene (512 mg, 3.0 mmol), Cs₂CO₃ (2.6 g, 7.5 mmol) and CH₃CN 15 mL). The crude product was purified by flash column chromatography (5:95 EtOAc:Hexanes) affording **23** as a clear oil (700 mg, 97 %). Proton NMR data matched previously reported literature values.²⁸ ¹H NMR (400 MHz, CDCl₃) δ 7.84 (d, *J* = 8.4 Hz, 2H), 7.58 (t, *J* = 7.3 Hz, 1H), 7.51 – 7.42 (m, 4H), 7.26 – 7.18 (m, 3H), 7.10 (t, *J* = 7.4 Hz, 1H), 7.05 (d, *J* = 8.7 Hz, 1H), 7.03 – 6.97 (m, 2H), 5.03 (s, 2H).



(2-(cyclopropylmethoxy)phenyl)(phenyl)methanone (21) was synthesized according to general procedure A using 2- hydroxybenzophenone 500 mg, 2.5 mmol), (bromomethyl)cyclopropane (416 mg, 3.0 mmol), Cs₂CO₃ (2 g, 7.5 mmol) and CH₃CN 20 mL). The crude product was purified by flash column chromatography (40:60 CH₂Cl₂:Hexanes) affording **21** as a yellow oil (400 mg, 63 %).¹H NMR (599 MHz, cdcl₃) δ 7.80 (d, *J* = 7.9 Hz, 2H), 7.62 – 7.49 (m, 1H), 7.49 – 7.34 (m, 4H), 7.10 – 7.00 (m, 1H), 6.94 (d, *J* = 8.3 Hz, 1H), 3.75 (d, *J* = 6.6 Hz, 2H), 0.97 – 0.76 (m, 1H), 0.34 (d, *J* = 7.9 Hz, 2H), 0.11 – -0.12 (m, 2H); ¹³C NMR (151 MHz, cdcl₃) δ 196.9, 156.8, 138.4, 132.6, 132.0, 129.8, 129.6, 129.3, 128.1, 120.7, 112.8, 72.7, 9.8, 2.7.

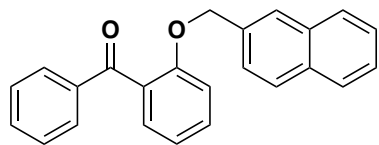


(2-((4-methoxybenzyl)oxy)phenyl)(phenyl)methanone (22) was synthesized according to general procedure A using 2-hydroxybenzophenone (1 g, 5 mmol), 1-(bromomethyl)-4-methoxybenzene (947 mg, 6 mmol), Cs_2CO_3 (4 g, 15 mmol) and CH_3CN 15 mL). The crude product was purified by flash column chromatography (40:60 CH_2Cl_2 :Hexanes) affording **22** as a clear oil (1.1 g, 72 %). Proton NMR data matched previously reported literature values.²⁸ ^1H NMR (599 MHz, CDCl_3) δ 7.80 (d, $J = 7.7$ Hz, 2H), 7.55 (t, $J = 7.5$ Hz, 1H), 7.48 – 7.38 (m, 4H), 7.12 – 6.99 (m, 2H), 6.89 (d, $J = 8.2$ Hz, 2H), 6.72 (d, $J = 8.1$ Hz, 2H), 4.92 (s, 2H), 3.75 (s, 3H).

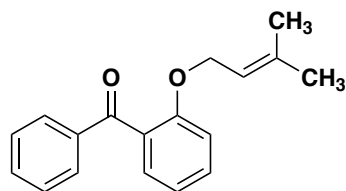


4-((2-benzoylphenoxy)methyl)benzonitrile (25) was synthesized according to general procedure A using 2-hydroxybenzophenone (2 g, 10 mmol), 4-((2-benzoylphenoxy)methyl)benzonitrile (2.3 g, 12 mmol), Cs_2CO_3 (9.6 g, 30 mmol) and CH_3CN 15 mL). The crude product was purified by flash column chromatography (15:85 EtOAc:Hexanes) affording **25** as a yellow oil (2 g, 64 %). Proton NMR data matched previously reported literature values.²⁸ ^1H NMR (400 MHz, CDCl_3) δ 7.84 (d, $J = 6.9$ Hz, 2H), 7.59 (t, $J = 7.5$ Hz, 1H), 7.56 – 7.42 (m, 6H), 7.15 (t, $J = 7.5$ Hz, 1H), 7.08 (d, $J = 8.1$

Hz, 2H), 7.02 (d, $J = 8.7$ Hz, 1H), 5.08 (s, 1H).

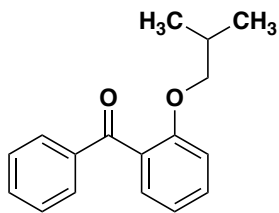


(2-(naphthalen-2-ylmethoxy)phenyl)(phenyl)methanone (18) was synthesized according to general procedure A using 2-hydroxybenzophenone (2 g, 10 mmol), 2-naphthylbromide (2.6 g, 12 mmol), Cs_2CO_3 (9.6 g, 30 mmol) and CH_3CN 15 mL. The crude product was purified by flash column chromatography (10:90 EtOAc:Hexanes) affording **18** as a clear oil (1.1 g, 33 %). ^1H NMR (599 MHz, CDCl_3) δ 7.90 – 7.84 (m, 2H), 7.80 – 7.73 (m, 1H), 7.70 – 7.62 (m, 2H), 7.60 – 7.52 (m, 1H), 7.51 – 7.41 (m, 5H), 7.38 (s, 1H), 7.13 – 7.04 (m, 3H), 5.16 (s, 2H); ^{13}C NMR (151 MHz, CDCl_3) δ 196.8, 156.4, 138.4, 133.8, 133.1, 132.9, 132.8, 132.1, 129.9, 129.8, 129.5, 128.4, 128.0, 127.9, 127.6, 126.1, 125.9, 125.4, 124.5, 121.1, 112.8, 70.2. AMM (ESI) m/z calcd for $\text{C}_{24}\text{H}_{19}\text{O}_2^+$ $[\text{M}+\text{H}]^+$ 339.1380, found 339.1381.

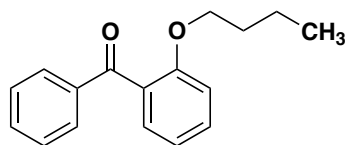


(2-((3-methylbut-2-en-1-yl)oxy)phenyl)(phenyl)methanone (24) was synthesized according to general procedure A using 2-hydroxybenzophenone (2 g, 10 mmol), 1-bromo-3-methylbut-2-ene (2 g, 12 mmol), Cs_2CO_3 (9 g, 30 mmol) and CH_3CN 15 mL. The crude product was purified by flash column chromatography (60:40 CH_2Cl_2 :Hexanes) affording **24** as a clear oil (450 mg, 17 %). Proton NMR data matched reported literature

values.²⁸ ¹H NMR (400 MHz, CDCl₃) δ 7.79 (d, *J* = 7.0 Hz, 2H), 7.54 (t, *J* = 7.4 Hz, 1H), 7.48 – 7.33 (m, 4H), 7.03 (t, *J* = 7.4 Hz, 1H), 6.98 (d, *J* = 8.3 Hz, 1H), 5.11 (t, *J* = 6.6 Hz, 1H), 4.45 (d, *J* = 6.5 Hz, 2H), 1.65 (s, 3H), 1.57 (s, 3H).

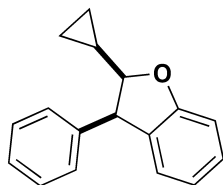


(2-isobutoxyphenyl)(phenyl)methanone (20) was synthesized according to general procedure A using 2- hydroxybenzophenone (2 g, 10 mmol), 1-bromo-2-methylpropane (1.6 g, 12 mmol), Cs₂CO₃ (9.6 mg, 30 mmol) and CH₃CN 15 mL. The crude product was purified by flash column chromatography (3:97 EtOAc:Hexanes) affording **20** as a clear oil (260 mg, 9 %). Proton NMR data matched previously reported literature values.²⁸ ¹H NMR (400 MHz, CDCl₃) δ 7.85 – 7.72 (m, 2H), 7.55 (t, *J* = 7.4 Hz, 1H), 7.50 – 7.36 (m, 4H), 7.06 (t, *J* = 7.4 Hz, 1H), 6.96 (d, *J* = 8.3 Hz, 1H), 3.66 (d, *J* = 6.2 Hz, 2H), 1.84 – 1.65 (m, 1H), 0.68 (d, *J* = 6.7 Hz, 6H).

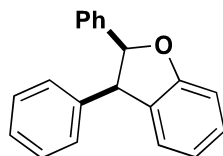


(2-butoxyphenyl)(phenyl)methanone (19) was synthesized according to general procedure A using 2- hydroxybenzophenone (2 g, 10 mmol), 1-bromobutane (1.4 g, 12 mmol), Cs₂CO₃ (9 g, 30 mmol) and CH₃CN 15 mL. The crude product was purified by flash column chromatography (10:90 EtOAc:Hexanes) affording **19** as a yellow oil (1.2 g, 47 %). Proton NMR data matched previously reported literature values²⁸. ¹H NMR (400 MHz, CDCl₃) δ 7.84 – 7.76 (m, 2H), 7.59 – 7.52 (m, 1H), 7.50 – 7.40 (m, 4H), 7.14 – 7.02

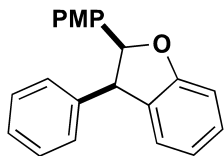
(m, 1H), 6.97 (d, $J = 8.3$ Hz, 1H), 3.89 (t, $J = 6.3$ Hz, 1H), 1.43 (p, $J = 6.3$ Hz, 2H), 1.07 (h, $J = 7.4$ Hz, 2H), 0.76 (t, $J = 7.4$ Hz, 3H).



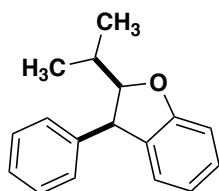
(2*R*,3*R*)-2-cyclopropyl-3-phenyl-2,3-dihydrobenzofuran (62) was synthesized by general procedure C using the requisite hydrazone (25 mg, 0.075 mmol), MnO₂ (52 mg, 0.60 mmol), and Rh₂(*R*-PTAD)₄ (1 mol%) in CH₃CN. The crude product was purified by flash column chromatography (50:50, CH₂Cl₂:hexanes) affording **62** as a white solid (16 mg, 97%, >95:5 dr). ¹H NMR (599 MHz, cdcl₃) δ 7.30 – 7.24 (m, 2H), 7.24 – 7.17 (m, 2H), 7.08 (d, $J = 7.4$ Hz, 1H), 7.04 (d, $J = 7.3$ Hz, 2H), 6.96 – 6.84 (m, 2H), 4.58 (d, $J = 8.5$ Hz, 1H), 4.11 (t, $J = 8.6$ Hz, 1H), 0.61 – 0.51 (m, 2H), 0.51 – 0.46 (m, 1H), 0.36 – 0.24 (m, 1H), 0.24 – 0.14 (m, 1H). ¹³C NMR (151 MHz, cdcl₃) δ 159.9, 140.3, 131.1, 129.2, 128.7, 128.1, 126.8, 125.8, 120.9, 109.7, 92.8, 51.5, 11.7, 4.2, 2.4.



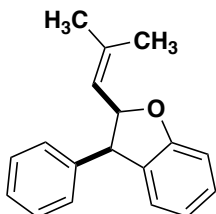
(2*S*,3*R*)-2,3-diphenyl-2,3-dihydrobenzofuran (63) was synthesized by general procedure C using the requisite hydrazone (25 mg, 0.066 mmol), MnO₂ (46 mg, 0.57 mmol), and dirhodium catalyst (1 mol%) in CH₃CN. Proton NMR data matched previously reported literature values.²⁸ ¹H NMR (400 MHz, CDCl₃) δ 7.35 – 7.26 (m, 1H), 7.18 – 7.00 (m, 10H), 7.00 – 6.93 (m, 1H), 6.79 – 6.66 (m, 2H), 6.06 (d, $J = 8.9$ Hz, 1H), 4.91 (d, $J = 8.9$ Hz, 1H).



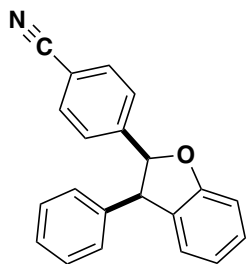
(2*S*,3*R*)-2-(4-methoxyphenyl)-3-phenyl-2,3-dihydrobenzofuran (64) was synthesized by general procedure C using the requisite hydrazone (15 mg, 0.045 mmol), MnO₂ (31 mg, 0.36 mmol), and dirhodium catalyst (1 mol%) in CH₃CN. Proton NMR data matched previously reported literature values.²⁸ ¹H NMR (400 MHz, CDCl₃) δ 7.30 – 7.23 (m, 1H), 7.10 (d, *J* = 7.4 Hz, 1H), 7.05 – 7.00 (m, 4H), 6.97 – 6.88 (m, 3H), 6.77 – 6.64 (m, 2H), 6.60 (d, *J* = 8.5 Hz, 2H), 5.97 (d, *J* = 8.8 Hz, 1H), 4.82 (d, *J* = 8.8 Hz, 1H), 3.68 (s, 3H).



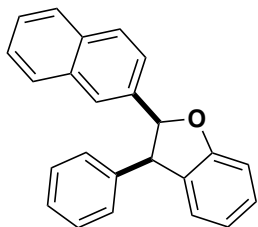
(2*R*,3*R*)-2-isopropyl-3-phenyl-2,3-dihydrobenzofuran (65) was synthesized by general procedure C using the requisite hydrazone (20 mg, 0.075 mmol), MnO₂ (52 mg, 0.6 mmol), and dirhodium catalyst (1 mol%) in CH₃CN. Proton NMR data matched previously reported literature values.²⁸ ¹H NMR (400 MHz, CDCl₃) δ 7.25 (t, *J* = 7.5 Hz, 2H), 7.24 – 7.16 (m, 2H), 7.09 – 7.02 (m, 3H), 6.94 (d, *J* = 8.0 Hz, 1H), 6.87 – 6.82 (m, 1H), 4.42 – 4.32 (m, 2H), 1.86 – 1.68 (m, 1H), 1.11 (d, *J* = 6.5 Hz, 3H), 0.78 (d, *J* = 6.5 Hz, 3H).



(2*R*,3*R*)-2-(2-methylprop-1-en-1-yl)-3-phenyl-2,3-dihydrobenzofuran (66) was synthesized by general procedure C using the requisite hydrazone (15 mg, 0.053 mmol), MnO₂ (37 mg, 0.42 mmol), and dirhodium catalyst (1 mol%) in CH₃CN. Proton NMR data matched previously reported literature values.²⁸ ¹H NMR (400 MHz, CDCl₃) δ 7.29 – 7.16 (m, 4H), 7.08 (d, *J* = 7.3 Hz, 1H), 6.98 – 6.81 (m, 4H), 5.61 (t, *J* = 8.9 Hz, 1H), 4.89 (d, *J* = 9.3 Hz, 1H), 4.54 (d, *J* = 8.5 Hz, 1H), 1.70 (s, 3H), 1.56 (s, 3H).

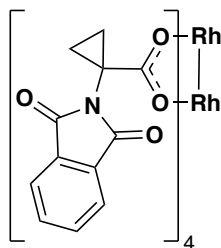


4-((2*S*,3*R*)-3-phenyl-2,3-dihydrobenzofuran-2-yl)benzonitrile (67) was synthesized by general procedure C using the requisite hydrazone (20 mg, 0.061 mmol), MnO₂ (42.5 mg, 0.49 mmol), and dirhodium catalyst (1 mol%) in CH₃CN. Proton NMR data matched previously reported literature values.²⁸ ¹H NMR (400 MHz, CDCl₃) δ 7.38 (d, *J* = 8.4 Hz, 2H), 7.31 (t, *J* = 8.2 Hz, 1H), 7.17 (d, *J* = 8.5 Hz, 2H), 7.14 – 7.01 (m, 5H), 6.99 (t, *J* = 7.4 Hz, 1H), 6.71 – 6.65 (m, 2H), 6.07 (d, *J* = 9.1 Hz, 2H), 4.97 (d, *J* = 9.1 Hz, 2H).

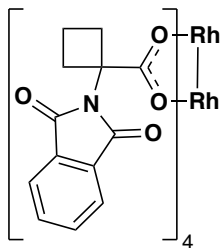


(2*S*,3*R*)-2-(naphthalen-2-yl)-3-phenyl-2,3-dihydrobenzofuran (68) was synthesized by general procedure C using the requisite hydrazone (20 mg, 0.056 mmol), MnO₂ (39.4 mg, 0.45 mmol), and Rh₂ (R-PTAD)₄ (1 mol%) in CH₃CN (isolated as a mixture of

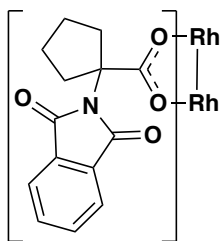
diastereomers). The crude product was purified by flash column chromatography (20:80, CH₂Cl₂:hexanes) affording **68** as a white solid (16 mg, 88%, 95:5 dr). ¹H NMR (major) (400 MHz, CD₂Cl₂) δ 7.71 – 7.65 (m, 2H), 7.62 (s, 1H), 7.50 (d, *J* = 8.5 Hz, 1H), 7.42 – 7.35 (m, 2H), 7.30 (td, *J* = 7.7, 1.4 Hz, 1H), 7.17 – 7.05 (m, 2H), 7.02 (dd, *J* = 8.5, 1.8 Hz, 1H), 6.99 – 6.87 (m, 4H), 6.77 – 6.63 (m, 2H), 6.18 (d, *J* = 8.9 Hz, 1H), 4.95 (d, *J* = 8.9 Hz, 1H).; ¹³C NMR (major) (151 MHz, cdcl₃) δ 160.5, 139.4 135.4, 133.1, 132.9, 131.0, 129.5, 129.2, 128.2, 128.1, 127.9, 127.5, 127.0, 126.4, 126.1, 126.0, 125.9, 124.8, 121.8, 110.2, 89.1, 54.2.



Rh₂(PTTCyP)₄ (46) was synthesized according to general procedure D 500 mg of the requisite ligand (2.10 mmol 8 eq), 1105mg (.26mmol 1 eq) of Rh₂(OAc)₄ and 20 ml chlorobenzene (0.1M). The product (150 mg 51%) was isolated by flash chromatography (3:97 MeOH CH₂Cl₂ as a green solid. AMM (ESI) *m/z* calcd for C₄₈H₃₂N₄O₁₆Rh₂ +, 1127.0002.,found 1127.0041

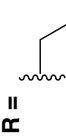
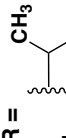
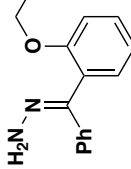
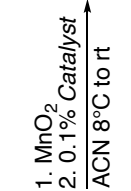
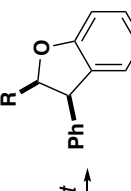





Rh₂(PTTB)₄ (47) was synthesized according to general procedure D 500 mg of the requisite ligand (2.00 mmol, 8 eq), 110 mg (.25 mmol, 1 eq) of Rh₂(OAc)₄ and 20 ml chlorobenzene (0.1M). The product (200 mg 67%) was isolated by flash chromatography (3:97 MeOH CH₂Cl₂) as a green solid. AMM (ESI) *m/z* for C₅₂H₄₀N₄O₁₆Rh₂⁺, calcd, 1183.0628., found, 1183.0536.



Rh₂(PTTP)₄ (48) was synthesized according to general procedure D 470 mg of the requisite ligand (1.81 mmol, 8 eq), 110 mg (0.25 mmol, 1 eq) of Rh₂(OAc)₄ and 20 ml chlorobenzene (0.1M). The product (250 mg 80%) was isolated by flash chromatography (3:97 MeOH CH₂Cl₂) as a green solid. AMM (ESI) *m/z* for C₅₄H₄₄N₄O₁₆Rh₂⁺, calcd, 1239.1254., found 1239.1182.

Training Set Data:

Catalyst	R = 	R = 	R = 	R = 	R = 	R = 	R = 	R = 
	d.r. (e.r.)	d.r. (e.r.)	d.r. (e.r.)	d.r. (e.r.)	d.r. (e.r.)	d.r. (e.r.)	d.r. (e.r.)	d.r. (e.r.)
cat. A	84:16	84:16	89:11 (—)	90:10 (—)	90:10 (—)	90:10 (—)	90:10 (—)	(—)
Rh ₂ (Mes) ₄	68:32	52:48	72:28 (—)	86:14 (—)	88:12 (—)	88:12 (—)	88:12 (—)	(—)
Rh ₂ (OAc) ₄	62:38	39:61	68:31 (—)	80:20 (—)	80:20 (—)	80:20 (—)	80:20 (—)	85:15
Rh ₂ (S-TCP TTL) ₄	46:54 (92:8)	50:50 (55:45)	82:18 (100:0)	100:0 (6:94)	100:0 (94:6)	100:0 (94:6)	100:0 (94:6)	(—)
Rh ₂ (R-PTAD) ₄	85:15 (97:3)	89:11 (97:3)	93:7 (100:0)	97:3 (96:4)	100:0 (99:1)	100:0 (99:1)	100:0 (94:6)	100:0 (94:6)
cat. B	72:28 (63:37)	72:28 (69:31)	85:15 (60:40)	90:10 (47:53)	87:13 (46:54)	87:13 (46:54)	87:13 (46:54)	(—)
Rh ₂ (S-BPTTL) ₄	94:6 (—)	74:26 (72:28)	(—)	94:6 (84:16)	94:6 (77:23)	94:6 (77:23)	94:6 (77:23)	(—)
Rh ₂ (S-NTTL) ₄	77:23 (90:10)	(—)	97:3 (93:7)	(—)	(—)	(—)	(—)	89:11 (80:20)
Rh ₂ (Et ₂ -Pr) ₄	(—)	(—)	(—)	(—)	(—)	(—)	(—)	94:6
Rh ₂ (t-Bu) ₄	(—)	(—)	(—)	(—)	(—)	(—)	(—)	87:13
Rh ₂ (Ph ₃) ₄	(—)	(—)	(—)	(—)	(—)	(—)	(—)	97:3
Rh ₂ (S,S,R,R-Di-OBnPhthal) ₄	(—)	(—)	(—)	(—)	(—)	(—)	(—)	96:4 (97:3)
Rh ₂ (R-BTPCP) ₄	(—)	(—)	(—)	(—)	(—)	(—)	(—)	98:2 (100:0)

- (1) Lam, Y. H.; Grayson, M. N.; Holland, M. C.; Simon, A.; Houk, K. N. *Acc. Chem. Res.* **2016**, *49*, 750–762.
- (2) Peng, Q.; Duarte, F.; Paton, R. S. *Chem. Soc. Rev.* **2016**, *45*, 6093–6107.
- (3) Roy, K.; Kar, S.; Das, R. N. *Understanding the Basics of QSAR for Applications in Pharmaceutical Sciences and Risk Assessment*.
- (4) Zahrt, A. F.; Athavale, S. V.; Denmark, S. E. *Chem. Rev.* **2020**, *120*, 1620–1689.
- (5) Lamb, K. N.; Squitieri, R. A.; Chintala, S. R.; Kwong, A. J.; Balmond, E. I.; Soldi, C.; Dmitrenko, O.; Castineira Reis, M.; Chung, R.; Addison, J. B.; et al. *Chemistry (Easton)*. **2017**, *23*, 11843–11855.
- (6) Laconsay, C. J.; Pla-Quintana, A.; Tantillo, D. J. *Organometallics* **2021**, *40*, 4120–4132.
- (7) Hammett, L. P. *J. Chem. Phys.* **1936**, *4*, 613–617.
- (8) Miller, J. J.; Sigman, M. S. *Angew. Chemie - Int. Ed.* **2008**, *47*, 771–774.
- (9) Brethomé, A. V.; Fletcher, S. P.; Paton, R. S. *ACS Catal.* **2019**, *9*, 2313–2323.
- (10) Miao, W.; Gao, Y.; Li, X.; Gao, Y.; Tang, G.; Zhao, Y. *Adv. Synth. Catal.* **2012**, *354*, 2659–2664.
- (11) Falivene, L.; Credendino, R.; Poater, A.; Petta, A.; Serra, L.; Oliva, R.; Scarano, V.; Cavallo, L. *Organometallics* **2016**, *35*, 2286–2293.
- (12) Cammarota, R. C.; Liu, W.; Bacsa, J.; Davies, H. M. L.; Sigman, M. S. *J. Am. Chem. Soc.* **2022**, *144*, 1881–1898.
- (13) Pettersen, E. F.; Goddard, T. D.; Huang, C. C.; Meng, E. C.; Couch, G. S.; Croll, T. I.; Morris, J. H.; Ferrin, T. E. *Protein Sci.* **2021**, *30*, 70–82.

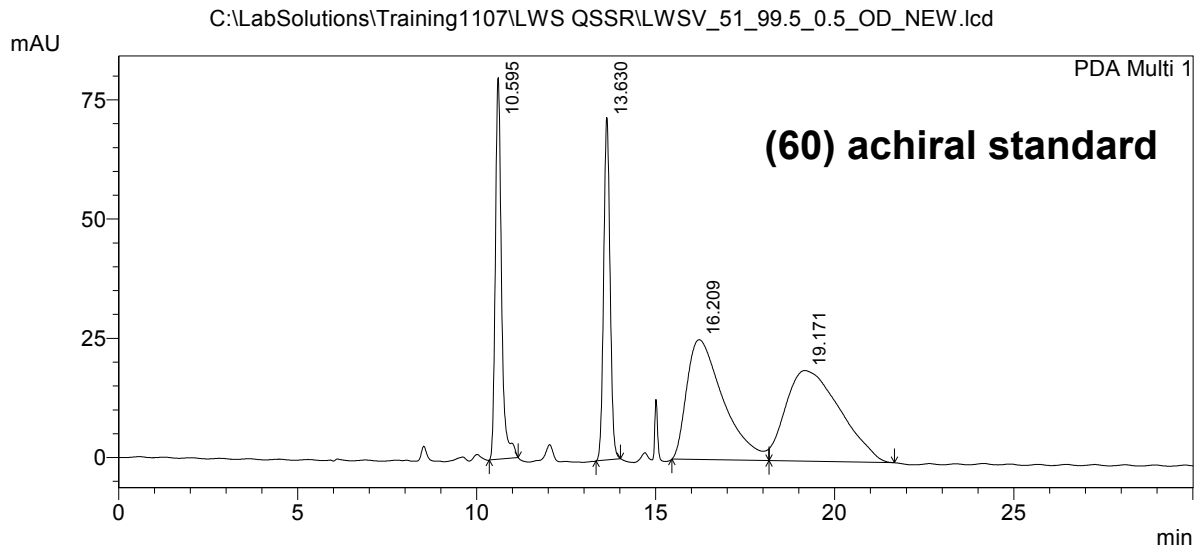
- (14) Davies, H. M. L.; Beckwith, R. E. J. *Chem. Rev.* **2003**, *103*, 2861–2904.
- (15) Becke, A. D. *Phys. Rev. A* **1988**, *38*, 3098–3100.
- (16) Weigend, F. *Phys. Chem. Chem. Phys.* **2006**, *8*, 1057–1065.
- (17) Laun, J.; Vilela Oliveira, D.; Bredow, T. *J. Comput. Chem.* **2018**, *39*, 1285–1290.
- (18) Mitin, A. V.; Merz Jr., K. M. *Int. J. Quantum Chem.* **2007**, *107*, 3028–3038.
- (19) Roy, L. E.; Hay, P. J.; Martin, R. L. *J. Chem. Theory Comput.* **2008**, *4*, 1029–1031.
- (20) Goerigk, L.; Grimme, S. *J. Chem. Phys.* **2010**, *132*.
- (21) Wang, Y.; Verma, P.; Jin, X.; Truhlar, D. G.; He, X. *Proc. Natl. Acad. Sci. U. S. A.* **2018**, *115*, 10257–10262.
- (22) Hehre, W. J.; Ditchfield, R.; Pople, J. A. *J. Chem. Phys.* **1972**, *56*, 2257–2261.
- (23) Zhao, Y.; Truhlar, D. G. *Theor. Chem. Acc.* **2008**, *120*, 215–241.
- (24) Frady G. Adly, Johncarlo Maddalena, A. G. **2011**, *43*, 34–43.
- (25) DeAngelis, A.; Panish, R.; Fox, J. M. *Acc. Chem. Res.* **2016**, *49*, 115–127.
- (26) Mattiza, J. T.; Fohrer, J. G. G.; Duddeck, H.; Gardiner, M. G.; Ghanem, A. *Org. Biomol. Chem.* **2011**, *9*, 6542–6550.
- (27) Bergstrom, B. D.; Nickerson, L. A.; Shaw, J. T.; Souza, L. W. **2021**, 6940–6954.
- (28) Soldi, C.; Lamb, K. N.; Squitieri, R. A.; González-López, M.; Di Maso, M. J.; Shaw, J. T. *J. Am. Chem. Soc.* **2014**, *136*, 15142–15145.
- (29) Lamb, K. N.; Squitieri, R. A.; Chintala, S. R.; Kwong, A. J.; Balmond, E. I.; Soldi, C.; Dmitrenko, O.; Castiñeira Reis, M.; Chung, R.; Addison, J. B.; et al. *Chem. - A Eur. J.* **2017**, *23*, 11843–11855.

==== HPLC Analysis Report ====

C:\LabSolutions\Training1107\LWS QSSR\LWSV_51_99.5_0.5_OD_NEW.lcd

Acquired by : Admin
 Sample Name : 1
 Sample ID : 1
 Tray# : 1
 Vial # : 46
 Injection Volume : 7 uL
 Data File Name : LWSV_51_99.5_0.5_OD_NEW.lcd
 Method File Name : OD-95_5_Hexane_IPA_30min_0.5mLmin.lcm
 Batch File Name : batch file 3.lcb
 Report File Name : UCD Default.lcr
 Data Acquired : 8/14/2006 3:37:27 AM
 Data Processed : 8/14/2006 4:07:29 AM

<Chromatogram>



< Peak Table >

PeakTable C:\LabSolutions\Training1107\LWS QSSR\LWSV_51_99.5_0.5_OD_NEW.lcd
 PDA Ch1 283nm 4nm

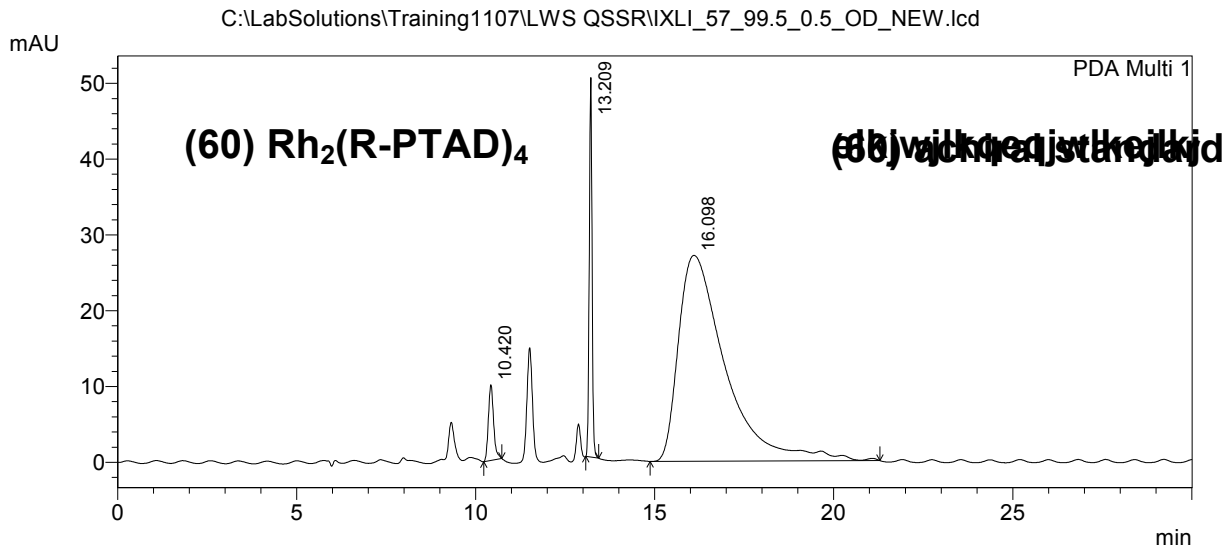
Peak#	Ret. Time	Area	Height	Area %	Height %
1	10.595	956370	80014	16.979	40.821
2	13.630	890262	71866	15.805	36.664
3	16.209	1786250	25117	31.712	12.814
4	19.171	1999847	19014	35.504	9.700
Total		5632728	196011	100.000	100.000



==== HPLC Analysis Report ====

Acquired by : Admin
 Sample Name : 1
 Sample ID : 1
 Tray# : 1
 Vail # : 95
 Injection Volume : 15 uL
 Data File Name : IXLI_57_99.5_0.5_OD_NEW.lcd
 Method File Name : OD-95_5_Hexane_IPA_30min_0.5mLmin.lcm
 Batch File Name : batch file 3.lcb
 Report File Name : UCD Default.lcr
 Data Acquired : 8/14/2006 5:04:41 AM
 Data Processed : 8/14/2006 5:34:44 AM

<Chromatogram>



< Peak Table >

PeakTable C:\LabSolutions\Training1107\LWS QSSR\IXLI_57_99.5_0.5_OD_NEW.lcd

PDA Ch1 275nm 4nm

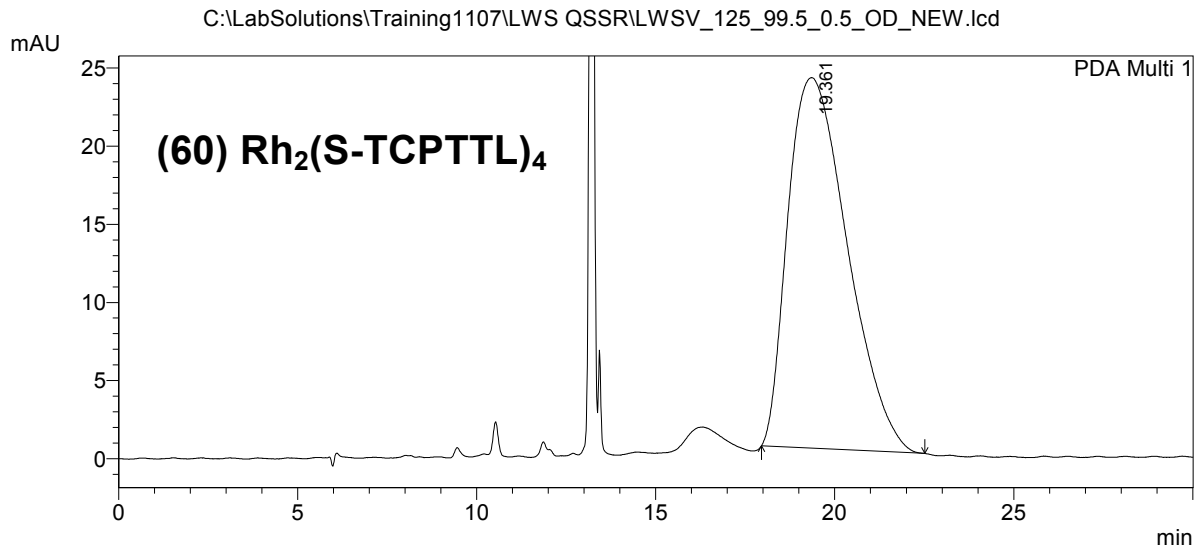
Peak#	Ret. Time	Area	Height	Area %	Height %
1	10.420	101256	9991	3.547	11.454
2	13.209	272162	50056	9.535	57.383
3	16.098	2480965	27185	86.918	31.164
Total		2854383	87232	100.000	100.000

==== HPLC Analysis Report ====

C:\LabSolutions\Training1107\LWS QSSR\LWSV_125_99.5_0.5_OD_NEW.lcd

Acquired by : Admin
 Sample Name : 1
 Sample ID : 1
 Tray# : 1
 Vial # : 96
 Injection Volume : 15 uL
 Data File Name : LWSV_125_99.5_0.5_OD_NEW.lcd
 Method File Name : OD-95_5_Hexane_IPA_30min_0.5mLmin.lcm
 Batch File Name : batch file 3.lcb
 Report File Name : UCD Default.lcr
 Data Acquired : 8/14/2006 7:49:42 AM
 Data Processed : 8/14/2006 8:19:44 AM

<Chromatogram>



< Peak Table >

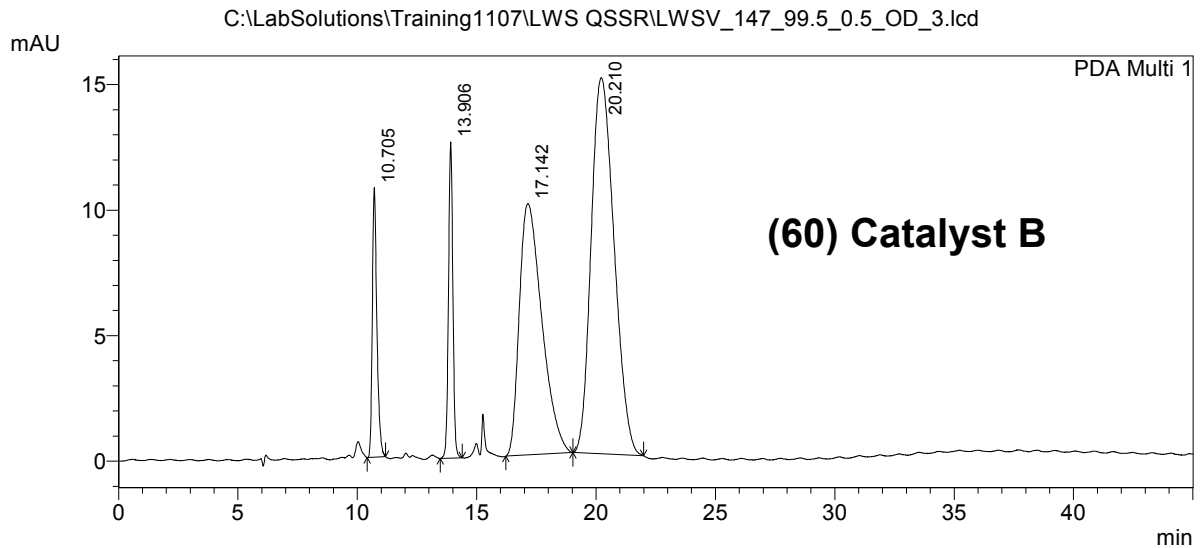
PeakTable C:\LabSolutions\Training1107\LWS QSSR\LWSV_125_99.5_0.5_OD_NEW.lcd
 PDA Ch1 291nm 4nm

Peak#	Ret. Time	Area	Height	Area %	Height %
1	19.361	2746210	23694	100.000	100.000
Total		2746210	23694	100.000	100.000

==== HPLC Analysis Report ====

C:\LabSolutions\Training1107\LWS QSSR\LWSV_147_99.5_0.5_OD_3.lcd
 Acquired by : Admin
 Sample Name : 1
 Sample ID : 1
 Tray# : 1
 Vial # : 44
 Injection Volume : 7 uL
 Data File Name : LWSV_147_99.5_0.5_OD_3.lcd
 Method File Name : OD-95_5_Hexane_IPA_45min_0.5mL.lcm
 Batch File Name : batch file 3.lcb
 Report File Name : UCD Default.lcr
 Data Acquired : 8/14/2006 1:16:56 AM
 Data Processed : 8/14/2006 2:01:58 AM

<Chromatogram>



< Peak Table >

PeakTable C:\LabSolutions\Training1107\LWS QSSR\LWSV_147_99.5_0.5_OD_3.lcd

PDA Ch1 292nm 4nm

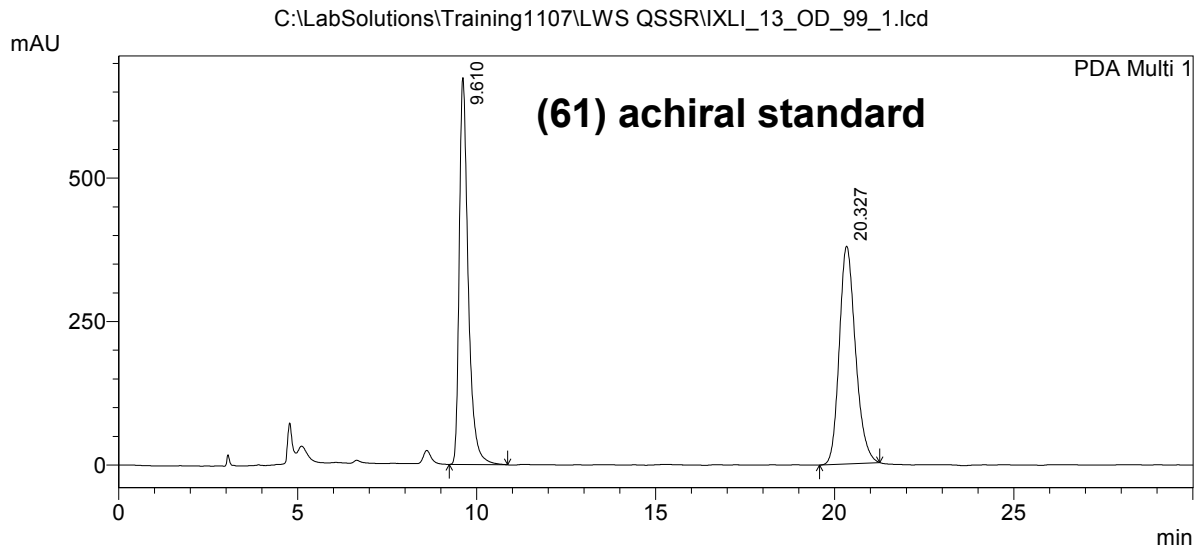
Peak#	Ret. Time	Area	Height	Area %	Height %
1	10.705	142306	10747	7.249	22.239
2	13.906	161265	12587	8.215	26.046
3	17.142	656802	10012	33.459	20.717
4	20.210	1002611	14981	51.076	30.999
Total		1962983	48326	100.000	100.000

==== HPLC Analysis Report ====

C:\LabSolutions\Training1107\LWS QSSR\IXLI_13_OD_99_1.lcd

Acquired by : Admin
 Sample Name : 1
 Sample ID : 1
 Tray# : 1
 Vial # : 65
 Injection Volume : 7 uL
 Data File Name : IXLI_13_OD_99_1.lcd
 Method File Name : OD-90_10_Hexane_IPA_30min.lcm
 Batch File Name : 09-27-2021-2npibusi-o-siphme2-enriched-98hex-08mlpermin.lcb
 Report File Name : UCD Default.lcr
 Data Acquired : 7/1/2006 3:03:09 AM
 Data Processed : 7/1/2006 3:33:11 AM

<Chromatogram>



< Peak Table >

PeakTable C:\LabSolutions\Training1107\LWS QSSR\IXLI_13_OD_99_1.lcd

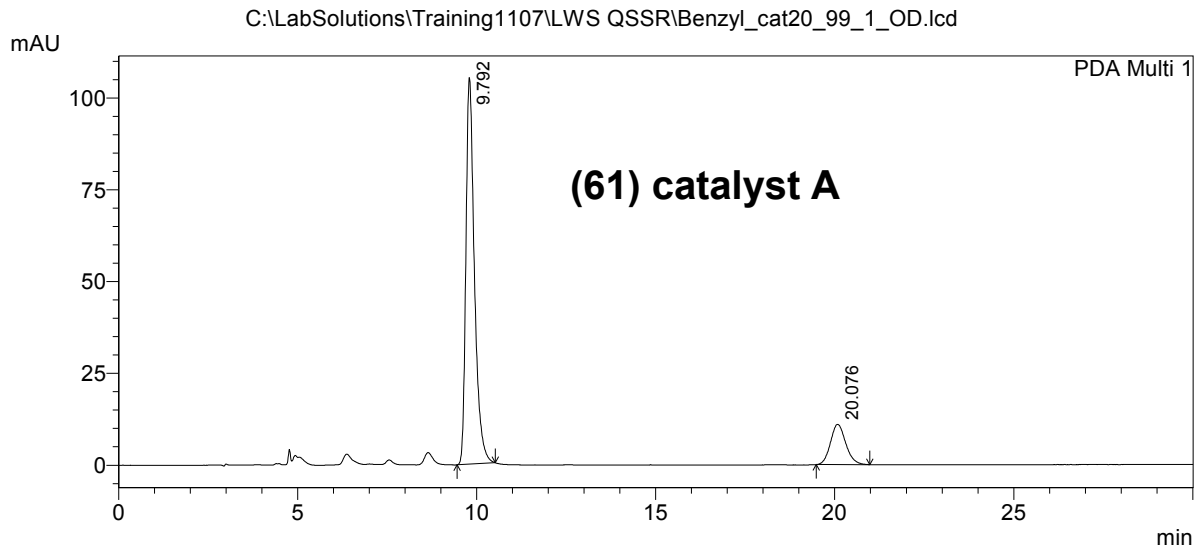
PDA Ch1 205nm 4nm

Peak#	Ret. Time	Area	Height	Area %	Height %
1	9.610	11708683	674224	49.538	63.963
2	20.327	11926950	379859	50.462	36.037
Total		23635633	1054082	100.000	100.000

==== HPLC Analysis Report ====

C:\LabSolutions\Training1107\LWS QSSR\Benzyl_cat20_99_1_OD.lcd
 Acquired by : Admin
 Sample Name : 1
 Sample ID : 1
 Tray# : 1
 Vial # : 58
 Injection Volume : 10 uL
 Data File Name : Benzyl_cat20_99_1_OD.lcd
 Method File Name : OD-90_10_Hexane_IPA_30min.lcm
 Batch File Name : batch file 3.lcb
 Report File Name : UCD Default.lcr
 Data Acquired : 8/13/2006 3:06:59 AM
 Data Processed : 8/13/2006 3:37:01 AM

<Chromatogram>



< Peak Table >

PeakTable C:\LabSolutions\Training1107\LWS QSSR\Benzyl_cat20_99_1_OD.lcd

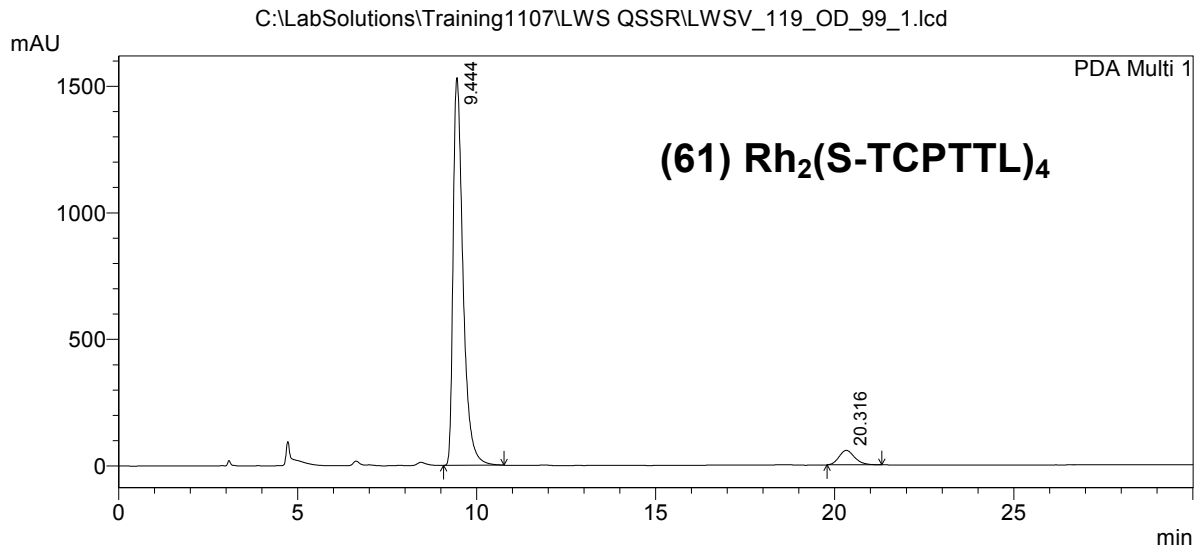
PDA Ch1 280nm 4nm

Peak#	Ret. Time	Area	Height	Area %	Height %
1	9.792	1739560	105248	84.209	90.559
2	20.076	326213	10973	15.791	9.441
Total		2065773	116220	100.000	100.000

==== HPLC Analysis Report ====

Acquired by : Admin
 Sample Name : 1
 Sample ID : 1
 Tray# : 1
 Vial # : 79
 Injection Volume : 7 uL
 Data File Name : LWSV_119_OD_99_1.lcd
 Method File Name : OD-90_10_Hexane_IPA_30min.lcm
 Batch File Name : 09-27-2021-2npibusi-o-siphme2-enriched-98hex-08mlpermin.lcb
 Report File Name : UCD Default.lcr
 Data Acquired : 6/29/2006 9:30:29 PM
 Data Processed : 6/29/2006 10:00:31 PM

<Chromatogram>



< Peak Table >

PeakTable C:\LabSolutions\Training1107\LWS QSSR\LWSV_119_OD_99_1.lcd

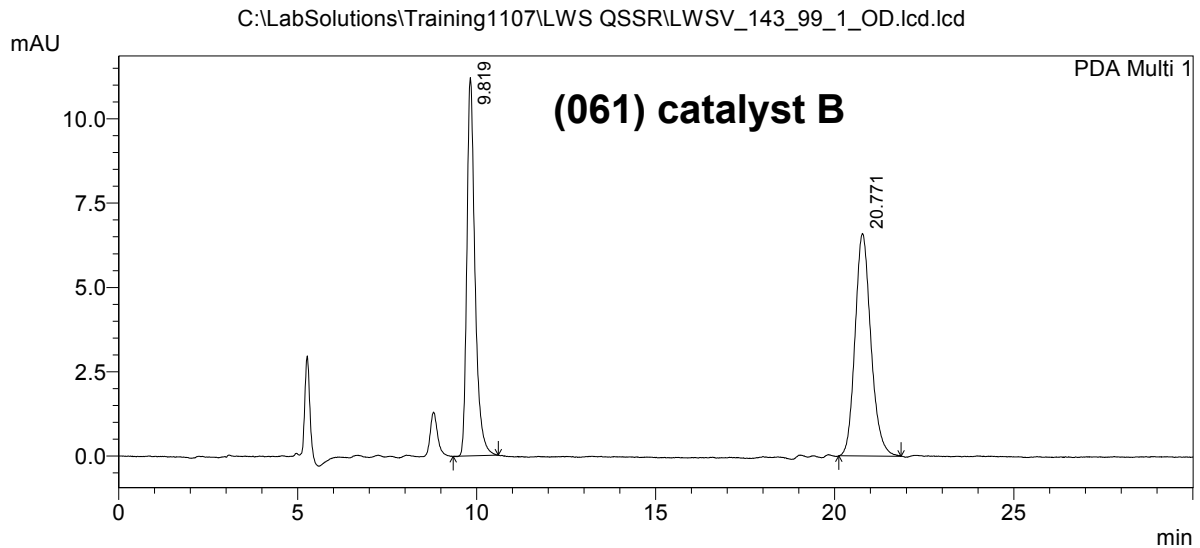
PDA Ch1 205nm 4nm

Peak#	Ret. Time	Area	Height	Area %	Height %
1	9.444	29419574	1531498	94.415	96.396
2	20.316	1740304	57254	5.585	3.604
Total		31159878	1588752	100.000	100.000

==== HPLC Analysis Report ====

C:\LabSolutions\Training1107\LWS QSSR\LWSV_143_99_1_OD.lcd.lcd
 Acquired by : Admin
 Sample Name : 1
 Sample ID : 1
 Tray# : 1
 Vial # : 63
 Injection Volume : 1 uL
 Data File Name : LWSV_143_99_1_OD.lcd.lcd
 Method File Name : OD-90_10_Hexane_IPA_30min.lcm
 Batch File Name : 09-27-2021-2npibusi-o-siphme2-enriched-98hex-08mlpermin.lcb
 Report File Name : UCD Default.lcr
 Data Acquired : 7/16/2006 2:15:25 AM
 Data Processed : 7/16/2006 2:45:27 AM

<Chromatogram>



< Peak Table >

PeakTable C:\LabSolutions\Training1107\LWS QSSR\LWSV_143_99_1_OD.lcd.lcd

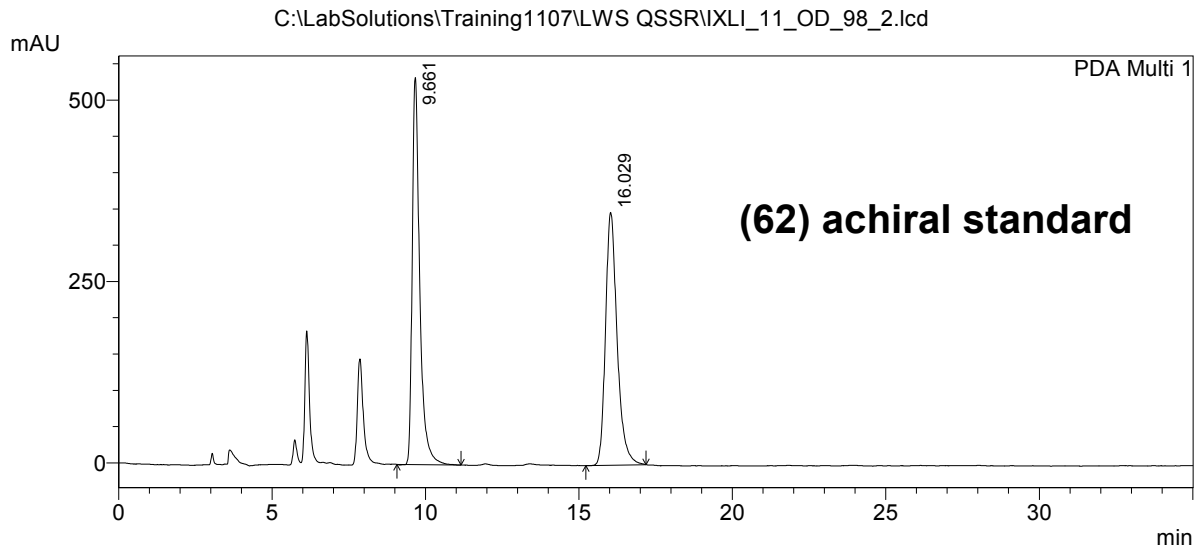
PDA Ch1 281nm 4nm

Peak#	Ret. Time	Area	Height	Area %	Height %
1	9.819	176293	11216	46.546	62.960
2	20.771	202459	6598	53.454	37.040
Total		378752	17814	100.000	100.000

==== HPLC Analysis Report ====

C:\LabSolutions\Training1107\LWS QSSR\IXLI_11_OD_98_2.lcd
 Acquired by : Admin
 Sample Name : 1
 Sample ID : 1
 Tray# : 1
 Vial # : 77
 Injection Volume : 7 uL
 Data File Name : IXLI_11_OD_98_2.lcd
 Method File Name : OD-80_20_Hexane_IPA_35min.lcm
 Batch File Name : 09-27-2021-2npibusi-o-siphme2-enriched-98hex-08mlpermin.lcb
 Report File Name : UCD Default.lcr
 Data Acquired : 7/1/2006 2:16:24 AM
 Data Processed : 7/1/2006 2:51:28 AM

<Chromatogram>



< Peak Table >

PeakTable C:\LabSolutions\Training1107\LWS QSSR\IXLI_11_OD_98_2.lcd

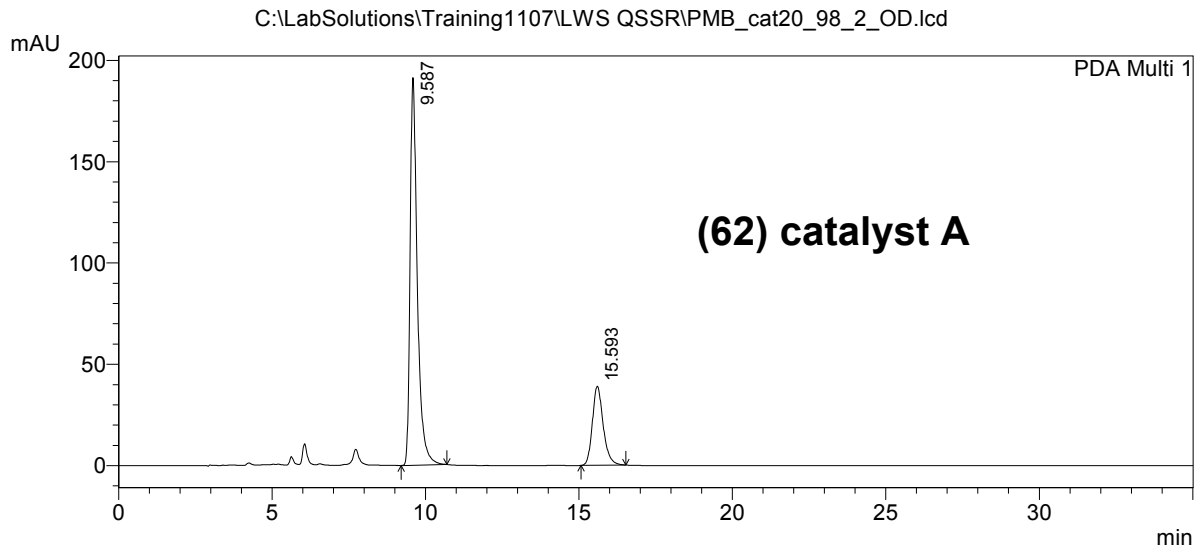
PDA Ch1 200nm 4nm

Peak#	Ret. Time	Area	Height	Area %	Height %
1	9.661	9052753	533214	49.668	60.474
2	16.029	9173857	348517	50.332	39.526
Total		18226611	881731	100.000	100.000

==== HPLC Analysis Report ====

C:\LabSolutions\Training1107\LWS QSSR\PMB_cat20_98_2_OD.lcd
 Acquired by : Admin
 Sample Name : 1
 Sample ID : 1
 Tray# : 1
 Vial # : 57
 Injection Volume : 10 uL
 Data File Name : PMB_cat20_98_2_OD.lcd
 Method File Name : OD-80_20_Hexane_IPA_35min.lcm
 Batch File Name : batch file 3.lcb
 Report File Name : UCD Default.lcr
 Data Acquired : 8/13/2006 2:21:19 AM
 Data Processed : 8/13/2006 2:56:21 AM

<Chromatogram>



< Peak Table >

PeakTable C:\LabSolutions\Training1107\LWS QSSR\PMB_cat20_98_2_OD.lcd

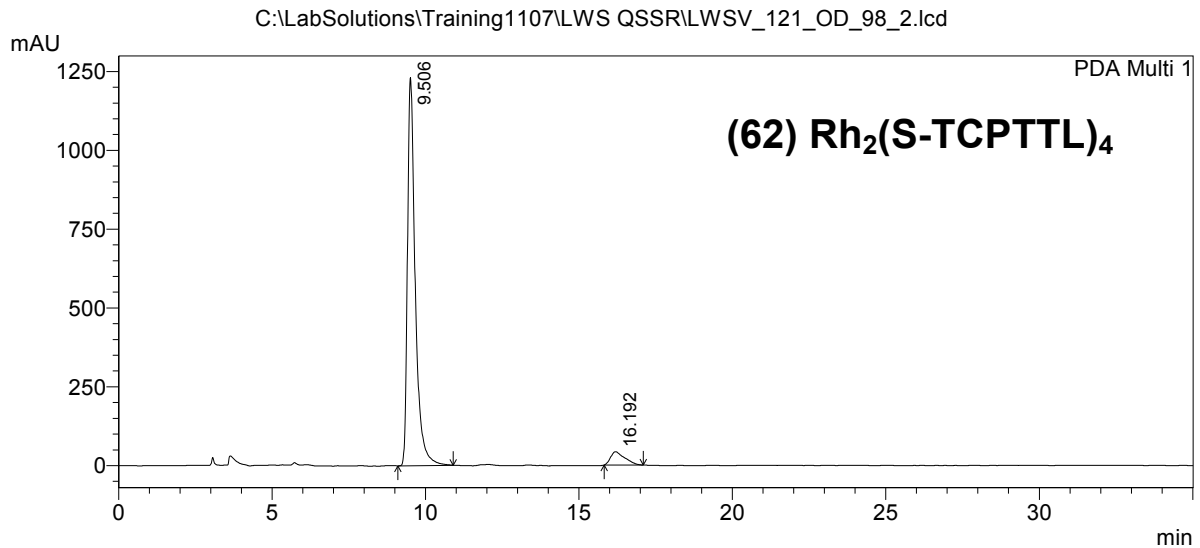
PDA Ch1 280nm 4nm

Peak#	Ret. Time	Area	Height	Area %	Height %
1	9.587	3137362	191265	76.605	83.056
2	15.593	958119	39019	23.395	16.944
Total		4095481	230284	100.000	100.000

==== HPLC Analysis Report ====

C:\LabSolutions\Training1107\LWS QSSR\LWSV_121_OD_98_2.lcd
 Acquired by : Admin
 Sample Name : 1
 Sample ID : 1
 Tray# : 1
 Vial # : 80
 Injection Volume : 7 uL
 Data File Name : LWSV_121_OD_98_2.lcd
 Method File Name : OD-80_20_Hexane_IPA_35min.lcm
 Batch File Name : 09-27-2021-2npibusi-o-siphme2-enriched-98hex-08mlpermin.lcb
 Report File Name : UCD Default.lcr
 Data Acquired : 6/29/2006 10:11:07 PM
 Data Processed : 6/29/2006 10:46:09 PM

<Chromatogram>



< Peak Table >

PeakTable C:\LabSolutions\Training1107\LWS QSSR\LWSV_121_OD_98_2.lcd

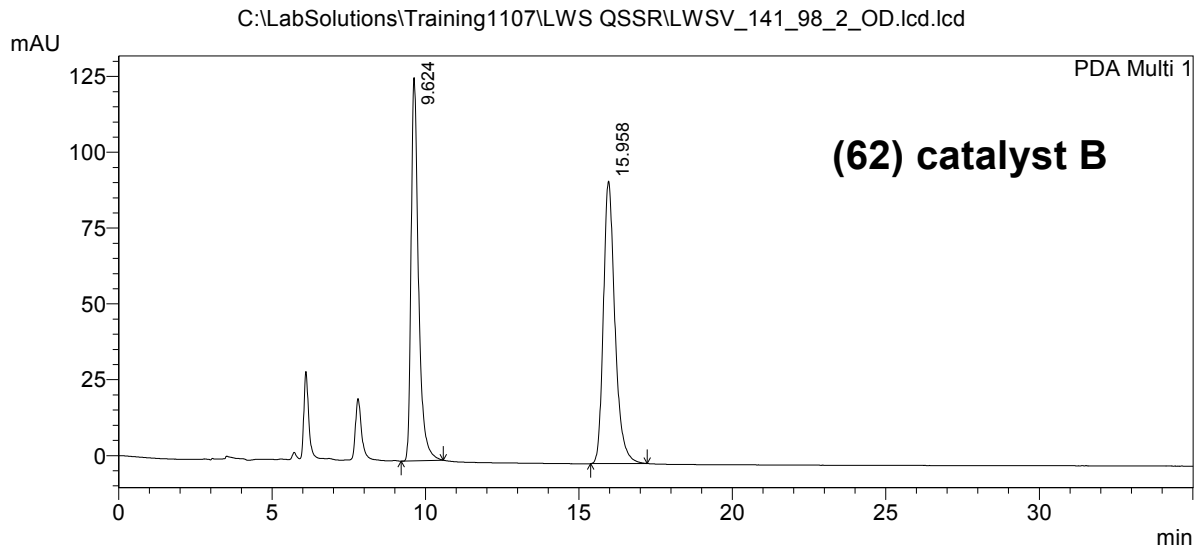
PDA Ch1 205nm 4nm

Peak#	Ret. Time	Area	Height	Area %	Height %
1	9.506	21729979	1230548	94.153	96.690
2	16.192	1349532	42121	5.847	3.310
Total		23079511	1272670	100.000	100.000

==== HPLC Analysis Report ====

C:\LabSolutions\Training1107\LWS QSSR\LWSV_141_98_2_OD.lcd.lcd
 Acquired by : Admin
 Sample Name : 1
 Sample ID : 1
 Tray# : 1
 Vail # : 62
 Injection Volume : 10 uL
 Data File Name : LWSV_141_98_2_OD.lcd.lcd
 Method File Name : OD-80_20_Hexane_IPA_35min.lcm
 Batch File Name : 09-27-2021-2npibusi-o-siphme2-enriched-98hex-08mlpermin.lcb
 Report File Name : UCD Default.lcr
 Data Acquired : 7/16/2006 1:29:46 AM
 Data Processed : 7/16/2006 2:04:50 AM

<Chromatogram>



< Peak Table >

PeakTable C:\LabSolutions\Training1107\LWS QSSR\LWSV_141_98_2_OD.lcd.lcd

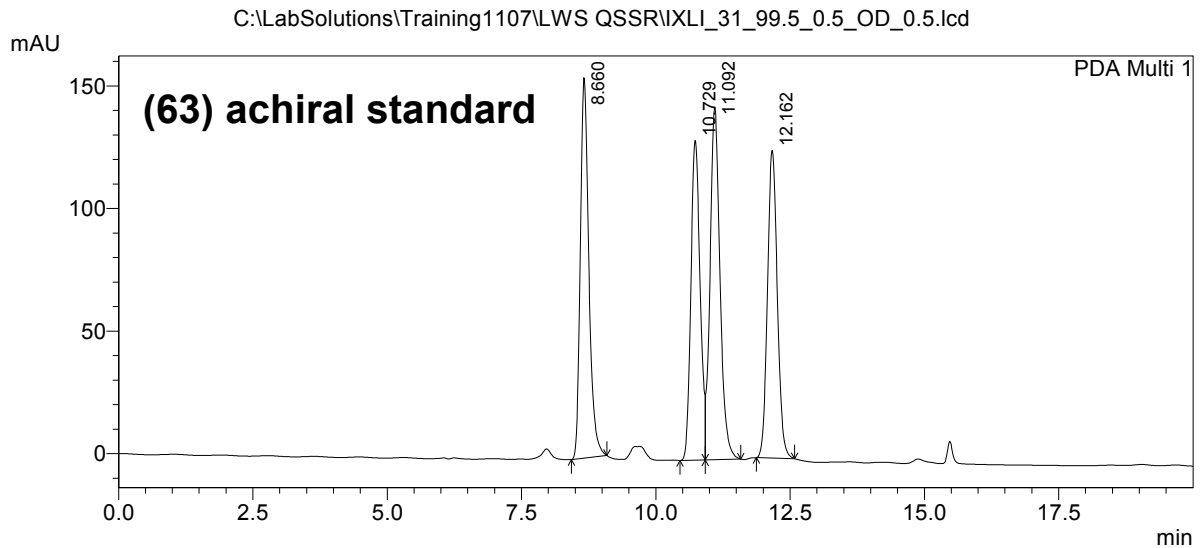
PDA Ch1 281nm 4nm

Peak#	Ret. Time	Area	Height	Area %	Height %
1	9.624	2117866	126366	46.495	57.569
2	15.958	2437177	93136	53.505	42.431
Total		4555044	219502	100.000	100.000

==== HPLC Analysis Report ====

C:\LabSolutions\Training1107\LWS QSSR\IXLI_31_99.5_0.5_OD_0.5.lcd
 Acquired by : Admin
 Sample Name : 1
 Sample ID : 1
 Tray# : 1
 Vial # : 66
 Injection Volume : 7 uL
 Data File Name : IXLI_31_99.5_0.5_OD_0.5.lcd
 Method File Name : OD-95_5_Hexane_IPA_20min_0.5mL.lcm
 Batch File Name : 09-27-2021-2npibusi-o-siphme2-enriched-98hex-08mlpermin.lcb
 Report File Name : UCD Default.lcr
 Data Acquired : 7/1/2006 8:36:02 PM
 Data Processed : 7/1/2006 8:56:04 PM

<Chromatogram>



1 PDA Multi 1/280nm 4nm

< Peak Table >

PeakTable C:\LabSolutions\Training1107\LWS QSSR\IXLI_31_99.5_0.5_OD_0.5.lcd

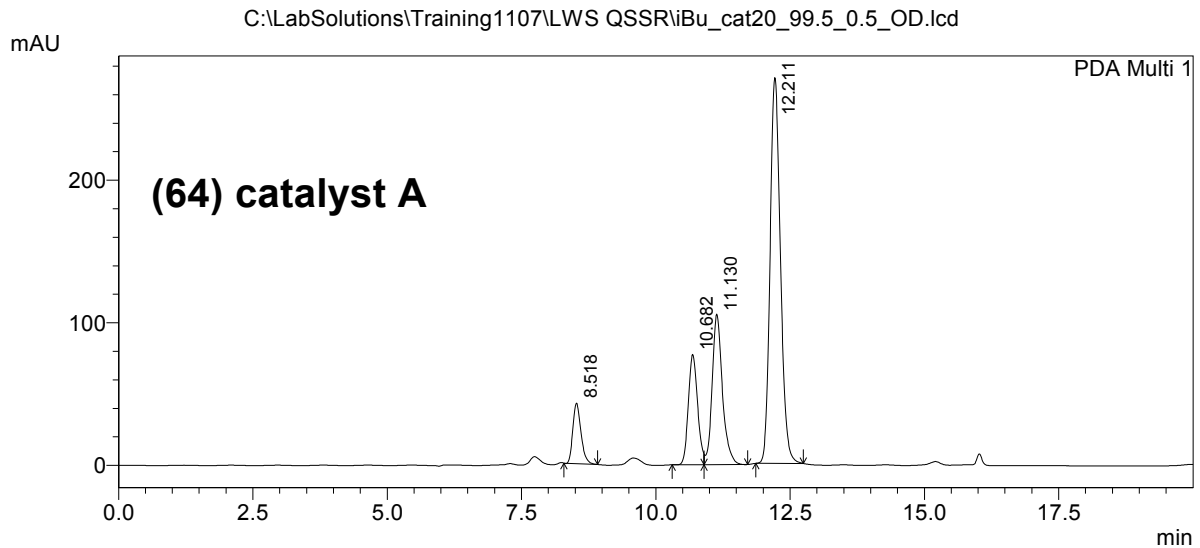
PDA Ch1 280nm 4nm

Peak#	Ret. Time	Area	Height	Area %	Height %
1	8.660	1715425	155247	25.542	27.969
2	10.729	1559107	130416	23.215	23.495
3	11.092	1845654	143849	27.481	25.915
4	12.162	1595870	125561	23.762	22.621
Total		6716056	555073	100.000	100.000

==== HPLC Analysis Report ====

C:\LabSolutions\Training1107\LWS QSSR\iBu_cat20_99.5_0.5_OD.lcd
 Acquired by : Admin
 Sample Name : 1
 Sample ID : 1
 Tray# : 1
 Vial # : 59
 Injection Volume : 10 uL
 Data File Name : iBu_cat20_99.5_0.5_OD.lcd
 Method File Name : OD-95_5_Hexane_IPA_20min_0.5mL.lcm
 Batch File Name : batch file 3.lcb
 Report File Name : UCD Default.lcr
 Data Acquired : 8/13/2006 3:47:38 AM
 Data Processed : 8/13/2006 4:07:40 AM

<Chromatogram>



< Peak Table >

PeakTable C:\LabSolutions\Training1107\LWS QSSR\iBu_cat20_99.5_0.5_OD.lcd

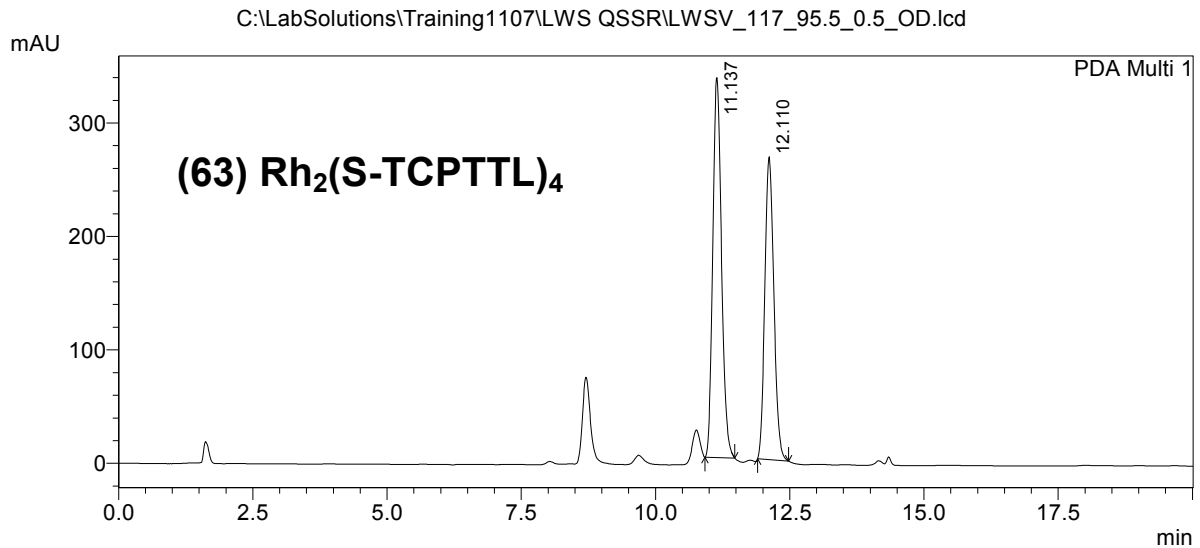
PDA Ch1 281nm 4nm

Peak#	Ret. Time	Area	Height	Area %	Height %
1	8.518	449453	42557	7.014	8.579
2	10.682	927889	77376	14.479	15.599
3	11.130	1405154	105556	21.927	21.280
4	12.211	3625856	270542	56.580	54.541
Total		6408351	496031	100.000	100.000

==== HPLC Analysis Report ====

Acquired by : Admin
 Sample Name : 1
 Sample ID : 1
 Tray# : 1
 Vial # : 78
 Injection Volume : 7 uL
 Data File Name : LWSV_117_95.5_0.5_OD.lcd
 Method File Name : OD-95_5_Hexane_IPA_20min_0.5mL.lcm
 Batch File Name : 09-27-2021-2npibusi-o-siphme2-enriched-98hex-08mlpermin.lcb
 Report File Name : UCD Default.lcr
 Data Acquired : 7/1/2006 10:24:16 PM
 Data Processed : 7/1/2006 10:44:18 PM

<Chromatogram>



1 PDA Multi 1/280nm 4nm

< Peak Table >

PeakTable C:\LabSolutions\Training1107\LWS QSSR\LWSV_117_95.5_0.5_OD.lcd

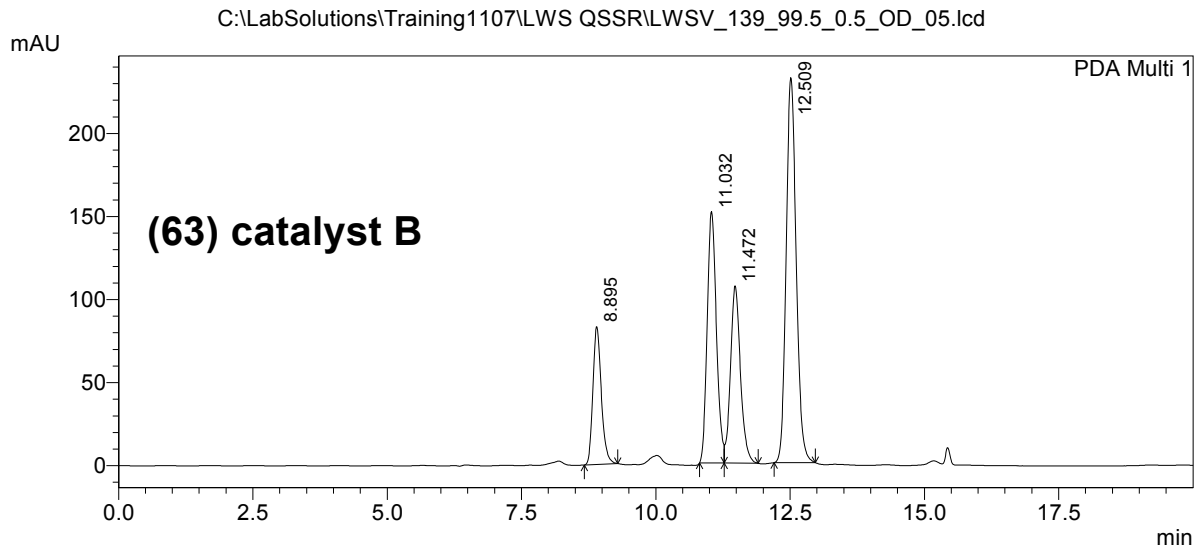
PDA Ch1 280nm 4nm

Peak#	Ret. Time	Area	Height	Area %	Height %
1	11.137	3788188	334828	54.743	55.630
2	12.110	3131714	267057	45.257	44.370
Total		6919902	601885	100.000	100.000

==== HPLC Analysis Report ====

C:\LabSolutions\Training1107\LWS QSSR\LWSV_139_99.5_0.5_OD_05.lcd
 Acquired by : Admin
 Sample Name : 1
 Sample ID : 1
 Tray# : 1
 Vial # : 41
 Injection Volume : 10 uL
 Data File Name : LWSV_139_99.5_0.5_OD_05.lcd
 Method File Name : OD-95_5_Hexane_IPA_20min_0.5mL.lcm
 Batch File Name : batch file 3.lcb
 Report File Name : UCD Default.lcr
 Data Acquired : 8/12/2006 4:20:11 AM
 Data Processed : 8/12/2006 4:40:13 AM

<Chromatogram>



< Peak Table >

PeakTable C:\LabSolutions\Training1107\LWS QSSR\LWSV_139_99.5_0.5_OD_05.lcd

PDA Ch1 280nm 4nm

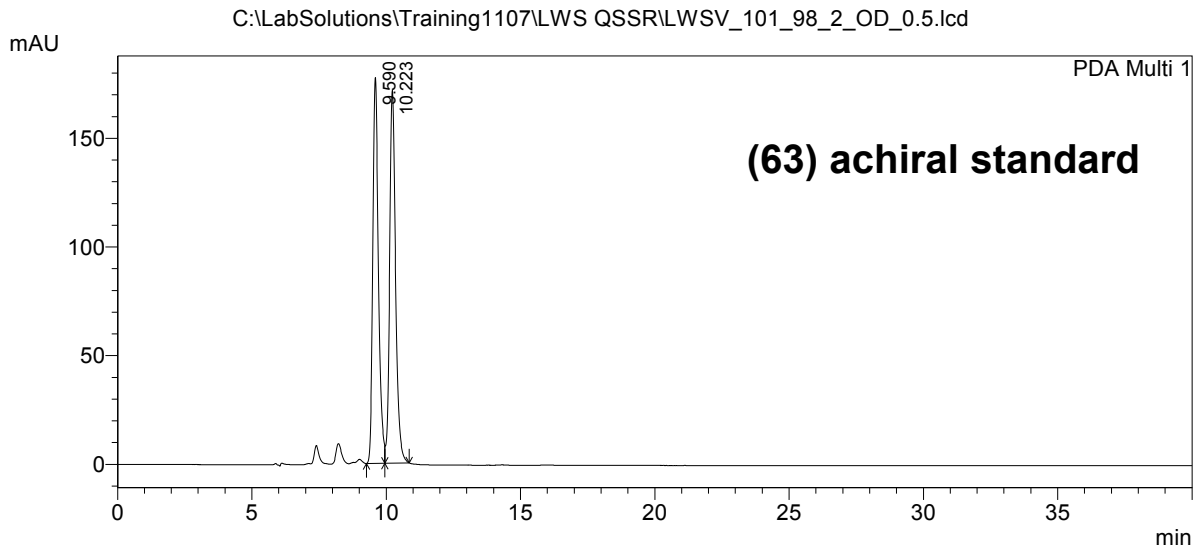
Peak#	Ret. Time	Area	Height	Area %	Height %
1	8.895	907974	82950	12.775	14.481
2	11.032	1810264	151345	25.471	26.420
3	11.472	1377218	106784	19.378	18.641
4	12.509	3011803	231753	42.376	40.457
Total		7107259	572832	100.000	100.000



==== HPLC Analysis Report ====

Acquired by : Admin
 Sample Name : 1
 Sample ID : 1
 Tray# : 1
 Vail # : 64
 Injection Volume : 10 uL
 Data File Name : LWSV_101_98_2_OD_0.5.lcd
 Method File Name : OD-50_50_Hexane_IPA_40min_0.5mLmin.lcm
 Batch File Name : batch file 3.lcb
 Report File Name : UCD Default.lcr
 Data Acquired : 8/17/2006 1:30:39 AM
 Data Processed : 8/17/2006 9:54:25 PM

<Chromatogram>



1 PDA Multi 1/280nm 4nm

< Peak Table >

PeakTable C:\LabSolutions\Training1107\LWS QSSR\LWSV_101_98_2_OD_0.5.lcd

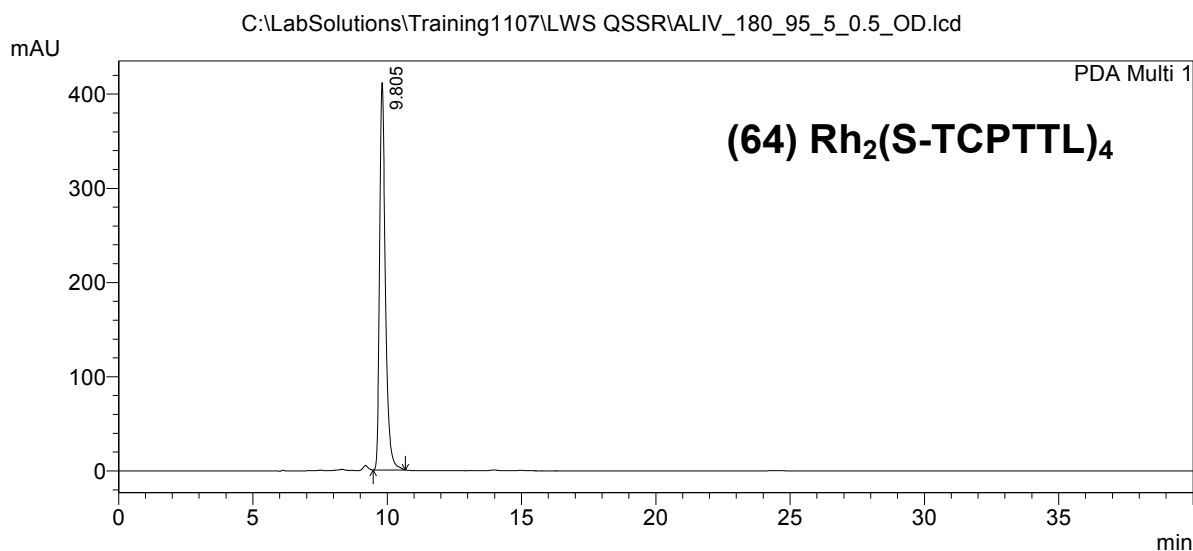
PDA Ch1 280nm 4nm

Peak#	Ret. Time	Area	Height	Area %	Height %
1	9.590	2583947	177448	49.459	50.854
2	10.223	2640428	171489	50.541	49.146
Total		5224375	348937	100.000	100.000

==== HPLC Analysis Report ====

C:\LabSolutions\Training1107\LWS QSSR\ALIV_180_95_5_0.5_OD.lcd
 Acquired by : Admin
 Sample Name : 1
 Sample ID : 1
 Tray# : 1
 Vial # : 75
 Injection Volume : 7 uL
 Data File Name : ALIV_180_95_5_0.5_OD.lcd
 Method File Name : OD-50_50_Hexane_IPA_25min_0.5mLmin.lcm
 Batch File Name : batch 7.lcb
 Report File Name : UCD Default.lcr
 Data Acquired : 12/7/2021 3:04:39 PM
 Data Processed : 12/7/2021 3:44:42 PM

<Chromatogram>



< Peak Table >

PeakTable C:\LabSolutions\Training1107\LWS QSSR\ALIV_180_95_5_0.5_OD.lcd

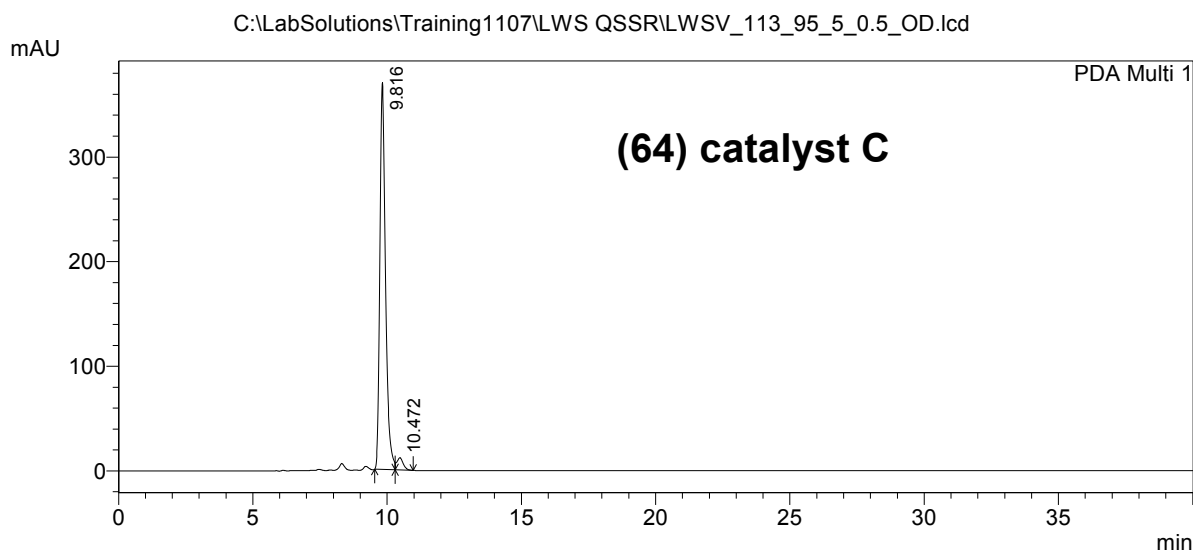
PDA Ch1 281nm 4nm

Peak#	Ret. Time	Area	Height	Area %	Height %
1	9.805	6166809	411285	100.000	100.000
Total		6166809	411285	100.000	100.000

==== HPLC Analysis Report ====

C:\LabSolutions\Training1107\LWS QSSR\LWSV_113_95_5_0.5_OD.lcd
 Acquired by : Admin
 Sample Name : 1
 Sample ID : 1
 Tray# : 1
 Vial # : 74
 Injection Volume : 7 uL
 Data File Name : LWSV_113_95_5_0.5_OD.lcd
 Method File Name : OD-50_50_Hexane_IPA_25min_0.5mLmin.lcm
 Batch File Name : batch 7.lcb
 Report File Name : UCD Default.lcr
 Data Acquired : 12/7/2021 2:14:02 PM
 Data Processed : 12/7/2021 2:54:06 PM

<Chromatogram>



< Peak Table >

PeakTable C:\LabSolutions\Training1107\LWS QSSR\LWSV_113_95_5_0.5_OD.lcd

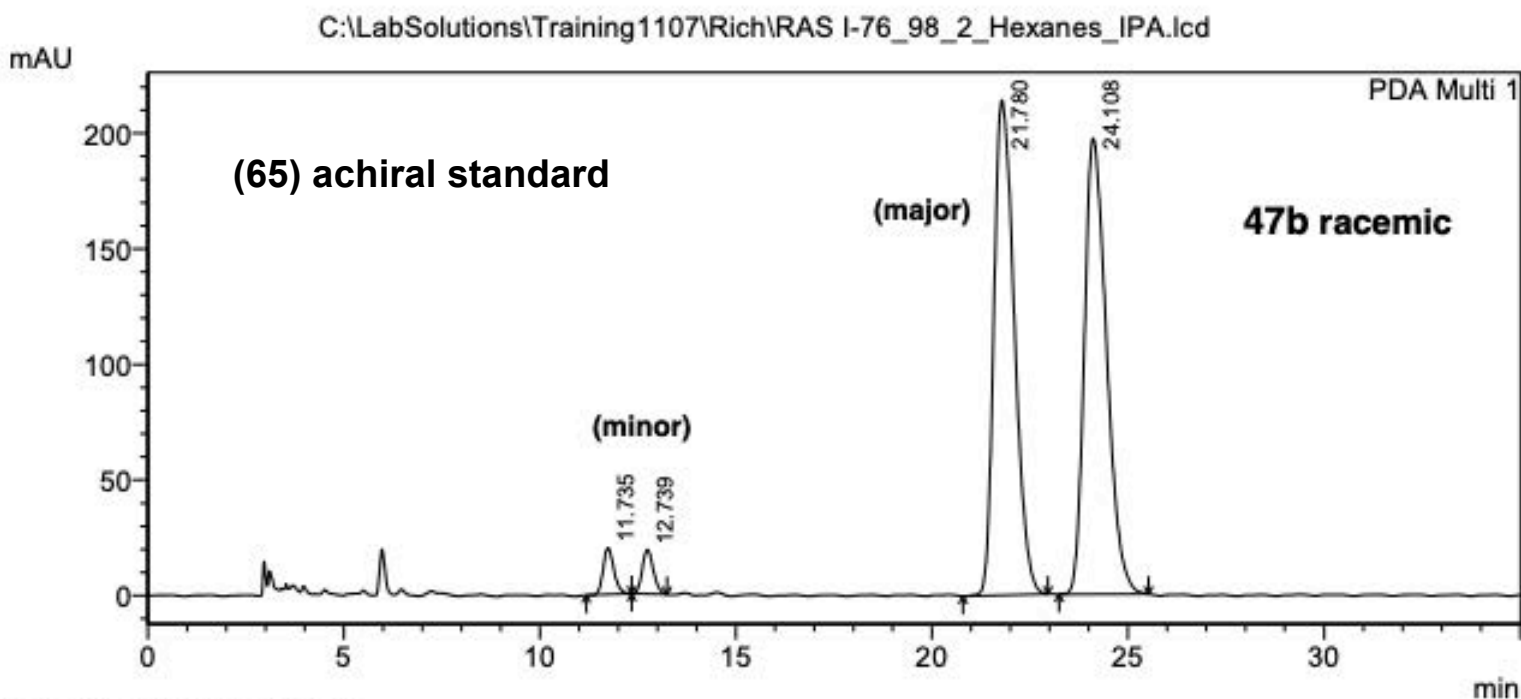
PDA Ch1 281nm 4nm

Peak#	Ret. Time	Area	Height	Area %	Height %
1	9.816	5440719	369699	96.561	96.908
2	10.472	193780	11798	3.439	3.092
Total		5634499	381496	100.000	100.000

==== HPLC Analysis Report ====

Acquired by : Admin
 Sample Name : RAS 1076_98_2_Hexanes_IPA
 Sample ID : RAS 1076_98_2_Hexanes_IPA
 Tray# : 1
 Vial # : 24
 Injection Volume : 10 uL
 Data File Name : RAS I-76_98_2_Hexanes_IPA.lcd
 Method File Name : OD-98_2_Hexane_IPA_35min.lcm
 Batch File Name : RAS_75_76_90_91.lcb
 Report File Name : UCD Default.lcr
 Data Acquired : 7/18/2013 4:34:03 PM
 Data Processed : 9/30/2014 1:58:52 PM

<Chromatogram>



< Peak Table >

PeakTable C:\LabSolutions\Training1107\Rich\RAS I-76_98_2_Hexanes_IPA.lcd

PDA Ch1 230nm 4nm

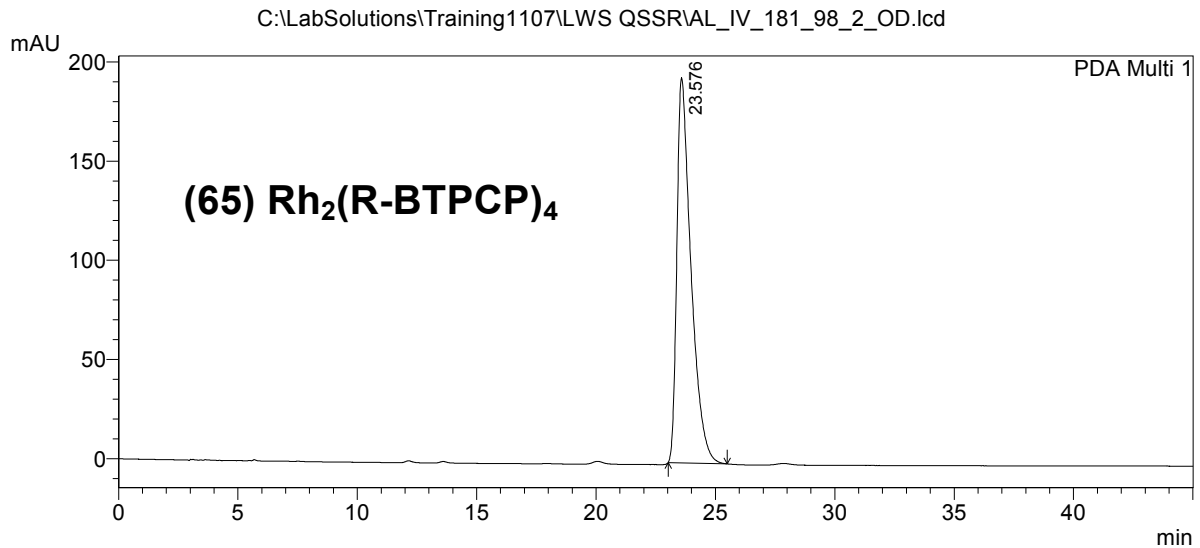
Peak#	Ret. Time	Area	Height	Area %	Height %
1	11.735	385406	20146	2.368	4.471
2	12.739	379548	19167	2.332	4.254
3	21.780	7755098	214050	47.656	47.502
4	24.108	7752865	197248	47.643	43.773
Total		16272917	450611	100.000	100.000

UCDAVIS Department of Chemistry
UNIVERSITY OF CALIFORNIA

==== HPLC Analysis Report ====

Acquired by : Admin
 Sample Name : 1
 Sample ID : 1
 Tray# : 1
 Vial # : 52
 Injection Volume : 10 uL
 Data File Name : AL_IV_181_98_2_OD.lcd
 Method File Name : OD-80_20_Hexane_IPA_45min.lcm
 Batch File Name : batch file 3.lcb
 Report File Name : UCD Default.lcr
 Data Acquired : 8/12/2006 11:13:51 PM
 Data Processed : 8/12/2006 11:58:53 PM

<Chromatogram>



1 PDA Multi 1/280nm 4nm

< Peak Table >

PeakTable C:\LabSolutions\Training1107\LWS QSSR\AL_IV_181_98_2_OD.lcd

PDA Ch1 280nm 4nm

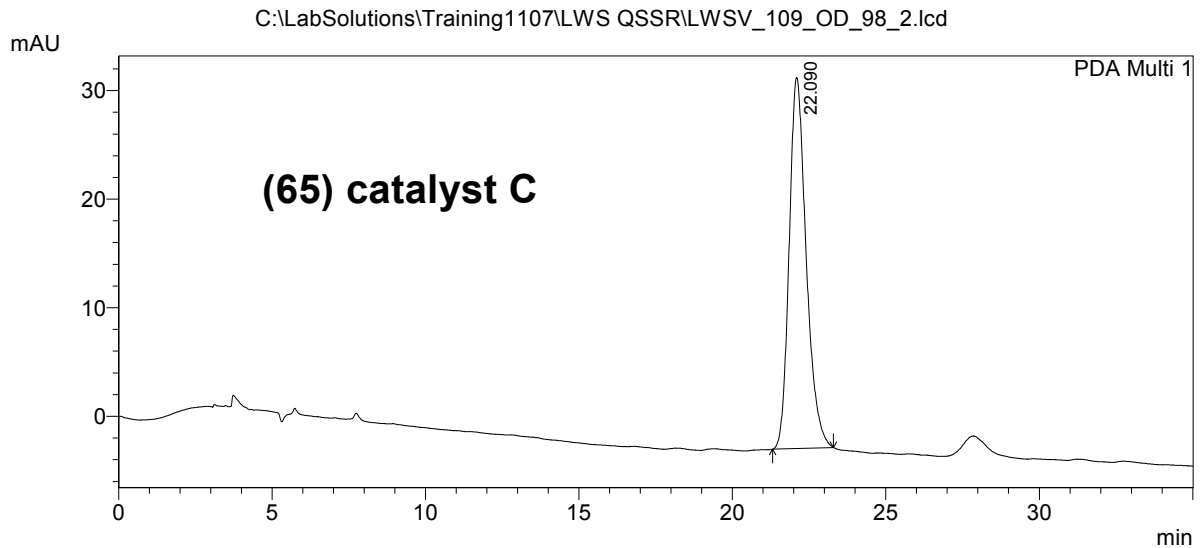
Peak#	Ret. Time	Area	Height	Area %	Height %
1	23.576	7984089	194055	100.000	100.000
Total		7984089	194055	100.000	100.000

UCDAVIS Department of Chemistry
UNIVERSITY OF CALIFORNIA

==== HPLC Analysis Report ====

Acquired by : Admin
 Sample Name : 1
 Sample ID : 1
 Tray# : 1
 Vial # : 86
 Injection Volume : 7 uL
 Data File Name : LWSV_109_OD_98_2.lcd
 Method File Name : OD-80_20_Hexane_IPA_35min.lcm
 Batch File Name : batch file 2.lcb
 Report File Name : UCD Default.lcr
 Data Acquired : 6/16/2006 9:10:17 PM
 Data Processed : 6/16/2006 9:45:19 PM

<Chromatogram>



< Peak Table >

PeakTable C:\LabSolutions\Training1107\LWS QSSR\LWSV_109_OD_98_2.lcd

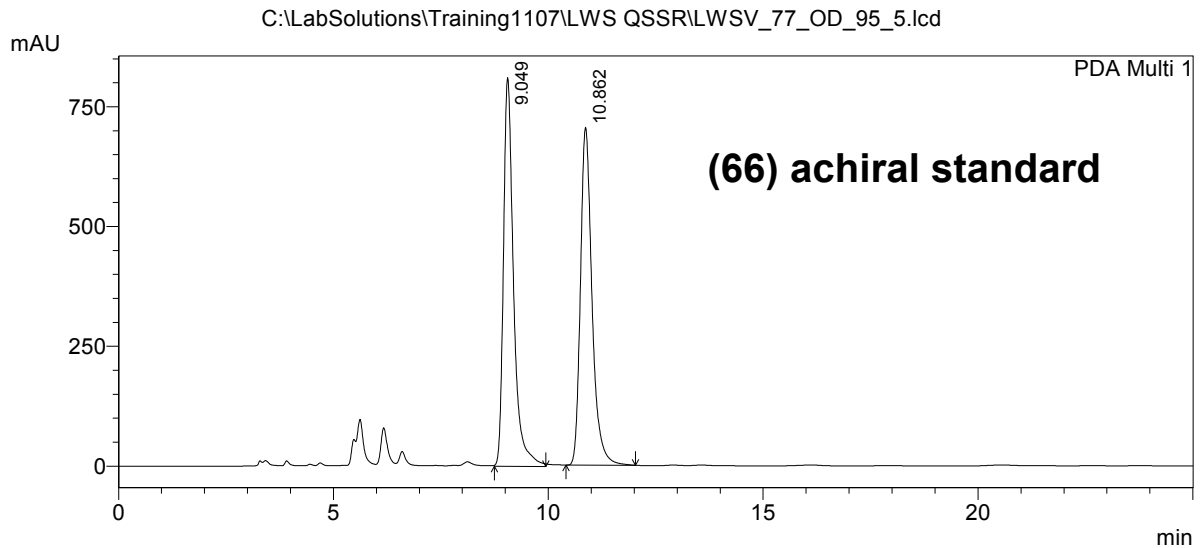
PDA Ch1 280nm 4nm

Peak#	Ret. Time	Area	Height	Area %	Height %
1	22.090	1320106	34156	100.000	100.000
Total		1320106	34156	100.000	100.000

==== HPLC Analysis Report ====

C:\LabSolutions\Training1107\LWS QSSR\LWSV_77_OD_95_5.lcd
 Acquired by : Admin
 Sample Name :
 Sample ID :
 Tray# : 1
 Vial # : 77
 Injection Volume : 10 uL
 Data File Name : LWSV_77_OD_95_5.lcd
 Method File Name : OD-50_50_Hexane_IPA_25min_1mLmin.lcm
 Batch File Name : Batch file 1.lcb
 Report File Name : UCD Default.lcr
 Data Acquired : 5/27/2006 11:03:14 PM
 Data Processed : 6/2/2006 11:43:04 PM

<Chromatogram>



< Peak Table >

PeakTable C:\LabSolutions\Training1107\LWS QSSR\LWSV_77_OD_95_5.lcd

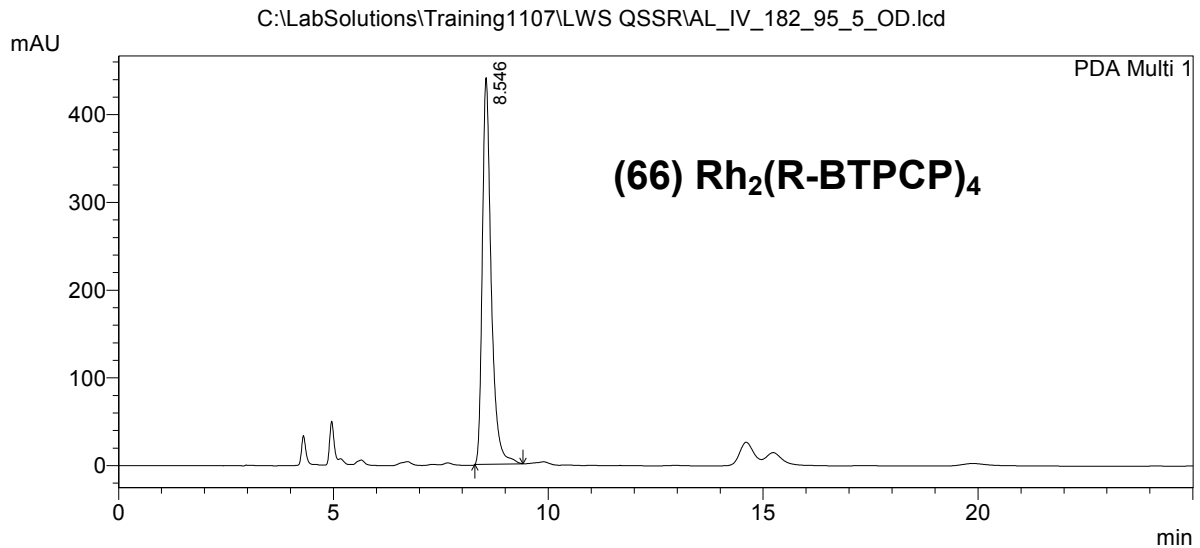
PDA Ch1 230nm 4nm

Peak#	Ret. Time	Area	Height	Area %	Height %
1	9.049	13275248	810871	50.137	53.493
2	10.862	13202436	704971	49.863	46.507
Total		26477685	1515842	100.000	100.000

==== HPLC Analysis Report ====

Acquired by : Admin
 Sample Name : 1
 Sample ID : 1
 Tray# : 1
 Vial # : 54
 Injection Volume : 10 uL
 Data File Name : AL_IV_182_95_5_OD.lcd
 Method File Name : OD-50_50_Hexane_IPA_25min_1mLmin.lcm
 Batch File Name : batch file 3.lcb
 Report File Name : UCD Default.lcr
 Data Acquired : 8/13/2006 12:35:05 AM
 Data Processed : 8/13/2006 1:00:07 AM

<Chromatogram>



< Peak Table >

PeakTable C:\LabSolutions\Training1107\LWS QSSR\AL_IV_182_95_5_OD.lcd

PDA Ch1 254nm 4nm

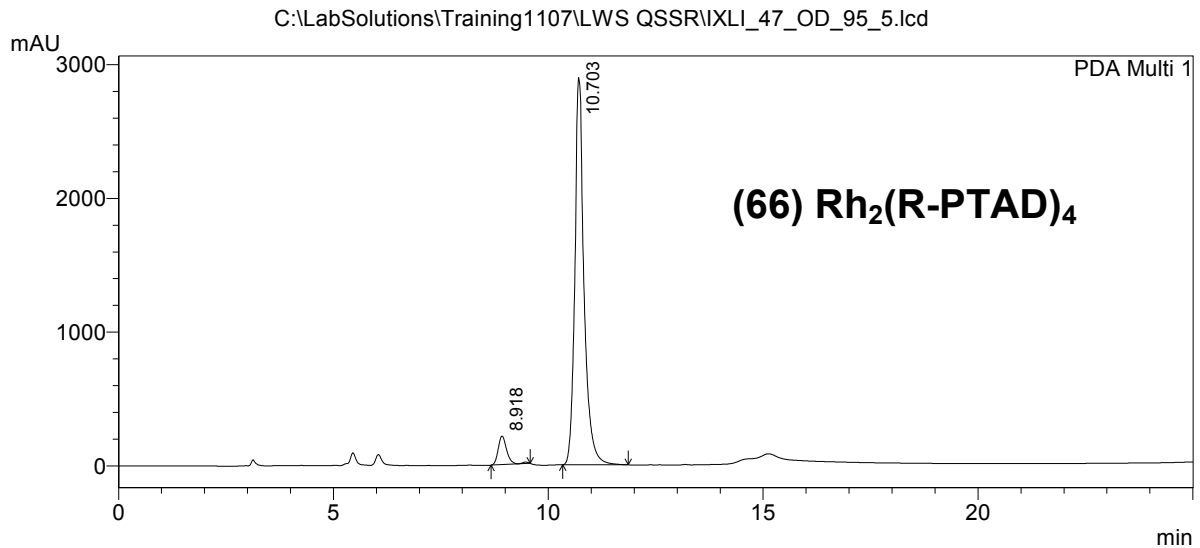
Peak#	Ret. Time	Area	Height	Area %	Height %
1	8.546	6330186	440574	100.000	100.000
Total		6330186	440574	100.000	100.000

UC DAVIS Department of Chemistry
UNIVERSITY OF CALIFORNIA

==== HPLC Analysis Report ====

C:\LabSolutions\Training1107\LWS QSSR\IXLI_47_OD_95_5.lcd
 Acquired by : Admin
 Sample Name : 1
 Sample ID : 1
 Tray# : 1
 Vial # : 83
 Injection Volume : 10 uL
 Data File Name : IXLI_47_OD_95_5.lcd
 Method File Name : OD-50_50_Hexane_IPA_25min_1mLmin.lcm
 Batch File Name : batch file 2.lcb
 Report File Name : UCD Default.lcr
 Data Acquired : 6/10/2006 9:15:19 PM
 Data Processed : 6/10/2006 9:40:23 PM

<Chromatogram>



< Peak Table >

PeakTable C:\LabSolutions\Training1107\LWS QSSR\IXLI_47_OD_95_5.lcd

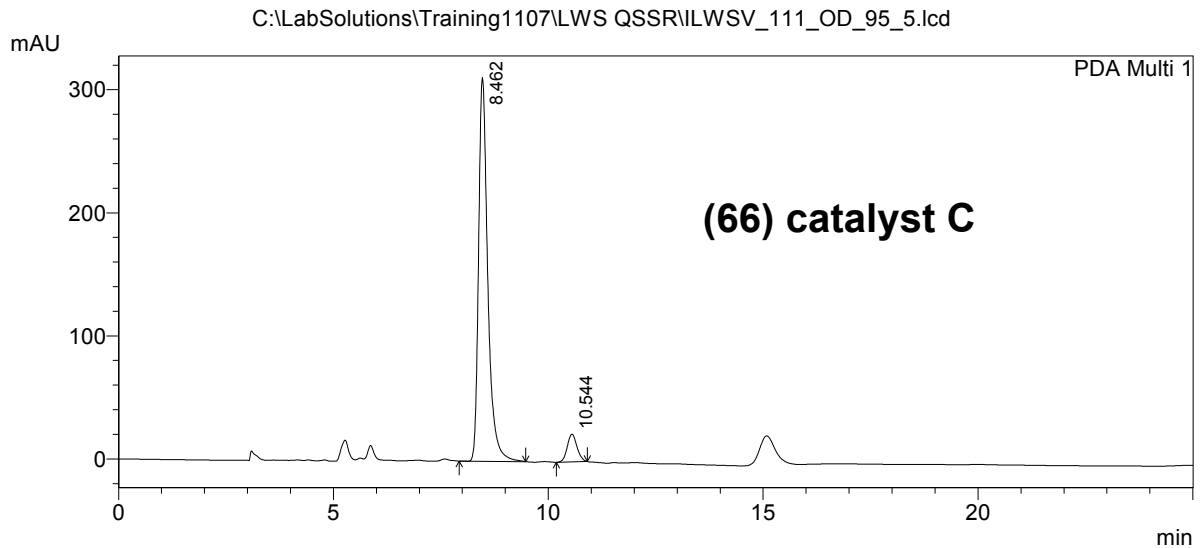
PDA Ch1 200nm 4nm

Peak#	Ret. Time	Area	Height	Area %	Height %
1	8.918	2986686	213717	6.482	6.873
2	10.703	43090859	2895743	93.518	93.127
Total		46077545	3109460	100.000	100.000

==== HPLC Analysis Report ====

C:\LabSolutions\Training1107\LWS QSSR\ILWSV_111_OD_95_5.lcd
 Acquired by : Admin
 Sample Name : 1
 Sample ID : 1
 Tray# : 1
 Vial # : 84
 Injection Volume : 13 uL
 Data File Name : ILWSV_111_OD_95_5.lcd
 Method File Name : OD-50_50_Hexane_IPA_25min_1mLmin.lcm
 Batch File Name : batch file 2.lcb
 Report File Name : UCD Default.lcr
 Data Acquired : 6/11/2006 12:23:51 AM
 Data Processed : 6/11/2006 12:48:53 AM

<Chromatogram>



< Peak Table >

PeakTable C:\LabSolutions\Training1107\LWS QSSR\ILWSV_111_OD_95_5.lcd

PDA Ch1 254nm 4nm

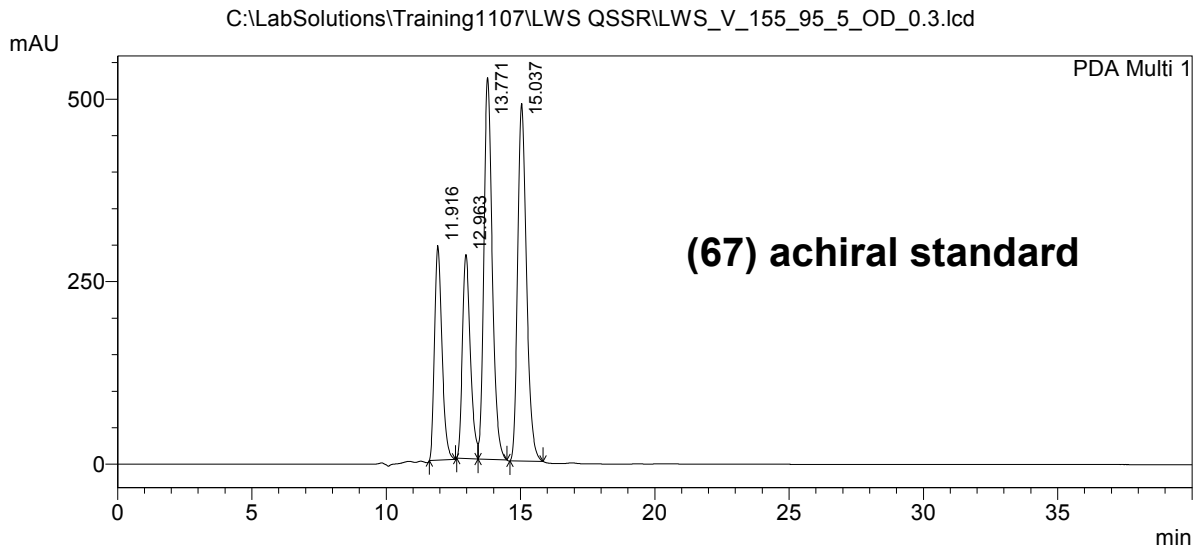
Peak#	Ret. Time	Area	Height	Area %	Height %
1	8.462	4647866	311766	92.874	93.241
2	10.544	356640	22602	7.126	6.759
Total		5004506	334368	100.000	100.000



==== HPLC Analysis Report ====

Acquired by : Admin
 Sample Name : 1
 Sample ID : 1
 Tray# : 1
 Vail # : 34
 Injection Volume : 10 uL
 Data File Name : LWS_V_155_95_5_OD_0.3.lcd
 Method File Name : OD-50_50_Hexane_IPA_40min_0.3mLmin.lcm
 Batch File Name : batch 4.lcb
 Report File Name : UCD Default.lcr
 Data Acquired : 12/2/2021 4:36:24 PM
 Data Processed : 12/2/2021 5:16:27 PM

<Chromatogram>



1 PDA Multi 1/280nm 4nm

< Peak Table >

PeakTable C:\LabSolutions\Training1107\LWS QSSR\LWS_V_155_95_5_OD_0.3.lcd

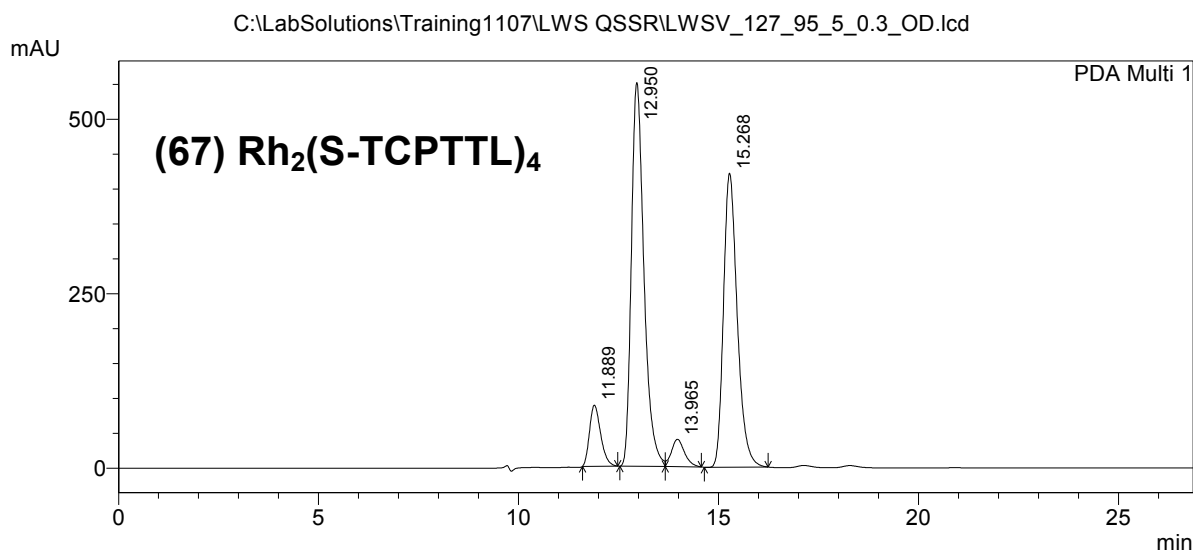
PDA Ch1 280nm 4nm

Peak#	Ret. Time	Area	Height	Area %	Height %
1	11.916	5692711	293869	16.758	18.532
2	12.963	5729796	279609	16.867	17.633
3	13.771	11319753	522610	33.323	32.957
4	15.037	11227386	489650	33.051	30.878
Total		33969646	1585738	100.000	100.000

==== HPLC Analysis Report ====

C:\LabSolutions\Training1107\LWS QSSR\LWSV_127_95_5_0.3_OD.lcd
 Acquired by : Admin
 Sample Name : 1
 Sample ID : 1
 Tray# : 1
 Vial # : 43
 Injection Volume : 7 uL
 Data File Name : LWSV_127_95_5_0.3_OD.lcd
 Method File Name : OD-50_50_Hexane_IPA_25min_0.3mLmin.lcm
 Batch File Name : batch 6.lcb
 Report File Name : UCD Default.lcr
 Data Acquired : 12/6/2021 4:34:09 PM
 Data Processed : 12/6/2021 5:01:02 PM

<Chromatogram>



< Peak Table >

PeakTable C:\LabSolutions\Training1107\LWS QSSR\LWSV_127_95_5_0.3_OD.lcd

PDA Ch1 280nm 4nm

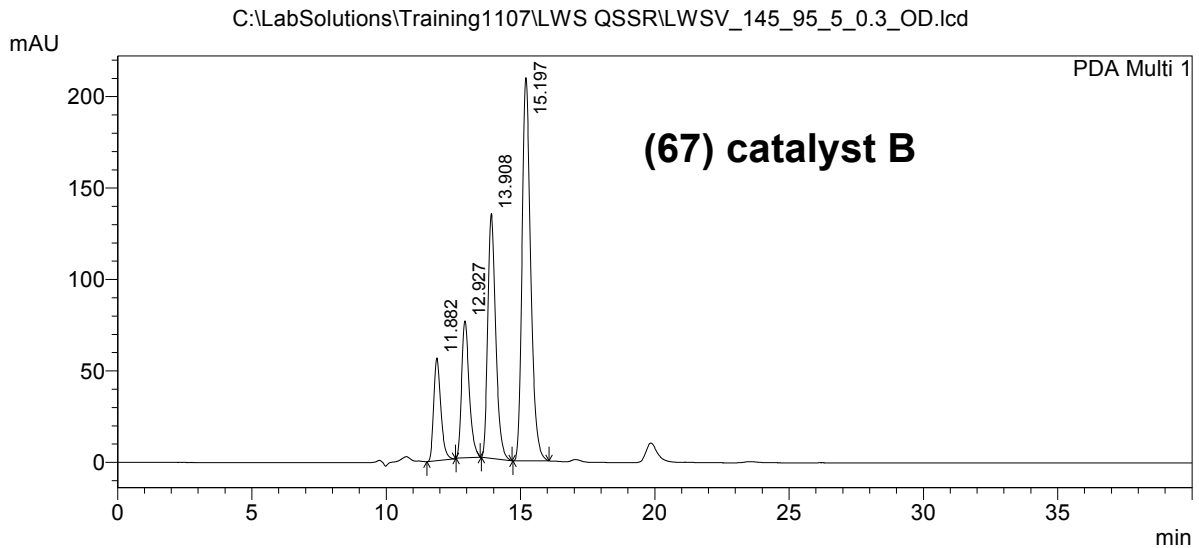
Peak#	Ret. Time	Area	Height	Area %	Height %
1	11.889	1697220	87660	6.879	7.985
2	12.950	12004490	549508	48.653	50.053
3	13.965	897805	39298	3.639	3.580
4	15.268	10074278	421381	40.830	38.382
Total		24673793	1097848	100.000	100.000



==== HPLC Analysis Report ====

Acquired by : Admin
 Sample Name : 1
 Sample ID : 1
 Tray# : 1
 Vail # : 42
 Injection Volume : 7 uL
 Data File Name : LWSV_145_95_5_0.3_OD.lcd
 Method File Name : OD-50_50_Hexane_IPA_25min_0.3mLmin.lcm
 Batch File Name : batch 6.lcb
 Report File Name : UCD Default.lcr
 Data Acquired : 12/6/2021 3:43:33 PM
 Data Processed : 12/6/2021 4:23:36 PM

<Chromatogram>



1 PDA Multi 1/280nm 4nm

< Peak Table >

PeakTable C:\LabSolutions\Training1107\LWS QSSR\LWSV_145_95_5_0.3_OD.lcd

PDA Ch1 280nm 4nm

Peak#	Ret. Time	Area	Height	Area %	Height %
1	11.882	1036896	56202	10.443	11.845
2	12.927	1466727	74912	14.772	15.789
3	13.908	2754728	133807	27.744	28.201
4	15.197	4670746	209548	47.041	44.165
Total		9929096	474468	100.000	100.000

Chapter 2. Enantioselective C–H Insertion Reactions of Donor/donor Carbenes for the Formation of Indolines and Indanes

2.1 Introduction

2.1.1 Metal Carbene Reactivity and History

Metal carbenes are reactive intermediates that undergo a wide variety of reactions.¹ Selective insertion into both C–H and X–H bonds by these intermediates forms the basis for many useful transformations.^{2–4} Foundational work in these fields by Taber, Doyle, Davies, and Hashimoto, among others, have revolutionized the field, making metal carbene chemistry convenient and accessible to the average chemist.^{5–7} Variations in the electronic character of metal carbenes have a significant influence on the chemoselectivity, regioselectivity, and stereo-selectivity of their subsequent reactivity (Figure 1). While carbenes featuring electron-withdrawing substituents are well represented in the literature,⁸ carbenes featuring electron donating substituents have been seeing increased attention only relatively recently.³ These donor/donor substituted carbenes show promising potential to synthesize a variety of important molecules. The focus of this work will be on stereoselective C–H insertion reactions of donor/donor carbenes to create indolines and indanes.

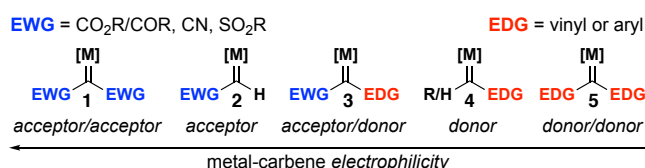


Figure 1: Reactivity of metal carbenes

2.1.2 Donor/Donor Metal Carbene Precursors

Catalytic reactions that proceed *via* carbene intermediates often employ diazo compounds as precursors to metal carbenes.⁸ In some cases these intermediates can be isolated, while in other cases they are generated *in situ*; when exposed to a catalyst, nitrogen gas is extruded, forming the metal. While diazo precursors for most acceptor-substituted carbenes are generated by diazo transfer to a stabilized anion, in the case of donor-substituted carbenes, diazo compounds are typically generated from hydrazone precursors (Figure 2).⁸

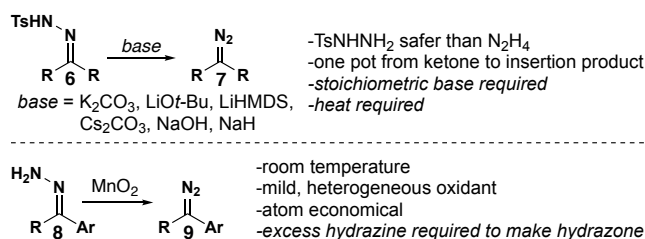


Figure 2. Hydrazone carbene precursors

Two different hydrazone precursors are typically employed in the generation of diazo precursors for donor-carbenes. Diazo compounds can be generated from tosylhydrazones by employing a stoichiometric amount of base, which typically requires the use of high temperatures.³ This method avoids the use of neat hydrazine, which is toxic and unstable, and can be performed as a one-pot procedure from the requisite ketones. As an alternative to tosylhydrazones, unsubstituted hydrazones can be oxidized with manganese dioxide to form diazo compounds.⁹ Although this method requires special handling of hydrazine, it benefits from the use of a heterogenous and chemoselective oxidant which operates without base or elevated temperature. In some

cases, the oxidation can be carried out in the presence of a metal catalyst (e.g., rhodium), enabling one-pot conversion of hydrazones to carbene insertion products.

Due to the reactive nature of metal carbenes and their requisite precursors, a variety of byproducts may be observed in the course of a typical reaction (Figure 3).³ Tosylhydrazone **16** is known to degrade to sulfone **11** at the elevated temperatures required to form the diazo compound **7**.¹⁰ Once formed, diazo intermediates themselves are potentially explosive and are often used on small scale and/or at low concentrations (e.g., dilute solutions and/or inverse addition). Donor/donor diazo compounds readily form metal carbenes; the process is nearly instantaneous at ambient and lower (e.g., -20 °C) temperatures.⁹ For hydrazone precursor **10**, when oxidation is slower than carbene formation, metal carbene **15** can react with hydrazone **10** to form imine **14**.⁹ This process can be avoided by filtering off the oxidant after diazo formation is complete, followed by addition of the catalyst. If the insertion reaction is slow, then the diazo **7** can react with the metal carbene to form azine **13**.⁹ Although most intramolecular insertions are fast enough to avoid this process, any unwanted azine formation can be suppressed using inverse addition of the diazo compound to a solution of catalyst. Another byproduct of slow insertion reactions is O–H insertion, which often occurs if the reaction is not kept sufficiently anhydrous.¹¹ If MnO₂ is present, **17** may be oxidized to ketone **18** when R=Ph.⁹ When the carbene is substituted with an alkyl group, β-hydride elimination can occur, forming alkene **19** or other degradation products. This byproduct can occasionally be suppressed based on the choice of catalyst/ligand and the character of the β-hydride, but is not a consistently reliable fix.² Under certain reaction conditions for N–H insertion,

imine **16** is observed as the byproduct of β -hydride elimination.¹² Finally, donor/donor carbenes can occasionally dimerize to form an alkene **19**.

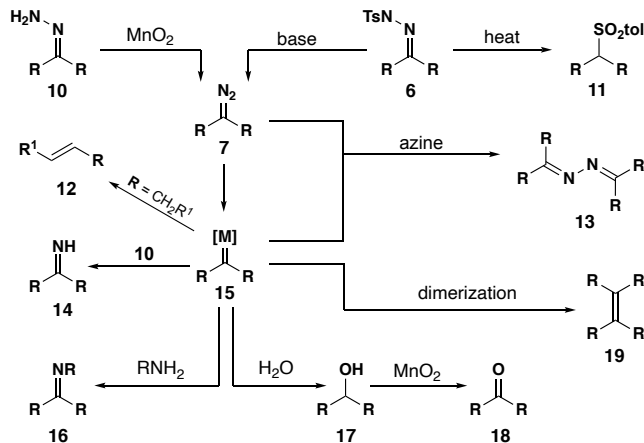
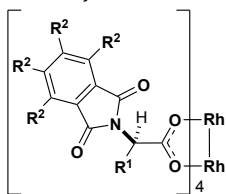


Figure 3. Metal carbene byproducts

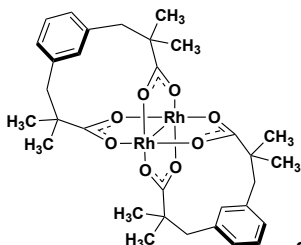
2.1.3 Catalysts Used in Donor/Donor Metal Carbene Insertions

The majority of donor/donor carbene insertion reactions are catalyzed by rhodium, ruthenium and copper catalysts (Figure 4).^{6,13–15} There have also been insertion reactions reported with gold, iron, silver, palladium, platinum and zinc catalysts, though these examples are relatively fewer in number. This work will focus primarily on dirhodium paddlewheel catalysts resembling **20–32** which serve as privileged reagents for insertion reactions of donor/donor metal carbenes in our lab.

Rhodium Catalysts



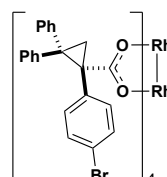
- 20, R¹ = *t*-Bu, R² = H, Rh₂(*R*-PTTL)₄
 21, R¹ = *t*-Bu, R² = F, Rh₂(*R*-TFPTTL)₄
 22, R¹ = *t*-Bu, R² = Cl, Rh₂(*R*-TCPTTL)₄
 23, R¹ = *t*-Bu, R² = Br, Rh₂(*R*-TBPTTL)₄
 24, R¹ = 1-adamantyl, R² = H, Rh₂(*R*-PTAD)₄



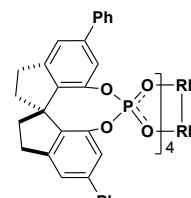
25, Rh₂(esp)₂



- 26, R = CH₃, Rh₂(OAc)₄
 27, R = CF₃, Rh₂(TFA)₄
 28, R = *t*-Bu, Rh₂(OPiv)₄
 29, R = mesityl, Rh₂(Mes)₄
 30, R = *n*-octyl, Rh₂(octanoate)₄

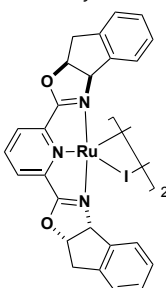


31, Rh₂(*R*-BTPCP)₄

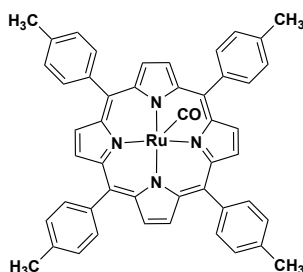


32, Rh₂(SPA)₄

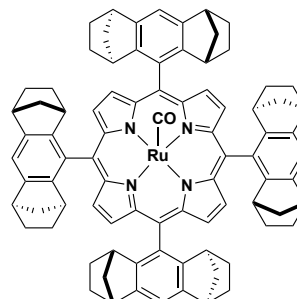
Ruthenium Catalysts



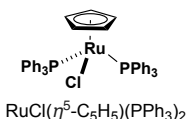
33, [Ru((3a*R*,8a*S*)-indapybox)]₂



34, Ru(TTP)(CO)

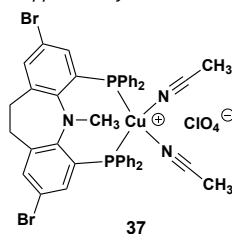


35, Ru(D₄-Por*)(CO)



36, RuCl(η⁵-C₅H₅)(PPh₃)₂

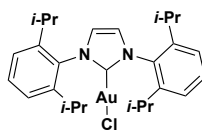
Copper Catalysts



37

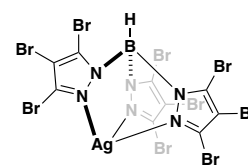
- 38, CuI
 39, Cu(acac)₂
 40, Cu(CH₃CN)₄BF₄⁻
 41, CuCl₂

Gold, Iron, Silver, Palladium, Platinum, and Zinc Catalysts

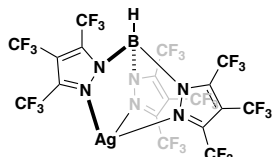


42, IPr-AuCl

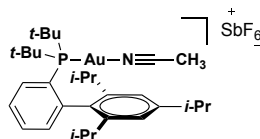
- 43, AgOTf; 44, Pd(*P**t*-Bu₃)₂
 45, *cis*-[Pt((PPh₃)₂(CH₃CN)₂][BF₄]₂
 46, ZnBr₂



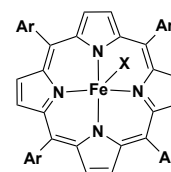
47, TpBr₃Ag(thf)



48, Tp(CF₃)₂Ag(thf)



49, [Au(*t*-BuXPhos)CH₃CN]SbF₆



50, Ar = Ph, X = Cl, Fe(TPP)Cl
 51, Ar = C₆F₅, X = adamantyl, Fe(TPFPP)Ad

Figure 4. Summary of catalysts used for insertion reactions of donor/donor carbenes.

2.1.4 Reaction Mechanisms and Scope of Donor/Donor Carbene Insertions

Donor/donor carbenes have demonstrated immense versatility in the types of insertion reactions they can accomplish. The mechanisms by which these insertions proceed are variable depending on the type of X–H bond and metal catalyst involved. This section will give an overview of the various types of donor/donor insertion reaction mechanisms as well as their reaction scopes which will provide the necessary context for the experimental work presented in this chapter. First, donor/donor carbene insertions to non-C–H bonds will be discussed. Then, C–H insertion reactions of donor/donor carbenes and their mechanism will be presented.

2.1.4.1 Mechanisms of Insertion Reactions of Non-C–H Bonds with Donor/Donor Carbenes

N–H and P–H insertions with donor/donor carbenes have been reported with copper (I) catalysts and proceed through similar mechanisms (Figure 5).^{17–19} First, tosylhydrazones react with base to generate diazo intermediates resembling **56**, which subsequently form metal carbenes in the presence of a copper (I) catalyst. The copper (I) catalyst results from reduction by the diazo precursor *in situ*.^{20,21} This metal carbene **58** can be nucleophilically attacked by a heteroatom (N or P) to produce zwitterionic intermediate **60**. Final proton transfer from the heteroatom to carbon facilitates the turnover of the copper catalyst and results in the X–H insertion product **61**.

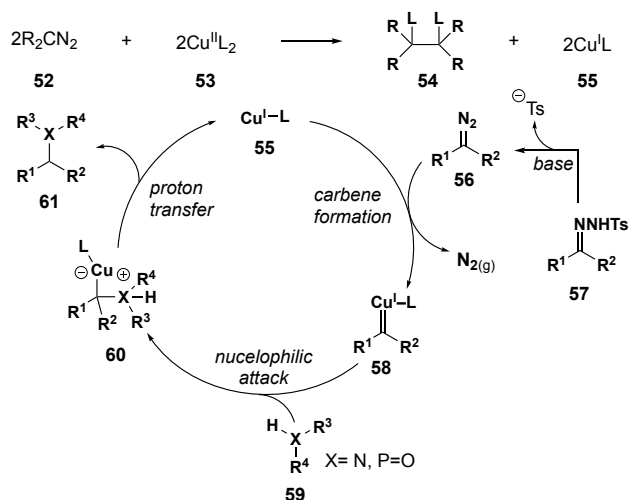


Figure 5. N–H and P–H insertion reaction mechanisms

Studies have suggested B–H and O–H insertion reactions proceed through concerted mechanisms (Figure 6).²² Rhodium or ruthenium carbenes form from diazo compound **63**. A subsequent concerted hydride transfer and C–B or C–O bond formation (transition state **66**) leads to insertion product **67**. Due to the strong hydridic character of borane hydrogens when coordinated to Lewis bases, B–H insertion can proceed intramolecularly. The mechanisms for B–H and O–H insertion also resemble the mechanism proposed for C–H insertion (i.e. explicit concerted asynchronous *hydride* transfer) discussed *vide infra*.

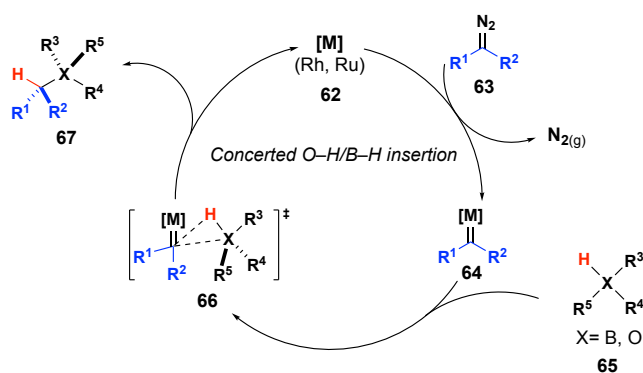


Figure 6. B–H and O–H insertion reaction mechanisms.

Reports of palladium-catalyzed Si–H insertion reactions with donor/donor carbenes propose a different mechanism of insertion relative to ones previously discussed (Figure 7).²³ A palladium (0) species can undergo oxidative addition with a silane Si–H bond leading to intermediate **70**. **70** reacts with diazo compound **72** to form metal carbene **74**. This intermediate could then undergo migratory insertion with either Si or H to form either **75** or **77**, respectively. Finally, reductive elimination furnishes the Si–H insertion product **76** and regenerates the active catalyst.

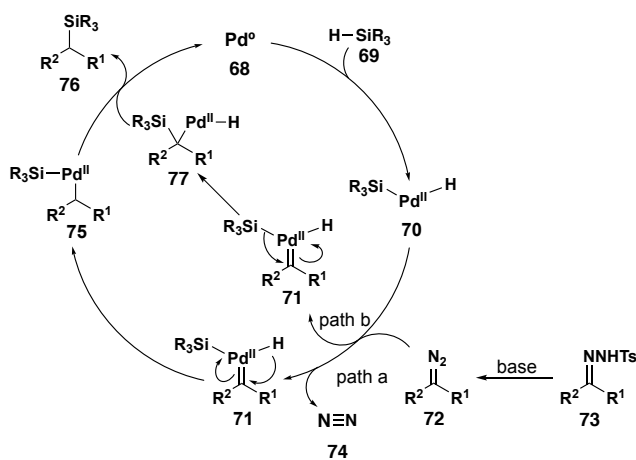


Figure 7. Palladium catalyzed Si–H insertion reaction mechanism

2.1.4.2 Scope of Insertion Reactions of Non-C–H Bonds with Donor/Donor Carbenes

There are many reported examples of N–H insertion reactions with donor/donor carbenes (Table 1). N–H insertion reactions with donor/donor carbenes lead to nitrogen containing products relevant to a variety of biologically active compounds and natural products. Alkyl- and aryl-tosylhydrazones have successfully reacted with copper-based catalysts in N–H insertion reactions to form secondary and tertiary amine and amide

products. The first example of N–H insertion was reported by De Zotto and co-workers using primary amines in the presence of diaryl diazo compounds and ruthenium catalyst (Table 1, entry 2).²⁴ Shortly thereafter, Cu(acac)₂ was shown to be effective in insertion reactions with imidazoles (Table 1, entry 4).²⁵ This development consequently led to successful insertions into aniline and alkyl N–H bonds (Table 1, entries 1 and 3). Impressively, Hamze and co-workers demonstrated that their procedure was highly chemoselective for N–H insertion over O–H moieties present in the substrate;^{12,17} Xu and co-workers were able to further expand this chemistry for the synthesis of amides (Table 4, entries 5-6).^{18,26} Unfortunately, in most of these examples using copper catalysts, byproducts formed through β-hydride elimination is common. While significant progress has been made in the field of N–H insertion reactions, enantioselective variants of these reactions are still elusive.

Reaction scheme: $\text{R}^1\text{-N(H)-R}^2$ (78) + Ar-C(=N-NHTs)-R^3 (79, Ar^a = Ph, substituted Ph) $\xrightarrow{\text{catalyst}}$ $\text{R}^1\text{-N(R}^2\text{)-CH(Ar)-R}^3$ (80)

entry	R ¹	R ²	R ³	catalyst	# examples	yield range
1	aryl	H/alkyl	aryl/H/alkyl	Cu(acac) ₂	40	50–93
2	alkyl	H/alkyl	H/alkyl	[RuCl(5-C ₅ H ₅)(PPh ₃) ₂]	10	10–48
3	alkyl	H/alkyl	aryl/H/alkyl	Cu(acac) ₂	22	40–84
4 ^b	imidazoles		aryl/H	Cu(acac) ₂	10	50–80
5 ^c	COR	H	H	Cu(CH ₃ CN) ₄ BF ₄	38	33–99
6	COR	H/alkyl/aryl	aryl/alkyl	CuI	38	40–98
7	imidazole, carbazole, morpholine		Ph	48	3	86–94
8	Ph, Bn	H	Ph	48	2	51–56

^a Includes Ar = pyridinyl, naphthyl (entry 1); Ar/R³ = fluorenyl (entry 2); Ar = naphthyl (entries 5 and 6). ^b Includes 2 examples with cyclohexanone-derived tosylhydrazones. ^c Includes 3 examples with tosylhydrazones derived from *n*-alkyl aldehydes.

Table 1: N–H insertion reaction scope

A variety of donor/donor carbenes undergo B–H insertion reactions to form alkylborane-amine complexes (Figure 8). Zhou and co-workers reported that B–H

insertion reactions readily occur between borane-Lewis base complexes **83** and metal carbenes (formed *in situ* from the decomposition of tosylhydrazones).²² As with many C–H insertion reactions with donor/donor carbenes, phthalimide and triphenyl cyclopropane-derived rhodium carboxylate catalysts provided impressive stereoselectivity. In contrast to this impressive selectivity, other efforts have shown that B₂Pin₂ and BHPin can also decompose aryl/aryl and aryl/alkyl diazo compounds to afford similar products as racemates without a metal catalyst or Lewis base additives.²⁷ Furthermore, β-hydride elimination is less consequential in these reactions despite the presence of β-hydrogen atoms.

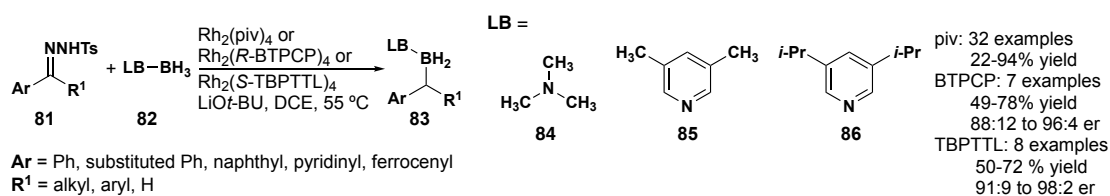
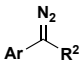
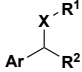


Figure 8. B–H insertion reaction scope

O–H insertion reactions with donor/donor carbenes allow unique access to functionalized ethers. Bertani et al. reported decomposition of 9-diazafluorene with neutral and cationic dirhodium carboxylate catalysts, giving poor yields of the O–H insertion product and a distribution of azine, ketone, and dimer byproducts.¹¹ However, when exposed to a platinum (II) phosphine catalyst, quantitative conversion to the O–H insertion product from methanol is observed (Table 2, entry 1). Later work by Barluenga and co-workers demonstrated that these substrates were susceptible to thermal

decomposition and formal O–H insertion *without* a transition metal catalyst, affording a broad variety of ethers.²⁸ This method used tosylhydrazones derived from acetophenones, alkyl aldehydes, and alkyl ketones without observing any Bamford-Stevens type elimination byproducts, suggesting that O–H insertion is faster than elimination without a metal catalyst. Similar work was recently accomplished by Che and co-workers in O–H insertion reactions using phenyl/phenyl carbenes and iron porphyrin catalyst to insert into phenyl, aryl, and alkyl alcohols (Table 2, entry 3).¹ This methodology proved amenable to S–H insertion reactions as well, affording phenyl and aryl thioethers in excellent yields and one example of an alkoxy thioether in poor yield (Table 2, entry 4). Currently there are reports of stereoselective variants for O–H or S–H insertion.

R ¹ –XH		+ 		catalyst			
87		88				89	
entry ^[a]	X	R ¹	Ar, R ²	# examples	yield range (%)		
1 ^[b]	O	CH ₃	Ar, R ² = fluorenyl	1	100		
2 ^[c]	O	Ph, Ar, 2-naphthyl, alkyl	Ar, R ² = Ph	5	31-92		
3 ^[c]	S	Ph, Ar, 2-pyridyl, alkyl	Ar, R ² = Ph	5	33-99		

[a] diazo compounds derived from tosylhydrazones for entries 1 and 2. [b] *cis*-[Pt(PPh₃)₂(CH₃CN)₂][BF₄]₂ **45** catalyst [c] Fe(TPFPP)Cl **51** as catalyst

Table 2. O–H and S–H insertion scope

There have been recent reports of insertion reactions into Si–, Ge–, and Sn–H bonds using a variety of transition metal catalysts. In 2017, Wang and co-workers demonstrated a successful donor/donor carbene insertion into a Sn–H bond in the absence of catalyst (Table 3, entry 3).²⁹ This report proposed two catalyst-free mechanisms: (1) direct attack of diazo **94** by alkyl tin and (2) formation of free carbene

95. Ultimately, the presence of a free carbene was corroborated by addition of a styrene derivative, which formed the corresponding cyclopropanation product **99**. Subsequently, Bi reported silver (I) triflate-catalyzed Si–, Ge–, and Sn–H insertion reactions using nosylhydrazones derived from aryl aldehydes and aryl ketones (Table 3, entry 4).³⁰ This method is high-yielding and tolerant of a wide range of functional groups. In 2018, Che demonstrated that iron porphyrins at low catalyst loading (i.e. 2 mol %) could be effective catalysts for Si–, Ge–, and Sn–H insertions (Table 3, entry 1).³¹ Unlike previous methods, this procedure allowed for the ability to insert into 3°, 2°, 1° Si–H bonds. Shortly after Che’s publication, Wang established a protocol for Si–H insertion using palladium catalyst **44** (Table 3, entry 2).²³ Though in all previous reports Si–H insertion into tosyl- or nosylhydrazones derived from aliphatic aldehydes or ketones was inaccessible, Wang and co-workers were able to generate several Si–H insertion examples in good yield using these intermediates.

Reaction scheme: $\text{R}^1-\overset{\text{R}^2}{\underset{\text{H}}{\text{X}}}-\text{R}^3 + \text{R}^4-\overset{\text{N}-\text{NHR}^6}{\text{C}}=\text{R}^5 \xrightarrow{\text{catalyst}} \text{R}^1-\overset{\text{R}^2}{\underset{\text{R}^4}{\text{X}}}-\text{R}^3-\text{R}^5$

entry ^[a]	X	R ¹ , R ² , R ³	R ⁴	R ⁵	R ⁶	catalyst	# examples	yield range (%)
1	Si, Ge, Sn	H, alkyl, aryl	Ph, Ar ^[a]	H, CH ₃ ^[b]	Ts	47	49	23-99
2	Si	alkyl, Ph	alkyl, alkynyl, Ph, Ar ^[a]	H, alkyl, aryl	Ts	44	41	35-98
3	Sn	alkyl	Ph, Ar ^[a]	H, alkyl	Ts	—	40	26-85
4	Si, Ge, Sn	alkyl, aryl	alkynyl, Ph, Ar ^[a]	H, alkyl, aryl	Ts	AgOTf	36	37-95

[a] Ar = substituted Ph, naphthyl (entry 1); Ar = substituted Ph, ferrocenyl, anthracenyl, naphthyl, pyridyl (entry 2); Ar = pyridyl, naphthyl (entry 3); Ar = naphthyl, furyl, thiophenyl, indolyl (entry 4). [b] 3 examples where X = Sn and Ge (30-44%).

Table 3. Si, Ge, Sn insertion scope

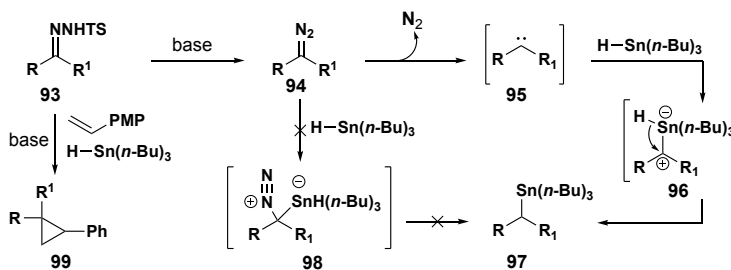


Figure 9. Donor/donor Sn–H insertion and potential mechanism

More recently, Franz and co-workers, in collaboration Shaw, developed conditions to undergo the first known stereoselective intermolecular Si–H insertion reaction with donor/donor carbenes to afford *chiral-at-silicon* products (Table 4, entries 1–2).³² After substantial optimization, this methodology demonstrated moderate to good enantioselectivity with catalyst **22** for the chiral silane products from symmetrical diazo compounds (Table 4, entry 1). Interestingly, when unsymmetrical, *prochiral* diazo compounds were used, enantioselectivity was more pronounced, giving up to 95:5 er, in addition to giving good to excellent diastereoselectivity (Table 4, entry 2).

entry	R ¹	R ²	R ³	R ⁴	dr	er	catalyst	# examples	yield range (%)
1	Ar	R ¹	alkyl, siloxy	H	NA	50:50 to 86:14 ^[b]	22	15	45-91
2	Ar	Ar ≠ R ¹	H, alkyl, aryl	H	61:39 to >95:5	61:39 to >95:5	22	9	55-95
3	aAr	Ar ≠ R	CH ₃ , Et, siloxy	R ³	NA	68:32 to 99.5:0.5 ^[c]	32	49	36-96

[a] Ar = Ph, substituted Ph, naphthyl, indolyl. [b] er denotes chirality at silicon. [c] er denotes chirality at carbon.

Table 4. Si–H insertion scope continued

Although ‘donor substituents’ on a carbene are typically aryl or alkyl, Micouin developed a unique donor carbene using alkynyl and trimethylsilyl substituents (Figure 10).³³ Using Rh₂(esp)₂ as catalyst, these carbenes resulted in excellent selectivity in Si–H insertions, though limited to 3° silanes and moderate yields. It was suggested that these donor carbenes are among the least electrophilic carbenes and could give very high levels of selectivity. and dioxane without observing any products from O–H, N–H, and C–H insertions. Cyclopropanation reactions with rhodium or copper catalysts was also unsuccessful, demonstrating the low electrophilicity and concomitant chemoselectivity of these carbenes.

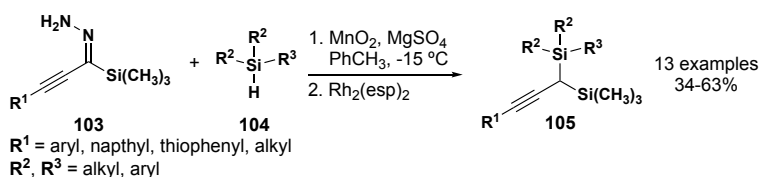


Figure 10. Si–H insertion reactions with alky/silyl carbenes

P–H insertion reactions result in alkyl phosphonates which are useful reagents in a variety of synthetic procedures. In 1990, Arbuzov and co-workers reported a method to synthesize dialkyl phosphonates by P–H insertion from donor/donor copper carbenes and hydrogen phosphites.³⁴ Aryl/aryl diazo species **107** and hydrogen phosphites resembling **106** were added to a refluxing solution of the copper catalyst to afford 5 examples of dialkyl phosphonates **108** in moderate yields (Table 5, entry 1). More recently, Wu and co-workers expanded P–H insertions to aryl phosphites, utilizing copper carbenes derived

from tosylhydrazones.¹⁹ This work reports the formation of alkylated diaryl phosphine oxides and alkylated dialkyl phosphonates in good yields and without any reported Bamford-Stevens type elimination products (Table 8, entry 2). Currently, no stereoselective variant is known.

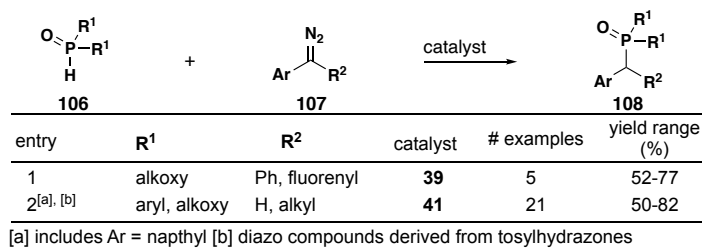


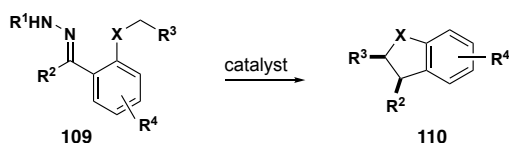
Table 5. P–H insertion scope

2.1.4.3 C–H Insertion Reactions of Donor/donor Carbenes

The functionalization of unactivated C–H bonds, namely sp³ C–H bonds, has been an attractive target in synthetic organic chemistry for decades.^{35,36} The ubiquity of this motif in all organic molecules and the potential for dramatic increases in the chemical and stereochemical diversity of simple starting materials have placed C–H activation/insertion methodology at the forefront of transition metal catalysis. While efforts towards intermolecular C–H insertion with acceptor-substituted metal carbenes have been successful, there are still only a few examples employing donor/donor carbenes. Intramolecular C–H insertion reactions with donor-substituted carbenes, on the other

hand, have been proven to proceed with high degrees of selectivity for a broad span of substrate classes.⁸

The most common C–H insertion products are benzene-fused 5-membered cyclic products, which are frequently generated with excellent stereoselectivity (Table 6). Che and co-workers first demonstrated this bond-construction using ruthenium porphyrin catalysts. Using these catalysts, they achieved the synthesis of benzodihydrofurans and a single example of an indoline using carbenes generated from tosylhydrazone precursors (Table 6, entries 1–2).^{1,37} As a result of the elevated temperatures required for the reaction to occur, reaction yields and diastereoselectivities were variable.



entry	R ¹	R ²	R ³	X	catalyst	# examples	yield range	dr (cis:trans)	er
1	Ts	methyl	PMP	O	Ru(TTP)(CO)	1	77	>98:2	-
2	Ts	methyl, Ph	Ar, ^a alkyl, CO ₂ CH ₃	O, NCH ₂ R ^{3b}	Ru(TTP)(CO)	8	62-89	34:66 to 99:1	98:2 ^c
3	H	Ar, ^a alkyl	Ar, alkyl, H, allylic ^d	O, NTs, CH ₂ ^e	Rh ₂ (<i>R</i> -PTAD) ₄	19	66-99	88:12 to 99:1	68:32 to 99:1
4	H	substituted Ph	PMP	O	Rh ₂ (<i>S</i> -TFPTTL) ₄	1	87	>95:5	98:2
5	H	Ar ^a	Ar, ^a alkyl	NR ^{5f} , CH ₂ , S	Rh ₂ (<i>R</i> -PTAD) ₄	22	65-99	80:20 to >95:5	75:25 to 99.5:0.5

^aAr = Ph, substituted Ph. ^bOne example where R³ = Ph. ^cOne example using Ru^{II}(D -Por*)(CO)] (D -H Por* = 5,10,15,20-tetrakis[(1*S*,4*R*,5*R*,8*S*)-1,2,3,4,5,6,7,8-octahydro-1,4:5,8-di-methanoanthracene-9-yl]porphyrin). ^dIncludes one example of R³ = propargylic (76%, 95:5 dr, 68:32 er). ^eOne example of X = NTs (98% 87:13 er) and one example of X = CH₂ (74%, >97:3 dr, 88:12 er). ^fR⁵ = H, Ts, alkyl.

Table 6. Previous work on intramolecular C–H insertion reactions of Donor/Donor carbenes

Our lab subsequently showed that not only could diazo formation be achieved at ambient temperature by MnO₂ oxidation of unsubstituted hydrazones, but also that metal carbene formation occurs rapidly at ambient or even reduced temperatures in the presence of dirhodium tetracarboxylates (occasionally referred to as paddlewheel

complexes).³⁸ Although initial reactions with achiral rhodium complexes showed only modest reactivity and diastereoselectivity, the use of chiral rhodium catalyst Rh₂(R-PTAD)₄ improved both the yield and diastereoselectivity while additionally enabling high degrees of enantioselectivity (Table 6, entry 3). This method was subsequently employed as the key bond constructing step for our synthesis of *E*- δ -viniferin, representing the first enantioselective synthesis of an oligoresveratrol natural product.³⁸

While relatively little is known about the exact mechanism(s) of insertion reactions with donor/donor carbenes, they can potentially undergo C–H/X–H insertion by several proposed pathways. Although both singlet and triplet carbenes are considered for reactions involving free carbenes, transition metals are known to stabilize the singlet carbene spin state to the degree that it becomes the energetic ground state.^{39–42} As such, transition metal catalyzed carbene reactions for C–H/X–H insertions are typically considered in the singlet state, supported by experimental selectivity and computational data.^{43–45}

Mechanistic insight into C–H insertion reactions with donor-substituted metal carbenes is currently limited to intramolecular reactions. For this process, discrete transition states have been proposed (Figure 11). The concerted pathway involves a three-centered transition state **115**, while the stepwise pathway produces a zwitterionic intermediate **113**. In support of the mechanism first proposed by Doyle,⁴¹ Nakamura and co-workers performed DFT calculations for acceptor-substituted rhodium carbenes, demonstrating a three-center concerted transition state.⁴⁶ This mechanism is corroborated implicitly or explicitly in several investigations into various donor-substituted

carbene insertions.^{7,23,47–49} In our previous work, the calculated reaction coordinate for a benzodihydrofuran substrate (e.g. Table 6) showed two discrete local maxima: one for hydride transfer and one for C–C bond formation, indicating the brief existence of an zwitterionic intermediate, i.e. a *stepwise mechanism* (Figure 11, **113**).⁹ Given the breadth of intramolecular insertion substrates to date, it is likely that changes to the substrate (e.g. substituents at the inserting carbon, the steric and electronic character of the carbene, and/or the size of the ring that is formed) can shift the pathway from stepwise to concerted. As donor/donor carbenes continue to be studied, additional experimental and computational mechanistic data will shed light on the factors that favor one pathway or the other.

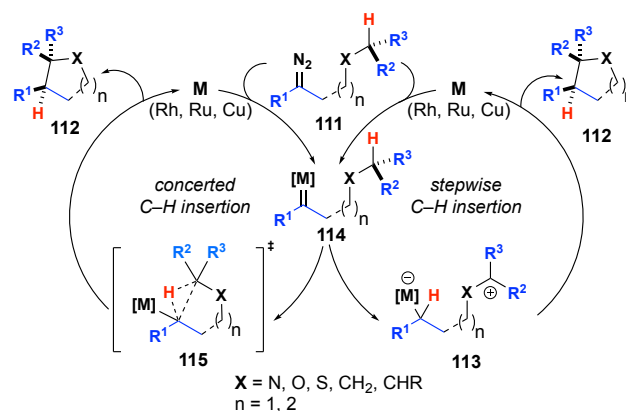


Figure 11. C–H insertion reaction mechanism summary.

2.1.4.4 Diazo-free Insertion Reactions of Donor/donor Carbenes

The presence of a diazo precursor in carbene formation presents a large safety and handling concern in carbene insertion chemistry. Diazo compounds are potentially explosive and handling them at large scale increases that risk. Therefore, it is often times

preferable or even necessary to explore diazo-free insertion methods, especially as reaction scale increases. Despite the focus of this chapter on carbenes generated from diazo precursors, examples of diazo-free insertion reactions are included in this part of the chapter with the intention of informing readers how to overcome their inherent risks.

Several methods have been developed to generate donor-substituted metal carbenes without diazo precursors. Most prominently, enynones, retro-Büchner ring expansion intermediates, and cyclopropenes can be manipulated in the presence of a transition metal catalyst to form the reactive carbene (Figure 12). Coordination of the alkyne moiety of an enynone (**116**) to a suitable rhodium or gold catalyst allows for the rearrangement of the structure to form a furyl-substituted metal carbene (**117**). Similarly, the alkene moiety of a strained cyclopropene (**118**) can coordinate to a rhodium or zinc catalyst, facilitating ring-opening and the formation of vinyl carbene (**119**). Finally, when the retro-Büchner ring expansion intermediate (**120**) is exposed to a rhodium or gold catalyst, the norcaradiene is decomposed to form a metal carbene (**121**) and benzene. These metal carbene species may then be used in further intra- or intermolecular insertion reactions.

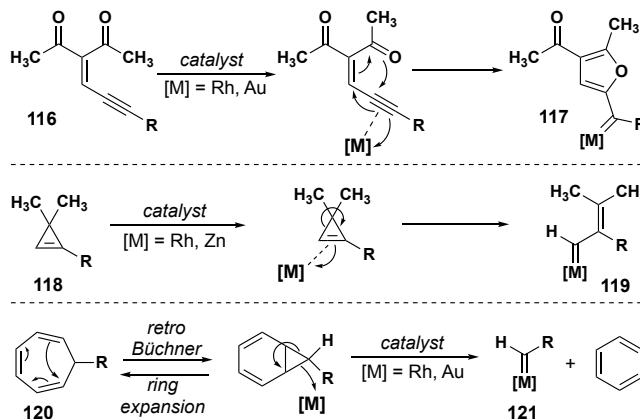


Figure 12. Donor-substituted metal carbene formation from diazo free substrates

Recent work by Zhu (South China University of Technology) circumvents potential safety issues through a novel *diazo-free* generation of donor/donor metal carbenes from the cyclization of enynes.⁵⁰ These metal carbenes then undergo diastereoselective and enantioselective C–H insertion to form furyl-substituted dihydroindole and dihydrobenzofuran structural cores (Table 7). Entry 1 demonstrates the utility of the methodology with a broad variety of both oxygen and *N*-acyl substrates; nearly all examples gave excellent diastereo- and enantio-selectivity at low catalyst loadings (1–5 mol %). Entry 3 describes the application of this methodology with a furyl/alkyl carbene, affording excellent yields of the tetrahydrofuran product but with diminished stereoselectivity compared to entry 1.

C–H insertion substrates with allylic or propargylic insertion sites often suffer from competing cyclopropanation (and cyclopropenation) reactions. Zhu and co-workers expanded upon their diazo-free methodology to include chemoselective reactions with

allylic and alkyl substrates by using an alternative catalyst.⁵¹ The dirhodium carboxylate catalyst used in entries 1 and 3, when applied to allylic insertion sites for *N*-acyl substrates, was found to give tetrahydroquinoline cyclopropanation products with excellent stereoselectivity. Outside of C–H insertion reactions, Zhu found that these diazo-free donor and donor/donor carbenes generated from enynones are productive in N–H, O–H, and Si–H insertion reactions, in addition to cyclopropanation reactions with gold catalysis (Figure 13).⁵² In a more recent report, Zhu and co-workers (Nankai University) used rhodium paddlewheel complexes with these enynone derived diazo-free carbenes to achieve enantioselective Si–H insertion for a wide selection of substrates.⁵³

entry	X	R ¹	R ²	R ³	dr	er	catalyst	# examples	yield range (%)
1 ^[a]	O, NAc	alkyl, alkoxy	alkyl	alkyl, alkenyl, NA	61:39 to >95:5	50:50 to >99:1	24	29	65-99
2 ^[c]	NAc	alkyl, alkoxy, Ph	alkyl, Ph	alkyl, alkenyl, NA	Ar ^[b]	91:9 to >99:1	33	34	43-97
3 ^[a]	NA	CH ₃	CH ₃	alkenyl, Ph		77:23 to 95:5 ^l	24	3	99

[a] reactions run -20 to -30 °C. [b] Ar = Ph, substituted Ph, naphthyl (entry 1); Ar = Ph, substituted Ph (entry 2). [c] reactions run 80-120 °C

Table 7. Diazo-free C–H insertion reactions of donor/ donor carbenes

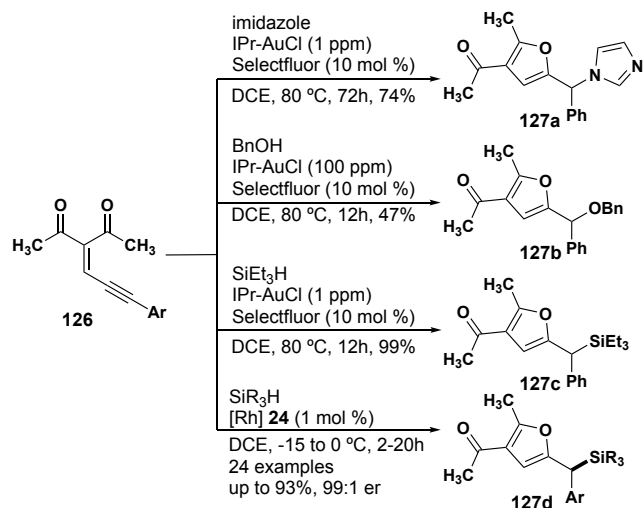


Figure 13. Diazo-free N–H, O–H, and Si–H insertion reactions with enynone-derived donor carbenes.

Echavarren and co-workers were able to generate diazo-free donor carbenes through a retro-Büchner ring expansion (Figure 14). With gold phosphine catalyst **49**, intramolecular C–H insertion to form an indane was achieved as the minor product, affording mostly cyclopropanation products.⁵⁴ In more recent efforts, the Echavarren group used dirhodium paddlewheel complex Rh₂(TFA)₄ (**27**) to better effect, generating numerous intermolecular Si–H insertion products (Figure 14).⁵⁵

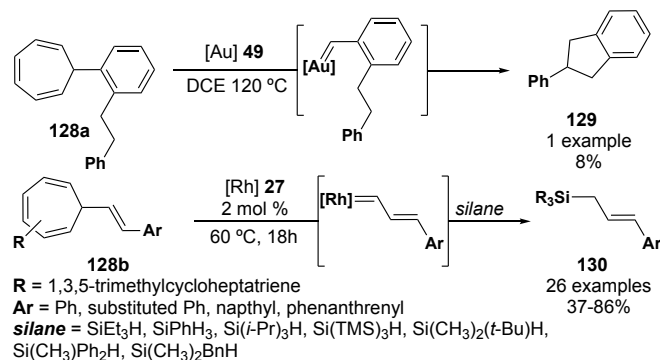


Figure 14. Formation of carbenes through retro-Büchner ring expansion

Another robust method for generating diazo-free donor metal carbenes is by the ring opening of substituted cyclopropenes. Early efforts by Cossy and co-workers demonstrated an impressive substrate scope using this method for intramolecular C–H insertion (Figure 15, **131-133**). With $\text{Rh}_2(\text{OAc})_4$ as the catalyst, substituted pyrans (**133**) were achieved with excellent diastereoselectivity at low catalyst loadings (0.5 mol %); a desymmetrization experiment furthermore demonstrated excellent stereoselectivity, affording **133** ($\text{R}^2 = \text{CH}_2\text{CH}_2\text{OR}$) as a single diastereomer. The authors also offered intriguing stereoselectivity models for these novel substrates and produced convincing evidence for a concerted mechanism for these insertion substrates *via* stereospecific deuterium labling experiments.⁴⁷

Vicente and co-workers also used substituted cyclopropenes as diazo-free donor metal carbene precursors with significant success. In a simple and cost-effective system using zinc bromide as the metal catalyst, Vicente was able to generate structurally unique allyl silanes (26 examples) from a variety of substrates and various silanes/siloxanes (Figure 15, **134-136**).⁵⁶ Notably, this method was applied in Ge–H insertion for the first ever zinc-catalyzed insertions into germanium hydrides. In a later report by Vicente and co-workers, cyclopropene-derived rhodium octanoate (**23**) carbenes were used to generate a broad scope of substrates (>35 examples) *via* intermolecular Si–H insertion reactions (Figure 15, **137-139**). This method was effective at low catalyst loadings (1 mol %) and tolerated other traditionally reactive moieties on the substrate (i.e. phenols,

allyl benzyl groups). For a specialized class of substrates, intramolecular Si–H insertion reactions were also achieved to produce racemic cyclic siloxanes. While these researchers have had considerable success with these diazo-free methodologies, there are still many opportunities to expand substrate scope, further develop enantioselective variants, and introduce new orthogonal diazo-free methods.

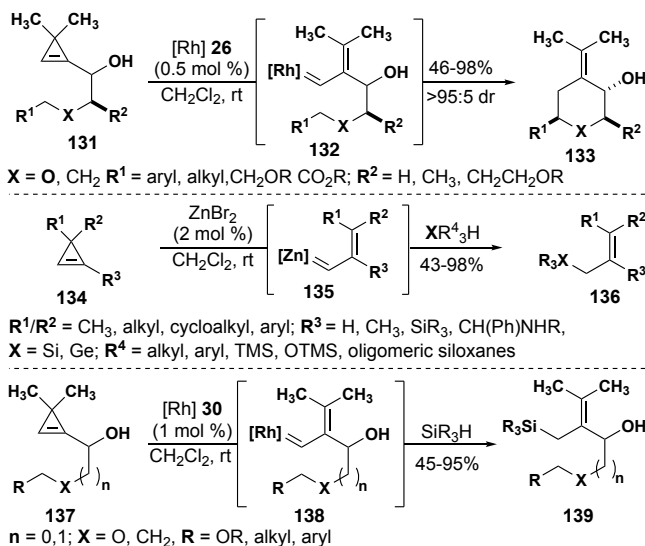


Figure 15. Cyclopropene-derived donor carbene insertion reactions.

2.1.5 Intramolecular C–H Insertion Reactions to Form Indolines and Indanes

Pioneering work in our group has developed the use of donor/donor metal carbenes for enantioselective C–H insertion reactions to form benzodihydrofurans.^{9,38} Using our methodology, we were interested in exploring insertion reactions utilizing substrates to form indolines and indanes, which are valuable motifs in many natural products and drug targets (Figure 16).^{57–59}

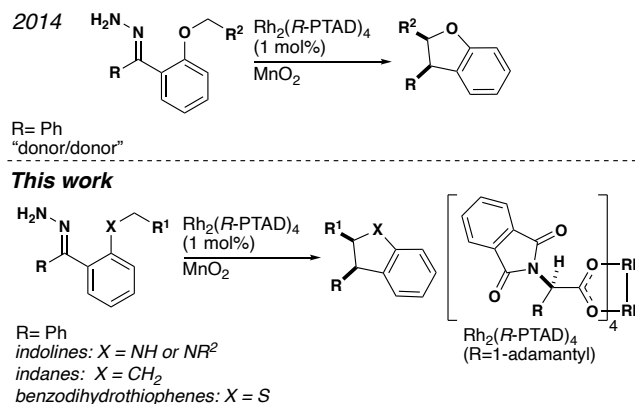


Figure 16. Summary of our previous work and this work

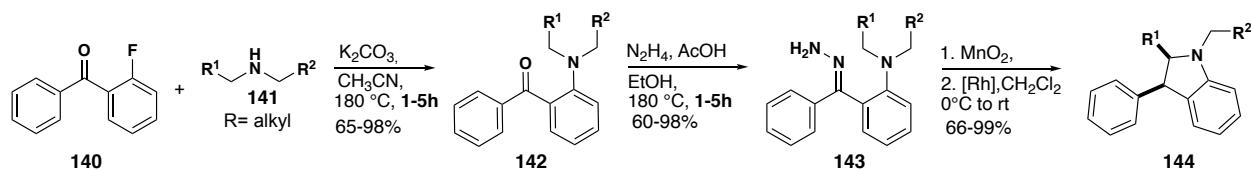
Although these heterocycles can be prepared by a variety of strategies, formation of the C2–C3 bond by C–H insertion offers the opportunity to create two stereogenic centers at once.⁶⁰ Intermolecular C–H insertion has been used previously for the synthesis of indolines, however few examples of substrates containing basic nitrogen have been shown to proceed with high levels of enantioselectivity.^{61–66} We documented the first enantioselective synthesis of an indoline from a donor/donor carbene, albeit with modest enantioselectivity, on a substrate lacking a basic nitrogen atom.³⁸ Recently, Zhu et. al. reported the enantioselective synthesis of indolines from donor/donor carbenes via a non-diazo approach.⁵⁰ Inspired by this approach, we set out to establish a robust method to construct indolines and indanes via C–H insertion reactions of donor/ donor carbenes.

2.2 Results

2.2.1 Indolines

To generate a wide range of indoline products, we developed a modular substrate synthesis (Scheme 1). 2-fluorobenzophenone **140** was coupled to amine **141** by an

S_NAr reaction. Next, the resultant ketone was treated with hydrazine and acetic acid to form hydrazone **143**. Hydrazone **143** could then be oxidized and treated with the requisite dirhodium catalyst to generate indoline **144**.



Scheme 1. Indoline substrate synthesis

A variety of indolines were synthesized with high levels of diastereo- and enantioselectivity (Figure 17). Fused indolines derived from cyclic anilines (**146a-d**) were formed in good to excellent er, dr, and yield. C–H Insertion into primary centers is known to be electronically unfavorable,^{67–69} however, indoline **146e** was produced in high yield and modest er. Increasing the steric demand of a methyl substituent to an ethyl substituent had a drastic effect on the enantioselectivity of the reaction, as indoline **146f** was produced as primarily one enantiomer. This observation suggests that increased steric bulk at the insertion center plays a key role in the high degree of stereoselectivity observed. An indoline derived from an *N*-tosyl protected amine was also tolerated (**146b**) allowing for further modification after deprotection. Additionally, hydrazone **145g** derived from a free amine was synthesized in excellent er, dr and yield (**146g**). X-ray crystallography of **146c** indicated that the relative and absolute configurations of the product were consistent with the sense of induction observed for the formation of benzodihydrofurans in our previous work.

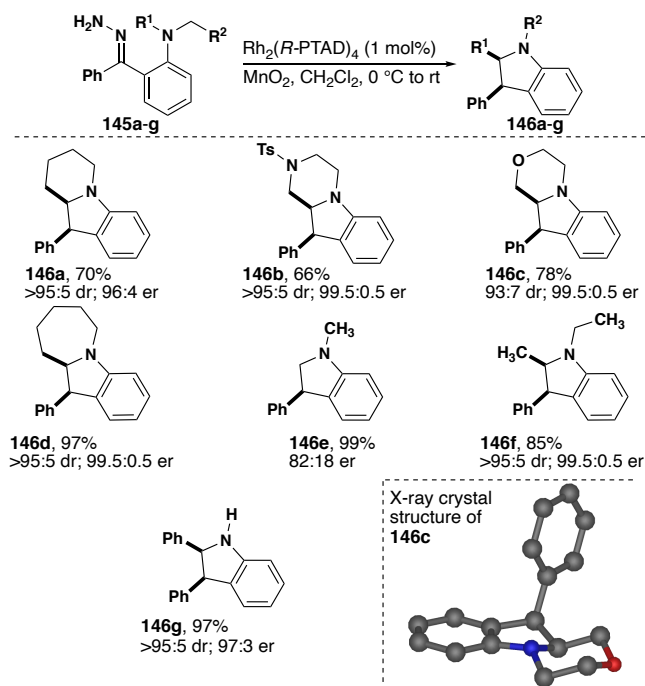


Figure 17. Indolines synthesized by C–H insertion reactions of donor/donor carbenes

A number of free amine containing indoline substrates were synthesized in an attempt to replicate the result of compound **146** (Figure 18). A free amine is an attractive functional group to target because it represents a benchmark for a high level of functional group tolerance for a particular reaction and additionally serves as a chemical handle for subsequent reactions. However, under optimized reaction conditions none of the desired products were observed. In each case treatment of the requisite hydrazone produced a complex reaction mixture with no identifiable major product. We hypothesize that this is due to the highly Lewis basic nature of the secondary amine, as well as the proclivity for N–H insertion reactions to occur.

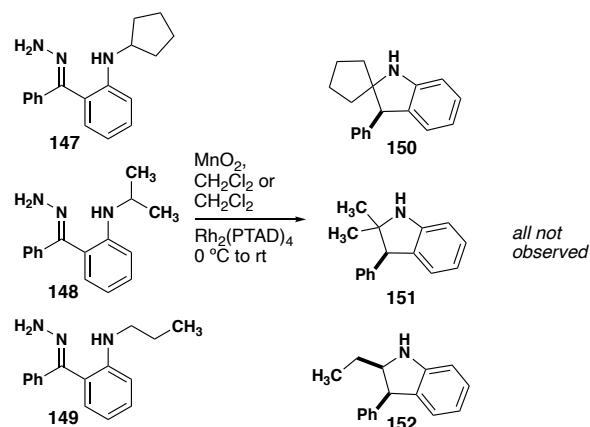
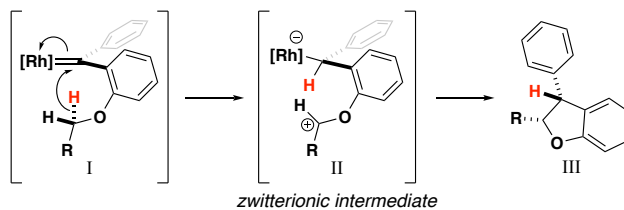


Figure 18. Secondary amine indoline substrates

2.2.2 Mechanistic Studies

Over the course of our synthesis of indolines, it became apparent that unsymmetrical aniline substrates presented the opportunity to insert into two chemically different C–H bonds. Inspired by mechanistic studies performed in our previous work,⁹ we set out to test the effects of steric bulk and electronics on the regiochemical outcomes of C–H insertion reactions to form indolines. In the case of benzodihydrofurans, the insertion proceeds stepwise, beginning with a hydride transfer followed by rapid collapse of the resultant zwitterionic intermediate II (Scheme 2). From an electronic perspective, insertion is favored by substituents that stabilize cations at the insertion carbon. From a steric perspective, on the other hand, steric demand near the insertion carbon can be unfavorable, especially when R paired with crowded chiral catalysts.



Scheme 2. Reaction mechanism postulated from our benzodihydrofuran work

To study the effects of shape and electronics on the regioselectivity of this chemistry, we synthesized a series of unsymmetrical hydrazones (**153a, b**) with both sterically and electronically favorable insertion sites (Table 7). In the presence of $\text{Rh}_2(\text{OAc})_4$, insertion at the more electronically favorable benzylic carbon of **153a** is observed, to form **155a** (Table 7, entry 1). Treatment with $\text{Rh}_2(\text{Mes})_4$ and $\text{Rh}_2(R\text{-PTAD})_4$, shows a decrease in selectivity for the electronically favorable center as the bulk of the catalyst increases (Table 7, entries 2, 3). When methyl is contrasted with isopropyl (**153b**), selectivity for the methyl carbon is modest with $\text{Rh}(\text{OAc})_4$ (Table 7, entry 4), and use of the $\text{Rh}_2(\text{Mes})_4$ catalyst heavily favors methyl insertion (entry 5). Finally, the reaction of **153b** with $\text{Rh}_2(R\text{-PTAD})_4$ also favors methyl insertion (**154b**), albeit to a lesser extent (Table 7, entry 6). The results indicate that both steric and electronic influences both play essential and often competing roles in determining the most favorable insertion pathway.

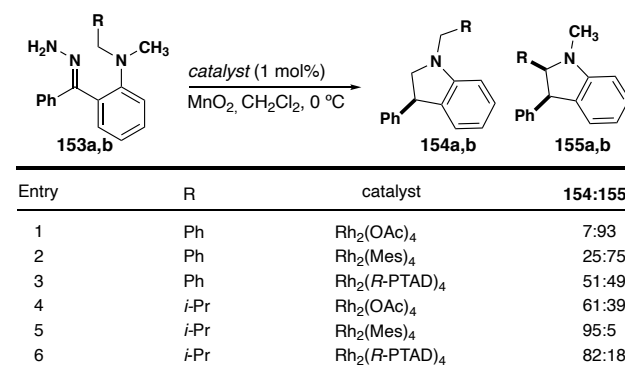
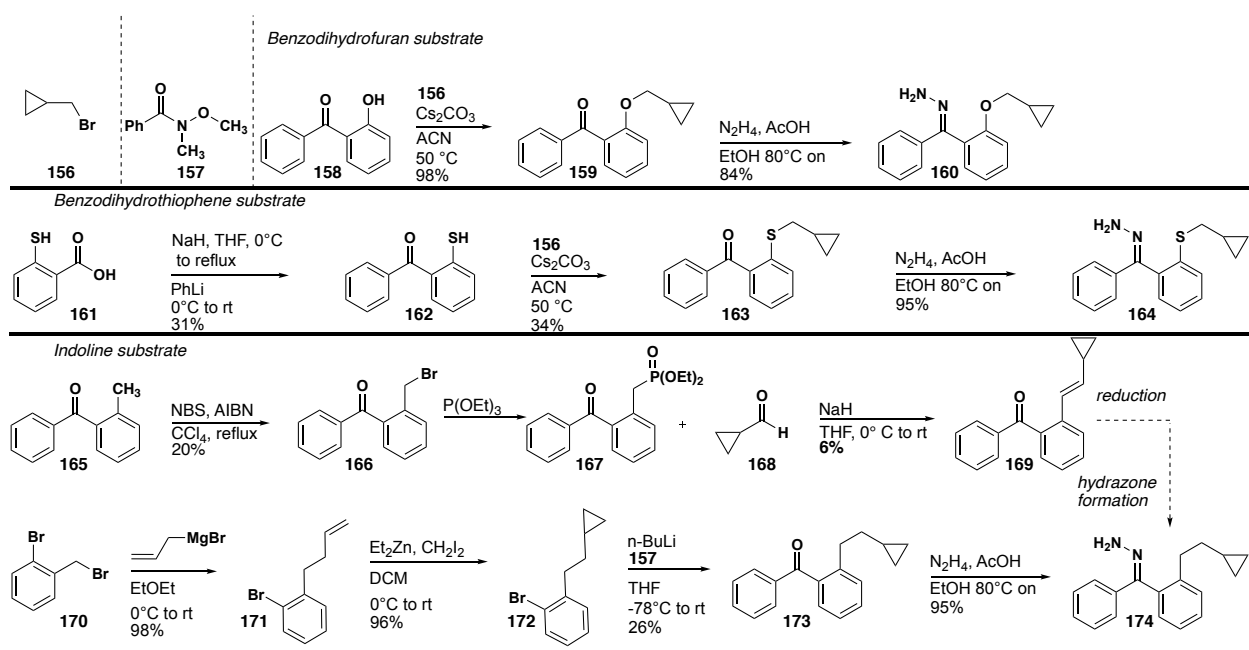


Table 7. Indoline regioselectivity study

We attempted to further probe the cationic character of the insertion carbon by synthesizing cyclopropane-based substrates (Scheme 3) with the intent of “trapping” the

cation via a ring expansion of the presumed zwitterionic insertion intermediate (Scheme 2, II). Firstly, we explored substrates leading to benzodihydrofuran products as most of the work in our lab up to this point has involved this class of substrates. The synthesis of the requisite hydrazone was carried out by alkylation of phenol **158** with bromide **156**, followed by hydrazone formation to yield **160**. We found that no ring expansion product was observed with **160** using the standard insertion conditions developed in the lab (Table 8, entries 1–3).



Scheme 3. Synthesis of cyclopropane derivatives

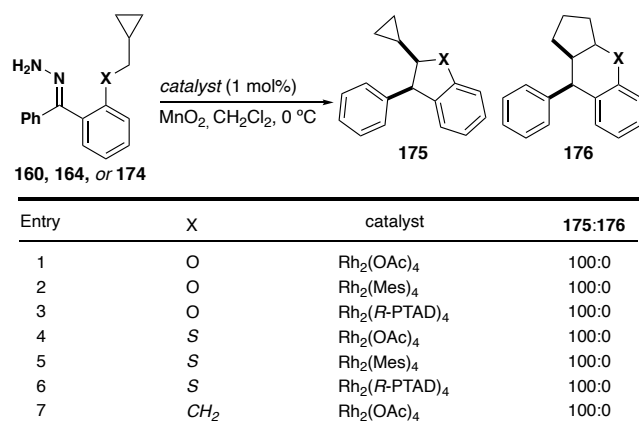


Table 8. Insertions of cyclopropane derivatives ratio of **175:176** measured by ¹H NMR

Following this result, we hypothesized that the insertion reaction was much faster than the desired ring expansion. To slow down the insertion reaction, we synthesized a less reactive sulfur substrate **164**. This involved the synthesis of thiol **162** by phenyl lithium addition to carboxylic acid **161**. Similar to the benzodihydrofuran substrate, alkylation of **162** followed by hydrazone formation furnished the desired sulfur containing hydrazone **164**. In analogy with benzodihydrofurans, these substrates also exclusively favored the benzodihydrothiophene product as opposed to the ring expansion product (Table 8, entries 4–6).

A final attempt was made at cyclization using the highly deactivated indane derived hydrazone **174** (Scheme 3). Our first synthesis involved halogenation of ketone **165** by NBS. Next, phosphonation followed by a Horner Wadsworth-Emmons (HWE) reaction with aldehyde **168** furnished ketone **169**. However, the HWE reaction gave an unsatisfactory yield due to the enolization of aldehyde **168**, generating a large amount of the homo-aldol product. As such, a new route was developed wherein bromide **170** was alkylated with allyl magnesium bromide to produce arene **171**. Next, a Johnson-Corey-

Chaykovsky reaction was used to generate cyclopropane **172**. Lithium halogen exchange followed by addition to benzoic acid-derived Weinreb amide **157** gave ketone **173**. Finally, treatment with hydrazine furnished the desired indane hydrazone precursor **174**. Unfortunately, insertion of this substrate with our least active catalyst, $\text{Rh}_2(\text{OAc})_4$, did not produce any of the desired rearrangement products and thus no more reactions were carried out on this material (Table 8, entry 7).

2.2.3 Indanes

In our seminal publication, we demonstrated that the formation of indanes by C–H insertion of donor/donor metal carbenes was possible in good yield and with a modest degree of stereoselectivity. In this work, we expand the scope of this chemistry to include a variety of indanes in excellent yield and selectivity (Figure 19). The synthesis of aliphatic, spirocyclic, five- and six-membered rings were particularly effective (Figure 19, **178a** and **c**). Heteroatoms were also tolerated to generate the corresponding spirocycles **178d** and **e** including a Boc-protected amine. Although disubstitution at the inserting carbon creates a high level of steric crowding, it stabilizes carbocation formation at the insertion center more readily. As such, these substrates react to form quaternary carbons in high yield and with high levels of stereoselectivity (**178b**). The absolute configuration of the new stereogenic center was demonstrated to be *S*, upon treatment with $\text{Rh}_2(R\text{-PTAD})_4$ in agreement with the sense of induction for both benzodihydrofurans and indolines. Substitution of the carbene pendant groups with halogens was also tolerated with excellent selectivity (**178f** and **g**). Furthermore, *J*-values of the relevant protons of these

products were consistent with the *cis* diastereomer observed both in this work and in our previous work.

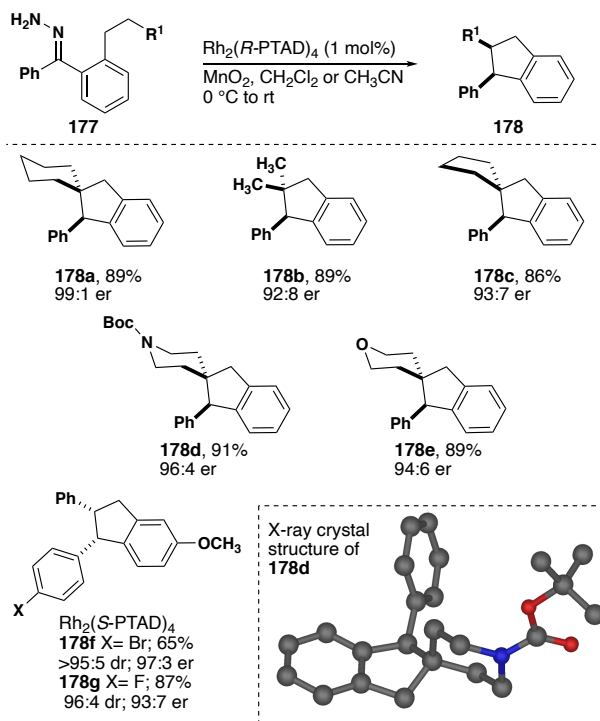
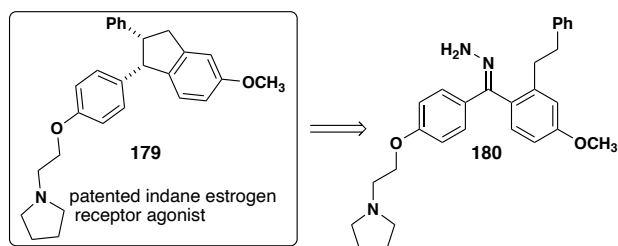


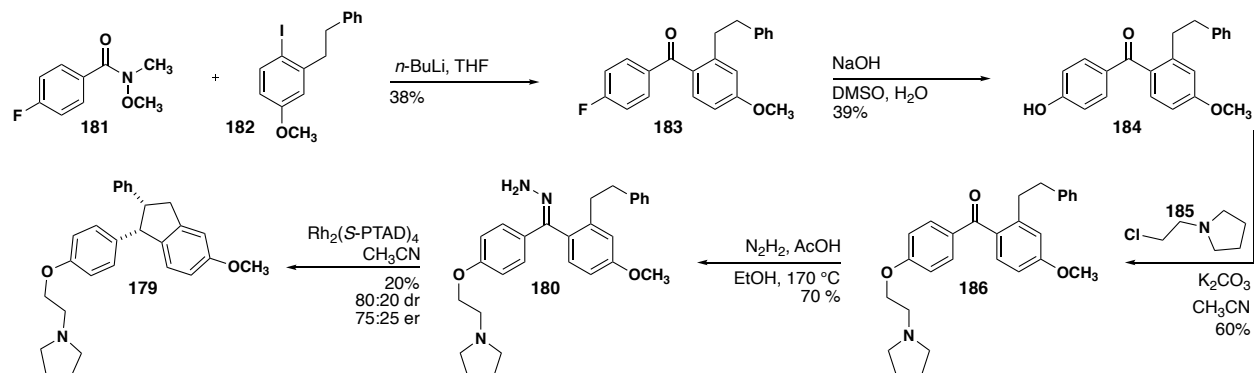
Figure 19. Indane reaction scope

2.2.4 Targeted Synthesis of Patented Indane Drug

Having established a robust method for the enantioselective synthesis of indanes, we decided to apply our method to the synthesis of a patented estrogen receptor agonist **179** (Scheme 4).⁷⁰ We hypothesized that the indane core of **179** could be accessed stereoselectively through our established methodology *via* insertion of hydrazone **180**. Therefore, the rest of the initial synthetic route was designed around the synthetic access of ketone **186** (Scheme 5).



Scheme 4. Retrosynthetic analysis of **179**



Scheme 5. Initial route to indane drug synthesis

Arene **182** was treated with butyllithium and Weinreb amide **181** yielding ketone **183**. However, the ortho substitution of ketone **183** proved troublesome to its synthesis which was reflected in its low yield. As such, extensive optimization was done (Table 9). First, the additions to the aldehyde were attempted with various organometallic sources and solvents (Table 9, entries 1–6). Of all the organometallic reagents used, *tert*-butyllithium led to the highest yield of product (Table 9, entry 2). Overall, the yield of these reactions was generally poor and extensive byproducts were observed resulting from over-alkylation. In order to eliminate potential byproducts resulting from over addition of the organometallic reagent to the aldehyde electrophile, reactions utilizing a benzyl-Weinreb amide were attempted (Table 9, entries 7–9). While the yield of these reactions was still poor, over alkylation was avoided and only product or proteo-deiodination were

recovered. Further changes in solvent and lithium source did not improve the yield by a significant margin and, as such, conditions in entry 7 were selected. Following the initial ketone synthesis, an S_NAr reaction with sodium hydroxide was used to install a phenol, followed by alkylation to furnish ketone **184**. Ketone **184** was then treated with hydrazine and acetic acid to furnish the desired hydrazone **180** in 70% yield.

Entry	R	Organometallic	Solvent	% Yield of XX
1	H	<i>n</i> -BuLi	THF	20
2	H	<i>tert</i> -BuLi	toluene	22
3	H	<i>i</i> -Pr-MgBr	THF	10
4	H	<i>n</i> -BuLi	EtOEt	12
5	H	<i>tert</i> -BuLi	toluene	18
6	H	<i>i</i> -Pr-MgBr	EtOEt	9
7	HNOCH ₃	<i>n</i> -BuLi	THF	38
8	HNOCH ₃	<i>tert</i> -BuLi	toluene	30
9	HNOCH ₃	<i>n</i> -BuLi	EtOEt	20

Table 9: Optimization of ketone **183** synthesis

The subsequent insertion reaction of hydrazone **180** also proved challenging (Table 10). Treatment with three of our previously highest performing catalysts under optimal conditions (Table 10, entries 1–3) showed that substrate **180** had remarkably low levels of reactivity. At the standard 0 °C to room temperature reaction conditions, the insertion reaction only proceeded when the highly electron-deficient catalyst Rh₂(TCPTTL)₄ was used (Table 10, entry 2). Changing the solvent had little effect on the reaction, however, refluxing finally caused the reaction to proceed with Rh₂(S-PTAD)₄, albeit with poor yields and stereoselectivity (Table 10, entry 6).

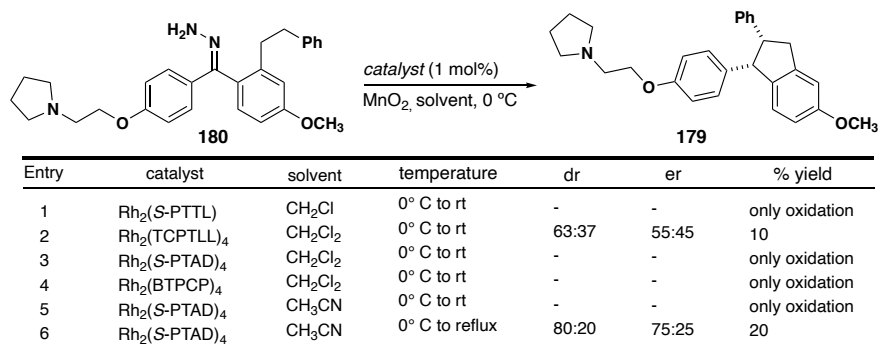
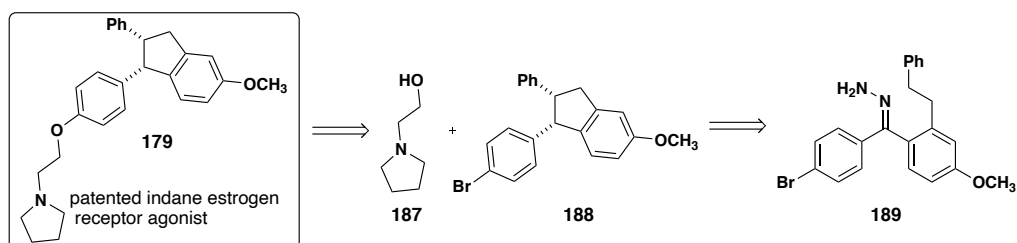


Table 10. Optimization of insertion reaction to synthesize **179**

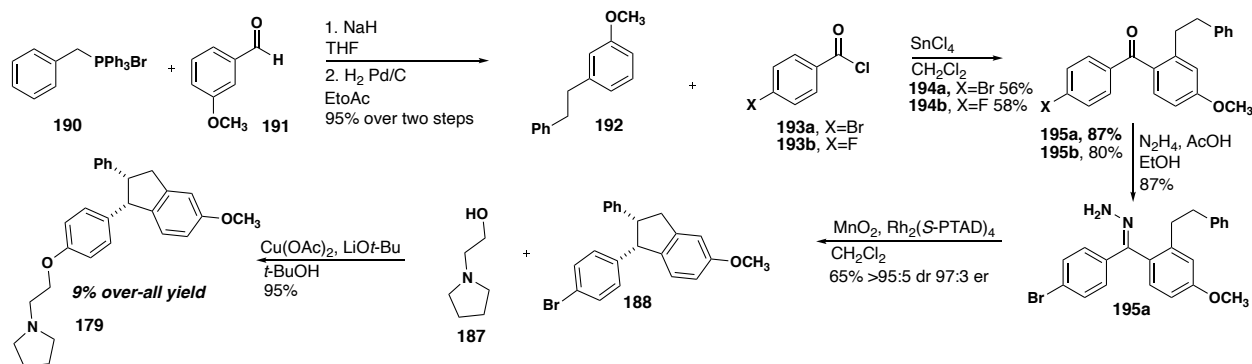
While these conditions ultimately yielded the desired product, we were unsatisfied with the low yield and poor levels of stereoselectivity. We hypothesized that the highly electron donating nature of the arene groups of hydrazone **180**, coupled with the presence of a Lewis basic tertiary amine, might be responsible for the subpar insertion result. As such, we decided to re-route the synthesis of **179** to include insertion of bromide **188** (Scheme 6). We hoped this would solve the electronic issues we were having while maintaining a bulky group on the arene, which might help with stereoselectivity and serve as a useful chemical handle. We planned to synthesize the final product by a modified Ullman coupling with commercially available amino alcohol **187**.



Scheme 6: Re-routed retrosynthesis including bromide **188**

To access bromide **188**, a Wittig reaction with **191** and **190** was carried out followed by reduction to furnish *meta*-substituted arene **192** in high yield over two steps

(Scheme 7). A Friedel-Crafts acylation was then conducted with acyl-chloride **193a** to produce ketone **194a**. Hydrazone formation followed by insertion using $\text{Rh}_2(\text{S-PTAD})_4$ yielded the desired indane core **188** in 65% (56% over two steps) with a high degree of stereocontrol. A modified Ullman coupling to install amino alcohol **187** produced the target compound in 95% yield after extensive optimization. Using this route, the synthesis of **179** was achieved in 6 steps with 9% overall yield.



Scheme 7. Enantioselective synthesis of patented estrogen receptor agonist **179**

Ullman coupling of bromide **188** was initially low-yielding and thus, required optimization. Initial results utilizing a literature precedent procedure (Table 11, entry 1) resulted in only 50% conversion by ^1H NMR. To combat this issue, the catalyst loading was increased up to stoichiometric amounts and still no increase in conversion was observed. We hypothesized that the catalyst might be getting poisoned, and the procedure was modified to allow for two portion-wise additions of 1 mol % catalyst between sessions of heating (Table 11, entry 5). We were pleased to see that this modification resulted in near quantitative yield of the desired coupled product **179**.

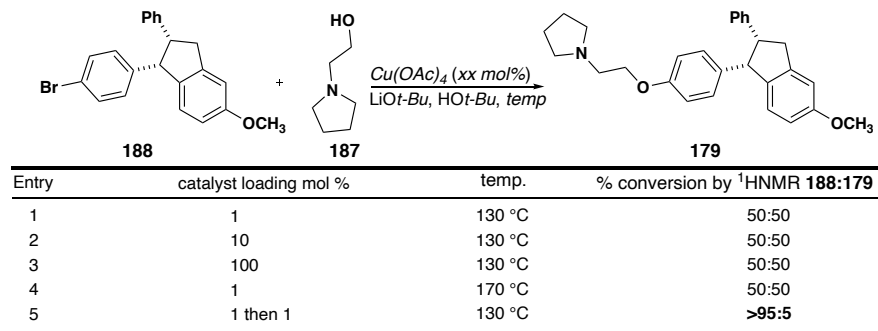


Table 11. Optimization of Ullman coupling

2.3 Conclusion

The construction of new carbon-carbon bonds is a fundamental endeavor of the organic chemist. Controlling the stereochemistry of their formation is arguably one of the most powerful methods chemists possess to control the downstream function of a molecule. Herein, we have presented a new method for the formation of indanes and indolines by intramolecular C–H insertion reactions of donor/donor carbenes. This methodology furnished a variety of indanes and indolines in moderate to high yields with a high degree of stereochemical control. Finally, this method development culminated in the first enantioselective synthesis of a patented drug molecule, highlighting the utility of this chemistry. Future work will focus on expanding this methodology to non-diaryl carbenes, and the construction of different sized heterocycles.

2.4 Experimental

General Comments. Chemicals were purchased and used without further purification unless otherwise specified. All reactions using anhydrous solvents were carried out under an atmosphere of industrial argon in flame-dried glassware with magnetic stirring. Anhydrous solvent was dispensed from a solvent purification system that passes solvent through two columns of dry neutral alumina. Reactions were monitored by thin layer chromatography (TLC, Merck), and detected by examination under UV light (254 nm and 365 nm). Flash column chromatography was performed using silica gel [230–400 mesh (40–63 μm)]. Extracts were concentrated *in vacuo* using both a rotary evaporator (bath temperatures up to 40 $^{\circ}\text{C}$) at a pressure of either 15 mmHg (diaphragm pump) or 0.1 mmHg (oil pump), as appropriate. High vacuum procedures were carried out at room temperature. ^1H and proton-decoupled ^{13}C spectra were measured in CDCl_3 at 400, or 600 MHz, and 101 or 151 MHz respectively unless otherwise noted. All spectra in CDCl_3 were referenced at TMS = 0 ppm. High-resolution mass spectrometry was performed on positive mode and ESI ionization techniques were used, unless otherwise noted. Melting points were taken on an EZ-melting apparatus and were uncorrected. Infrared spectra were taken on a Bruker Tensor 27 spectrometer. All microwave experiments were run in a biotage initiator EXP EU 400W microwave synthesizer 2.0 serial number 11031.

General Procedure A (nucleophilic aromatic substitution). To an oven-dried 20 mL microwave vial was added K_2CO_3 (3 equiv). The vial was evacuated under vacuum and backfilled with argon. To the vial was added DMF or CH_3CN (1.0 M), the respective amine (1.2 equiv), and 2-fluorobenzophenone (1 equiv). The mixture was heated to 180 °C in a microwave reactor for 2-4 hours. Upon completion by TLC, the crude mixture was poured into water (50 mL) and extracted with CH_2Cl_2 (3 x 75 mL). The combined organic layers were dried over Na_2SO_4 , filtered, and concentrated *in vacuo*. The crude reaction mixture was purified by flash column chromatography or recrystallization to yield the desired ketone.

General Procedure B (alkylation of 2-mercaptobenzophenone). To a flame-dried 50 mL round bottom flask was added 2-mercaptobenzophenone (1.0 equiv). The flask was evacuated under high vacuum and backfilled with argon. To the flask was added acetonitrile (0.1 M), the respective bromide (1.3-1.5 equiv), and K_2CO_3 or Cs_2CO_3 (3 equiv). The mixture was then heated to 65 °C for 18 hours and then cooled to room temperature. The reaction was gravity filtered through fluted filter paper to remove K_2CO_3 or Cs_2CO_3 . The filtrate was concentrated *in vacuo* and the crude mixture was purified by flash column chromatography.

General Procedure C (alkylation of 2-mercaptobenzophenone). To a flame-dried 50 mL round bottom flask was added 2-mercaptobenzophenone (1.0 equiv). The flask was evacuated under high vacuum and backfilled with argon. To the flask was added acetonitrile (0.1 M), the respective bromide (1.3-1.5 equiv), and K_2CO_3 or Cs_2CO_3 (3

equiv). The mixture was then stirred at room temperature for 18 hours. Upon completion by TLC, the reaction was gravity filtered through fluted filter paper to remove K_2CO_3 or Cs_2CO_3 . The filtrate was concentrated *in vacuo* and the crude mixture was purified by flash column chromatography.

General Procedure D (microwave hydrazone formation). To an oven-dried 5-25 mL argon backfilled microwave vial was added a solution of the respective ketone (1 equiv) in anhydrous EtOH (0.1 M). To the vial was added AcOH (2 equiv) and anhydrous hydrazine (10 equiv). The vial was heated in a microwave reactor at 170 °C for 2-5 hours. The reaction mixture was then concentrated *in vacuo*, dissolved in diethyl ether (50 mL), and washed with H_2O (3 x 30 mL). The organic layer was dried over Na_2SO_4 , filtered, concentrated *in vacuo*, and purified by flash column chromatography to yield the desired hydrazone.

General Procedure E (hydrazone formation). Following literature precedent,⁽¹⁾ to the desired alkylated benzophenone (1 equiv) in anhydrous EtOH (0.06 M) was added anhydrous hydrazine (12-20 equiv.) and glacial acetic acid (1.2 equiv). The reaction was heated to 80 °C for 18-120 h with additional hydrazine and AcOH added as needed if poor conversion was observed by TLC. The reaction was allowed to cool and EtOH was removed *in vacuo*. The residue was taken up in diethyl ether (30 mL) and H_2O (20 mL). The layers were separated, and the organic layer was washed with H_2O (2 x 20 mL). The combined organic layers were dried over Na_2SO_4 , filtered, and concentrated *in vacuo*.

General Procedure F (reduction after hydrazone). Argon was bubbled through a solution of the crude hydrazone from general procedure E (1 equiv) in CH_3OH (0.3 M) for

15 minutes. 10% Palladium on carbon (0.05-0.1 equiv) was added and argon was bubbled through the mixture for an additional 5 minutes. The reaction was sparged with H₂ (g) for 5 minutes and then stirred for 18-28 h at room temperature under 1 atm of H₂ (g). The crude product was filtered through Celite with CH₂Cl₂ and concentrated *in vacuo*. In some cases, the ¹H NMR of the crude reaction mixture showed incomplete conversion and the crude material was resubmitted under the same reaction conditions for an additional 18 h. The crude product was purified by flash column chromatography using 2-40 % EtOAc:hexanes as the eluent on neutral alumina.

General Procedure G (sequential one-pot insertion). To a flame-dried 7 mL scintillation vial under argon atmosphere was added the desired hydrazone (1 equiv) followed by anhydrous CH₂Cl₂ or CH₃CN (0.01 M). To the vial was added MnO₂ (8 equiv). The resulting dark suspension was stirred until full conversion of the starting material was observed by TLC. Upon pausing stirring, a color change from clear to magenta was observed from formation of the diazo. The vial was then cooled to 0 °C and the desired rhodium catalyst was added (0.01 equiv). The reaction mixture was warmed to room temperature and allowed to react from 10 min to 12 h. The crude reaction mixture was filtered over Celite to remove MnO₂, concentrated *in vacuo*, and purified by flash column chromatography to yield the desired insertion product.

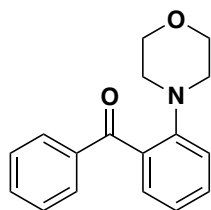
General Procedure H (two-pot insertion). To a flame-dried scintillation vial under argon atmosphere was added the desired hydrazone (1 equiv) followed by anhydrous CH₂Cl₂ or CH₃CN (0.01 M). To the vial was added MnO₂ (8 equiv). The resulting dark suspension was stirred until full conversion of the starting material was observed by TLC. The reaction

mixture was filtered over Celite into a new flame-dried, argon backfilled 20 mL scintillation vial using the same solvent. The magenta solution was cooled to 0 °C and the desired rhodium catalyst was added (0.01 equiv). The reaction mixture was warmed to room temperature and allowed to stir from 10 min to 12 h. The crude reaction mixture was concentrated *in vacuo* and purified by flash column chromatography to yield the desired insertion product.

General Procedure I (one-pot insertion). To a flame-dried scintillation vial under argon atmosphere was added the desired hydrazone (1 equiv) followed by anhydrous CH₂Cl₂ or CH₃CN (0.01 M). The vial was cooled to 0 °C and MnO₂ (8 equiv) and the desired rhodium catalyst (0.01 equiv) were added. The resulting dark suspension was warmed to room temperature and allowed to stir from 10 min to 12 h. The crude reaction mixture was filtered over Celite, concentrated *in vacuo*, and purified by flash column chromatography to yield the desired insertion product.

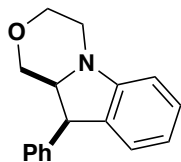
Note: Hydrazones were often isolated as a mixture of *E/Z* isomers or used without further purification. As such ¹H NMR peaks have been reported only for selected examples.

INDOLINES

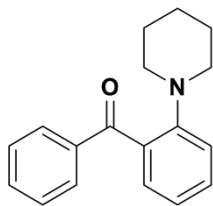


(2-morpholinophenyl)(phenyl)methanone (196) was synthesized according to general procedure A using 2-fluorobenzophenone (2.0 mL, 12 mmol), morpholine (1.2 mL, 14

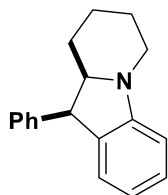
mmol), K₂CO₃ (4.90 g, 35.5 mmol) and CH₃CN (2.4 mL). The crude product was purified by flash column chromatography (10:90, EtOAc:hexanes) affording **196** as a yellow solid (286 mg, 90%). ¹H NMR (400 MHz, CDCl₃) δ 7.75 (dd, *J* = 8.3, 1.4 Hz, 2H), 7.59 – 7.52 (m, 1H), 7.51 – 7.37 (m, 4H), 7.16 (td, *J* = 7.5, 1.1 Hz, 1H), 7.07 (dd, *J* = 8.1, 1.0 Hz, 1H), 3.31 – 3.26 (m, 4H), 3.04 – 2.84 (m, 4H). Proton NMR data of the crude material was consistent with the reported literature values.⁷¹



10-phenyl-3,4,10,10a-tetrahydro-1H-[1,4]oxazino[4,3-a]indole (146c) was synthesized according to general procedure H using hydrazone **145c** (23 mg, 0.083 mmol), MnO₂ (58 mg, 0.66 mmol), and Rh₂(*R*-PTAD)₄ (1 mg, 0.0006 mmol) in CH₂Cl₂ (0.01 M). The crude product was purified by flash column chromatography (7:93, EtOAc:hexanes) affording **68c** as a white solid (16 mg, 78%, 100:0 er, 93:7 dr). ¹H NMR (400 MHz, CDCl₃) δ 7.25 (m, , 3H), 7.18 (td, *J* = 7.7, 1.3 Hz, 1H), 7.07 (m, 3H), 6.74 (td, *J* = 7.4, 1.0 Hz, 1H), 6.58 (d, *J* = 7.8 Hz, 1H), 4.43 (d, *J* = 8.4 Hz, 1H), 3.82 (dd, *J* = 10.4, 3.4 Hz, 1H), 3.70 (ddd, *J* = 10.7, 8.3, 3.2 Hz, 1H), 3.62 – 3.38 (m, 3H), 3.18 – 3.02 (m, 2H). ¹³C NMR (101 MHz, CDCl₃) δ 151.4, 138.4, 132.1, 128.6, 128.3, 128.2, 126.9, 125.5, 118.7, 106.7, 68.5, 65.7, 65.3, 48.8, 45. AMM (ESI) *m/z* calcd for C₁₇H₁₈NO⁺ [M+H]⁺ 252.1383, found 252.1381. [α]_D²³ = -0.189 (c = 33.75, CHCl₃).

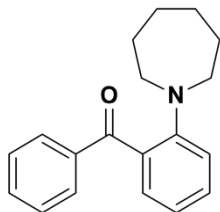


phenyl(2-(piperidin-1-yl)phenyl)methanone (197) was synthesized according to general procedure A using 2-fluorobenzophenone (1.71 mL, 9.90 mmol), cyclohexyl amine (1.13 mL, 11.0 mmol), K_2CO_3 (4.17 g, 39.8 mmol) and DMF (10 mL). The crude product was recrystallized (35:65 $H_2O:CH_3OH$) affording **197** as an off-white solid (922 mg, 35%). 1H NMR (400 MHz, $CDCl_3$) 7.78 – 7.74 (m, 2H), 7.59 – 7.49 (m, 1H), 7.48 – 7.34 (m, 4H), 7.15 – 6.98 (m, 2H), 2.84 (dd, $J = 6.0, 4.6$ Hz, 4H), 1.27 (td, $J = 7.3, 6.4, 4.1$ Hz, 2H), 1.21 – 1.06 (m, 4H). Proton NMR data of the crude material was consistent with the reported literature values.⁷¹

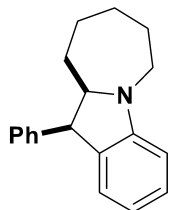


10-phenyl-6,7,8,9,9a,10-hexahydropyrido[1,2-a]indole (146a) was synthesized according to general procedure G using hydrazone **145a** (26 mg, 0.09 mmol), MnO_2 (87 mg, 0.73 mmol), and $Rh_2(R-PTAD)_4$ (1 mg, 0.0006 μ mol) in CH_3CN (0.01 M). The crude product was purified by flash column chromatography (6:94, EtOAc:hexanes) affording **68a** as a yellow oil (16 mg, 70%, 96:4 er, >95:5 dr). 1H NMR (600 MHz, Chloroform- d) δ 7.26 – 7.22 (m, 2H), 7.23 – 7.18 (m, 1H), 7.16 (t, $J = 7.7$ Hz, 1H), 7.04 (d, $J = 7.3$ Hz, 3H), 6.69 (t, $J = 7.4$ Hz, 1H), 6.57 (d, $J = 7.9$ Hz, 1H), 4.27 (d, $J = 8.2$ Hz, 1H), 3.68 (d, $J = 3.6$ Hz, 1H), 3.40 (s, 1H), 2.63 (td, $J = 12.0, 3.0$ Hz, 1H), 1.81 – 1.72 (m, 1H), 1.66 (d, $J =$

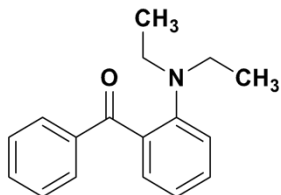
13.3 Hz, 1H), 1.52 – 1.40 (m, 2H), 1.34 (qt, $J = 13.2, 3.8$ Hz, 1H), 0.93 (qd, $J = 12.5, 3.8$ Hz, 1H); ^{13}C NMR (101 MHz, CDCl_3) δ 151.8, 141.3, 132.3, 129.0, 128.4, 127.6, 126.8, 124.5, 118.1, 106.0, 74.6, 54.6, 45.6, 29.3, 25.0, 24.3. ν_{max} 2929, 2821, 1485, 748 cm^{-1} ; AMM (ESI) m/z calcd for $\text{C}_{18}\text{H}_{20}\text{N}^+$ $[\text{M}+\text{H}]^+$ 250.1590, found 250.1585. $[\alpha]_{\text{D}}^{23} = -0.0325$ ($c = 83.8, \text{CHCl}_3$).



(2-(azepan-1-yl)phenyl)(phenyl)methanone (198) was synthesized according to general procedure A using 2-fluorobenzophenone (1.70 mL, 9.90 mmol), cycloheptyl amine (1.12 mL, 11.4 mmol), K_2CO_3 (3.00 g, 24.8 mmol) and DMF (8.00 mL). The crude product was purified by flash column chromatography (4:96 EtOAc:hexanes) affording **119** as a yellow oil (1.25 g, 44%). ^1H NMR (400 MHz, CDCl_3) δ 7.83 (dd, $J = 8.3, 1.4$ Hz, 2H), 7.61 – 7.47 (m, 1H), 7.46 – 7.39 (m, 2H), 7.36 (ddd, $J = 8.7, 7.2, 1.8$ Hz, 1H), 7.29 (dd, $J = 7.6, 1.7$ Hz, 1H), 7.04 (dd, $J = 8.4, 0.9$ Hz, 1H), 6.84 (td, $J = 7.4, 1.0$ Hz, 1H), 3.70 – 2.39 (m, 4H), 1.63 – 1.53 (m, 4H), 1.46 – 1.38 (m, 4H); ^{13}C NMR (101 MHz, CDCl_3) δ 198.0, 151.9, 138.0, 132.5, 131.2, 130.7, 130.0, 128.5, 128.1, 118.0, 117.4, 53.6, 28.5, 27.7; IR (neat): ν_{max} 2923, 2851, 1651, 1592, 704 cm^{-1} ; AMM (ESI) m/z calcd for $\text{C}_{19}\text{H}_{22}\text{NO}^+$ $[\text{M}+\text{H}]^+$ 280.1696, found 280.1693.

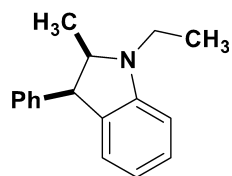


1-phenyl-7,8,9,10,10a,11-hexahydro-6H-azepino[1,2-a]indole (146d) was synthesized by general procedure G using hydrazone **145d** (25 mg, 0.084 mol), MnO₂ (58 mg, 0.67 mmol), and Rh₂(*R*-PTAD)₄ (1 mg, 0.0006mmol) in CH₂Cl₂. The crude product was purified by flash column chromatography (2:98, EtOAc:hexanes) affording **146d** as a yellow oil (16 mg, 97%, 100:0 er, >95:5 dr). ¹H NMR (600 MHz, CDCl₃) δ 7.27 – 7.24 (m, 2H), 7.23 – 7.17 (m, 1H), 7.14 – 7.07 (m, 3H), 6.90 (d, *J* = 7.2 Hz, 1H), 6.61 (t, *J* = 7.3 Hz, 1H), 6.47 (d, *J* = 7.9 Hz, 1H), 4.49 (d, *J* = 9.4 Hz, 1H), 3.93 (td, *J* = 9.7, 2.3 Hz, 1H), 3.51 – 3.41 (m, 1H), 3.22 – 3.10 (m, 1H), 1.95 – 1.84 (m, 1H), 1.84 – 1.73 (m, 1H), 1.74 – 1.65 (m, 1H), 1.66 – 1.59 (m, 1H), 1.50 – 1.41 (m, 1H), 1.43 – 1.34 (m, 1H), 1.35 – 1.23 (m, 1H), 1.21 – 1.08 (m, 1H); ¹³C NMR (151 MHz, CDCl₃) δ 153.1, 140.9, 132.5, 129.6, 128.0, 127.9, 126.5, 124.9, 117.1, 106.5, 69.4, 52.2, 48.7, 31.6, 28.2, 26.9, 26.7; ν_{max} 3049, 2921, 1493, 769 cm⁻¹; AMM (ESI) *m/z* calcd for C₁₉H₂₂N⁺ 264.1747, found 264.1744. [α]_D²³ = -0.007 (c = 72.9, CHCl₃).

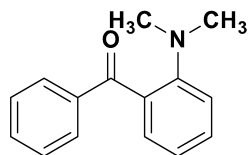


(2-(diethylamino)phenyl)(phenyl)methanone (199) was synthesized according to general procedure A using 2-fluorobenzophenone (1.70 mL, 9.97 mmol), diethylamine (1.9 mL, 11 mmol), K₂CO₃ (4.46 g, 32.3 mmol) and DMF (10 mL). The crude product was

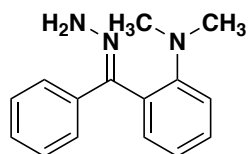
purified by flash column chromatography (50:50 toluene:hexanes) affording **199** as a yellow oil (626 mg, 27%). ^1H NMR (400 MHz, CDCl_3) δ 7.74 (dd, $J = 8.3, 1.4$ Hz, 2H), 7.54 – 7.46 (t, $J = 7.5, 4.8$, 1H), 7.44 – 7.32 (m, 4H), 7.11 – 6.97 (m, 2H), 2.95 (q, $J = 7.1$ Hz, 4H), 0.81 (t, $J = 7.1$ Hz, 6H); ^{13}C NMR (101 MHz, CDCl_3) δ 199.2, 149.8, 137.8, 134.3, 132.5, 130.7, 129.7, 129.7, 127.9, 121.3, 120.5, 46.7, 11.7; IR (neat): ν_{max} 2971, 2930, 1655, 1484, 1314, cm^{-1} ; AMM (ESI) m/z calcd for $\text{C}_{17}\text{H}_{20}\text{NO}^+$ $[\text{M}+\text{H}]^+$ 254.1539, found 254.1537.



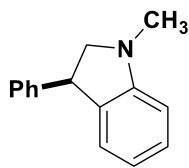
1-ethyl-2-methyl-3-phenylindoline (146f) was synthesized according to general procedure g using hydrazone **145f** (24 mg, 0.90 mmol), MnO_2 (63 mg, 0.72 mmol), and $\text{Rh}_2(\text{R-PTAD})_4$ (1 mg, 0.0006 mmol) in CH_2Cl_2 . The crude product was purified by flash column chromatography (4:96, EtOAc:hexanes) affording indoline **146f** as a yellow oil (18 mg, 86%, 100:0 er, >95:5 dr). ^1H NMR (600 MHz, Chloroform- d) δ 7.28 – 7.22 (m, 2H), 7.21 – 7.16 (m, 1H), 7.13 (t, $J = 7.7$ Hz, 1H), 7.05 (d, $J = 7.5$ Hz, 2H), 6.96 (d, $J = 7.2$ Hz, 1H), 6.63 (t, $J = 7.3$ Hz, 1H), 6.53 (d, $J = 7.9$ Hz, 1H), 4.33 (d, $J = 8.8$ Hz, 1H), 4.08 – 3.84 (m, 1H), 3.49 – 3.32 (m, 1H), 3.20 – 3.04 (m, 1H), 1.11 (td, $J = 7.2, 1.1$ Hz, 3H), 0.84 (d, $J = 6.6, 1.1$ Hz, 3H); ^{13}C NMR (151 MHz, CDCl_3) δ 152.0, 140.5, 133.1, 129.3, 128.0, 127.9, 126.5, 125.2, 117.5, 106.9, 61.5, 51.6, 38.7, 14.5, 10.5.; ν_{max} 3025, 2868, 1483, 2929, 1605 cm^{-1} ; AMM (ESI) m/z calcd for $\text{C}_{17}\text{H}_{20}\text{N}^+$ $[\text{M}+\text{H}]^+$ 238.1590, found 238.1586. $[\alpha]_{\text{D}}^{23} = 0.002$ ($c = 86.02$, CHCl_3).



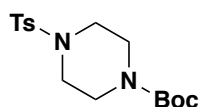
(2-(dimethylamino)phenyl)(phenyl)methanone (200) was isolated as a byproduct from general procedure A using 2-fluorobenzophenone (1.70 mL, 9.97 mmol), 4-methylcyclohexylamine (1.42 mL, 10.7 mmol), K_2CO_3 (1.66 g, 12.0 mmol) and DMF (8.0 mL). The crude product was purified by flash column chromatography (3.5:96.5, EtOAc:hexanes) affording ketone **120** as a yellow oil (700 mg, 30%). 1H NMR (600 MHz, $CDCl_3$) δ 7.87 – 7.79 (m, 2H), 7.60 – 7.50 (m, 1H), 7.48 – 7.36 (m, 3H), 7.32 (s, 1H), 7.03 – 6.98 (m, 1H), 6.94 – 6.86 (m, 1H), 2.70 (s, 6H). Proton NMR data of the crude material was consistent with the reported literature values.⁷¹



(E)-2-(hydrazineylidene(phenyl)methyl)-N,N-dimethylaniline (145e) was synthesized according to general procedure D using ketone **200** (188 mg, 0.834 mmol), hydrazine (0.262 mL, 8.58 mmol), acetic acid (0.091 mL, 1.55 mmol), and anhydrous ethanol (2.8 mL). The crude product was purified by flash column chromatography (66:34, EtOAc:hexanes) affording hydrazone **145e** as a white solid (269 mg, 85%). 1H NMR (600 MHz, $CDCl_3$) δ 7.58 – 7.52 (m, 2H), 7.34 (ddd, $J = 8.3, 7.2, 1.7$ Hz, 1H), 7.32 – 7.25 (m, 3H), 7.06 – 7.00 (m, 2H), 6.98 – 6.91 (m, 1H), 5.85 (s, 2H), 2.75 (s, 6H).

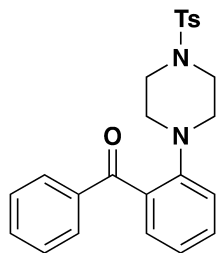


1-methyl-3-phenylindoline (146e) was synthesized by general procedure G using hydrazone **145e** (25 mg, 0.11 mol), MnO₂ (75 mg, 0.86 mmol), and Rh₂(*R*-PTAD)₄ (1 mg, 0.0006 mmol) in CH₂Cl₂ (4.0 mL) over 4 hours. The crude product was purified by flash column chromatography (5:95, EtOAc:hexanes) affording indoline **146e** as a brown oil (18 mg, 99%, 82:18 er). ¹H NMR (600 MHz, Chloroform-*d*) δ 7.36 – 7.27 (m, 4H), 7.28 – 7.21 (m, 1H), 7.18 – 7.12 (m, 1H), 6.93 – 6.87 (m, 1H), 6.74 – 6.66 (m, 1H), 6.59 (d, *J* = 7.9 Hz, 1H), 4.41 (t, *J* = 8.8 Hz, 1H), 3.74 (td, *J* = 8.8, 0.7 Hz, 1H), 3.22 (td, *J* = 8.8, 0.8 Hz, 1H), 2.81 (d, *J* = 0.8 Hz, 3H); ¹³C NMR (151 MHz, CDCl₃) δ 153.4, 143.1, 133.2, 128.5, 128.2, 127.86, 126.7, 124.6, 118.2, 107.5, 65.1, 47.4, 36.2; ν_{max} 2805, 1724, 1606, 1490, 747 cm⁻¹; AMM (ESI) *m/z* calcd for C₁₅H₁₅N⁺ [M+H]⁺ 210.1283, found 210.1271. [α]_D²³ = -0.136(c = 88.3, CHCl₃).

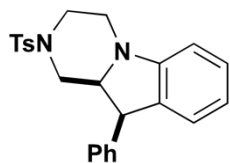


tert-butyl 4-tosylpiperazine-1-carboxylate (201). To a solution of *N*-boc-piperazine (3.0g, 16 mmol) in dry CH₂Cl₂ (80 mL) was added triethylamine (6.6 g, 55 mmol) followed by tosyl chloride (2.2 g, 35 mmol). The mixture was cooled to room temperature then diluted in CH₂Cl₂ (50 mL). The reaction mixture was washed with 1 M HCl (3 x 25 mL) and brine (50 mL), dried over Na₂SO₄, filtered, and concentrated *in vacuo*. The solid was purified by flash chromatography (20:80 EtOAc/hexanes) to yield the product as white

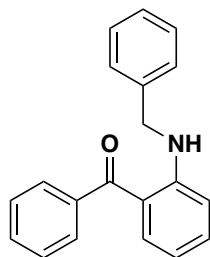
solid (0.790 g, 14%). ^1H NMR (600 MHz, CDCl_3) δ 7.61 (d, $J = 8.3$ Hz, 2H), 7.32 (d, $J = 7.9$ Hz, 2H), 3.52 – 3.45 (m, 4H), 2.96 – 2.89 (m, 4H), 2.42 (s, 3H), 1.39 (s, 9H). Proton NMR data was consistent with the reported literature values.⁷²



phenyl(2-(4-tosylpiperazin-1-yl)phenyl)methanone (202). Piperazine (**201**) (822 mg, 2.31 mmol) was stirred with 4 M HCl in dioxane (10.0 mL, 40 mmol) for 12 hours and the crude product was isolated by concentration *in vacuo*. The crude deprotected material was used to synthesize ketone **202** according to general procedure A using 2-fluorobenzophenone (0.26 mL, 2.3 mmol), crude deprotected piperazine **201** (650 mg, 2.7 mmol), K_2CO_3 (1.10 g, 30 mmol) and CH_3CN (10 mL). The crude product was purified by flash column chromatography (30:70 EtOAc:hexanes) affording the desired ketone as a yellow crystalline solid (139 mg, 14% over two steps). ^1H NMR (600 MHz, CDCl_3) δ 7.55 (d, $J = 7.2$ Hz, 2H), 7.52 – 7.38 (m, 4H), 7.33 (d, $J = 7.9$ Hz, 2H), 7.22 – 7.08 (m, 4H), 7.04 (d, $J = 8.1$ Hz, 1H), 2.94 (t, $J = 4.9$ Hz, 4H), 2.52 (s, 7H); ^{13}C NMR (151 MHz, CDCl_3) δ 198.3, 150.4, 143.5, 137.5, 133.6, 132.2, 132.0, 131.9, 130.2, 129.5, 129.3, 127.8, 127.6, 123.4, 119.3, 51.3, 45.6, 21.6; IR (neat): 2955, 2916, 1648, 1449, 1165, cm^{-1} ; AMM (ESI) m/z calcd for $\text{C}_{17}\text{H}_{20}\text{NO}^+$ $[\text{M}+\text{H}]^+$ 421.1586, found 421.1576; m.p. 171.1-172.9 $^\circ\text{C}$.

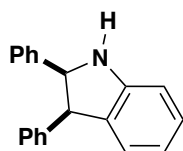


10-phenyl-2-tosyl-1,2,3,4,10,10a-hexahydropyrazino[1,2-*a*]indole (146b) was synthesized by general procedure G using hydrazone **145b** (2 mg, 0.05 mmol), MnO₂ (32 mg, 0.37 mmol), and Rh₂(*R*-PTAD)₄ (1 mg, 0.0006 mmol) in CH₂Cl₂. The crude product was purified by flash column chromatography (60:40, CH₂Cl₂:hexanes) affording indoline **68b** as a white solid (13.1. mg, 68%, 100:0 er, >95:5 dr). ¹H NMR (600 MHz, CDCl₃) δ 7.45 (d, *J* = 8.3 Hz, 2H), 7.26 – 7.19 (m, 5H), 7.16-7.12 (m, 1H), 7.06 – 6.97 (m, 3H), 6.75-6.71 (m, 1H), 6.52 (d, *J* = 7.8 Hz, 1H), 4.47 (d, *J* = 8.4 Hz, 1H), 3.75 – 3.66 (m, 2H), 3.63-3.59 (m, 1H), 3.43-3.39 (m, 1H), 3.07-3.01 (m, 1H), 2.38 (s, 3H), 2.37-2.31 (m, 1H), 1.87 (t, *J* = 11.2 Hz, 1H); ¹³C NMR (151 MHz, CDCl₃) δ 150.5, 143.6, 137.8, 133.0, 131.9, 129.6, 128.7, 128.4, 128.2, 127.4, 127.1, 125.6, 119.1, 107.0, 65.4, 49.3, 47.4, 44.4, 44.0, 21.5; ; ν_{max} 2920, 1450, 1482, 1166 cm⁻¹; AMM (ESI) *m/z* calcd for C₂₄H₂₅N₂O₂S⁺ [M+H]⁺ 405.1631, found 405.1627. [α]_D²³ = 0.076 (c = 42, CHCl₃); m.p. 180.9-182.1 °C.

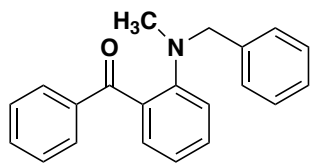


(2-(benzylamino)phenyl)(phenyl)methanone (203) To a flame-dried round-bottom flask under Ar was added dry CH₂Cl₂ (35.5 mL, 0.1M) followed by 2-aminobenzophenone (700 mg, 3.54 mmol), benzaldehyde (0.43 mL, 4.3 mmol) and two drops of acetic acid. The mixture stirred at room temperature for 15 min. To the flask was added Na(AcO)₃BH (1.5 g, 7.1 mmol) by quickly removing and replacing the rubber septa. The reaction was stirred for 5 min at which point full conversion was observed by TLC. The reaction was concentrated by rotary evaporation and isolated by silica column chromatography (8:92

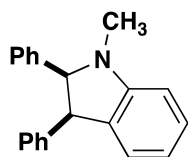
EtOAc:hexanes) to yield **123** as a yellow oil (785 mg, 77%). ^1H NMR (600 MHz, CDCl_3) δ 9.04 (t, $J = 5.5$ Hz, 1H), 7.67 – 7.62 (m, 2H), 7.56 – 7.51 (m, 2H), 7.50 – 7.44 (m, 2H), 7.42 (d, $J = 7.4$ Hz, 2H), 7.39 – 7.32 (m, 3H), 7.29 (t, $J = 7.3$ Hz, 1H), 6.76 (d, $J = 8.5$ Hz, 1H), 6.57 (t, $J = 7.5$ Hz, 1H), 4.53 (d, $J = 5.6$ Hz, 2H). Proton NMR data was consistent with reported literature values.⁷³



(2S,3R)-2,3-diphenylindoline (146g) was synthesized by general procedure H using hydrazone **145g** (25 mg, 0.083 mmol), MnO_2 (32 mg, 0.66 mmol), and $\text{Rh}_2(\text{R-PTAD})_4$ (1 mg, 0.0006 mmol) in CH_3CN . The crude product was purified by flash column chromatography (4:95.5:0.5, EtOAc₂:hexanes:Et₃N) affording indoline **146g** as a yellow amorphous solid (21.6 mg, 97%, >99.05:0.5 er, >95:5 dr). ^1H NMR (600 MHz, Chloroform-*d*) δ 7.17 (t, $J = 7.6$ Hz, 1H), 7.07 – 6.95 (m, 9H), 6.84 (d, $J = 7.8$ Hz, 1H), 6.78 (t, $J = 7.4$ Hz, 1H), 6.75 – 6.69 (m, 2H), 5.24 (d, $J = 9.1$ Hz, 1H), 4.73 (d, $J = 9.0$ Hz, 1H).; ^{13}C NMR (151 MHz, CDCl_3) δ 151.7, 140.0, 139.3, 131.2, 129.3, 128.1, 127.6, 127.5, 127.2, 126.9, 126.2, 125.8, 119.3, 109.1, 68.9, 54.1; AMM (ESI) m/z calcd for $\text{C}_{20}\text{H}_{18}\text{N}^+$ $[\text{M}+\text{H}]^+$ 272.1434, found 272.1431. $[\alpha]_{\text{D}}^{23} = -0.039$ ($c = 15.3$, CHCl_3).



(2-(benzyl(methyl)amino)phenyl)(phenyl)methanone (204) was synthesized according to general procedure A using 2-fluorobenzophenone (0.35 mL, 2.0 mmol), *N*-benzylmethylamine (260 mg, 1.74 mmol), K₂CO₃ (829 mg, 5.99 mmol) and CH₃CN (10 mL). The crude product was purified by flash column chromatography (5:95 EtOAc:hexanes) affording **124** as a yellow oil (368.1 mg, 72%). ¹H NMR (400 MHz, CDCl₃) δ 7.84 (d, *J* = 7.7 Hz, 2H), 7.68 – 7.55 (m, 1H), 7.47 (t, *J* = 7.8 Hz, 3H), 7.44 – 7.36 (m, 1H), 7.25 – 7.16 (m, 3H), 7.12 (d, *J* = 8.2 Hz, 1H), 7.06 (t, *J* = 7.4 Hz, 1H), 7.00 – 6.84 (m, 2H), 4.16 (s, 2H), 2.58 (s, 3H); ¹³C NMR (151 MHz, CDCl₃) δ 198.6, 151.5, 137.9, 137.8, 132.7, 131.5, 131.3, 130.1, 129.8, 128.3, 128.2, 127.8, 126.9, 120.6, 118.6, 59.9, 41.1 AMM (ESI) *m/z* calcd for C₁₇H₂₀NO⁺ [M+H]⁺302.1539, found 302.1540.

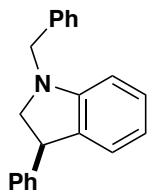


1-methyl-2,3-diphenylindoline (155a) was synthesized by general procedure G using hydrazone **153a** (25 mg, 0.08 mmol), MnO₂ (55 mg, 0.63 mmol), and Rh₂(OAc)₄ (1 mg, 0.002 mmol) in CH₂Cl₂. The crude product was purified by flash column chromatography (20:80 CH₂Cl₂:hexanes) affording indoline **155a** as a white amorphous solid (17 mg, 76%, >95:5 dr). ¹H NMR (600 MHz, Acetone-*d*₆) δ 7.21 (td, *J* = 7.7, 1.3 Hz, 1H), 7.10 – 7.01 (m, 5H), 7.01 – 6.91 (m, 4H), 6.78 (d, *J* = 7.9 Hz, 1H), 6.74 (td, *J* = 7.4, 1.0 Hz, 1H), 6.71 – 6.64 (m, 2H), 4.73 (d, *J* = 8.9 Hz, 1H), 4.63 (d, *J* = 8.9 Hz, 1H), 2.65 (s, 3H); ¹³C NMR

(151 MHz, CDCl₃) δ 154.0, 140.0, 137.7, 132.2, 129.3, 128.3, 128.1, 127.6, 127.4, 126.9, 126.0, 125.4, 118.9, 107.9, 76.6, 53.4, 34.4; IR 3035, 2799, 1599, 1481, 700; AMM (ESI) m/z calcd for C₂₁H₂₀N⁺[M+H]⁺ 286.1590, found 286.1586.

1-methyl-2,3-diphenylindoline (155a) was synthesized by general procedure G using hydrazone **153a** (25 mg, 0.079 mmol), MnO₂ (55 mg, 0.63 mmol), and Rh₂(Mes)₄ (1 mg, 0.00094 mmol) in CH₂Cl₂. The crude product was purified by flash column chromatography (20:80 CH₃Cl₂/Hexanes) affording indoline **155a** as a white amorphous solid (12.5 mg, 56% >95:5dr). Proton NMR data was consistent with characterization described above.

1-methyl-2,3-diphenylindoline (155a) was synthesized by general procedure G using hydrazone **153a** (25 mg, 0.079 mmol), MnO₂ (55 mg, 0.63 mmol), and Rh₂(*R*-PTAD)₄ (1 mg, 0.00079 mmol) in CH₂Cl₂. The crude product was purified by flash column chromatography (20:80 CH₃Cl₂/Hexanes) affording indoline **155a** as a white amorphous solid (8.9 mg, 39% >95:5 dr). Proton NMR data was consistent with characterization described above.

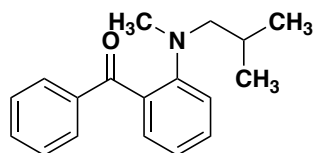


1-benzyl-3-phenylindoline (154a) was synthesized by general procedure G using hydrazone **153a** (25 mg, 0.079 mmol), MnO₂ (55 mg, 0.63 mmol), and Rh₂(OAc)₄ (1 mg, 0.002 mmol) in CH₂Cl₂. The crude product was purified by flash column chromatography (20:80 CH₂Cl₂:hexanes) affording indoline **154a** as a yellow oil (1 mg, 4%). ¹H NMR (400

MHz, Chloroform-*d*) δ 7.45 – 7.27 (m, 10H), 7.14 (t, $J = 7.5, 1.0$ Hz, 1H), 6.92 (d, $J = 7.4, 1.3$ Hz, 1H), 6.71 (d, $J = 7.4, 1.0$ Hz, 1H), 6.64 (d, $J = 7.9$ Hz, 1H), 4.51 – 4.39 (m, 2H), 4.21 (d, $J = 14.7$ Hz, 1H), 3.76 (t, $J = 9.1$ Hz, 1H), 3.26 (t, $J = 8.9$ Hz, 1H); ^{13}C NMR (151 MHz, CDCl_3) δ 152.5, 143.4, 138.2, 133.1, 128.51, 128.50, 128.2, 128.0, 127.8, 127.2, 126.7, 124.9, 118.1, 107.4, 62.6, 53.6, 47.3; IR 3033, 2819, 1598, 1234, 738: ν_{max} : 1598 cm^{-1} ; AMM (ESI) m/z calcd for $\text{C}_{21}\text{H}_{20}\text{N}^+[\text{M}+\text{H}]^+$ 286.1590, found 286.1586.

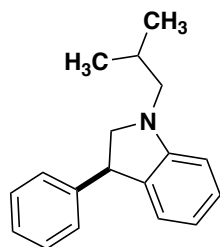
1-benzyl-3-phenylindoline (154a) was synthesized by general procedure G using hydrazone **153a** (25 mg, 0.079 mmol), MnO_2 (40 mg, 0.48 mmol), and $\text{Rh}_2(\text{Mes})_4$ (1 mg, 0.0009 mmol) in CH_2Cl_2 . The crude product was purified by flash column chromatography affording indoline **154a** as a yellow oil (4 mg, 19 %). Proton NMR data was consistent with characterization described above.

1-benzyl-3-phenylindoline (154a) (9 mg, 39%) was synthesized by general procedure G using hydrazone **153a** (25 mg, 0.079 mmol), MnO_2 (55 mg, 0.63 mmol), and $\text{Rh}_2(\text{R-PTAD})_4$ (1 mg, 0.0008 mmol) in CH_2Cl_2 . The crude product was purified by flash column chromatography affording indoline **154a** as a yellow oil. Proton NMR data was consistent with characterization described above.



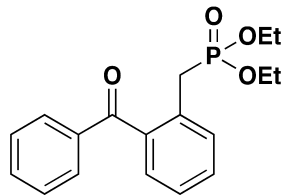
(2-(isobutyl(methyl)amino)phenyl)(phenyl)methanone (205) was synthesized according to general procedure A using 2-fluorobenzophenone (1.20 mL, 7.01 mmol), *N*-methylisobutylamine (1.00 mL, 8.37 mmol), K_2CO_3 (2.30g, 16.6 mmol) and DMF (8.00

mL). The crude product was purified by flash column chromatography (10:90, DCM:hexanes) affording ketone **205** as a yellow oil (828 mg, 44%). ¹H NMR (600 MHz, CDCl₃) δ 7.82 – 7.73 (m, 2H), 7.54 – 7.48 (m, 1H), 7.46 – 7.34 (m, 3H), 7.29 (dd, *J* = 7.5, 1.7 Hz, 1H), 7.04 (d, *J* = 8.3 Hz, 1H), 6.92 (td, *J* = 7.4, 0.9 Hz, 1H), 2.73 (d, *J* = 7.3 Hz, 2H), 2.64 (s, 3H), 1.87 – 1.71 (m, 1H), 0.66 (d, *J* = 6.6 Hz, 6H); ¹³C NMR (151 MHz, CDCl₃) δ 198.6, 152.0, 138.0, 132.6, 131.1, 130.7, 130.2, 129.8, 128.1, 119.4, 118.0, 63.1, 41.9, 26.7, 20.2.; IR 2954, 1655, 1594, 1448, 698: ν_{\max} 1594 cm⁻¹; AMM (ESI) *m/z* calcd for C₁₈H₂₂NO⁺ 268.1696, found 268.1696.

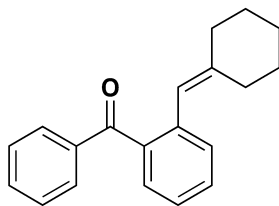


1-isobutyl-3-phenylindoline (154b) was synthesized by general procedure G using hydrazone **153b** (15 mg, 0.055 mmol), MnO₂ (38 mg, 0.44 mmol), and Rh₂(Mes)₄ (1 mg, 0.0009 mmol) in CH₂Cl₂. The crude product was purified by flash column chromatography (20:80 CH₂Cl₂:hexanes) affording indoline **154b** as a yellow oil (10 mg, 80 %). ¹H NMR (400 MHz, CDCl₃) δ 7.34 – 7.15 (m, 5H), 7.14 – 7.05 (m, 1H), 6.85 (dt, *J* = 7.3, 1.3 Hz, 1H), 6.61 (td, *J* = 7.4, 1.0 Hz, 1H), 6.53 (d, *J* = 7.8 Hz, 1H), 4.41 (t, *J* = 8.9 Hz, 1H), 3.81 (t, *J* = 9.2 Hz, 1H), 3.28 (t, *J* = 8.7 Hz, 1H), 2.95 (dd, *J* = 13.2, 7.6 Hz, 1H), 2.82 (dd, *J* = 13.0, 7.1 Hz, 1H), 1.97 – 1.90 (m, 1H), 0.98 (t, *J* = 6.6 Hz, 6H). Regioisomers of this compound proved difficult to isolate by a myriad of chromatography techniques. As such we have included a proton NMR of a mixture of 95:5, 6b:7b.

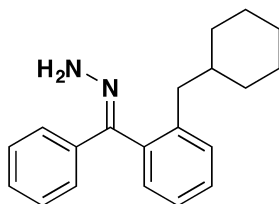
INDANES



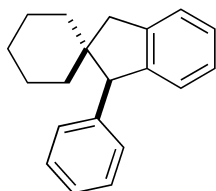
Diethyl 2-benzoylphenylmethylphosphonate (206). Following a modified literature procedure,⁷⁴ to a solution of 2-methylbenzophenone (2.0 mL, 11 mmol) and *N*-bromosuccinimide (2.2 g, 12 mmol) in CCl₄ (100 mL) under argon was added 2,2'-azobis(2-methylpropionitrile) (AIBN, 0.091 g, 0.55 mmol). The reaction mixture was stirred at reflux for 3 h and then more AIBN (0.091 g, 0.55 mmol) was added. The reaction mixture was refluxed for another 2 h and then allowed to cool to room temperature. The solution was added to H₂O (200 mL), extracted with CH₂Cl₂ (2 x 50 mL), dried over Na₂SO₄, filtered, and concentrated *in vacuo* to afford the desired crude bromo-compound as a red oil. The crude material was dissolved in triethyl phosphite (4.2 mL, 24 mmol) and the reaction mixture was stirred at reflux for 18 h and then allowed to cool to room temperature. The solution was added to H₂O (20 mL), extracted with CH₂Cl₂ (2 x 20 mL), dried over Na₂SO₄, filtered, concentrated *in vacuo*, and purified by flash column chromatography (60:40, EtOAc:hexanes) to afford the desired phosphonate ester **126** as a yellow oil (1.05 g, 29%). ¹H NMR (600 MHz, CDCl₃) δ 7.83 (dd, *J* = 8.3, 1.4 Hz, 2H), 7.58 (tt, *J* = 7.4, 1.2 Hz, 1H), 7.52-7.49 (m, 1H), 7.48-7.44 (m, 3H), 7.35 (d, *J* = 7.5 Hz, 1H), 7.33-7.28 (m, 1H), 3.98-3.84 (m, 4H), 3.53 (d, ¹*J*_{H-P} = 22.3 Hz, 2H), 1.10 (t, *J* = 7.1 Hz, 6H). ¹H NMR is consistent with published data.⁷⁵



2-(Cyclohexylidene)methylbenzophenone (207). Following a literature procedure,⁷⁶ to a solution of phosphonate **206** (0.522 g, 1.57 mmol) and cyclohexanone (0.16 mL, 1.6 mmol) in anhydrous THF (6.0 mL) was added NaH (60% in mineral oil, 0.075 g, 1.9 mmol) at 0 °C. The reaction mixture was allowed to warm to room temperature and stirred for 18 h. The reaction mixture was quenched with H₂O (20 mL), extracted with CH₂Cl₂ (2 x 20 mL), dried over Na₂SO₄, filtered, concentrated *in vacuo*, and purified by flash column chromatography (5:95, EtOAc:hexanes) to afford the desired benzophenone **127** as a clear oil (0.310 g, 72%). ¹H NMR (600 MHz, CDCl₃) δ 7.73 (d, *J* = 7.3 Hz, 2H), 7.53 (t, *J* = 7.4 Hz, 1H), 7.45-7.37 (m, 4H), 7.30 (t, *J* = 7.5 Hz, 1H), 7.23 (d, *J* = 7.6 Hz, 1H), 6.04 (s, 1H), 2.13 (t, *J* = 6.1 Hz, 2H), 1.97 (t, *J* = 6.1 Hz, 2H), 1.50-1.34 (m, 6H); ¹³C NMR (151 MHz, CDCl₃) δ 198.9, 144.6, 139.2, 138.1, 137.2, 132.9, 130.3, 130.0, 129.9, 128.3, 128.2, 126.1, 120.5, 37.1, 29.7, 28.3, 27.5, 26.6.; AMM (ESI) *m/z* calcd for C₂₀H₂₁O⁺ [M+H]⁺ 277.1587 found 277.1597; IR (neat): 1666, 2854, 2925, 1599 cm⁻¹.

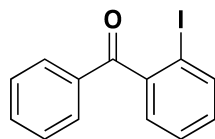


(2-Cyclohexylmethyl)benzophenone hydrazone (177a) was synthesized according to general procedure E, benzophenone **207** (0.329 g, 1.19 mmol), N₂H₄ (0.60 mL, 18 mmol), AcOH (0.080 mL, 1.4 mmol) and anhydrous EtOH (18.0 mL) were used. The crude reaction mixture was taken into general procedure F, 10% palladium on carbon (0.064 g, 0.060 mmol) and CH₃OH (4.0 mL) were used. Following purification by flash column chromatography on neutral alumina (97:3, hexanes:EtOAc), hydrazone **177a** was obtained as a yellow oil (0.164 g, 47%). ¹H NMR (600 MHz, CDCl₃) δ 7.47 – 7.43 (m, 2H), 7.40 – 7.30 (m, 3H), 7.30 – 7.23 (m, 3H), 7.13 (d, *J* = 7.2 Hz, 1H), 5.33 (s, 2H), 2.35 – 2.27 (m, 2H), 1.63 – 1.58 (m, 1H), 1.57 – 1.52 (m, 3H), 1.52 – 1.47 (m, 1H), 1.47 – 1.40 (m, 1H), 1.10 – 0.97 (m, 3H), 0.82 (qd, *J* = 12.1, 3.6 Hz, 1H), 0.73 (qd, *J* = 12.1, 3.2 Hz, 1H); ¹³C NMR (151 MHz, CDCl₃) δ 149.2, 140.3, 138.3, 132.6, 130.7, 129.0, 128.8, 128.1, 128.0, 126.7, 126.0, 41.1, 38.1, 33.3, 33.3, 26.4, 26.2, 26.2; AMM (ESI) *m/z* calcd for C₂₀H₂₅N₂⁺ [M+H]⁺ 293.2012 found 293.2012.

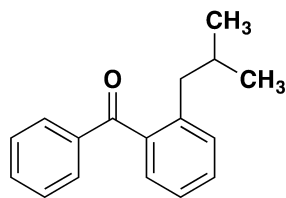


1-Phenylspiro(cyclohexane-1,2'-indane) (178a) was synthesized by general procedure H using hydrazone **177a** (42 mg, 0.14 mmol), MnO₂ (100 mg, 1.14 mmol), and Rh₂(*R*-PTAD)₄ (2 mg, 0.001 mmol) in CH₂Cl₂ (9 mL). The crude product was purified by flash column chromatography (4:96, EtOAc:hexanes) affording indane **178a** as a white solid (34 mg, 89%, 99:1 er). ¹H NMR (600 MHz, CDCl₃) δ 7.30 – 7.20 (m, 4H), 7.18 (t, *J* = 7.4 Hz, 1H), 7.12 (t, *J* = 7.4 Hz, 1H), 7.05 (d, *J* = 6.9 Hz, 2H), 7.02 (d, *J* = 7.5 Hz, 1H), 4.01

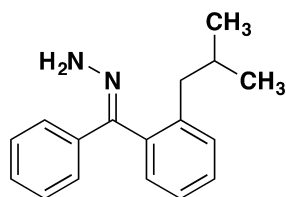
(s, 1H), 3.04 (d, $J = 15.7$ Hz, 1H), 2.79 (d, $J = 15.6$ Hz, 1H), 1.69 (d, $J = 11.8$ Hz, 1H), 1.66 – 1.59 (m, 1H), 1.59 – 1.53 (m, 1H), 1.53 – 1.48 (m, 1H), 1.48 – 1.40 (m, 2H), 1.38 – 1.29 (m, 1H), 1.14 (d, $J = 13.5$ Hz, 1H), 1.11 – 1.02 (m, 1H), 0.79 (td, $J = 12.7, 4.0$ Hz, 1H); ^{13}C NMR (151 MHz, CDCl_3) δ 146.0, 143.3, 141.0, 123.0, 127.9, 126.6, 126.4, 126.4, 125.6, 124.9, 63.3, 48.8, 42.0, 38.0, 32.6, 26.2, 23.9, 23.1; IR (neat) 3024, 2927, 1451, 720 cm^{-1} ; AMM (ESI) m/z calcd for $\text{C}_{20}\text{H}_{26}\text{N}^+$ $[\text{M}+\text{NH}_4]^+$ 280.2060 found 280.2074; m.p. 94 $^\circ\text{C}$; $[\alpha]_{\text{D}}^{24} = 31.8$ ($c = 0.30$, CHCl_3).



2-Iodobenzophenone (208). A solution of 2-aminobenzophenone (6.00 g, 30.4 mmol) and concentrated H_2SO_4 (35.8 mL, 645 mmol) in H_2O (17.9 mL) was stirred vigorously at room temperature for 45 minutes. The solution was cooled to 0 $^\circ\text{C}$ and a solution of NaNO_2 (2.73 g, 39.6 mmol) in H_2O (6.10 mL) was added dropwise. The solution was stirred at 0 $^\circ\text{C}$ for 2.5 h at which time a solution of KI (25.2 g, 152 mmol) in H_2O (28.7 mL) was slowly added. The reaction mixture was allowed to warm to room temperature and stirred for 27 h. EtOAc (80 mL) was added and the organic layer was washed with brine (50 mL), saturated $\text{Na}_2\text{S}_2\text{O}_3$ (2 x 50 mL), and then H_2O (50 mL). The organic layer was dried over Na_2SO_4 , filtered, concentrated *in vacuo*, and purified by flash column chromatography (95:5, hexanes:EtOAc) to afford the desired benzophenone **128** as a yellow oil (6.49 g, 69%). ^1H NMR (400 MHz, CDCl_3) δ 7.95 (dd, $J = 8.0, 1.1$ Hz, 1H), 7.87 – 7.81 (m, 2H), 7.64 (tt, $J = 7.4, 1.2$ Hz, 1H), 7.53 – 7.44 (m, 3H), 7.33 (dd, $J = 7.6, 1.7$ Hz, 1H), 7.21 (td, $J = 7.7, 1.7$ Hz, 1H). ^1H NMR is consistent with published data.⁷⁷

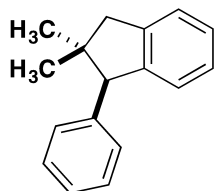


(2-Methylpropyl)benzophenone (209). Following a modified literature procedure,⁷⁸ a solution of **208** (0.250 g, 0.811 mmol), isobutylboronic acid (0.165 g, 1.57 mmol), K₂CO₃ (0.335 g, 2.42 mmol) and Ag₂O (0.470 g, 2.03 mmol) in anhydrous toluene (2.5 mL) was heated at 120 °C for 18 h and then allowed to cool to room temperature. The reaction mixture was filtered through Celite with diethyl ether (25 mL), concentrated *in vacuo*, and purified by flash column chromatography (4:96, EtOAc:hexanes) to afford the desired benzophenone **209** as a clear oil (0.088 g, 46%). ¹H NMR (400 MHz, CDCl₃) δ 7.82 – 7.76 (m, 2H), 7.58 – 7.52 (m, 1H), 7.46 – 7.36 (m, 3H), 7.30 – 7.20 (m, 3H), 2.57 (d, *J* = 7.3 Hz, 2H), 1.87 – 1.72 (m, 1H), 0.80 (d, *J* = 6.6 Hz, 6H); ¹³C NMR (101 MHz, CDCl₃) δ 198.8, 140.7, 138.9, 138.0, 133.2, 131.0, 130.2, 123.0, 128.6, 128.5, 125.2, 42.4, 30.3, 22.5; AMM (ESI) *m/z* calcd for C₁₇H₁₉O⁺ [M+H]⁺ 239.1430 found 239.1431; IR (neat): 1666, 1599, 2925, 2869, 2955 cm⁻¹.

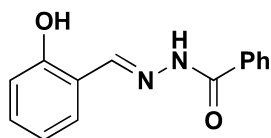


(2-Methylpropyl)benzophenone hydrazone (177b) was synthesized according to general procedure E, benzophenone **209** (0.400 g, 1.68 mmol), N₂H₄ (1.6 mL, 50 mmol), AcOH (0.17 mL, 3.0 mmol) and anhydrous EtOH (28.0 mL) were used. Following

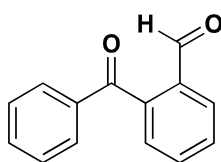
purification by flash column chromatography (10:90, EtOAc:hexanes), hydrazone **177b** was obtained as a light-yellow solid (0.279 g, 66%). ¹H NMR (400 MHz, CDCl₃) δ 7.49 – 7.42 (m, 2H), 7.41 – 7.30 (m, 3H), 7.30 – 7.24 (m, 3H), 7.13 (d, *J* = 7.4 Hz, 1H), 5.33 (br s, 2H), 2.30 (dd, *J* = 7.4, 1.8 Hz, 2H), 1.84 – 1.74 (m, 1H), 0.81 (d, *J* = 6.6 Hz, 3H), 0.74 (d, *J* = 6.6 Hz, 3H); ¹³C NMR (101 MHz, CDCl₃) δ 149.1, 140.7, 138.3, 132.5, 130.6, 129.0, 128.9, 128.1, 128.0, 126.8, 126.0, 42.5, 28.7, 22.7, 22.6; AMM (ESI) *m/z* calcd for C₁₇H₂₁N₂⁺ [M+H]⁺ 253.1699 found 253.1699.



2,2-Dimethyl-1-phenylindane (178b) was synthesized according to general procedure I using hydrazone **177b** (37 mg, 0.15 mmol), MnO₂ (102 mg, 1.17 mmol), and Rh₂(R-PTAD)₄ (2 mg, 0.001 mmol) in CH₂Cl₂ (9.0 mL). The crude product was purified by flash column chromatography (4:96, EtOAc:hexanes) affording indane **178b** as a white solid (24 mg, 73%, 92:8 er). ¹H NMR (600 MHz, CDCl₃) δ 7.30 (t, *J* = 7.4 Hz, 2H), 7.26-7.22 (m, 2H), 7.19 (t, *J* = 7.3 Hz, 1H), 7.15 (t, *J* = 7.3 Hz, 1H), 7.10 (d, *J* = 7.1 Hz, 2H), 7.05 (d, *J* = 7.4 Hz, 1H), 4.04 (s, 1H), 2.85 (d, *J* = 15.3 Hz, 1 H), 2.80 (d, *J* = 15.3 Hz, 1 H), 1.24 (s, 3H), 0.66 (s, 3H); ¹³C NMR (101 MHz, CDCl₃) δ 145.9, 143.6, 140.7, 129.7, 128.0, 126.7, 126.5, 126.3, 125.6, 124.8, 62.3, 47.4, 45.5, 28.6, 24.5; AMM (ESI) *m/z* calcd for C₁₇H₂₂N⁺ [M+NH₄]⁺ 240.1747 found 240.1757; m.p. 64 °C; [α]_D²⁴ = 80.8(c = 0.70, CHCl₃).

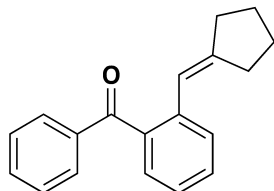


(E)-N-(2-hydroxybenzylidene)benzohydrazide (210). To a solution of benzhydrazide (2.70 g, 19.8 mmol) in ethanol (10.0 mL) was added salicylaldehyde (2.10 mL, 19.8mmol) in ethanol (20.0 mL). The reaction mixture was stirred at room temperature for 12 hours before it was filtered and washed with additional ethanol and concentrated to afford hydrazone **210** as a white solid (3.54 g, 84%). ¹H NMR (400 MHz, DMSO-d₆) δ 12.11 (s, 1H), 11.29 (s, 1H), 8.65 (s, 1H), 7.94 (d, *J* = 7.9, 2H), 7.64-7.53 (m, 4H), 7.31 (t, *J* = 7.9 Hz, 1H), 6.93 (t, *J* = 8.1 Hz, 2H). Proton NMR data of the crude material was consistent with the reported literature values.⁷⁹



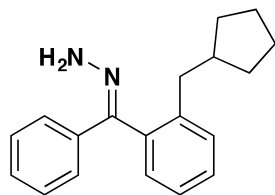
2-Benzoylbenzaldehyde (211). Following a literature procedure,⁸⁰ lead (IV) acetate (1.86 g, 4.20 mmol) was added slowly to a solution of **210** (1.00 g, 4.21 mmol) in THF (25.0 mL) in a flame-dried flask. Upon addition of lead (IV) acetate the mixture bubbled and turned yellow. After stirring for two hours the reaction was concentrated *in vacuo* and

purified by flash column chromatography (5:95 to 20:80, EtOAc:hexanes) to afford **211** as an off-white solid (0.749 g, 85%). ¹H NMR (600 MHz, CDCl₃) δ 10.03 (s, 1H), 8.06 – 8.01 (m, 1H), 7.80 (dd, *J* = 8.2, 1.4 Hz, 2H), 7.73 – 7.66 (m, 2H), 7.63 – 7.58 (m, 1H), 7.53 – 7.49 (m, 1H), 7.49 – 7.45 (m, 2H). ¹H NMR is consistent with published data. ⁸¹

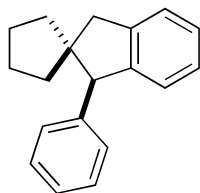


2-(Cycloheptylidene)methyl)benzophenone (212) Following a literature procedure,⁸² to a solution of cyclopentyl triphenylphosphonium bromide (0.616 g, 1.49 mmol) in THF (2.25 mL) was added 1 M KO*t*-Bu in THF (1.60 mL, 1.60 mmol). The reaction mixture was stirred for 1 h at room temperature and then a solution of benzaldehyde **211** (0.300 g, 1.42mmol) in THF (2.3 mL) was added. The reaction mixture was stirred at room temperature for an additional 2 h, concentrated *in vacuo*, and flushed through a plug of silica (5:95, EtOAc:hexanes) to afford the desired benzophenone **212** as a light-yellow oil (0.328 g, 88%). ¹H NMR (600 MHz, CDCl₃) δ 7.76 (d, *J* = 7.6 Hz, 2H), 7.54 (t, *J* = 7.4 Hz, 1H), 7.49 – 7.43 (m, 2H), 7.43 – 7.39 (m, 2H), 7.35 (d, *J* = 7.5 Hz, 1H), 7.27 – 7.23 (m, 1H), 6.27 – 6.24 (m, 1H), 2.40 (t, *J* = 7.2 Hz, 2H), 2.23 (t, *J* = 7.2 Hz, 2H), 1.67 (p, *J* = 7.0 Hz, 2H), 1.56 (p, *J* = 7.0 Hz, 2H); ¹³C NMR (151 MHz, CDCl₃) δ 198.9, 149.0, 138.2, 137.9, 137.7, 133.0, 130.1, 129.9, 128.6, 128.3, 128.2, 125.4, 118.5, 35.1, 31.1, 26.8, 25.4; AMM (ESI) *m/z* calcd for C₁₉H₁₉O⁺ [M+H]⁺ 263.1430 found 263.1428; IR (neat): ν_{max}

2951, 2869, 1599, 1663 cm^{-1} .

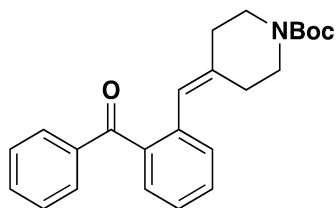


(2-Cyclopentylmethyl)benzophenone hydrazone (177c) was synthesized according to general procedure E, benzophenone **212** (0.325 g, 1.24 mmol), N_2H_4 (1.0 mL, 32 mmol), AcOH (0.14 mL, 2.4 mmol) and anhydrous EtOH (21 mL) were used. The crude reaction material was taken into general procedure F, 10% palladium on carbon (0.067 g, 0.063 mmol) and CH_3OH (4.2 mL) were used. Following purification by flash column chromatography on neutral alumina (5:95, EtOAc:hexanes), hydrazone **177c** was obtained as a yellow solid (0.257 g, 75%). ^1H NMR (600 MHz, CDCl_3) δ 7.47 – 7.44 (m, 2H), 7.42 – 7.36 (m, 2H), 7.33 (tt, $J = 7.1, 1.9$ Hz, 1H), 7.30 – 7.23 (m, 3H), 7.12 (d, $J = 7.4$ Hz, 1H), 5.33 (s, 2H), 2.49 – 2.40 (m, 2H), 2.08 – 1.99 (m, 1H), 1.68 – 1.60 (m, 1H), 1.59 – 1.46 (m, 3H), 1.46 – 1.35 (m, 2H), 1.12 – 1.04 (m, 1H), 1.04 – 0.96 (m, 1H); ^{13}C NMR (151 MHz, CDCl_3) δ 149.2, 141.3, 138.3, 132.3, 130.2, 128.9, 128.9, 128.1, 128.0, 126.7, 126.0, 40.3, 39.0, 32.7, 32.6, 24.8, 24.8; AMM (ESI) m/z calcd for $\text{C}_{19}\text{H}_{23}\text{N}_2^+$ $[\text{M}+\text{H}]^+$ 279.1856 found 279.1857.



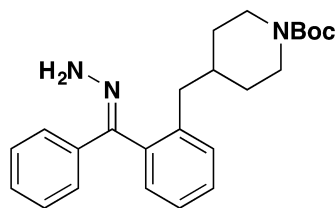
1-Phenylspiro(cyclopentane-1,2'-indane) (178c) was synthesized according to general

procedure I using hydrazone **177c** (51 mg, 0.18 mmol), MnO₂ (126 mg, 1.48 mmol), and Rh₂(*R*-PTAD)₄ (2 mg, 0.001 mmol) in CH₂Cl₂ (9.0 mL). The crude product was purified by flash column chromatography (4:96, EtOAc:hexanes) affording indane **178c** as a clear oil (39 mg, 86 %, 93:7 er). ¹H NMR (600 MHz, CDCl₃) δ 7.29 – 7.23 (m, 3H), 7.23 – 7.16 (m, 2H), 7.13 (t, *J* = 7.4 Hz, 1H), 7.07 – 7.00 (m, 3H), 4.16 (s, 1H), 2.99 (d, *J* = 15.4 Hz, 1H), 2.78 (d, *J* = 15.5 Hz, 1H), 1.74 – 1.61 (m, 4H), 1.62 – 1.54 (m, 1H), 1.52 – 1.44 (m, 1H), 1.23 – 1.16 (m, 1H), 1.15 – 1.08 (m, 1H); ¹³C NMR (151 MHz, CDCl₃) δ 146.8, 143.6, 142.1, 129.5, 128.1, 126.7, 126.4, 126.4, 125.4, 124.7, 60.1, 57.2, 44.9, 39.3, 33.8, 23.5, 23.4; IR (neat) 3024, 2952, 2871, 745, 703 cm⁻¹; AMM (ESI) *m/z* calcd for C₁₉H₂₄N⁺ [M+NH₄]⁺ 266.1903 found 266.1915; [α]_D²⁶ = -1.32 (c = 0.79, CHCl₃).



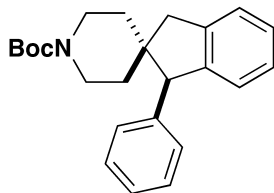
tert-butyl 4-(2-benzoylbenzylidene)piperidine-1-carboxylate (213). Following a literature procedure,⁷⁶ to a solution of phosphonate **206** (0.162 g, 0.517 mmol) and 1-boc-4-piperidone (0.099 g, 0.497 mmol) in anhydrous THF (2 mL) was added NaH (60% in mineral oil, 0.021 g, 0.525 mmol) at 0 °C. The reaction mixture was allowed to warm to room temperature and stirred for 18 h. The reaction mixture was quenched with H₂O (10 mL), extracted with CH₂Cl₂ (2 x 10 mL), dried over Na₂SO₄, filtered, and concentrated *in vacuo*. The crude material was purified by flash column chromatography (15:85, EtOAc:hexanes) to afford the desired benzophenone **213** as an off-white amorphous solid (0.142 g, 77%). ¹H NMR (600 MHz, CDCl₃) δ 7.72 (d, *J* = 7.6 Hz, 2H), 7.55 (td, *J* = 7.4,

1.3 Hz, 1H), 7.49 – 7.45 (m, 1H), 7.45 – 7.38 (m, 3H), 7.34 (t, $J = 7.5$ Hz, 1H), 7.22 (d, $J = 7.6$ Hz, 1H), 6.20 (s, 1H), 3.26 (dt, $J = 15.3, 5.9$ Hz, 4H), 2.20 (bs, 2H), 2.08 – 2.03 (m, 2H), 1.44 (s, 9H); ^{13}C NMR (151 MHz, CDCl_3) δ 198.6, 154.7, 139.8, 139.0, 138.0, 136.2, 133.0, 130.1, 130.1, 129.9, 128.4, 126.6, 123.0, 79.56, 45.6, 44.8, 44.0, 35.8, 29.4, 28.5; AMM (ESI) m/z calcd for $\text{C}_{24}\text{H}_{28}\text{NO}_3^+$ $[\text{M}+\text{H}]^+$ 378.2064 found 378.2071; IR (neat): 2936, 2869, 1693, 1666, 1599 cm^{-1} . Note: This compound forms rotamers due to the Boc protecting group. The final indane structure was proved by crystal structure.



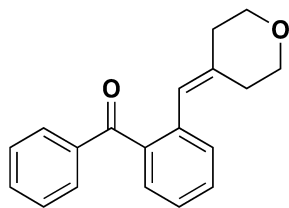
tert-butyl (E)-4-(2-(hydrazineylidene(phenyl)methyl)benzylidene)piperidine-1-carboxylate (177d) was synthesized according to general procedure E, benzophenone **213** (0.207 g, 0.548 mmol), N_2H_4 (0.20 mL, 7.0 mmol), AcOH (0.040 mL, 0.70 mmol) and anhydrous EtOH (8.3 mL) were used. The crude reaction mixture was taken into general procedure F, 10% palladium on carbon (0.030 g, 0.028 mmol) and CH_3OH (1.9 mL) were used. Purification by flash column chromatography on neutral alumina (12:88, EtOAc:hexanes), hydrazone **177d** was obtained as a white solid (0.162 g, 75%). ^1H NMR (600 MHz, CDCl_3) δ 7.44 (d, $J = 6.8$ Hz, 2H), 7.41 – 7.34 (m, 2H), 7.33 (d, $J = 7.4$ Hz, 1H), 7.30 – 7.26 (m, 3H), 7.15 (d, $J = 7.3$ Hz, 1H), 5.35 (s, 2H), 3.95 (br s, 2H), 2.56 – 2.27 (m, 4H), 1.61 – 1.44 (m, 3H), 1.41 (s, 9H), 1.06 – 0.89 (m, 2H); ^{13}C NMR (151 MHz, CDCl_3) δ 154.8, 148.8, 139.4, 138.2, 132.6, 130.9, 129.2, 128.9, 128.2, 128.1, 127.1,

125.9, 79.1, 44.1, 43.5, 40.3, 36.4, 32.1, 28.4; AMM (ESI) m/z calcd for $C_{24}H_{32}N_3O_2^+$ $[M+H]^+$ 394.2489 found 394.2505. Note: This compound forms rotamers due to the Boc protecting group. The final indane structure was proved by crystal structure.

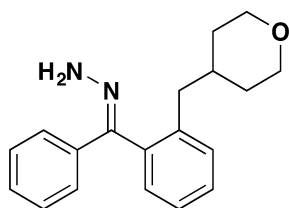


1-Phenylspiro((*tert*-butyl 4-methylidenepiperidine-1-carboxylate)-1,2'-indane)

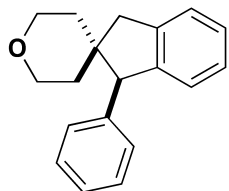
(178d) was synthesized according to general procedure H using hydrazone **177d** (32 mg, 0.081 mmol), MnO_2 (56 mg, 0.64 mmol), and $Rh_2(R-PTAD)_4$ (2 mg, 0.001 mmol) in CH_2Cl_2 (5.4 mL). The crude product was purified by flash column chromatography (10:90, EtOAc:hexanes) affording indane **178d** as a white solid (30 mg, 91 %, 96:4er). 1H NMR (600 MHz, $CDCl_3$) δ 7.30 – 7.25 (m, 3H), 7.26 – 7.19 (m, 2H), 7.15 (t, $J = 7.4$ Hz, 1H), 7.05 (d, $J = 7.4$ Hz, 1H), 7.04 – 6.98 (m, 2H), 4.06 (s, 1H), 3.92 (br s, 1H), 3.73 (br s, 1H), 3.07 (d, $J = 15.7$ Hz, 1H), 3.02 (t, $J = 11.8$ Hz, 1H), 2.95 – 2.88 (m, 1H), 2.86 (d, $J = 15.6$ Hz, 1H), 1.75 – 1.63 (m, 2H), 1.41 (s, 9H), 1.14 – 1.01 (m, 2H); ^{13}C NMR (151 MHz, $CDCl_3$) δ 155.0, 145.4, 142.2, 140.2, 129.8, 128.2, 127.0, 126.8, 125.7, 125.0, 79.4, 62.4, 46.9, 40.8, 37.0, 32.2, 28.6; IR (neat) 3023.8, 2930.9, 1694.0, 1423.4, 748.4 cm^{-1} ; AMM (ESI) m/z calcd for $C_{24}H_{29}NO_2Na^+$ $[M+Na]^+$ 386.2091, found 386.2095 m.p. 96.3 °C; $[\alpha]_D^{25} = -12.1$ ($c = 0.45$, $CHCl_3$). Note: This compound forms rotamers due to the Boc protecting group. The final structure was proved by crystal structure.



2-(4-Benzylidenetetrahydro-2H-pyran)benzophenone (214) Following a literature procedure,⁷⁶ to a solution of phosphonate **206** (0.560 g, 1.69 mmol) and tetrahydro-4H-pyran-4-one (0.160 mL, 1.73 mmol) in anhydrous THF (7 mL) was added NaH (60% in mineral oil, 0.0740 g, 1.85 mmol) at 0 °C. The reaction mixture was allowed to warm to room temperature and stirred for 18 h. The reaction mixture was quenched with H₂O (20 mL), extracted with CH₂Cl₂ (2 x 20 mL), dried over Na₂SO₄, filtered, and concentrated *in vacuo*. The crude material was purified by flash column chromatography (15:85, EtOAc:hexanes) to afford the desired benzophenone **214** as a light-yellow oil (0.142 g, 77%). ¹H NMR (600 MHz, CDCl₃) δ 7.73 (d, *J* = 8.2 Hz, 2H), 7.56 (td, *J* = 7.6, 1.2 Hz, 1H), 7.49 – 7.40 (m, 4H), 7.34 (t, *J* = 7.5 Hz, 1H), 7.24 (d, *J* = 7.7 Hz, 1H), 6.17 (s, 1H), 3.53 (q, *J* = 5.7 Hz, 4H), 2.28 (t, *J* = 5.5 Hz, 2H), 2.13 (t, *J* = 5.4 Hz, 2H); ¹³C NMR (151 MHz, CDCl₃) δ 198.7, 139.1, 138.0, 136.2, 133.1, 130.2, 130.1, 130.0, 128.5, 128.5, 126.6, 122.3, 110.1, 69.2, 68.4, 36.8, 30.9; AMM (ESI) *m/z* calcd for C₁₉H₁₉O₂⁺ [M+H]⁺ 279.1380 found 279.1393; IR (neat): *v*_{max} 2907, 2847, 1663, 1599 cm⁻¹.

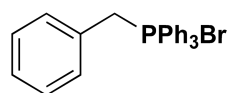


2-((Tetrahydro-2H-pyran-4-yl)methyl)benzophenone hydrazone (177e) was synthesized according to general procedure E, benzophenone **214** (0.293 g, 1.05mmol), N₂H₄ (0.40 mL, 13 mmol), AcOH (0.070 mL, 1.2 mmol) and anhydrous EtOH (17.0 mL) were used. The crude reaction mixture was taken into general procedure F, 10% palladium on carbon (0.057 g, 0.054 mmol) and CH₃OH (3.6 mL) were used. Following purification by flash column chromatography on neutral alumina (88:12 to 60:40, hexanes:EtOAc), hydrazone **177e** was obtained as a yellow oil (0.222 g, 72%). ¹H NMR (600 MHz, CDCl₃) δ 7.47 – 7.42 (m, 2H), 7.42 – 7.32 (m, 3H), 7.30 – 7.24 (m, 3H), 7.16 (dd, *J* = 7.3, 1.6 Hz, 1H), 5.35 (s, 2H), 3.84 (dd, *J* = 11.1, 3.1 Hz, 1H), 3.79 (dd, *J* = 10.9, 3.2 Hz, 1H), 3.17 (td, *J* = 11.8, 2.3 Hz, 1H), 3.13 (td, *J* = 11.7, 2.3 Hz, 1H), 2.42 – 2.33 (m, 2H), 1.69 – 1.60 (m, 1H), 1.45 – 1.40 (m, 1H), 1.38 – 1.33 (m, 1H), 1.25 – 1.18 (m, 1H), 1.16 – 1.08 (m, 1H); ¹³C NMR (151 MHz, CDCl₃) δ 148.8, 139.2, 138.2, 132.6, 130.9, 129.1, 128.9, 128.2, 128.1, 127.1, 125.9, 67.9, 67.8, 40.6, 35.4, 33.1, 33.0; AMM (ESI) *m/z* calcd for C₁₉H₂₂N₂O⁺ [M+H]⁺ 295.1805 found 295.1806.

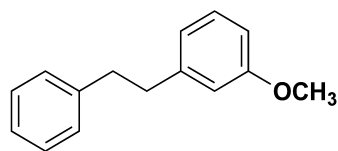


1-Phenylspiro((tetrahydro-2H-pyran-4-yl)-1,2'-indane) (178e) was synthesized according to general procedure I using hydrazone **177e** (38 mg, 0.13 mmol), MnO₂ (89 mg, 1.0 mmol), and Rh₂(*R*-PTAD)₄ (2 mg, 0.001 mmol) in CH₂Cl₂ (8 mL). The crude product was purified by flash column chromatography (10:90, EtOAc:hexanes) affording indane **178e** as a white solid (30 mg, 89 %, 94:6 er). ¹H NMR (600 MHz, CDCl₃) δ 7.30 –

7.26 (m, 3H), 7.25 – 7.19 (m, 2H), 7.15 (t, $J = 7.4$ Hz, 1H), 7.05 (d, $J = 7.5$ Hz, 1H), 7.02 (d, $J = 7.3$ Hz, 2H), 4.06 (s, 1H), 3.87 (dt, $J = 11.7, 3.9$ Hz, 1H), 3.69 (dt, $J = 11.7, 4.0$ Hz, 1H), 3.64 (td, $J = 11.5, 2.6$ Hz, 1H), 3.52 (td, $J = 11.4, 2.5$ Hz, 1H), 3.13 (d, $J = 15.6$ Hz, 1H), 2.92 (d, $J = 15.6$ Hz, 1H), 1.87 (ddd, $J = 13.4, 11.2, 4.5$ Hz, 1H), 1.61 (dq, $J = 13.8, 2.9$ Hz, 1H), 1.25 (ddd, $J = 13.6, 11.2, 4.6$ Hz, 1H), 1.05 (dq, $J = 13.6, 2.3$ Hz, 1H); ^{13}C NMR (151 MHz, CDCl_3) δ 145.4, 142.3, 140.2, 129.8, 128.2, 127.0, 126.8, 126.78, 125.8, 125.0, 65.4, 65.1, 62.8, 46.1, 41.6, 37.8, 33.1; IR (neat): 3020, 2918, 2845, 1453, 1102 cm^{-1} ; AMM (ESI) m/z calcd for $\text{C}_{19}\text{H}_{24}\text{NO}^+ [\text{M}+\text{NH}_4]^+$ 282.1852 found 282.2846; m.p. 126.5 $^\circ\text{C}$; $[\alpha]_{\text{D}}^{26} = 7.70$ ($c = 0.50, \text{CHCl}_3$).

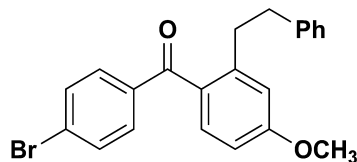


Benzyltriphenylphosphonium bromide (190). Following a modified literature procedure,⁸³ triphenylphosphine (1.69 g, 6.44 mmol) was added to a solution of benzyl bromide (0.69 mL, 5.9 mmol) in anhydrous toluene (10 mL). The reaction mixture was refluxed open to air overnight. The white precipitate formed was collected by vacuum filtration and the filter cake was rinsed with toluene and hexanes and then dried by pulling air through the cake for 2 h to give the phosphonium salt as a white powder (2.47 g, 97%) which was used without further purification.



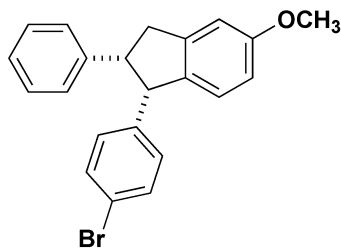
1-Methoxy-3-phenethylbenzene (192). Following a modified literature procedure,⁸⁴ sodium hydride (60% in mineral oil, 0.112 g, 3.05 mmol) was added to a solution of Wittig

salt **190** (1.00 g, 2.31 mmol) and anhydrous THF (23 mL) in a flame-dried flask at 0 °C. A solution of m-anisaldehyde (0.28 mL, 2.3 mmol) in THF (23 mL) was added to the sodium hydride mixture dropwise and allowed to warm to room temperature. After 23 hours, the reaction was quenched by the addition of H₂O (40 mL) and extracted with EtOAc (3 x 30 mL). The combined organic layers were washed with H₂O (1 x 30 mL), brine (1 x 30 mL), dried over Na₂SO₄, filtered, concentrated *in vacuo* and purified by flash column chromatography (1:99 to 5:95, EtOAc:hexanes) to afford the alkene product as mixture of isomers (0.483 g, 98%). Hydrogenation: A solution of the alkene isomers in EtOAc (23.0 mL) was added to a flask with palladium on carbon (10% Pd/C, 0.0759 g) under argon. The solution was sparged with hydrogen gas while stirring for five minutes and the reaction was left to stir overnight under an atmosphere of hydrogen. The flask was flushed with argon gas prior to filtering through Celite and concentrating *in vacuo* to afford the product **192** as a clear oil (0.473 g, 97%) with no purification necessary. ¹H NMR (600 MHz, CDCl₃) δ 7.31 – 7.26 (m, 2H), 7.23 – 7.16 (m, 4H), 6.79 (d, *J* = 7.4 Hz, 1H), 6.77 – 6.71 (m, 2H), 3.78 (s, 3H), 2.96 – 2.87 (m, 4H). ¹H NMR is consistent with published data.⁸⁴



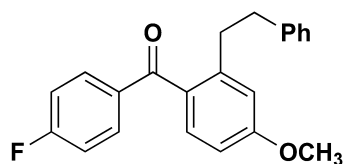
(4-Bromophenyl)(4-methoxy-2-phenethylphenyl)methanone (194a). Following a modified literature procedure,⁸⁵ tin (IV) chloride in CH₂Cl₂ (1.0 M, 3.5 mL, 3.5 mmol) was added to a solution of **192** (0.455 g, 2.14 mmol) in CH₂Cl₂ (6.3 mL) in a flame-dried flask at 0 °C. A solution of 4-bromobenzoyl chloride (0.713 g, 3.25 mmol) in CH₂Cl₂ (6.3 mL)

was slowly added to the tin (IV) chloride mixture. After addition was complete, the reaction was warmed to room temperature and stirred for 24 hours. The reaction was quenched by pouring into H₂O (40 mL) and extracted with Et₂O (3 x 30 mL). The combined organic layers were dried over Na₂SO₄, filtered, concentrated *in vacuo*, and purified by flash column chromatography (5:95 to 65:35, CH₂Cl₂) to yield ketone **194a** as a white amorphous solid (0.476 g, 56%). ¹H NMR (600 MHz, CDCl₃) δ 7.59 (d, *J* = 8.1 Hz, 2H), 7.54 (d, *J* = 8.3 Hz, 2H), 7.25 (d, *J* = 8.5 Hz, 1H), 7.23 – 7.17 (m, 2H), 7.12 (d, *J* = 7.4 Hz, 3H), 6.79 (s, 1H), 6.72 (d, *J* = 7.9 Hz, 1H), 3.78 (s, 3H), 3.10 – 3.02 (m, 2H), 2.94 – 2.86 (m, 2H); ¹³C NMR (151 MHz, CDCl₃) δ 196.4, 161.5, 144.7, 141.5, 137.6, 132.2, 131.6, 131.6, 129.9, 128.6, 128.3, 127.7, 126.0, 116.4, 110.5, 55.4, 38.2, 35.8; AMM (ESI) *m/z* calcd C₂₂H₂₀BrO₂Na⁺ [M+Na]⁺ 417.0459 found 417.0466.



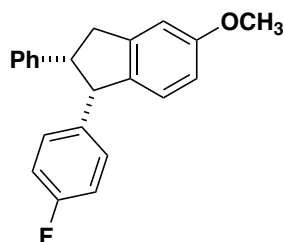
(1S,2R)-1-(4-bromophenyl)-5-methoxy-2-phenyl-2,3-dihydro-1H-indene (188) was synthesized according to general procedure H using hydrazone **195a** (25 mg, 0.061 mmol), MnO₂ (42 mg, 0.49 mmol), and Rh₂(S-PTAD)₄ (1.0 mg, 0.0006 mmol) in CH₂Cl₂. The crude product was purified by flash column chromatography (60:40, CH₂Cl₂:hexanes) affording indane **188** as a clear oil (15 mg, 65%, 97:3 er, >95:5 dr). ¹H

NMR (600 MHz, CDCl₃) δ 7.14 – 7.08 (m, 2H), 7.08 – 7.02 (m, 3H), 7.00 – 6.91 (m, 2H), 6.81 – 6.78 (m, 2H), 6.76 (dd, *J* = 8.3, 2.5 Hz, 1H), 6.47 – 6.40 (m, 2H), 4.55 (d, *J* = 8.0 Hz, 1H), 4.05 – 3.98 (m, 1H), 3.85 (s, 3H), 3.32 (dd, *J* = 15.8, 8.5 Hz, 1H), 3.21 (dd, *J* = 15.8, 7.5 Hz, 1H); ¹³C NMR (151 MHz, CDCl₃) δ 159.3, 145.4, 140.8, 140.3, 136.9, 130.7, 130.6, 128.3, 127.8, 126.2, 125.9, 119.8, 112.8, 109.8, 55.5, 55.4, 52.1, 37.0; AMM (ESI) *m/z* calcd for C₂₂H₁₉BrONa⁺ [M+Na]⁺ 401.0511, found 401.0533; [α]_D²³ = 0.147 (c = 70, CHCl₃).

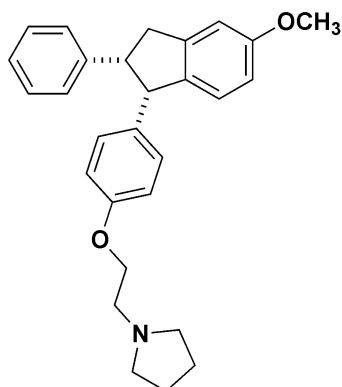


(4-fluorophenyl)(4-methoxy-2-phenethylphenyl)methanone (195b) Following a modified literature procedure,⁸⁵ tin (IV) chloride in CH₂Cl₂ (1.0 M, 4.1 mL, 4.1 mmol) was added to a solution of **192** (0.531 g, 2.50 mmol) in CH₂Cl₂ (7.5 mL) in a flame-dried flask at 0 °C. A solution of 4-fluorobenzoyl chloride (0.531 g, 3.34 mmol) in CH₂Cl₂ (7.5 mL) was slowly added to the tin (IV) chloride mixture. After addition was complete the reaction was warmed to room temperature and stirred for 24 hours. The reaction was quenched by pouring into H₂O (40 mL) and extracted with Et₂O (3 x 30 mL). The combined organic layers were dried over Na₂SO₄, filtered, concentrated *in vacuo*, and purified by flash column chromatography (0:100 to 10:90, EtOAc:hexanes) to yield ketone **195b** as a white amorphous solid (0.296 g, 36%). ¹H NMR (600 MHz, CDCl₃) δ 7.78 – 7.72 (m, 2H), 7.27 (d, *J* = 8.5 Hz, 1H), 7.24 – 7.17 (m, 2H), 7.17 – 7.00 (m, 5H), 6.79 (d, *J* = 2.6 Hz, 1H), 6.74 (dd, *J* = 8.4, 2.6 Hz, 1H), 3.80 (s, 3H), 3.09 – 3.01 (m, 2H), 2.94 – 2.86 (m, 2H); ¹³C NMR (151 MHz, CDCl₃) δ 196.2, 165.5 (d, *J* = 254.3 Hz), 161.4, 144.5, 141.6, 135.2 (d,

$J = 2.9$ Hz), 132.8 (d, $J = 9.2$ Hz), 132.0, 130.4, 128.6, 128.4, 126.0, 116.3, 115.4 (d, $J = 21.9$ Hz), 110.6, 55.4, 38.2, 35.9; AMM (ESI) m/z calcd $C_{22}H_{20}FO_2^+$ $[M+H]^+$ 335.1442 found 335.1443.

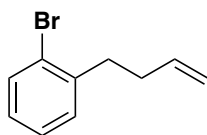


(1*S*,2*R*)-1-(4-fluorophenyl)-5-methoxy-2-phenyl-2,3-dihydro-1*H*-indene (215) was synthesized according to general procedure H using hydrazone **195b** (25mg, 0.072 mmol), MnO_2 (50 mg, 0.58 mmol), and $Rh_2(S-PTAD)_4$ (1.0 mg, 0.0006 mmol) in CH_2Cl_2 . The crude product was purified by flash column chromatography (2:98, EtOAc:hexanes) affording indane **215** as a clear oil (14.5 mg, 93%, 92:8 er, >95:5 dr). 1H NMR (600 MHz, $CDCl_3$) δ 7.07 – 7.01 (m, 3H), 7.00 – 6.93 (m, 2H), 6.81 – 6.74 (m, 3H), 6.72 – 6.65 (m, 2H), 6.54 – 6.47 (m, 2H), 4.58 (d, $J = 8.0$ Hz, 1H), 4.04 – 3.95 (m, 1H), 3.85 (s, 3H), 3.32 (dd, $J = 15.7, 8.5$ Hz, 1H), 3.21 (dd, $J = 15.8, 7.5$ Hz, 1H); ^{13}C NMR (151 MHz, $CDCl_3$) δ 161.27 (d, $J = 243.9$ Hz), 159.2, 145.4, 141.0, 137.3, 136.9, (d, $J = 3.0$ Hz), 130.3 (d, $J = 7.6$ Hz), 128.36, 127.7, 126.1, 126.0, 114.3 (d, $J = 21.2$ Hz), 112.8, 109.7, 55.4, 55.3, 52.2, 37.0; AMM (ESI) m/z calcd for $C_{22}H_{20}FO^+$ $[M]^+$ 318.1420 found 318.1408; $[\alpha]_D^{23} = -0.143$ (c = 71.5, $CHCl_3$).

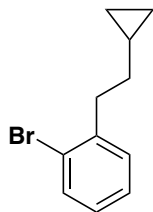


1-(2-(4-((1*S*,2*R*)-5-methoxy-2-phenyl-2,3-dihydro-1*H*-inden-1-yl)phenoxy)ethyl)pyrrolidine (179) was synthesized following a modified literature procedure.⁸⁶ To a flame-dried 5 mL μ W vial was added $\text{Cu}(\text{OAc})_2$ (1 mg, 0.006 mmol). The vial was capped and backfilled with argon. To a separate 20 mL flame-dried scintillation vial was added lithium *tert*-butoxide (32 mg, 0.40 mmol) and the vial was sealed with a septum and backfilled with argon. To the vial was added amine **187** (2.00 mL, 0.07 M) and bromide **188** (50 mg 0.132 mmol). The contents of the vial containing the catalyst, amine and base were added to the vial containing the $\text{Cu}(\text{OAc})_4$. The combined reaction mixture was heated in a microwave reactor for 20 min at 130 °C. The vial was removed from the reactor and $\text{Cu}(\text{OAc})_2$ (1 mg, 0.006 mmol) was added by quickly removing the microwave cap and replacing it. This process was repeated by adding $\text{Cu}(\text{OAc})_2$ (1 mg, 0.006 mmol) every 20 min for 2 h. The crude product was dissolved in H_2O (25 mL) and extracted with CH_2Cl_2 . (3 x 10 mL). The organic layers were combined and washed with H_2O (3 x 25 mL) and brine (1 x 25 mL). The organic layer was dried over anhydrous Na_2SO_4 , concentrated *in vacuo* and purified by flash column chromatography (5:95, $\text{CH}_3\text{OH}:\text{CH}_3\text{Cl}$) affording **179** as a brown oil (25.9 mg, 95%). ^1H

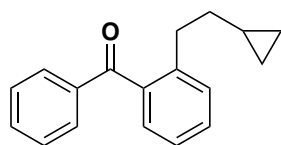
NMR (600 MHz, CDCl₃) δ 7.06 – 7.03 (m, 3H), 7.01 (d, *J* = 8.2 Hz, 1H), 6.95 (s, 1H), 6.82 – 6.78 (m, 2H), 6.77 (dd, *J* = 8.4, 2.4 Hz, 1H), 6.56 (d, *J* = 8.3 Hz, 2H), 6.47 (d, *J* = 8.3 Hz, 2H), 4.55 (d, *J* = 7.9 Hz, 1H), 4.03 – 3.93 (m, 3H), 3.85 (s, 3H), 3.32 (dd, *J* = 15.7, 8.6 Hz, 1H), 3.19 (dd, *J* = 15.7, 7.5 Hz, 1H), 2.85 (t, *J* = 6.0 Hz, 2H), 2.62 (s, 4H), 1.88 – 1.73 (m, 4H); ¹³C NMR (151 MHz, CDCl₃) δ 159.0, 156.9, 145.4, 141.4, 137.8, 133.6, 129.9, 128.5, 127.56, 126.0, 125.95, 113.7, 112.7, 109.7, 66.4, 55.4, 55.2, 54.9, 54.6, 52.4, 37.1, 23.4; AMM (ESI) *m/z* calcd for C₂₈H₃₂NO₂⁺ [M+H]⁺ 414.2428, found 414.2428; [α]_D²³ = -0.033 (c = 16.5, CHCl₃)



1-bromo-2-(but-3-en-1-yl)benzene (71). Was synthesized according to a modified literature procedure.⁸⁷ To a flame dried 250 mL round-bottomed flask was added a solution of 1-bromo-2-(bromomethyl)benzene (1 equiv, 4.00 mmol) as a solution in diethyl ether (1 M). The reaction was cooled to 0 °C and allyl magnesium bromide (2 equiv, 8 mmol) was added. The flask was then allowed to stir overnight and warm to room temperature. . After stirring, the reaction was then cooled to 0 °C and quenched with 100 mL of DI water. The crude reaction mixture was extracted 3x with 25 mL of ethyl acetate, washed with brine, dried over anhydrous Na₂SO₄, and solvent was removed by rotary evaporation affording the desired product without further purification in 99% yield as a clear oil. ¹HNMR was consistent with reported literature values.⁸⁷

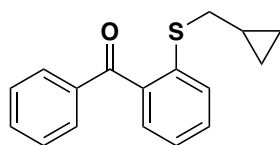


1-bromo-2-(2-cyclopropylethyl)benzene (172). To a flame dried argon backfilled 100 mL round-bottomed flask was added a solution of Et₂Zn in hexanes at 0 °C (2 equiv, 4.8 mmol). To the flask was added TFA dropwise (2 equiv, 4.8 mmol) and the resultant mixture was stirred for 20 mins at 0 °C. To the flask was added a solution of CH₂I₂ (2 equiv, 4.8 mmol) in dry THF (2M) at 0 °C. Finally , a solution of 1-bromo-2-(but-3-en-1-yl)benzene (**171**) (1 equiv, 2.4 mmol) was added in dry THF (1 M) at 0 °C. and the reaction was allowed to warm to room temperature overnight. The reaction mixture was diluted in DI water (100 mL) and extracted with 3x 25 mL of EtOEt. The organic layers were combined, washed with 100 mL of brine, and dried over anhydrous Na₂SO₄. Solvent was removed by rotary evaporation to afford the product in 99 % yield without further purification as a yellow oil.. ¹H NMR (599 MHz, cdcl₃) δ 7.51 (d, *J* = 7.8 Hz, 1H), 7.24 – 7.15 (m, 2H), 7.12 – 7.00 (m, 1H), 2.90 – 2.70 (m, 2H), 1.50 (q, *J* = 7.2 Hz, 2H), 0.83 – 0.65 (m, 1H), 0.44 (d, *J* = 8.1 Hz, 2H), 0.06 (d, *J* = 4.9 Hz, 2H). ¹³C NMR (151 MHz, cdcl₃) δ 141.8, 132.7, 130.5, 127.4, 127.3, 124.5, 36.39, 35.1, 10.8, 4.7.



(2-(2-cyclopropylethyl)phenyl)(phenyl)methanone (173). To a flame dried 100 mL

argon backfilled round-bottomed flask was added 1-bromo-2-(2-cyclopropylethyl)benzene (**172**) (1 equiv, 0.45 mmol) and THF (0.2M). The reaction was cooled to -78 °C and *n*-BuLi (0.8 equiv, 1.7 mmol) was added. The reaction mixture was then warmed to room temperature over 2 hours. The reaction was then cooled to 0 °C and *N*-methoxy-*N*-methylbenzamide (1.2 equiv, 2.6 mmol) was added as a solution in THF (0.8M). The mixture was then warmed to room temperature overnight. Following overnight stirring, the reaction was cooled to 0 °C and quenched with DI water. The quenched mixture was extracted 3x with 25 mL of EtOAc dried over brine and anhydrous Na₂SO₄. Solvent was then removed by rotary evaporation to afford the crude product. The crude product was purified by flash chromatography 80:20 CH₂Cl₂:Hexanes affording **173** as a clear oil (150 mg 27%) ¹H NMR (599 MHz, CDCl₃) δ 7.80 (d, *J* = 8.2 Hz, 2H), 7.58 (t, *J* = 7.4 Hz, 1H), 7.45 (t, *J* = 7.6 Hz, 2H), 7.41 (td, *J* = 7.4, 1.6 Hz, 1H), 7.33 (d, *J* = 7.7 Hz, 1H), 7.29 – 7.27 (m, 1H), 7.26 – 7.22 (m, 1H), 2.75 (dd, *J* = 8.8, 6.9 Hz, 2H), 1.43 (q, *J* = 7.2 Hz, 2H), 0.68 – 0.50 (m, 1H), 0.45 – 0.23 (m, 2H), -0.04 – -0.16 (m, 2H). ¹³C NMR (151 MHz, CDCl₃) δ 198.7, 141.4, 138.5, 137.9, 133.1, 130.2, 130.2, 130.1, 128.4, 128.4, 125.2, 36.9, 33.4, 10.8, 4.4.



(2-((cyclopropylmethyl)thio)phenyl)(phenyl)methanone (163). To a 20 mL oven dried microwave vial was added oven dried Cs₂CO₃ (3 equiv, 7.05 mmol) followed by (2-mercaptophenyl)(phenyl)methanone. (1 equiv, 2.35 mmol) and

(bromomethyl)cyclopropane (1.5 equiv, 3.5 mmol) and dry CH₃CN (0.2 M). The reaction was capped and heated at 65 °C for 24 hours and monitored by TLC. The reaction was then cooled to room temperature and diluted in 100 mL of DI water. The reaction mixture was then extracted 3x with 25 mL of ethyl acetate. The organic layers were combined and dried with brine (100 ml) and anhydrous sodium sulfate. The resultant suspension was filtered and solvent was removed by rotary evaporation to afford the crude product as a yellow oil. The crude material was purified by flash chromatography on silica gel 45:65 CH₂Cl₂:Hexanes. Affording 220mg of **163** in 35% yield as a clear oil. ¹H NMR (400 MHz, CDCl₃) δ 7.82 (d, *J* = 8.0 Hz, 2H), 7.60 (t, *J* = 7.4 Hz, 1H), 7.54 (d, *J* = 7.9 Hz, 1H), 7.46 (q, *J* = 7.9 Hz, 3H), 7.38 (d, *J* = 7.5 Hz, 1H), 7.35 – 7.20 (m, 1H), 2.81 (d, *J* = 7.1 Hz, 2H), 1.03 – 0.85 (m, 1H), 0.53 (d, *J* = 8.0 Hz, 2H), 0.19 (d, *J* = 5.0 Hz, 2H).

2.5 References:

- (1) Wang, H. X.; Wan, Q.; Low, K. H.; Zhou, C. Y.; Huang, J. S.; Zhang, J. L.; Che, C. *M. Chem. Sci.* **2020**, *11*, 2243–2259.
- (2) DeAngelis, A.; Panish, R.; Fox, J. M. *Acc. Chem. Res.* **2016**, *49*, 115–127.
- (3) Bergstrom, B. D.; Nickerson, L. A.; Shaw, J. T.; Souza, L. W. **2021**, 6940–6954.
- (4) Soldi, C.; Lamb, K. N.; Squitieri, R. A.; González-López, M.; Di Maso, M. J.; Shaw, J. T. *J. Am. Chem. Soc.* **2014**, *136*, 15142–15145.
- (5) Davies, H. M. L.; Beckwith, R. E. *J. Chem. Rev.* **2003**, *103*, 2861–2904.
- (6) Doyle, M. P.; Duffy, R.; Ratnikov, M.; Zhou, L. *Chem. Rev.* **2010**, *110*, 704–724.
- (7) Wang, B.; Qiu, D.; Zhang, Y.; Wang, J. *Beilstein J. Org. Chem.* **2016**, *12*, 796–804.
- (8) Davies, H. M. L.; Morton, D. *Chem. Soc. Rev.* **2011**, *40*, 1857–1869.
- (9) Lamb, K. N.; Squitieri, R. A.; Chintala, S. R.; Kwong, A. J.; Balmond, E. I.; Soldi, C.; Dmitrenko, O.; Castiñeira Reis, M.; Chung, R.; Addison, J. B.; et al. *Chem. - A Eur. J.* **2017**, *23*, 11843–11855.
- (10) Xu, P.; Qi, F. L.; Han, F. S.; Wang, Y. H. *Chem. - An Asian J.* **2016**, *11*, 2030–2034.
- (11) Bertani, R.; Michelin, R. A.; Mozzon, M.; Sassi, A.; Basato, M.; Biffis, A.; Martinati,

- G.; Zecca, M. *Inorg. Chem. Commun.* **2001**, *4*, 281–284.
- (12) Aziz, J.; Brion, J. D.; Hamze, A.; Alami, M. *Adv. Synth. Catal.* **2013**, *355*, 2417–2429.
- (13) Hansen, J.; Davies, H. M. L. *Coord. Chem. Rev.* **2008**, *252*, 545–555.
- (14) Timmons, D. J.; Doyle, M. P. *J. Organomet. Chem.* **2001**, *617–618*, 98–104.
- (15) Adly, F. G.; Bollard, H.; Gardiner, M. G.; Ghanem, A. *Catalysts* . 2018.
- (16) Hamze, A.; Tréguier, B.; Brion, J. D.; Alami, M. *Org. Biomol. Chem.* **2011**, *9*, 6200–6204.
- (17) Hamze, A.; Tréguier, B.; Brion, J. D.; Alami, M. *Org. Biomol. Chem.* **2011**, *9*, 6200–6204.
- (18) Xu, P.; Qi, F. L.; Han, F. S.; Wang, Y. H. *Chem. Asian J.* **2016**, *11*, 2030–2034.
- (19) Wu, L.; Zhang, X.; Chen, Q. Q.; Zhou, A. K. *Org. Biomol. Chem.* **2012**, *10*, 7859–7862.
- (20) Salomon, R. G.; Kochi, J. K. *J. Am. Chem. Soc.* **1973**, *95*, 3300–3310.
- (21) Shirafuji, T.; Yamamoto, Y.; Nozaki, H. *Tetrahedron* **1971**, *27*, 5353–5358.
- (22) Pang, Y.; He, Q.; Li, Z.-Q.; Yang, J.-M.; Yu, J.-H.; Zhu, S.-F.; Zhou, Q.-L. *J. Am. Chem. Soc.* **2018**, *140*, 10663–10668.

- (23) Liu, Z.; Huo, J.; Fu, T.; Tan, H.; Ye, F.; Hossain, M. L.; Wang, J. *Chem. Commun.* **2018**, *54*, 11419–11422.
- (24) Del Zotto, A.; Baratta, W.; Miani, F.; Verardo, G.; Rigo, P. *Inorganica Chim. Acta* **2003**, *349*, 249–252.
- (25) Cuevas-Yañez, E.; Serrano, J. M.; Huerta, G.; Muchowski, J. M.; Cruz-Almanza, R. *Tetrahedron* **60**, 9391–9396.
- (26) Xu, P.; Han, F. S.; Wang, Y. H. *Adv. Synth. Catal.* **2015**, *357*, 3441–3446.
- (27) Li, H.; Wang, L.; Zhang, Y.; Wang, J. *Angew. Chem. Int. Ed.* **2012**, *51*, 2943–2946.
- (28) Barluenga, J.; Tomás-Gamasa, M.; Aznar, F.; Valdé, C. *Angew. Chem. Int. Ed.* **2010**, *49*, 4993–4996.
- (29) Qiu, D.; Wang, S.; Meng, H.; Tang, S.; Zhang, Y.; Wang, J. *J. Org. Chem.* **2017**, *82*, 624–632.
- (30) Liu, Z.; Li, Q.; Yang, Y.; Bi, X. *Chem. Commun.* **2017**, *53*, 2503–2506.
- (31) Wang, E.-H.; Ping, Y.-J.; Li, Z.-R.; Qin, H.; Xu, Z.-J.; Che, C.-M. *Org. Lett.* **2018**, *20*, 4641–4644.
- (32) Jagannathan, J. R.; Fettinger, J. C.; Shaw, J. T.; Franz, A. K. *J. Am. Chem. Soc.* **2020**.

- (33) Courant, T.; Kumar, R.; Turcaud, S.; Micouin, L. *Org. Lett.* **2016**, *18*, 4818–4820.
- (34) Polozov, A. M.; Polezhaeva, N. A.; Mustaphin, A. H.; Khotinen, A. V.; Arbuzov, B. A. *Synthesis (Stuttg)*. **1990**, 515–517.
- (35) Bard, A. J.; Whitesides, G. M.; Zare, R. N.; McLafferty, F. W. *Acc. Chem. Res.* **1995**, *28*, 91.
- (36) Arndtsen, B. A.; Bergman, R. G.; Mobley, T. A.; Peterson, T. H. *Acc. Chem. Res.* **1995**, *28*, 154–162.
- (37) Cheung, W. H.; Zheng, S. L.; Yu, W. Y.; Zhou, G. C.; Che, C. M. *Org. Lett.* **2003**, *5*, 2535–2538.
- (38) Soldi, C.; Lamb, K. N.; Squitieri, R. A.; González-López, M.; Di Maso, M. J.; Shaw, J. T. *J. Am. Chem. Soc.* **2014**, *136*, 15142–15145.
- (39) Grasse, P. B.; Brauer, B. E.; Zupancic, J. J.; Kaufmann, K. J.; Schuster, G. B. *J. Am. Chem. Soc.* **1983**, *105*, 6833–6845.
- (40) Leutzsch, M.; Wolf, L. M.; Gupta, P.; Fuchs, M.; Thiel, W.; Farès, C.; Fürstner, A. *Angew. Chemie - Int. Ed.* **2015**, *54*, 12431–12436.
- (41) Doyle, M. P.; Westrum, L. J.; Wolthuis, W. N. E.; See, M. M.; Boone, W. P.; Bagheri, V.; Pearson, M. M. *J. Am. Chem. Soc.* **1993**, *115*, 958–964.
- (42) Collins, L. R.; Van Gastel, M.; Neese, F.; Fürstner, A. *J. Am. Chem. Soc.* **2018**, *140*, 13042–13055.

- (43) Philip S. Skell, R. C. W. *J. Am. Chem. Soc.* **1974**, *314*, 7–8.
- (44) Davies, H. M. L.; Bruzinski, P. R.; Lake, D. H.; Kong, N.; Fall, M. J. *J. Am. Chem. Soc.* **1996**, *118*, 6897–6907.
- (45) Hansen, J.; Autschbach, J.; Davies, H. M. L. *J. Org. Chem.* **2009**, *74*, 6555–6563.
- (46) Nakamura, E.; Yoshikai, N.; Yamanaka, M. *J. Am. Chem. Soc.* **2002**, *124*, 7181–7192.
- (47) Archambeau, A.; Miege, F.; Meyer, C.; Cossy, J. *Angew. Chem. Int. Ed.* **2012**, *124*, 11540–11544.
- (48) Dong, K.; Fan, X.; Pei, C.; Zheng, Y.; Chang, S.; Cai, J.; Qiu, L.; Yu, Z. X.; Xu, X. *Nat. Commun.* **2020**, *11*, 1–10.
- (49) Zhao, X.; Wu, G.; Zhang, Y.; Wang, J. *J. Am. Chem. Soc.* **2011**, *133*, 3296–3299.
- (50) Zhu, D.; Ma, J.; Luo, K.; Fu, H.; Zhang, L.; Zhu, S. *Angew. Chemie - Int. Ed.* **2016**, *55*, 8452–8456.
- (51) Zhu, D.; Chen, L.; Zhang, H.; Ma, Z.; Jiang, H.; Zhu, S. *Angew. Chemie - Int. Ed.* **2018**, *57*, 12405–12409.
- (52) Ma, J.; Jiang, H.; Zhu, S. *Org. Lett.* **2014**, *16*, 4472–4475.
- (53) Huang, M. Y.; Yang, J. M.; Zhao, Y. T.; Zhu, S. F. *ACS Catal.* **2019**, *2*, 5353–5357.

- (54) Solorio-Alvarado, C. R.; Wang, Y.; Echavarren, A. M. *J. Am. Chem. Soc.* **2011**, *133*, 11952–11955.
- (55) Mato, M.; Echavarren, A. M. *Angew. Chem. Int. Ed.* **2019**, *58*, 2088–2092.
- (56) Mata, S.; López, L. A.; Vicente, R. *Angew. Chem. Int. Ed.* **2017**, *56*, 7930–7934.
- (57) Dejon, L.; Mohammed, H.; Du, P.; Jacob, C.; Speicher, A. *Medchemcomm* **2013**, *4*, 1580–1583.
- (58) Ngantchou, I.; Nyasse, B.; Denier, C.; Blonski, C.; Hannaert, V.; Schneider, B. *Bioorg. Med. Chem. Lett.* **2010**, *20*, 3495–3498.
- (59) Zhang, Y.-B.; Zhang, X.-L.; Chen, N.-H.; Wu, Z.-N.; Ye, W.-C.; Li, Y.-L.; Wang, G.-C. *Org. Lett.* **2017**, *19*, 424–427.
- (60) Solé, D.; Mariani, F.; Bennasar, M. L.; Fernández, I. *Angew. Chemie - Int. Ed.* **2016**, *55*, 6467–6470.
- (61) R. Garner. *Tetrahedron Lett.* **1968**, No. 2, 221–224.
- (62) Krogsgaard-Larsen, N.; Begtrup, M.; Herth, M. M.; Kehler, J. *Synthesis (Stuttg.)*. **2010**, No. 24, 4287–4299.
- (63) Lee, S.; Lim, H. J.; Cha, K. L.; Sulikowski, G. A. *Tetrahedron* **1997**, *53*, 16521–16532.
- (64) Ester, D.; Lim, H.; Sulikowski, G. A. **1995**, No. 8, 2326–2327.

- (65) Mahoney, S. J.; Fillion, E. *Chem. - A Eur. J.* **2012**, *18*, 68–71.
- (66) Reddy, A. R.; Hao, F.; Wu, K.; Zhou, C. Y.; Che, C. M. *Angew. Chemie - Int. Ed.* **2016**, *55*, 1810–1815.
- (67) Davies, H. M. L.; Hansen, T.; Churchill, M. R. *J. Am. Chem. Soc.* **2000**, *122*, 3063–3070.
- (68) Demonceau, A.; Noels, A. F.; Hubert, A. J.; Teyssié, P. *J. Chem. Soc. Chem. Commun.* **1981**, No. 14, 688–689.
- (69) Demonceau, A.; Noels, A. F.; Hubert, A. J.; Teyssié, P. *Bull. des Sociétés Chim. Belges* **1984**, *93*, 945–948.
- (70) Govek, S. P.; Smith, N. D. *Preparation of Indane Derivatives for Use as Estrogen Receptor Modulators.*, 2011.
- (71) Dubrovskiy, A. V.; Larock, R. C. *J. Org. Chem.* **2012**, *77*, 11232–11256.
- (72) Buathongjan, C.; Beukeaw, D.; Yotphan, S. *European J. Org. Chem.* **2015**, *2015*, 1575–1582.
- (73) Wu, Y.; Feng, L. J.; Lu, X.; Yee Kwong, F.; Luo, H. Bin. *Chem. Commun.* **2014**, *50*, 15352–15354.
- (74) Gra; Janczyk, W.; Sperl, B.; Elumalai, N.; Kozany, C.; Hausch, F.; Holak, T. A.; Berg, T. *ACS Chem. Biol.* **2011**, *6*, 1008–1014.

- (75) Takahashi, H.; Inagaki, S.; Yoshii, N.; Gao, F.; Nishihara, Y.; Takagi, K. **2009**, 12527–12530.
- (76) Willemse, R. J.; Piet, J. J.; Warman, J. M.; Hartl, F.; Verhoeven, J. W.; Brouwer, A. M. *J. Am. Chem. Soc.* **2000**, *122*, 3721–3730.
- (77) He, C.; Zhang, X.; Huang, R.; Pan, J.; Li, J.; Ling, X.; Xiong, Y.; Zhu, X. *Tetrahedron Lett.* **2014**, *55*, 4458–4462.
- (78) Zou, G.; Reddy, Y. K.; Falck, J. R. **2001**, *42*, 7213–7215.
- (79) Jacq, J.; Einhorn, C.; Einhorn, J. *Org. Lett.* **2008**, *10*, 3757–3760.
- (80) Kotali, A.; Papapetrou, M.; Dimos, V.; Harris, P. A. *Org. Prep. Proced. Int.* **1998**, *30*, 177–181.
- (81) Lei, P.; Meng, G.; Ling, Y.; An, J.; Nolan, S. P.; Szostak, M. *Org. Lett.* **2017**, *19*, 6510–6513.
- (82) Wang, W. J.; Zhao, X.; Tong, L.; Chen, J. H.; Zhang, X. J.; Yan, M. *J. Org. Chem.* **2014**, *79*, 8557–8565.
- (83) Smith, J. A.; Moeller, K. D. *Org. Lett.* **2013**, *15*, 5818–5821.
- (84) Moodie, L. W. K.; Trepos, R.; Cervin, G.; Brathen, K. A.; Lindgard, B.; Reiersen, R.; Cahill, P.; Pavia, H.; Hellio, C.; Svenson, J. *J. Nat. Prod.* **2017**, *80*, 2001–2011.

- (85) Bradshaw, D. P.; Jones, D. W.; Tideswell, J. **1991**, 169–173.
- (86) Huang, J.; Chen, Y.; Chan, J.; Ronk, M. L.; Larsen, R. D.; Faul, M. M. *Synlett* **2011**, No. 10, 1419–1422.
- (87) Lekky, A.; Ruengsatra, T.; Ruchirawat, S.; Ploypradith, P. *J. Org. Chem.* **2019**, *84*, 5277–5291.

146a achiral

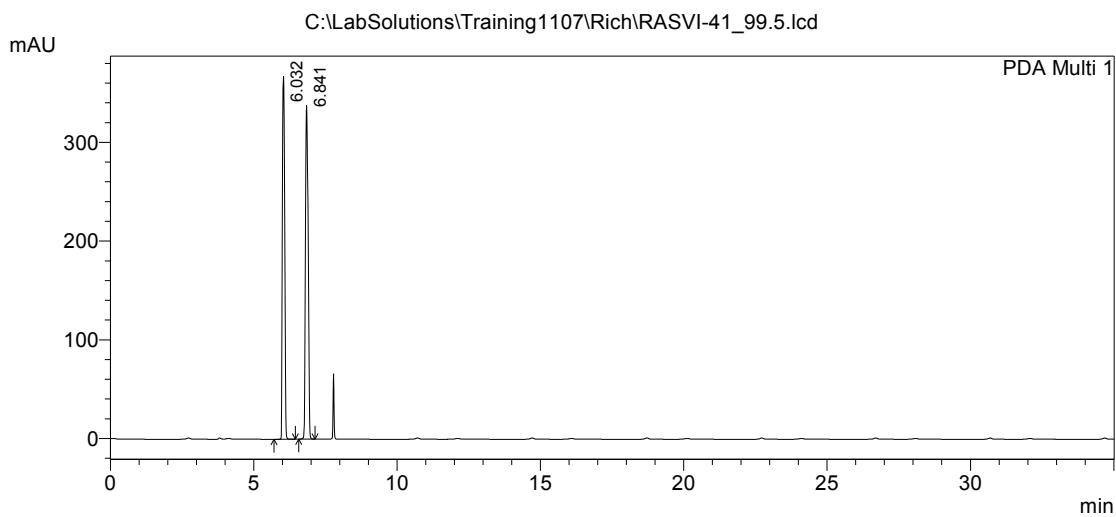


==== HPLC Analysis Report ====

C:\LabSolutions\Training1107\Rich\RASVI-41_99.5.lcd

Acquired by : Admin
 Sample Name : RASVI-41
 Sample ID : RASVI-41
 Tray# : 1
 Vial # : 59
 Injection Volume : 5 uL
 Data File Name : RASVI-41_99.5.lcd
 Method File Name : OD-99.5_0.5_Hexane_IPA_35min.lcm
 Batch File Name : 7.12.17.lcb
 Report File Name : UCD Default.lcr
 Data Acquired : 7/12/2017 5:43:44 PM
 Data Processed : 7/12/2017 6:18:46 PM

<Chromatogram>



1 PDA Multi 1/217nm 4nm

< Peak Table >

PeakTable C:\LabSolutions\Training1107\Rich\RASVI-41_99.5.lcd

PDA Ch1 217nm 4nm

Peak#	Ret. Time	Area	Height	Area %	Height %
1	6.032	2075466	367578	47.676	52.100
2	6.841	2277773	337944	52.324	47.900
Total		4353240	705522	100.000	100.000

146a chiral

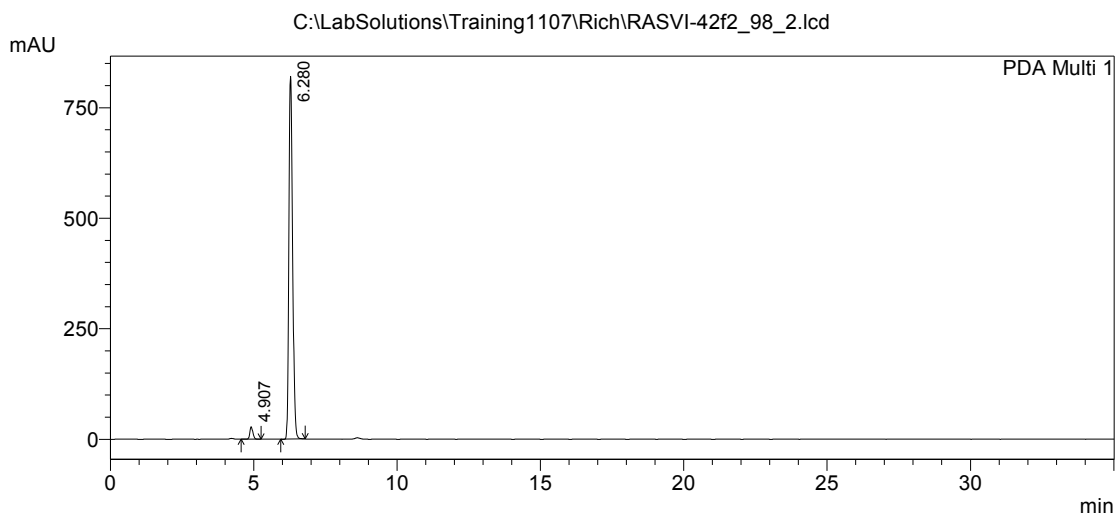


==== HPLC Analysis Report ====

C:\LabSolutions\Training1107\Rich\RASVI-42f2_98_2.lcd

Acquired by : Admin
 Sample Name : RASVI-42f2
 Sample ID : RASVI-42f2
 Tray# : 1
 Vial # : 58
 Injection Volume : 5 uL
 Data File Name : RASVI-42f2_98_2.lcd
 Method File Name : OD-98_2_Hexane_IPA_35min.lcm
 Batch File Name : 7.11.17.lcb
 Report File Name : UCD Default.lcr
 Data Acquired : 7/11/2017 5:19:53 PM
 Data Processed : 7/11/2017 5:54:56 PM

<Chromatogram>



1 PDA Multi 1/257nm 4nm

< Peak Table >

PeakTable C:\LabSolutions\Training1107\Rich\RASVI-42f2_98_2.lcd

PDA Ch1 257nm 4nm

Peak#	Ret. Time	Area	Height	Area %	Height %
1	4.907	206843	27805	2.727	3.278
2	6.280	7379043	820387	97.273	96.722
Total		7585886	848191	100.000	100.000

146b achiral

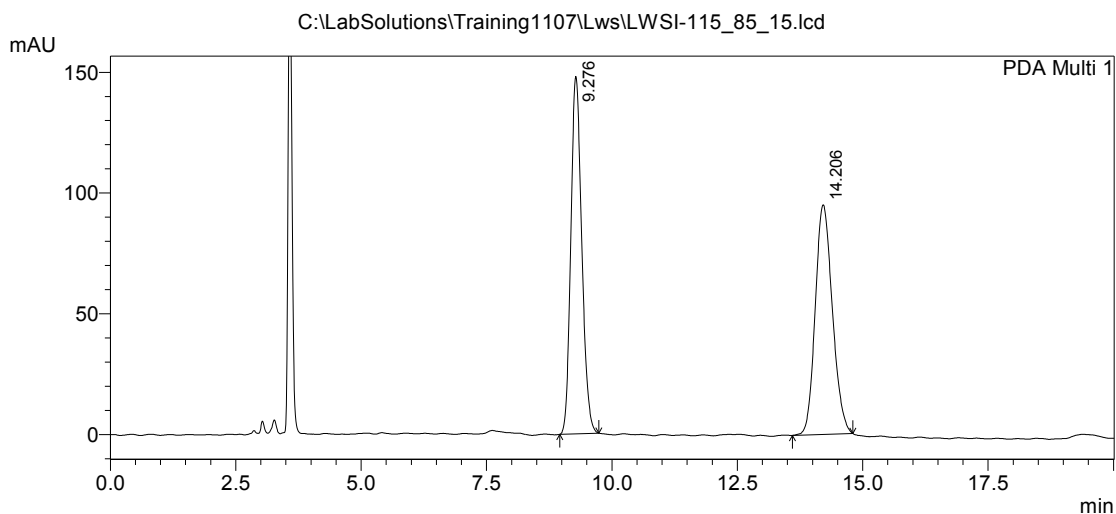


==== HPLC Analysis Report ====

C:\LabSolutions\Training1107\Lws\LWSI-115_85_15.lcd

Acquired by : Admin
 Sample Name : LWSI115
 Sample ID : LWSI-115
 Tray# : 1
 Vial # : 60
 Injection Volume : 1 uL
 Data File Name : LWSI-115_85_15.lcd
 Method File Name : OD-85_15_Hexane_IPA_20min.lcm
 Batch File Name : 8.4.17_new.lcb
 Report File Name : UCD Default.lcr
 Data Acquired : 8/4/2017 5:19:03 PM
 Data Processed : 8/4/2017 5:39:07 PM

<Chromatogram>



1 PDA Multi 1/207nm 4nm

< Peak Table >

PeakTable C:\LabSolutions\Training1107\Lws\LWSI-115_85_15.lcd

PDA Ch1 207nm 4nm

Peak#	Ret. Time	Area	Height	Area %	Height %
1	9.276	2239216	147945	49.759	60.876
2	14.206	2260931	95083	50.241	39.124
Total		4500146	243029	100.000	100.000

146b chiral

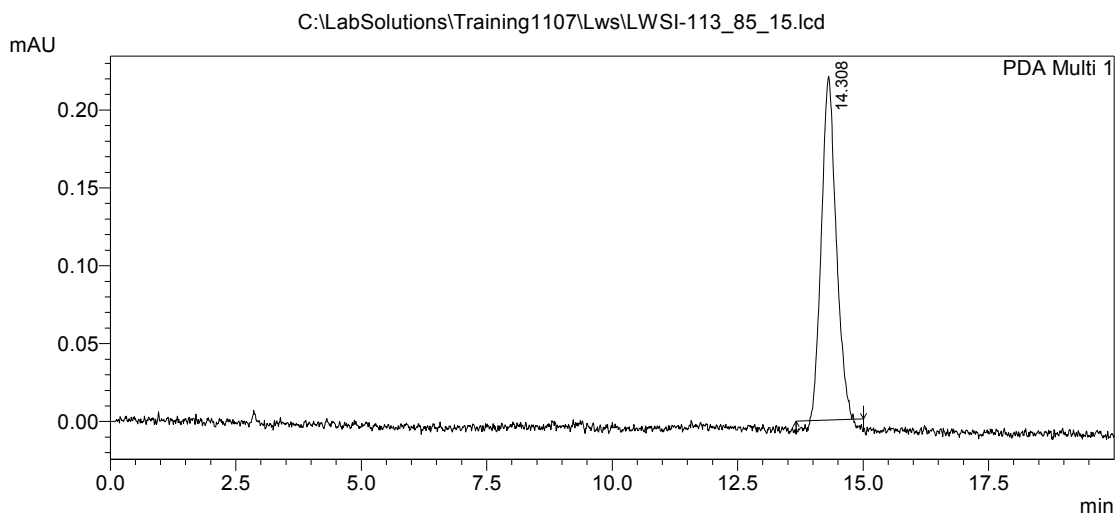


==== HPLC Analysis Report ====

C:\LabSolutions\Training1107\Lws\LWSI-113_85_15.lcd

Acquired by : Admin
 Sample Name : LWSI113
 Sample ID : LWSI-113
 Tray# : 1
 Vial # : 59
 Injection Volume : 1 uL
 Data File Name : LWSI-113_85_15.lcd
 Method File Name : OD-85_15_Hexane_IPA_20min.lcm
 Batch File Name : 8.3.17_new2.lcb
 Report File Name : UCD Default.lcr
 Data Acquired : 8/3/2017 2:26:51 PM
 Data Processed : 8/3/2017 2:46:53 PM

<Chromatogram>



< Peak Table >

PeakTable C:\LabSolutions\Training1107\Lws\LWSI-113_85_15.lcd

PDA Ch1 254nm 4nm

Peak#	Ret. Time	Area	Height	Area %	Height %
1	14.308	4393	221	100.000	100.000
Total		4393	221	100.000	100.000

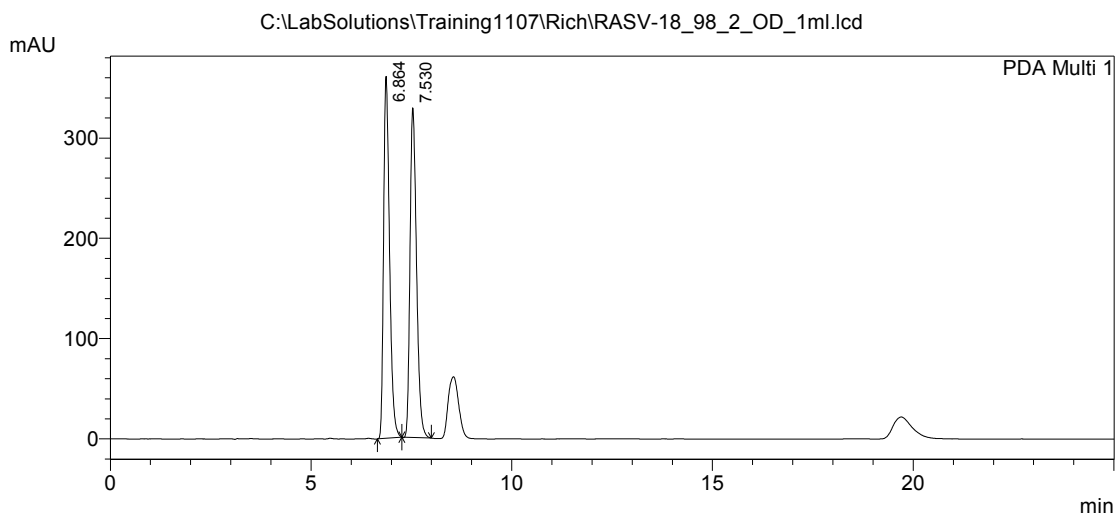
146c achiral



==== HPLC Analysis Report ====

C:\LabSolutions\Training1107\Rich\RASV-18_98_2_OD_1ml.lcd
 Acquired by : Admin
 Sample Name : RASV-18
 Sample ID : RASV-18
 Tray# : 1
 Vial # : 28
 Injection Volume : 10 uL
 Data File Name : RASV-18_98_2_OD_1ml.lcd
 Method File Name : OD-98_2_Hexane_IPA_25min.lcm
 Batch File Name : 8.10.16.lcb
 Report File Name : UCD Default.lcr
 Data Acquired : 8/10/2016 3:37:30 PM
 Data Processed : 8/10/2016 4:02:32 PM

<Chromatogram>



1 PDA Multi 1/313nm 4nm

< Peak Table >

PeakTable C:\LabSolutions\Training1107\Rich\RASV-18_98_2_OD_1ml.lcd

PDA Ch1 313nm 4nm

Peak#	Ret. Time	Area	Height	Area %	Height %
1	6.864	3709067	360905	50.008	52.340
2	7.530	3707899	328635	49.992	47.660
Total		7416965	689540	100.000	100.000

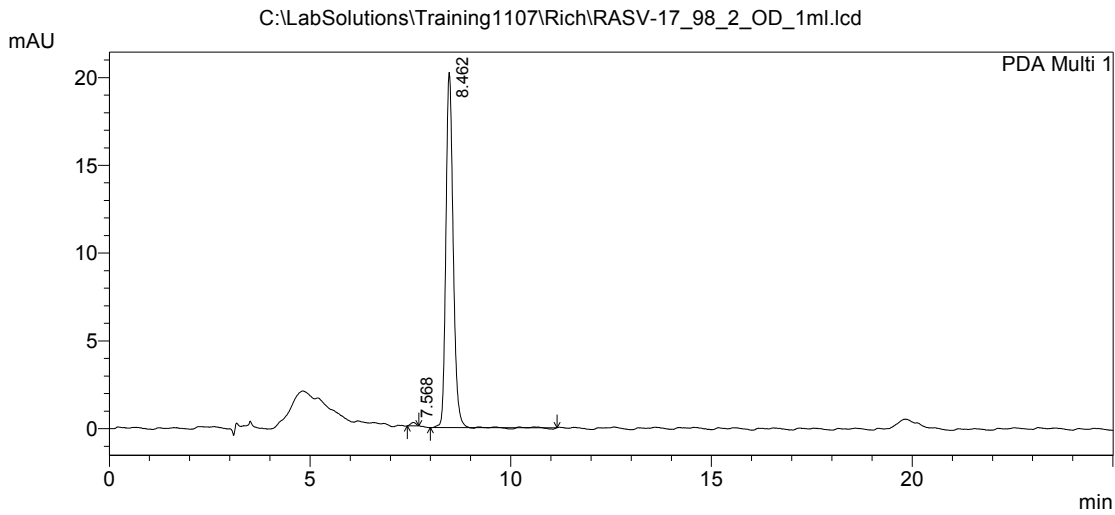
146c chiral



==== HPLC Analysis Report ====

C:\LabSolutions\Training1107\Rich\RASV-17_98_2_OD_1ml.lcd
 Acquired by : Admin
 Sample Name : RASV-18
 Sample ID : RASV-18
 Tray# : 1
 Vial # : 28
 Injection Volume : 10 uL
 Data File Name : RASV-17_98_2_OD_1ml.lcd
 Method File Name : OD-98_2_Hexane_IPA_25min.lcm
 Batch File Name : 8.10.16.lcb
 Report File Name : UCD Default.lcr
 Data Acquired : 8/10/2016 4:02:59 PM
 Data Processed : 8/10/2016 4:28:01 PM

<Chromatogram>



1 PDA Multi 1/313nm 4nm

< Peak Table >

PeakTable C:\LabSolutions\Training1107\Rich\RASV-17_98_2_OD_1ml.lcd

PDA Ch1 313nm 4nm

Peak#	Ret. Time	Area	Height	Area %	Height %
1	7.568	1714	198	0.673	0.971
2	8.462	253135	20233	99.327	99.029
Total		254849	20431	100.000	100.000

146d achiral

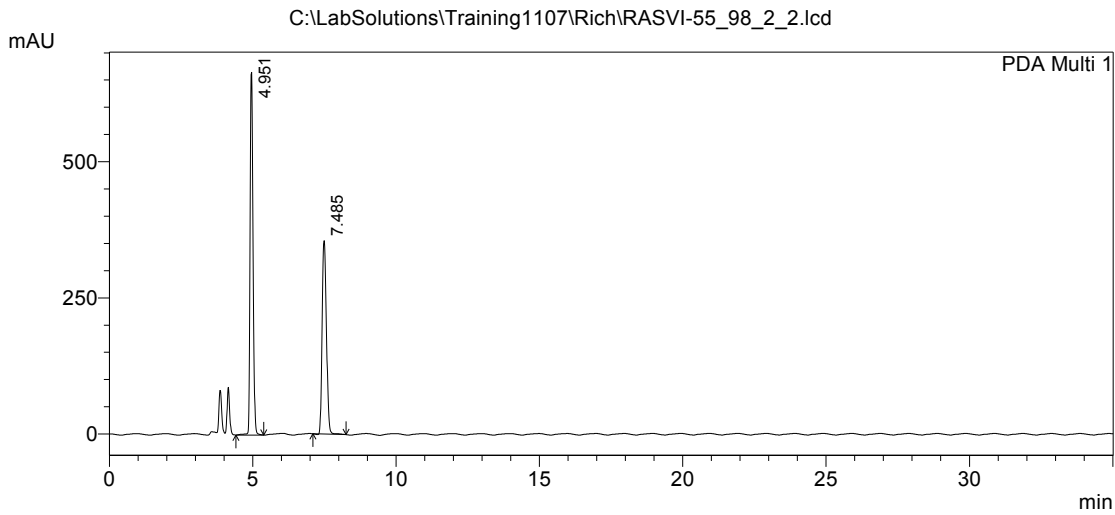


==== HPLC Analysis Report ====

C:\LabSolutions\Training1107\Rich\RASVI-55_98_2_2.lcd

Acquired by : Admin
 Sample Name : RASVI-55
 Sample ID : RASVI-55
 Tray# : 1
 Vial # : 60
 Injection Volume : 5 uL
 Data File Name : RASVI-55_98_2_2.lcd
 Method File Name : OD-98_2_Hexane_IPA_35min.lcm
 Batch File Name : 7.20.17.lcb
 Report File Name : UCD Default.lcr
 Data Acquired : 7/20/2017 9:07:19 PM
 Data Processed : 7/20/2017 9:42:22 PM

<Chromatogram>



< Peak Table >

PeakTable C:\LabSolutions\Training1107\Rich\RASVI-55_98_2_2.lcd

PDA Ch1 254nm 4nm

Peak#	Ret. Time	Area	Height	Area %	Height %
1	4.951	4716536	665822	56.019	65.196
2	7.485	3702927	355438	43.981	34.804
Total		8419463	1021260	100.000	100.000

146d chiral

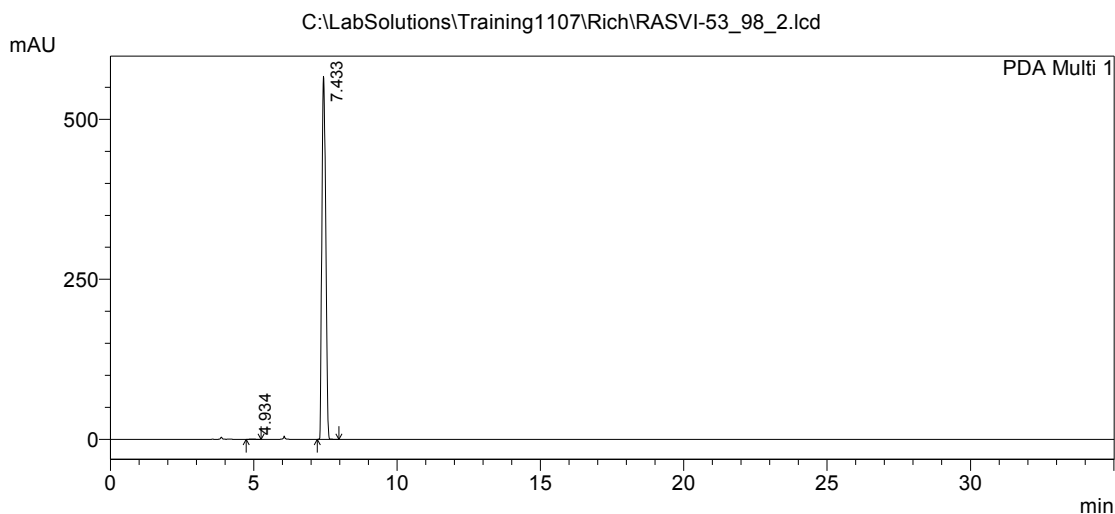


==== HPLC Analysis Report ====

C:\LabSolutions\Training1107\Rich\RASVI-53_98_2.lcd

Acquired by : Admin
 Sample Name : RASVI-53
 Sample ID : RASVI-53
 Tray# : 1
 Vial # : 59
 Injection Volume : 5 uL
 Data File Name : RASVI-53_98_2.lcd
 Method File Name : OD-98_2_Hexane_IPA_35min.lcm
 Batch File Name : 7.20.17.lcb
 Report File Name : UCD Default.lcr
 Data Acquired : 7/20/2017 4:29:33 PM
 Data Processed : 7/20/2017 5:04:36 PM

<Chromatogram>



1 PDA Multi 1/262nm 4nm

< Peak Table >

PeakTable C:\LabSolutions\Training1107\Rich\RASVI-53_98_2.lcd

PDA Ch1 262nm 4nm

Peak#	Ret. Time	Area	Height	Area %	Height %
1	4.934	3699	458	0.069	0.081
2	7.433	5324069	567075	99.931	99.919
Total		5327767	567532	100.000	100.000

146e achiral

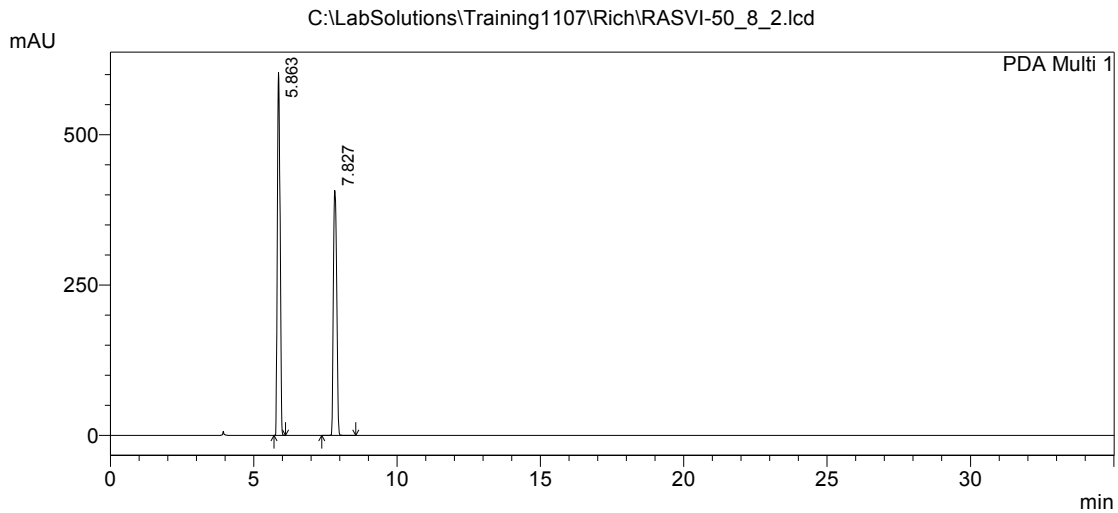


==== HPLC Analysis Report ====

C:\LabSolutions\Training1107\Rich\RASVI-50_8_2.lcd

Acquired by : Admin
 Sample Name : RASVI-50
 Sample ID : RASVI-50
 Tray# : 1
 Vial # : 58
 Injection Volume : 5 uL
 Data File Name : RASVI-50_8_2.lcd
 Method File Name : OD-98_2_Hexane_IPA_35min.lcm
 Batch File Name : 7.14.17.lcb
 Report File Name : UCD Default.lcr
 Data Acquired : 7/15/2017 3:14:27 AM
 Data Processed : 7/15/2017 3:49:29 AM

<Chromatogram>



1 PDA Multi 1/263nm 4nm

< Peak Table >

PeakTable C:\LabSolutions\Training1107\Rich\RASVI-50_8_2.lcd

PDA Ch1 263nm 4nm

Peak#	Ret. Time	Area	Height	Area %	Height %
1	5.863	4074594	603587	54.977	59.702
2	7.827	3336797	407406	45.023	40.298
Total		7411392	1010993	100.000	100.000

146e chiral

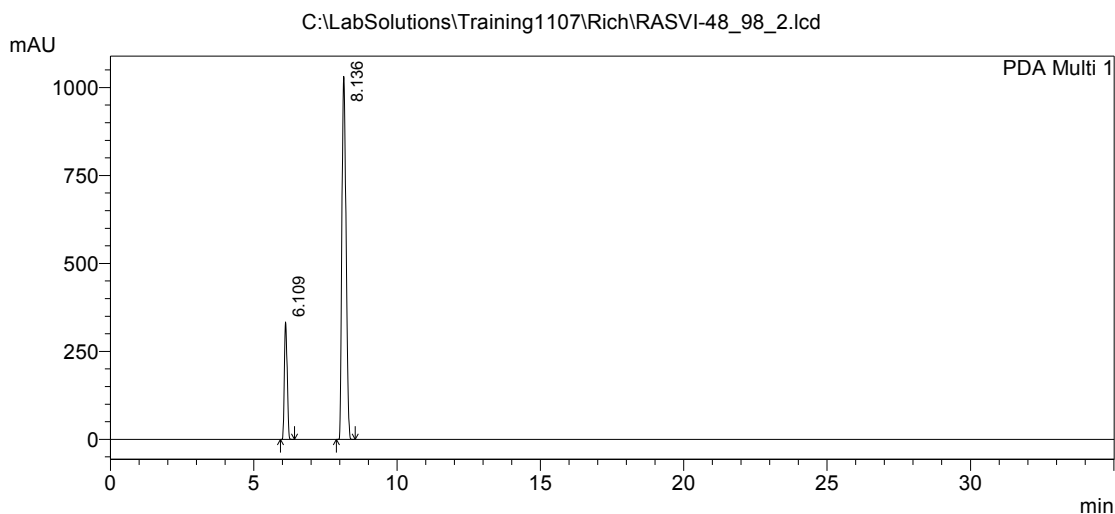


==== HPLC Analysis Report ====

C:\LabSolutions\Training1107\Rich\RASVI-48_98_2.lcd

Acquired by : Admin
 Sample Name : RASVI-48
 Sample ID : RASVI-48
 Tray# : 1
 Vial # : 60
 Injection Volume : 5 uL
 Data File Name : RASVI-48_98_2.lcd
 Method File Name : OD-98_2_Hexane_IPA_35min.lcm
 Batch File Name : 7.14.17.lcb
 Report File Name : UCD Default.lcr
 Data Acquired : 7/15/2017 2:03:33 AM
 Data Processed : 7/15/2017 2:38:35 AM

<Chromatogram>



1 PDA Multi 1/254nm 4nm

< Peak Table >

PeakTable C:\LabSolutions\Training1107\Rich\RASVI-48_98_2.lcd

PDA Ch1 254nm 4nm

Peak#	Ret. Time	Area	Height	Area %	Height %
1	6.109	2321027	333310	18.284	24.419
2	8.136	10373425	1031660	81.716	75.581
Total		12694452	1364970	100.000	100.000

146f achiral

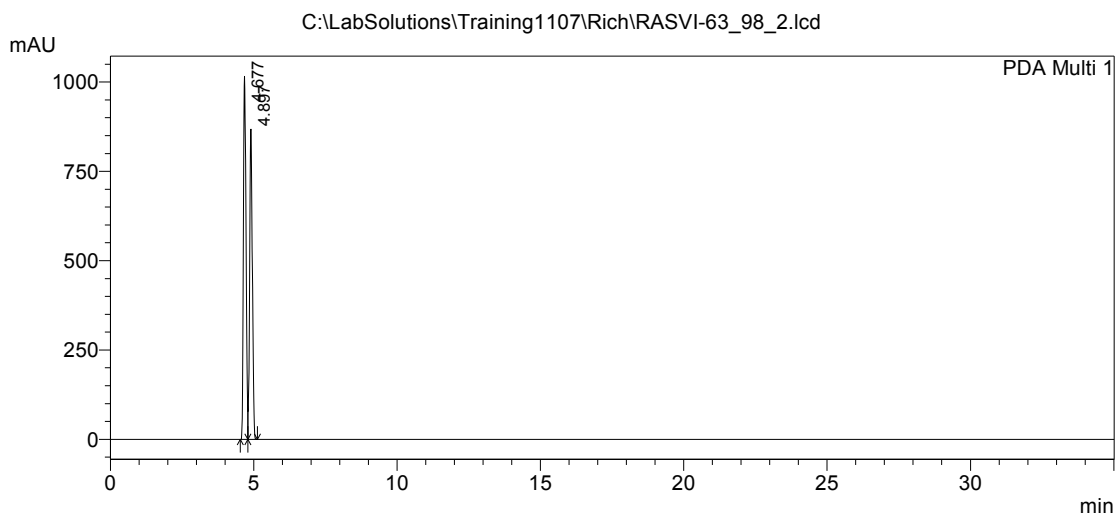


==== HPLC Analysis Report ====

C:\LabSolutions\Training1107\Rich\RASVI-63_98_2.lcd

Acquired by : Admin
 Sample Name : RASVI-63
 Sample ID : RASVI-63
 Tray# : 1
 Vial # : 56
 Injection Volume : 5 uL
 Data File Name : RASVI-63_98_2.lcd
 Method File Name : OD-98_2_Hexane_IPA_35min.lcm
 Batch File Name : 8.1.17.lcb
 Report File Name : UCD Default.lcr
 Data Acquired : 8/2/2017 1:18:26 AM
 Data Processed : 8/2/2017 1:53:27 AM

<Chromatogram>



1 PDA Multi 1/254nm 4nm

< Peak Table >

PeakTable C:\LabSolutions\Training1107\Rich\RASVI-63_98_2.lcd

PDA Ch1 254nm 4nm

Peak#	Ret. Time	Area	Height	Area %	Height %
1	4.677	6521163	1015780	52.875	53.929
2	4.897	5811944	867780	47.125	46.071
Total		12333107	1883560	100.000	100.000

146f chiral

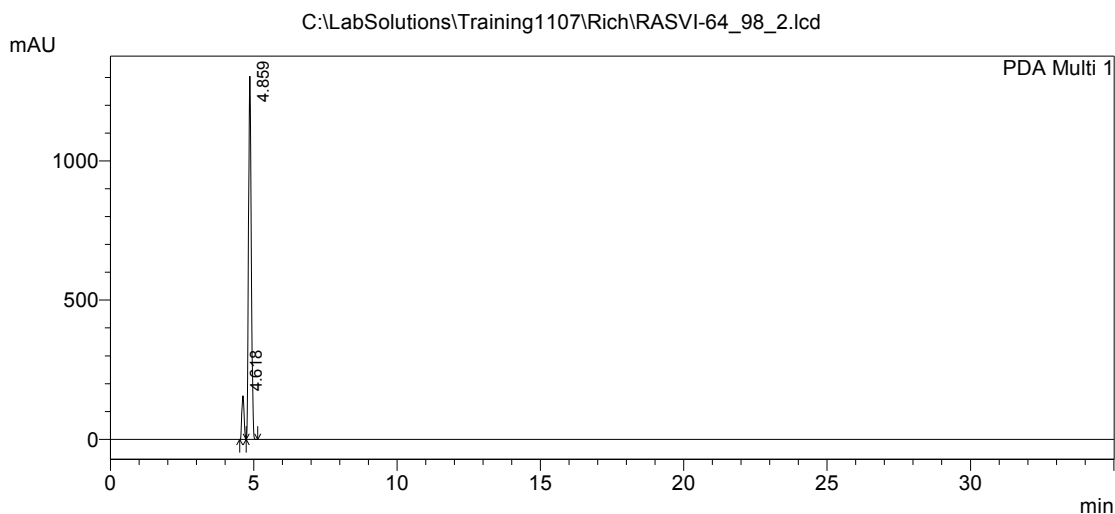


==== HPLC Analysis Report ====

C:\LabSolutions\Training1107\Rich\RASVI-64_98_2.lcd

Acquired by : Admin
 Sample Name : RASVI-63
 Sample ID : RASVI-63
 Tray# : 1
 Vial # : 55
 Injection Volume : 5 uL
 Data File Name : RASVI-64_98_2.lcd
 Method File Name : OD-98_2_Hexane_IPA_35min.lcm
 Batch File Name : 8.1.17.lcb
 Report File Name : UCD Default.lcr
 Data Acquired : 8/2/2017 1:53:51 AM
 Data Processed : 8/2/2017 2:28:53 AM

<Chromatogram>



1 PDA Multi 1/254nm 4nm

< Peak Table >

PeakTable C:\LabSolutions\Training1107\Rich\RASVI-64_98_2.lcd

PDA Ch1 254nm 4nm

Peak#	Ret. Time	Area	Height	Area %	Height %
1	4.618	863113	155935	9.006	10.684
2	4.859	8720681	1303524	90.994	89.316
Total		9583794	1459459	100.000	100.000

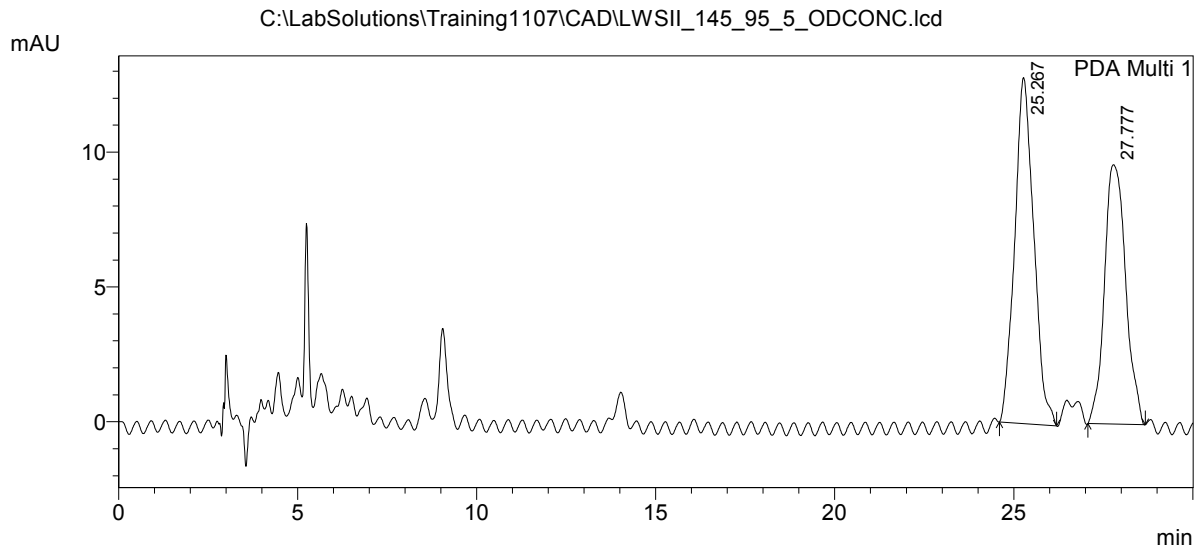
146g achiral

UC DAVIS Department of Chemistry
UNIVERSITY OF CALIFORNIA

==== HPLC Analysis Report ====

Acquired by : Admin
 Sample Name : 1
 Sample ID : 1
 Tray# : 1
 Vial # : 76
 Injection Volume : 20 uL
 Data File Name : LWSII_145_95_5_ODCONC.lcd
 Method File Name : OD-95_5_Hexane_IPA_30min.lcm
 Batch File Name : 8.22.17_CADRUNS.lcb
 Report File Name : UCD Default.lcr
 Data Acquired : 8/5/2018 11:58:35 AM
 Data Processed : 8/5/2018 12:28:38 PM

<Chromatogram>



< Peak Table >

PeakTable C:\LabSolutions\Training1107\CAD\LWSII_145_95_5_ODCONC.lcd

PDA Ch1 254nm 4nm

Peak#	Ret. Time	Area	Height	Area %	Height %
1	25.267	476172	12834	54.563	57.165
2	27.777	396531	9617	45.437	42.835
Total		872703	22450	100.000	100.000

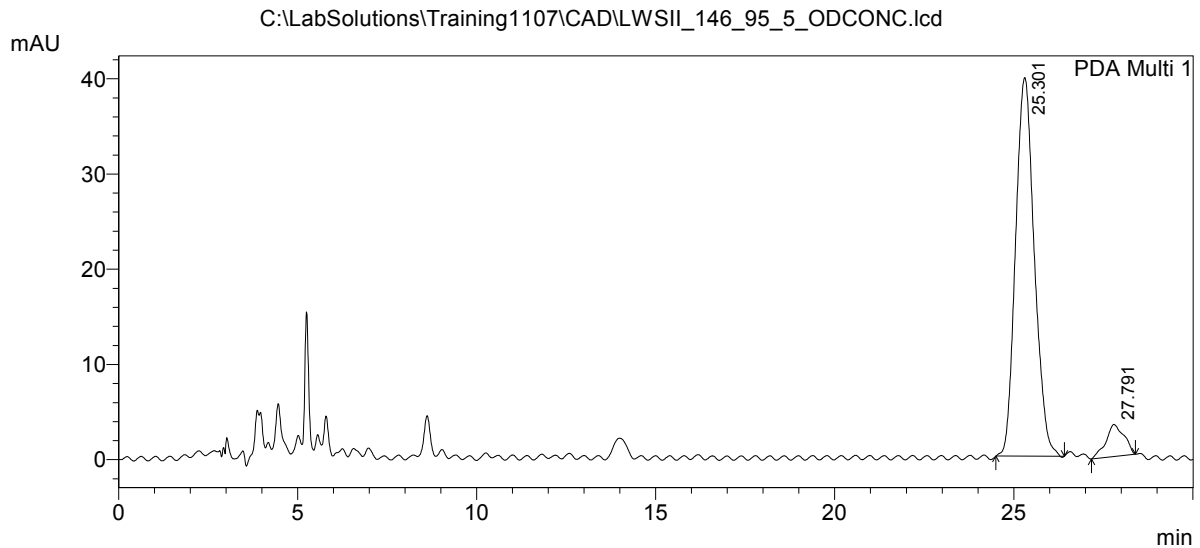
146g chiral



==== HPLC Analysis Report ====

C:\LabSolutions\Training1107\CAD\LWSII_146_95_5_ODCONC.lcd
 Acquired by : Admin
 Sample Name : 1
 Sample ID : 1
 Tray# : 1
 Vial # : 77
 Injection Volume : 20 uL
 Data File Name : LWSII_146_95_5_ODCONC.lcd
 Method File Name : OD-95_5_Hexane_IPA_30min.lcm
 Batch File Name : 8.22.17_CADRUNS.lcb
 Report File Name : UCD Default.lcr
 Data Acquired : 8/5/2018 11:28:08 AM
 Data Processed : 8/5/2018 11:58:10 AM

<Chromatogram>



< Peak Table >

PeakTable C:\LabSolutions\Training1107\CAD\LWSII_146_95_5_ODCONC.lcd

PDA Ch1 254nm 4nm

Peak#	Ret. Time	Area	Height	Area %	Height %
1	25.301	1448245	39751	92.454	92.207
2	27.791	118200	3359	7.546	7.793
Total		1566445	43110	100.000	100.000

178a achiral

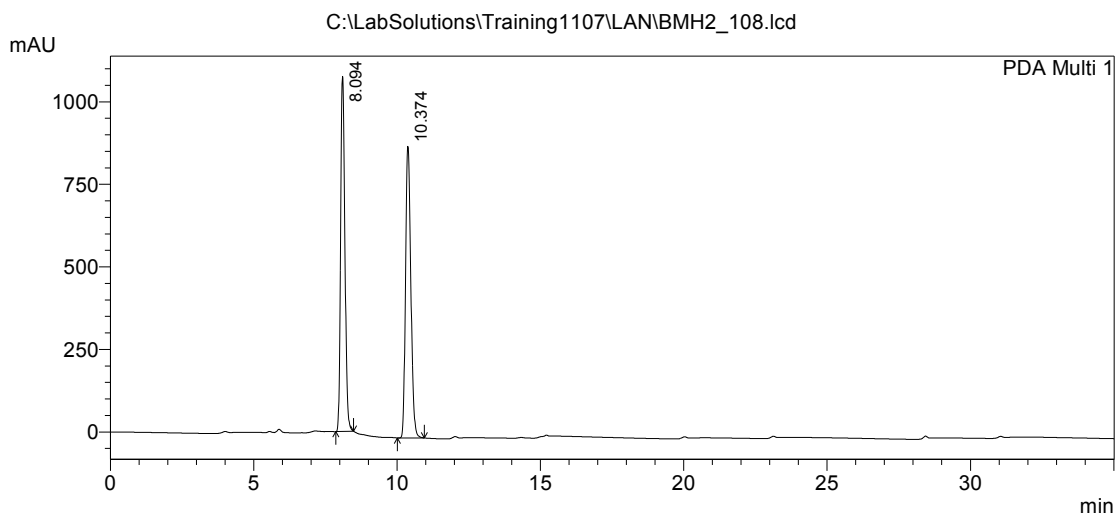


==== HPLC Analysis Report ====

C:\LabSolutions\Training1107\LAN\BMH2_108.lcd

Acquired by : Admin
 Sample Name : 1
 Sample ID : 1
 Tray# : 1
 Vial # : 77
 Injection Volume : 5 uL
 Data File Name : BMH2_108.lcd
 Method File Name : OD-99.5_5_Hexane_IPA_35min_0.5ml.lcm
 Batch File Name : 12.20.17.lcb
 Report File Name : UCD Default.lcr
 Data Acquired : 12/21/2017 10:01:12 AM
 Data Processed : 1/2/2018 5:56:45 PM

<Chromatogram>



1 PDA Multi 1/210nm 4nm

< Peak Table >

PeakTable C:\LabSolutions\Training1107\LAN\BMH2_108.lcd

PDA Ch1 210nm 4nm

Peak#	Ret. Time	Area	Height	Area %	Height %
1	8.094	11182934	1075245	49.573	54.903
2	10.374	11375650	883216	50.427	45.097
Total		22558584	1958461	100.000	100.000

178a chiral

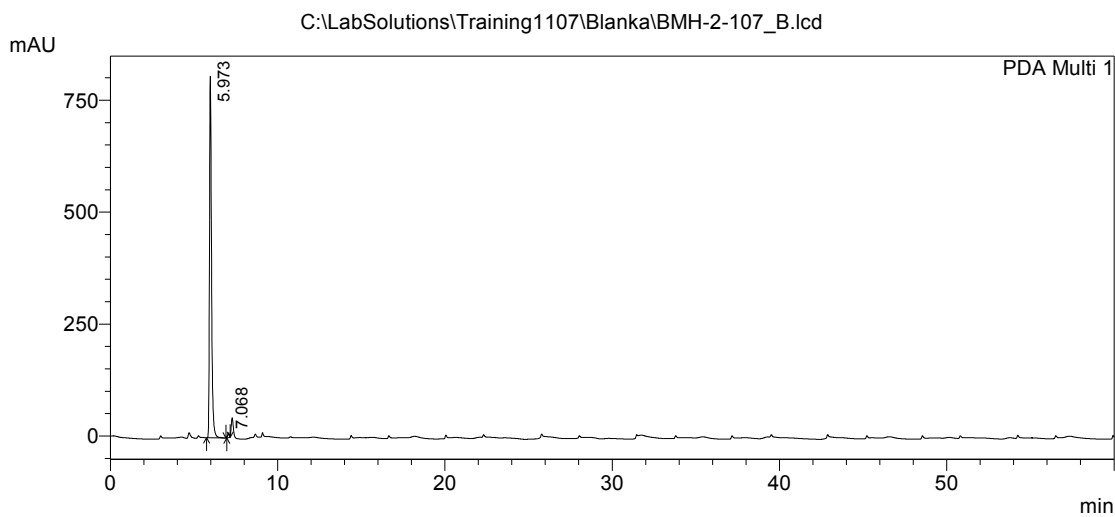


==== HPLC Analysis Report ====

C:\LabSolutions\Training1107\Blanka\BMH-2-107_B.lcd

Acquired by : Admin
 Sample Name : BMH-2-107
 Sample ID : BMH-2-107
 Tray# : 1
 Vial # : 9
 Injection Volume : 7 uL
 Data File Name : BMH-2-107_B.lcd
 Method File Name : OD-99.5_5_Hexane_IPA_60min_0.7mLmin.lcm
 Batch File Name : BMH 2-107 redo.lcb
 Report File Name : UCD Default.lcr
 Data Acquired : 3/11/2016 11:33:40 AM
 Data Processed : 10/12/2017 12:40:52 PM

<Chromatogram>



1 PDA Multi 1/218nm 4nm

< Peak Table >

PeakTable C:\LabSolutions\Training1107\Blanka\BMH-2-107_B.lcd

PDA Ch1 218nm 4nm

Peak#	Ret. Time	Area	Height	Area %	Height %
1	5.973	6811649	806989	98.867	98.763
2	7.068	78079	10111	1.133	1.237
Total		6889728	817099	100.000	100.000

178b achiral

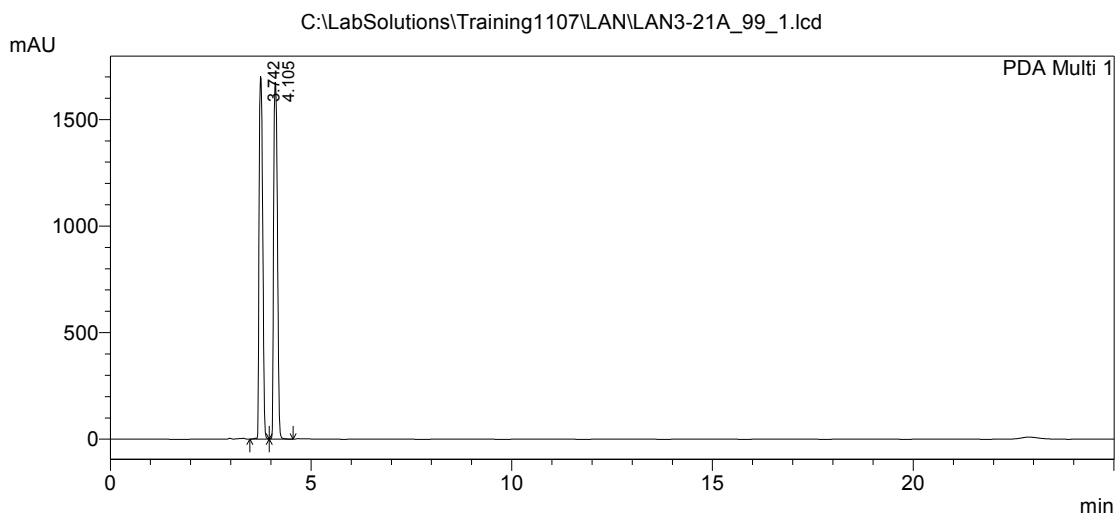


==== HPLC Analysis Report ====

C:\LabSolutions\Training1107\LAN\LAN3-21A_99_1.lcd

Acquired by : Admin
 Sample Name : LAN3-21A
 Sample ID : LAN3-21A
 Tray# : 1
 Vial # : 13
 Injection Volume : 10 uL
 Data File Name : LAN3-21A_99_1.lcd
 Method File Name : OD-99_1_Hexane_IPA_25min.lcm
 Batch File Name : 9.5.17.lcb
 Report File Name : UCD Default.lcr
 Data Acquired : 9/5/2017 3:52:49 PM
 Data Processed : 10/12/2017 12:53:50 PM

<Chromatogram>



1 PDA Multi 1/212nm 4nm

< Peak Table >

PeakTable C:\LabSolutions\Training1107\LAN\LAN3-21A_99_1.lcd

PDA Ch1 212nm 4nm

Peak#	Ret. Time	Area	Height	Area %	Height %
1	3.742	10574888	1702164	48.770	50.408
2	4.105	11108112	1674630	51.230	49.592
Total		21683000	3376794	100.000	100.000

178b chiral

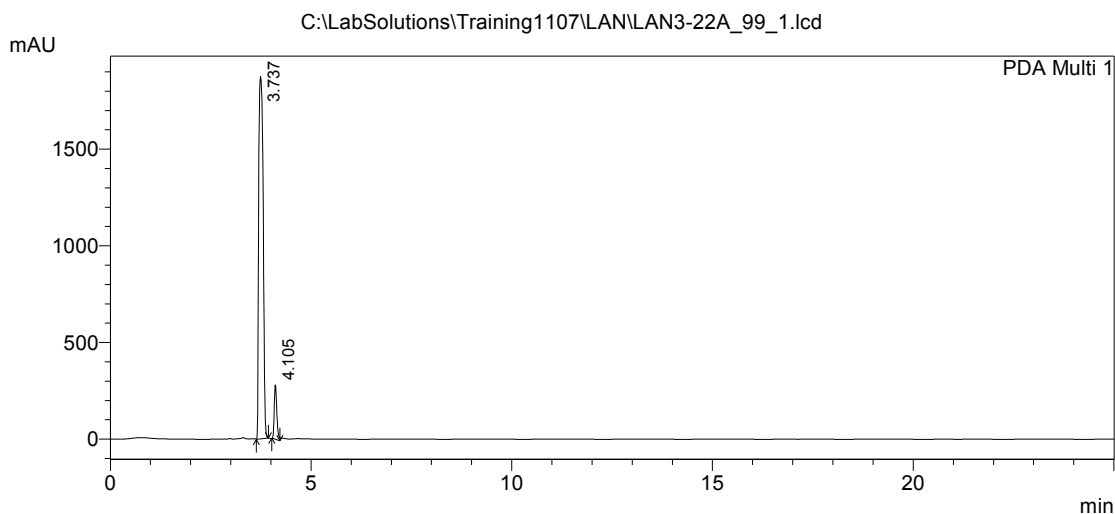


==== HPLC Analysis Report ====

C:\LabSolutions\Training1107\LAN\LAN3-22A_99_1.lcd

Acquired by : Admin
 Sample Name : LAN3-22A
 Sample ID : LAN3-22A
 Tray# : 1
 Vial # : 14
 Injection Volume : 10 uL
 Data File Name : LAN3-22A_99_1.lcd
 Method File Name : OD-99_1_Hexane_IPA_25min.lcm
 Batch File Name : 9.5.17.lcb
 Report File Name : UCD Default.lcr
 Data Acquired : 9/5/2017 4:18:18 PM
 Data Processed : 10/12/2017 1:02:52 PM

<Chromatogram>



1 PDA Multi 1/212nm 4nm

< Peak Table >

PeakTable C:\LabSolutions\Training1107\LAN\LAN3-22A_99_1.lcd

PDA Ch1 212nm 4nm

Peak#	Ret. Time	Area	Height	Area %	Height %
1	3.737	14330793	1874825	91.894	87.016
2	4.105	1264063	279746	8.106	12.984
Total		15594855	2154571	100.000	100.000

178c achiral

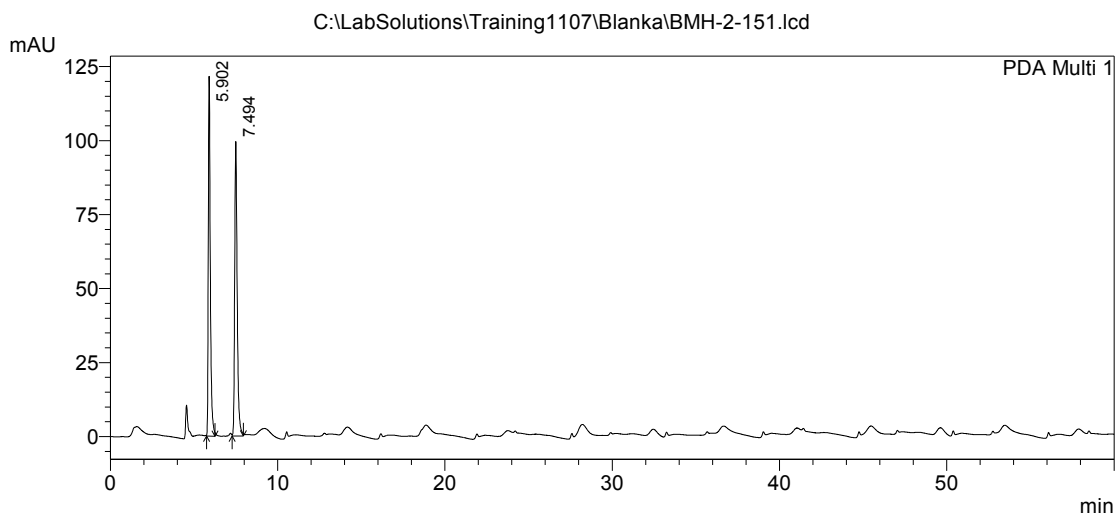


==== HPLC Analysis Report ====

C:\LabSolutions\Training1107\Blanka\BMH-2-151.lcd

Acquired by : Admin
 Sample Name : BMH-2-151
 Sample ID : BMH-2-151
 Tray# : 1
 Vial # : 9
 Injection Volume : 7 uL
 Data File Name : BMH-2-151.lcd
 Method File Name : OD-99.5_5_Hexane_IPA_60min_0.7mLmin.lcm
 Batch File Name : BMH 2-107 redo.lcb
 Report File Name : UCD Default.lcr
 Data Acquired : 4/18/2016 11:06:17 AM
 Data Processed : 6/7/2016 1:51:49 PM

<Chromatogram>



< Peak Table >

PeakTable C:\LabSolutions\Training1107\Blanka\BMH-2-151.lcd

PDA Ch1 222nm 4nm

Peak#	Ret. Time	Area	Height	Area %	Height %
1	5.902	1016211	121550	49.493	54.984
2	7.494	1037047	99512	50.507	45.016
Total		2053258	221062	100.000	100.000

178c chiral

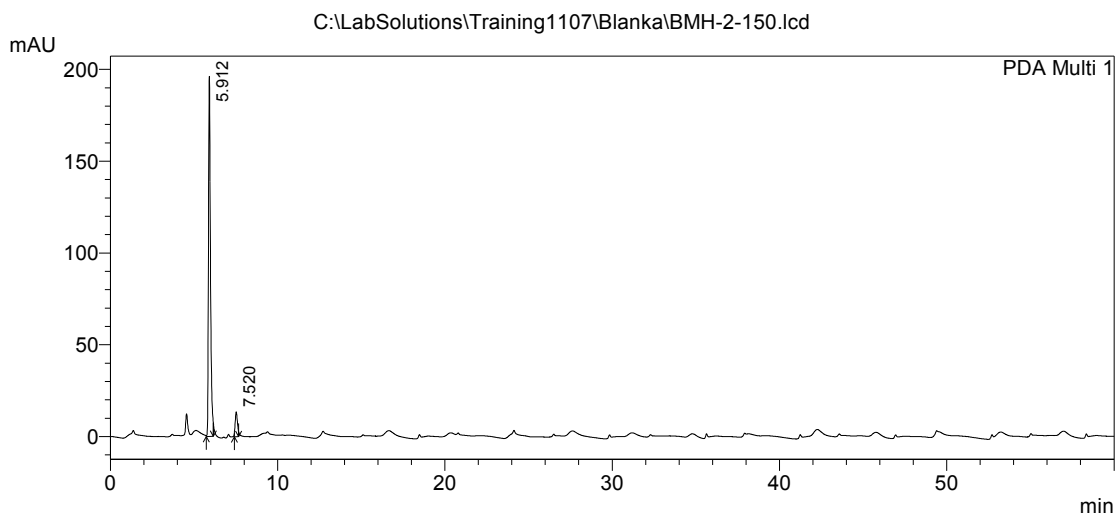


==== HPLC Analysis Report ====

C:\LabSolutions\Training1107\Blanka\BMH-2-150.lcd

Acquired by : Admin
 Sample Name : BMH-2-150
 Sample ID : BMH-2-150
 Tray# : 1
 Vial # : 8
 Injection Volume : 7 uL
 Data File Name : BMH-2-150.lcd
 Method File Name : OD-99.5_5_Hexane_IPA_60min_0.7mLmin.lcm
 Batch File Name : BMH 2-107 redo.lcb
 Report File Name : UCD Default.lcr
 Data Acquired : 4/18/2016 12:06:46 PM
 Data Processed : 6/7/2016 2:00:48 PM

<Chromatogram>



1 PDA Multi 1/222nm 4nm

< Peak Table >

PeakTable C:\LabSolutions\Training1107\Blanka\BMH-2-150.lcd

PDA Ch1 222nm 4nm

Peak#	Ret. Time	Area	Height	Area %	Height %
1	5.912	1622912	196099	92.778	93.534
2	7.520	126325	13556	7.222	6.466
Total		1749237	209655	100.000	100.000

178d achiral

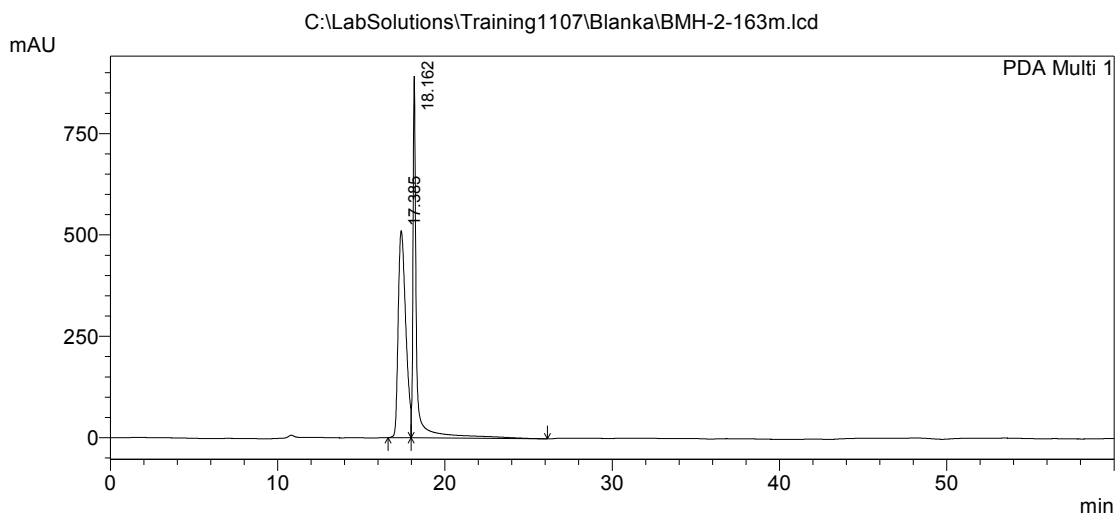


==== HPLC Analysis Report ====

C:\LabSolutions\Training1107\Blanka\BMH-2-163m.lcd

Acquired by : Admin
 Sample Name : BMH-2-163
 Sample ID : BMH-2-163
 Tray# : 1
 Vial # : 5
 Injection Volume : 7 uL
 Data File Name : BMH-2-163m.lcd
 Method File Name : AS-99.8_2_Hexane_IPA_60min-0.3mlmin.lcm
 Batch File Name : BMH 2-161m.lcb
 Report File Name : UCD Default.lcr
 Data Acquired : 5/19/2016 9:33:06 AM
 Data Processed : 5/19/2016 10:56:00 AM

<Chromatogram>



1 PDA Multi 1/217nm 4nm

< Peak Table >

PeakTable C:\LabSolutions\Training1107\Blanka\BMH-2-163m.lcd

PDA Ch1 217nm 4nm

Peak#	Ret. Time	Area	Height	Area %	Height %
1	17.385	16060524	510924	54.595	36.437
2	18.162	13357047	891302	45.405	63.563
Total		29417571	1402226	100.000	100.000

178d chiral

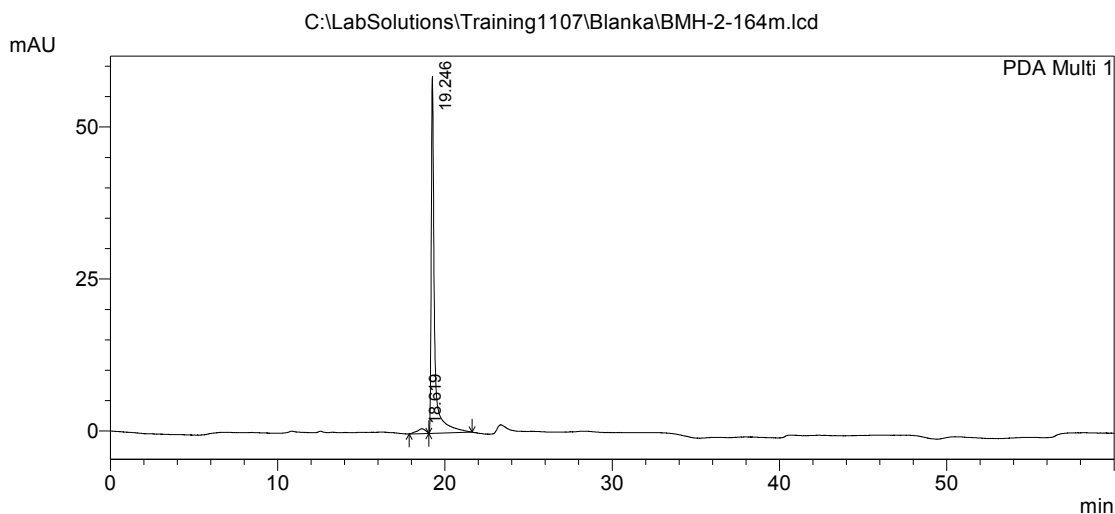


==== HPLC Analysis Report ====

C:\LabSolutions\Training1107\Blanka\BMH-2-164m.lcd

Acquired by : Admin
 Sample Name : BMH-2-164
 Sample ID : BMH-2-164
 Tray# : 1
 Vial # : 7
 Injection Volume : 7 uL
 Data File Name : BMH-2-164m.lcd
 Method File Name : AS-99.8_2_Hexane_IPA_60min-0.3mlmin.lcm
 Batch File Name : BMH 2-161m.lcb
 Report File Name : UCD Default.lcr
 Data Acquired : 5/19/2016 11:34:03 AM
 Data Processed : 5/19/2016 1:15:16 PM

<Chromatogram>



1 PDA Multi 1/254nm 4nm

< Peak Table >

PeakTable C:\LabSolutions\Training1107\Blanka\BMH-2-164m.lcd

PDA Ch1 254nm 4nm

Peak#	Ret. Time	Area	Height	Area %	Height %
1	18.619	27985	790	3.419	1.328
2	19.246	790619	58698	96.581	98.672
Total		818603	59488	100.000	100.000

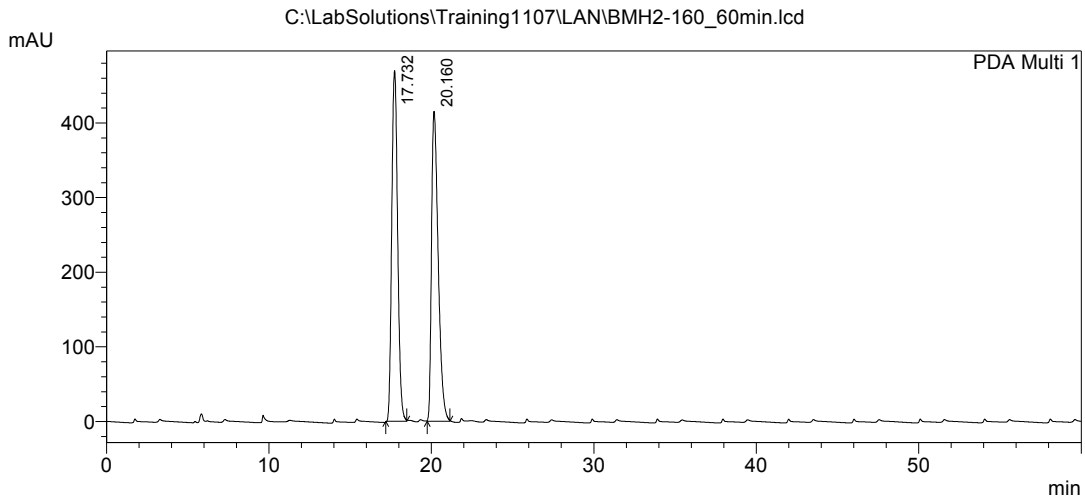


==== HPLC Analysis Report ====

C:\LabSolutions\Training1107\LAN\BMH2-160_60min.lcd

Acquired by : Admin
 Sample Name : 1
 Sample ID : 1
 Tray# : 1
 Vial # : 78
 Injection Volume : 5 uL
 Data File Name : BMH2-160_60min.lcd
 Method File Name : OD-99_1_Hexane_IPA_60min_0.5mL.lcm
 Batch File Name : 12.20.17.lcb
 Report File Name : UCD Default.lcr
 Data Acquired : 12/21/2017 8:54:01 PM
 Data Processed : 1/2/2018 6:05:55 PM

<Chromatogram>



1 PDA Multi 1/214nm 4nm

< Peak Table >

PeakTable C:\LabSolutions\Training1107\LAN\BMH2-160_60min.lcd

PDA Ch1 214nm 4nm

Peak#	Ret. Time	Area	Height	Area %	Height %
1	17.732	11858354	469881	49.932	53.081
2	20.160	11890636	415336	50.068	46.919
Total		23748989	885216	100.000	100.000

flow rate 0.5 mL/

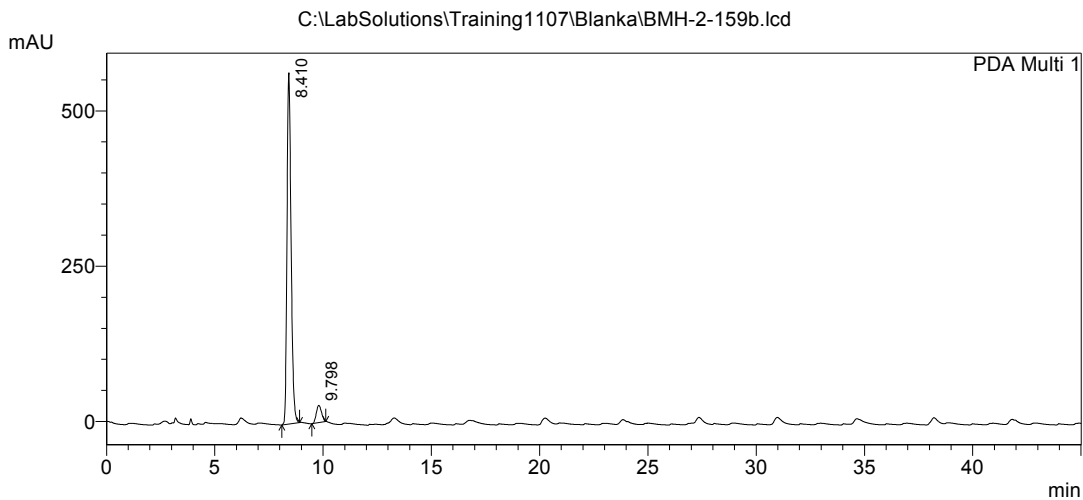


==== HPLC Analysis Report ====

C:\LabSolutions\Training1107\Blanka\BMH-2-159b.lcd

Acquired by : Admin
 Sample Name : BMH-2-159
 Sample ID : BMH-2-159
 Tray# : 1
 Vail # : 4
 Injection Volume : 7 uL
 Data File Name : BMH-2-159b.lcd
 Method File Name : OD-99_1_Hexane_IPA_45min.lcm
 Batch File Name : BMH-2-159_161b.lcb
 Report File Name : UCD Default.lcr
 Data Acquired : 5/6/2016 10:54:09 AM
 Data Processed : 5/6/2016 3:35:02 PM

<Chromatogram>



< Peak Table >

PeakTable C:\LabSolutions\Training1107\Blanka\BMH-2-159b.lcd

PDA Ch1 217nm 4nm

Peak#	Ret. Time	Area	Height	Area %	Height %
1	8.410	7387065	565215	94.033	95.285
2	9.798	468727	27967	5.967	4.715
Total		7855792	593182	100.000	100.000

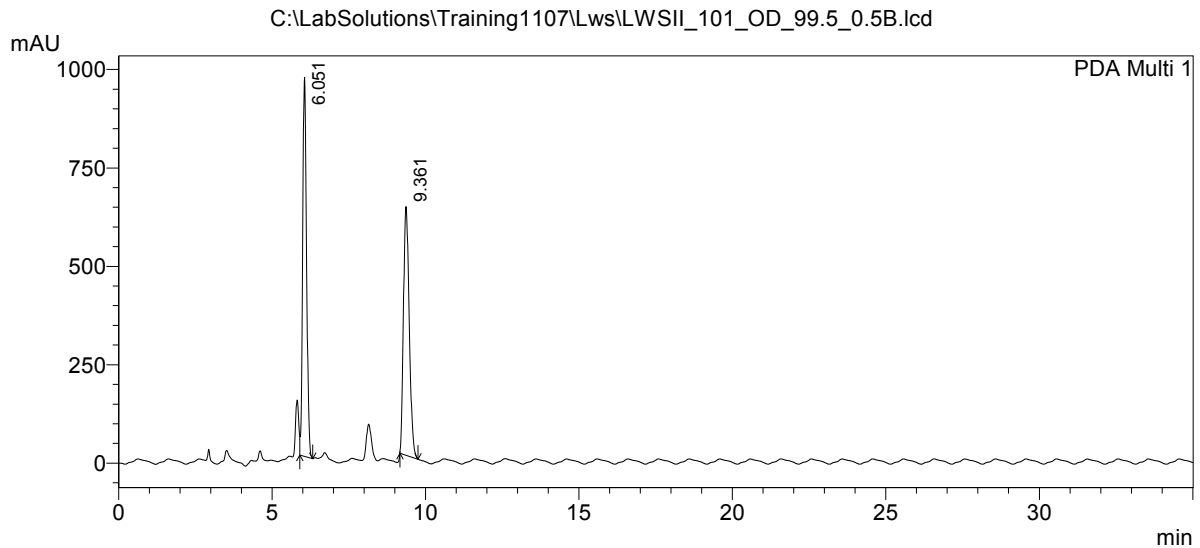
178f achiral



==== HPLC Analysis Report ====

C:\LabSolutions\Training1107\Lws\LWSII_101_OD_99.5_0.5B.lcd
 Acquired by : Admin
 Sample Name : 1
 Sample ID : 1
 Tray# : 1
 Vial # : 62
 Injection Volume : 10 uL
 Data File Name : LWSII_101_OD_99.5_0.5B.lcd
 Method File Name : OD-98_2_Hexane_IPA_35min.lcm
 Batch File Name : 4-16-18.lcb
 Report File Name : UCD Default.lcr
 Data Acquired : 5/23/2018 8:13:35 PM
 Data Processed : 5/23/2018 8:48:36 PM

<Chromatogram>



< Peak Table >

PeakTable C:\LabSolutions\Training1107\Lws\LWSII_101_OD_99.5_0.5B.lcd

PDA Ch1 215nm 4nm

Peak#	Ret. Time	Area	Height	Area %	Height %
1	6.051	8444380	961915	50.535	60.362
2	9.361	8265497	631650	49.465	39.638
Total		16709878	1593565	100.000	100.000

178f chiral

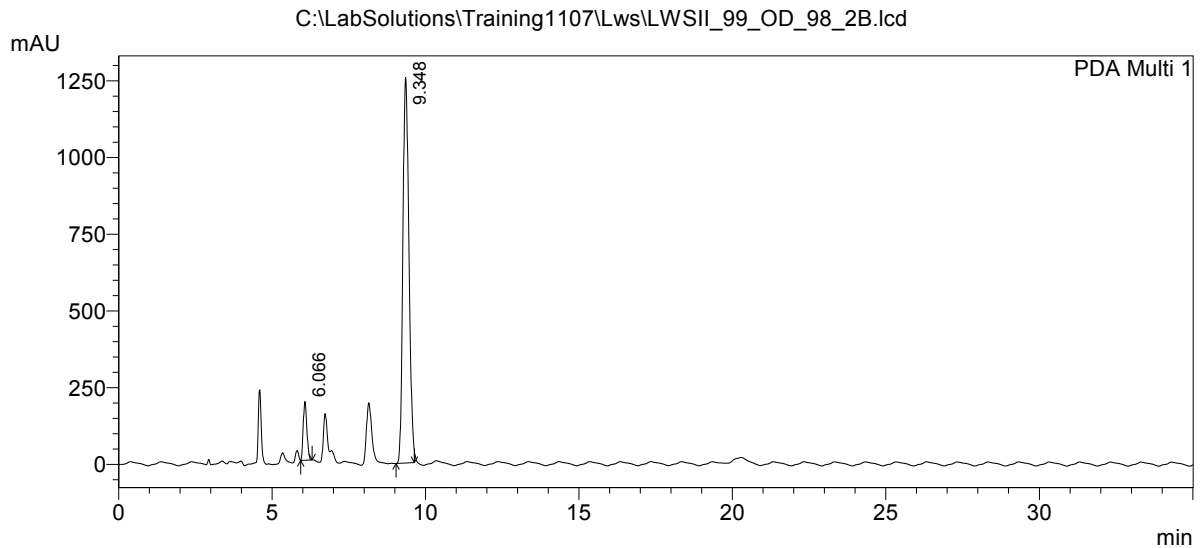


==== HPLC Analysis Report ====

C:\LabSolutions\Training1107\Lws\LWSII_99_OD_98_2B.lcd

Acquired by : Admin
 Sample Name : 1
 Sample ID : 1
 Tray# : 1
 Vial # : 61
 Injection Volume : 10 uL
 Data File Name : LWSII_99_OD_98_2B.lcd
 Method File Name : OD-98_2_Hexane_IPA_35min.lcm
 Batch File Name : 4-16-18.lcb
 Report File Name : UCD Default.lcr
 Data Acquired : 5/23/2018 7:02:58 PM
 Data Processed : 5/23/2018 7:37:59 PM

<Chromatogram>



< Peak Table >

PeakTable C:\LabSolutions\Training1107\Lws\LWSII_99_OD_98_2B.lcd

PDA Ch1 215nm 4nm

Peak#	Ret. Time	Area	Height	Area %	Height %
1	6.066	1580582	190838	8.403	13.194
2	9.348	17229527	1255613	91.597	86.806
Total		18810109	1446451	100.000	100.000

178g
achiral

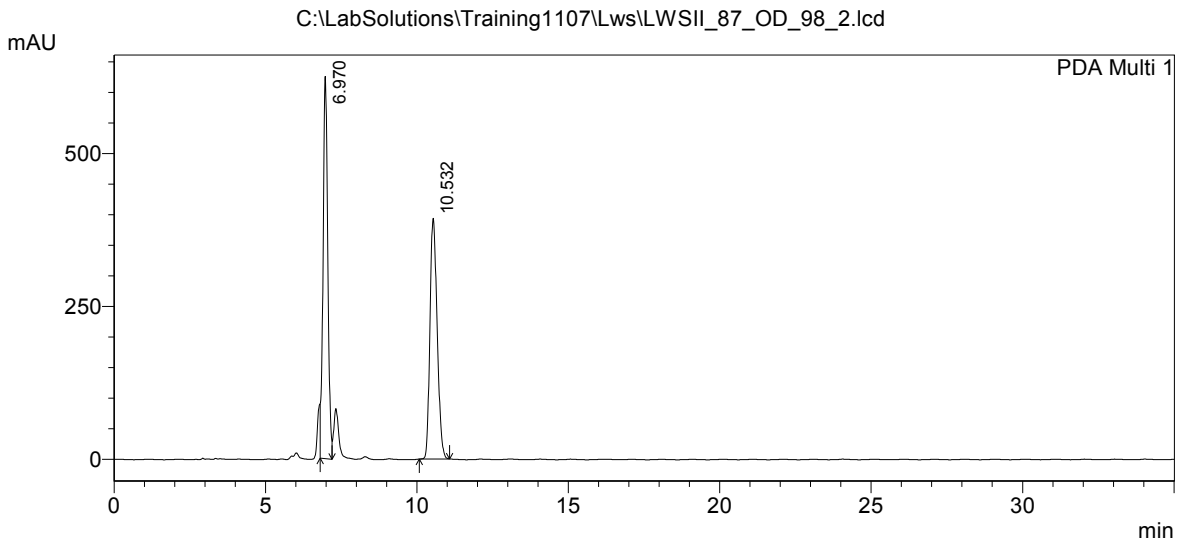


==== HPLC Analysis Report ====

C:\LabSolutions\Training1107\Lws\LWSII_87_OD_98_2.lcd

Acquired by : Admin
 Sample Name : 1
 Sample ID : 1
 Tray# : 1
 Vial # : 31
 Injection Volume : 10 uL
 Data File Name : LWSII_87_OD_98_2.lcd
 Method File Name : OD-98_2_Hexane_IPA_35min.lcm
 Batch File Name : 4-9-18.lcb
 Report File Name : UCD Default.lcr
 Data Acquired : 4/12/2018 6:30:58 PM
 Data Processed : 4/12/2018 7:05:59 PM

<Chromatogram>



< Peak Table >

PeakTable C:\LabSolutions\Training1107\Lws\LWSII_87_OD_98_2.lcd

PDA Ch1 237nm 4nm

Peak#	Ret. Time	Area	Height	Area %	Height %
1	6.970	6786552	625100	51.038	61.372
2	10.532	6510558	393434	48.962	38.628
Total		13297110	1018534	100.000	100.000

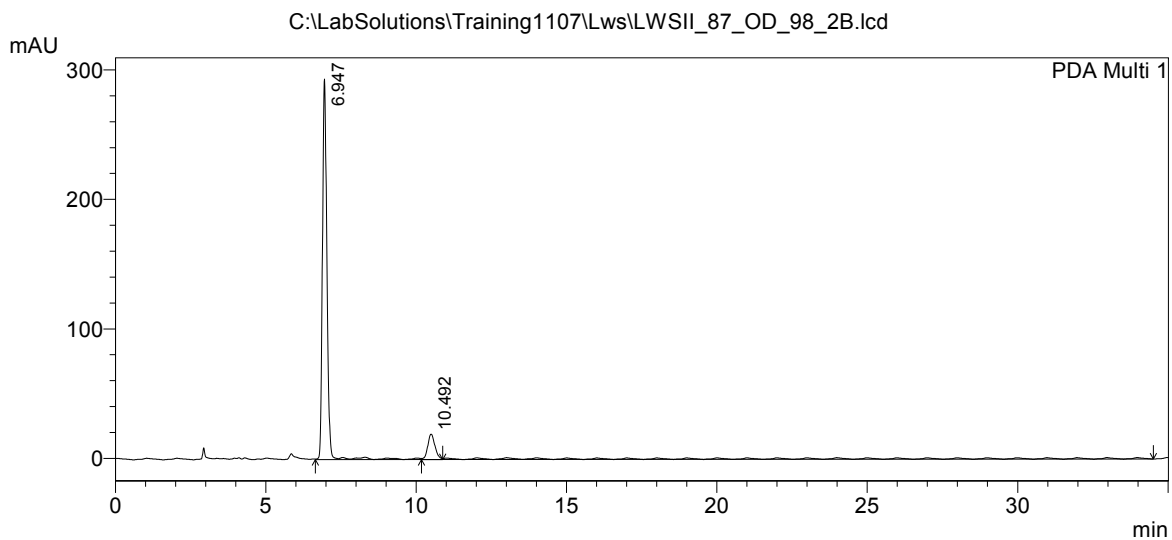
178g
chiral



==== HPLC Analysis Report ====

C:\LabSolutions\Training1107\Lws\LWSII_87_OD_98_2B.lcd
Acquired by : Admin
Sample Name : 1
Sample ID : 1
Tray# : 1
Vail # : 33
Injection Volume : 10 uL
Data File Name : LWSII_87_OD_98_2B.lcd
Method File Name : OD-98_2_Hexane_IPA_35min.lcm
Batch File Name : 4-16-18.lcb
Report File Name : UCD Default.lcr
Data Acquired : 4/16/2018 4:03:35 PM
Data Processed : 4/16/2018 4:38:38 PM

<Chromatogram>



1 PDA Multi 1/230nm 4nm

< Peak Table >

PeakTable C:\LabSolutions\Training1107\Lws\LWSII_87_OD_98_2B.lcd

PDA Ch1 230nm 4nm

Peak#	Ret. Time	Area	Height	Area %	Height %
1	6.947	3023143	293915	90.188	93.753
2	10.492	328909	19583	9.812	6.247
Total		3352052	313498	100.000	100.000